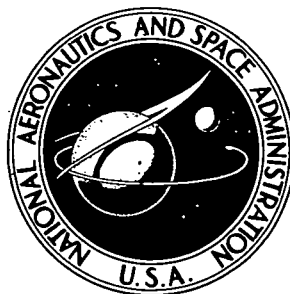


**NASA CONTRACTOR  
REPORT**



**NASA CR-2478**

**NASA CR-2478**

**DEMONSTRATION OF A STERILIZABLE  
SOLID ROCKET MOTOR SYSTEM**

*by E. J. Mastrolia, G. M. Santerre, and W. L. Lambert*

*Prepared by*

**AEROJET SOLID PROPULSION COMPANY**

**Sacramento, Calif. 95813**

*for Langley Research Center*



**NATIONAL AERONAUTICS AND SPACE ADMINISTRATION • WASHINGTON, D. C. • FEBRUARY 1975**

1. Report No. NASA CR-2478		2. Government Accession No.		3. Recipient's Catalog No.	
4. Title and Subtitle DEMONSTRATION OF A STERILIZABLE SOLID ROCKET MOTOR SYSTEM				5. Report Date FEBRUARY 1975	
				6. Performing Organization Code	
7. Author(s) E. J. Mastrolia, G. M. Santerre, and W. L. Lambers				8. Performing Organization Report No.	
9. Performing Organization Name and Address Aerojet Solid Propulsion Company P. O. Box 13400 Sacramento, CA 95813				10. Work Unit No.	
				11. Contract or Grant No. NAS1-10861	
12. Sponsoring Agency Name and Address National Aeronautics & Space Administration Washington, DC 20546				13. Type of Report and Period Covered Contractor Report	
				14. Sponsoring Agency Code	
15. Supplementary Notes FINAL REPORT					
16. Abstract A solid propellant rocket motor containing 60.9 Kg (134-lb) of propellant was successfully static fired after being subjected to eight heat sterilization cycles (three 54-hour cycles plus five 40-hour cycles) at 125°C (257°F). The test motor, a modified SVM-3 chamber, incorporated a flexible grain retention system of EPR rubber to relieve thermal shrinkage stresses. The propellant used in the motor was ANB-3438, and 84 wt% solids system (18 wt% aluminum) containing 66 wt% stabilized ammonium perchlorate oxidizer and a saturated hydroxyl-terminated polybutadiene binder. Bonding of the propellant to the EPR insulation (GenGard V-4030) was provided by the use of SD-886, an epoxy urethane restriction.					
17. Key Words (Suggested by Author(s)) Heat sterilization Solid propellant Polymers				18. Distribution Statement  Unclassified - Unlimited  STAR CATEGORY 27	
19. Security Classif. (of this report) Unclassified		20. Security Classif. (of this page) Unclassified		21. No. of Pages 200	
				22. Price* \$7.00	

Page Intentionally Left Blank

## TABLE OF CONTENTS

	<u>Page</u>
I. <u>INTRODUCTION</u> . . . . .	1
II. <u>SUMMARY</u> . . . . .	2
III. <u>TECHNICAL DISCUSSION</u> . . . . .	3
A.   SUMMARY OF PREVIOUS WORK. . . . .	3
B.   MOTOR DESIGN. . . . .	5
1. <u>Requirements</u> . . . . .	5
2. <u>Propellant Grain and Grain Retention System</u> . . . . .	7
3. <u>Hardware Components</u> . . . . .	36
C.   PROPELLANT VERIFICATION . . . . .	53
1. <u>Raw Materials</u> . . . . .	53
2. <u>Heat Sterilization of Small Grains</u> . . . . .	61
3. <u>Heat Sterilization of Large Grains</u> . . . . .	65
D.   DEMONSTRATION MOTOR PROCESSING AND HEAT STERILIZATION . . . . .	107
1. <u>Demonstration Motor Processing</u> . . . . .	107
2. <u>Heat Sterilization of Demonstration Motors</u> . . . . .	108
3. <u>Selection of Motor for Static Test Firing</u> . . . . .	119
4. <u>Testing of Small-Size Samples</u> . . . . .	119
E.   STATIC TEST FIRING OF THE HEAT STERILIZED MOTOR . . . . .	138
1. <u>Nozzle Throat Modification</u> . . . . .	138
2. <u>Motor Assembly</u> . . . . .	138
3. <u>Temperature Conditioning</u> . . . . .	141
4. <u>Test Installation</u> . . . . .	141
5. <u>Ballistic Performance</u> . . . . .	142
6. <u>Component Performance</u> . . . . .	150
APPENDIX A . . . . .	156
APPENDIX B . . . . .	185
REFERENCES . . . . .	192

## LIST OF FIGURES

<u>Figure</u>		<u>Page</u>
1	Formulations of Heat Sterilizable Propellant and Liner . . . . .	6
2	Preliminary Grain Design - Sterilizable Motor . . . . .	8
3	Grain Retention Disk Installation . . . . .	10
4	Master Relaxation Curve for V-4030 Rubber . . . . .	12
5	Time-Temperature Shift Factor for V-4030 Rubber . . . . .	13
6	Tensile Stress vs Time to Failure for V-4030 Rubber Bonded to V-4030 Rubber with EC-2216 . . . . .	14
7	Comparison of Theoretical Prediction and Test Results of Disk Grain Support for Tangential Loads, V-4030 Rubber . . . . .	16
8	Comparison of Theoretical Prediction and Tests Results of Disk Grain Support for Radial Load, V-4030 Rubber . . . . .	17
9	Test Results of Disk Grain Support for Radial Load . . . . .	19
10	Test Results of Disk Grain Support for Tangential Load . . . . .	20
11	Deformation of Motor Inner Bore at 4°C (40°F) . . . . .	21
12	Interface Stresses and Inner Bore Shape of Sterilizable Motor Subjected to 15g Axial Acceleration . . . . .	23
13	Summary of Propellant Grain and Retention System Structural Margins . . . . .	25
14	Motor Pressurization Using Two-Bottle Model . . . . .	26
15	Motor Pressurization, Four-Bottle Model . . . . .	28
16	Motor Pressurization Using Four-Bottle Model . . . . .	29
17	Effect of Oxidizer Blend on ANB-3289-3 Burning Rate . . . . .	31
18	Revised Grain Configuration . . . . .	32
19	Predicted Ballistic Performance Summary - Sterilizable Motor at 21°C (70°F), Sea Level . . . . .	33
20	Sterilizable Motor Predicted Ballistic Performance at 21°C (70°F), Sea Level . . . . .	34
21	Formulation of ANB-3438 Propellant . . . . .	35
22	Ballistic Performance Comparison . . . . .	37
23	SVM-3 Nozzle Cross Section . . . . .	38
24	Nozzle Throat Structural Analysis . . . . .	42
25	Sterilizable Motor Insulated Chamber . . . . .	43
26	Sterilizable Motor Chamber Insulator . . . . .	45
27	Arc Image Furnace Data - ANB-3289 -3 Propellant . . . . .	51
28	Ignition Time as a Function of Pressure, ANB-3289-3 Propel- lant, Batch 72-92 . . . . .	52

# LIST OF FIGURES (cont)

<u>Figure</u>		<u>Page</u>
29	Analyses of Telagen-S HTPB Prepolymers . . . . .	54
30	DTA Thermograms of PEPCON Produced Oxidizer . . . . .	56
31	TGA Thermograms of PEPCON Produced Oxidizers . . . . .	57
32	Effect of Heat Sterilization on Mechanical Properties of ANB-3289-3 Propellant Prepared with Different Oxidizer Lots . . . . .	59
33	Solid Strand Burning Rates for Batch 72-92, ANB-3289-3 Propellant . . . . .	62
34	Effect of Heat Sterilization on Mechanical Properties of ANB-3289-3 Propellant . . . . .	63
35	Solid Strand Burning Rate for Batch 73-30-70, ANB-3438 Propellant . . . . .	66
36	Analytical Data from 0.11 m <sup>3</sup> (30-gal) Size Mix of ANB-3289-3, Propellant . . . . .	68
37	Propellant Viscosity as a Function of Shear Stress and Time from Curing Agent Addition . . . . .	69
38	Burning Rates of Solid and Liquid Strands for ANB-3289-3, Batch 72-92 . . . . .	70
39	Propellant Compositions of Scale-Up Batches . . . . .	71
40	Analytical Data from 0.11 m <sup>3</sup> (30-gal) Size Batch Mixes of ANB-3289-3 Type Propellants . . . . .	72
41	Analytical Data from ANB-3438 Propellant Prepared in 0.02 m <sup>3</sup> (5-gal) and 0.11 m <sup>3</sup> (30-gal) Batches . . . . .	73
42	Propellant Viscosity as a Function of Shear Stress and Time from Curing Agent Addition . . . . .	74
43	Propellant Viscosity as a Function of Shear Stress and Time from Curing Agent Addition . . . . .	75
44	Propellant Viscosity as a Function of Shear Stress and Time from Curing Agent Addition . . . . .	76
45	Propellant Viscosity as a Function of Shear Stress and Time from Curing Agent Addition . . . . .	77
46	Diagram of 38 cm (15-in.) Diameter Propellant Grain Used in Heat Sterilization Tests . . . . .	79
47	Nominal Grain Sterilization Conditions . . . . .	80
48	Calculated Thermal Gradients in Sample Cross Sections . . . . .	82
49	Assumed Thermal Gradients and Calculated Maximum Tensile Stress in Actual Sample . . . . .	83
50	Calculated Thermal Stresses Occurring During Heat Sterili- zation of Propellant Grain . . . . .	84

# LIST OF FIGURES (cont)

<u>Figure</u>		<u>Page</u>
51	Effect of Crosslinker Level on Mechanical Properties of ANB-3289-3 and ANB-3438 Propellants Prepared with Telagen-S Prepolymer Master Blend . . . . .	87
52	Effect of Telagen-S Prepolymer Lot on Modulus/Crosslinker Level Relationship of ANB-3289-3 Propellant . . . . .	88
53	Effect of Telagen-S Prepolymer Lot on Modulus/Crosslinker Level Relationship of ANB-3438 Propellant . . . . .	89
54	Liquid Strand Burning Rate (LSBR) of Propellant Prepared in 0.11 m <sup>3</sup> (30-gal) Vertical Mixer Batches . . . . .	92
55	Solid Strand Burning Rate (SSBR) of Propellant Prepared in 0.11 in. <sup>3</sup> (30-gal) Vertical Mixer Batches . . . . .	93
56	Mechanical Properties of Propellants Prepared in 0.11 m <sup>3</sup> (30-gal) Vertical Mixer . . . . .	94
57	Oven Temperature Profile, Two-Step Heating Rate . . . . .	95
58	Oven Temperature Profile, Four-Step Heating Rate . . . . .	96
59	Oven Temperature Profile, Heating Rate of 11°C/hr (~20°F/hr) . . . . .	97
60	Large Grain Heat Sterilization Schedule . . . . .	99
61	Oven and Grain Temperature Profile, Two-Step Heating Rate . . . . .	100
62	Oven and Grain Temperature Profile, 4-Step Heating Rate . . . . .	101
63	Grain Temperature Profile at Oven Heating Rate of 11°C/hr (20°F/hr) . . . . .	102
64	Results of Heat Sterilization of Large Grains . . . . .	103
65	Effect of Heat Sterilization on Mechanical Properties of ANB-3438 Propellant . . . . .	105
66	Analytical Data from ANB-3438 Propellant Prepared in 0.02 m <sup>3</sup> (5-gal) and 0.11 m <sup>3</sup> (30-gal) batches . . . . .	109
67	Propellant Viscosity as a Function of Shear Stress and Time from Curing Agent Addition . . . . .	110
68	Liquid Strand Burning Rates of ANB-3438 Propellant . . . . .	111
69	Heat Sterilization Cycle No. 1 at 135°C (275°F) Demonstration Motor No. 1 . . . . .	113
70	Heat Sterilization Cycle No. 2 at 135°C (275°F) Demonstration Motor No. 1 . . . . .	114
71	Heat Sterilization Cycle No. 3 at 135°C (275°F) Demonstration Motor No. 1 . . . . .	115
72	Heat Sterilization Cycle No. 4 at 135°C (275°F) Demonstration Motor No. 1 . . . . .	116

# LIST OF FIGURES (cont)

<u>Figure</u>		<u>Page</u>
73	Heat Sterilization Cycle No. 5 at 135°C (275°F) Demonstration Motor No. 1 . . . . .	117
74	Heat Sterilization Cycle No. 6 at 135°C (275°F) Demonstration Motor No. 1 . . . . .	118
75	Heat Sterilization Cycle No. 1 at 125°C (257°F) Demonstration Motor No. 2 . . . . .	120
76	Heat Sterilization Cycle No. 2 at 125°C (257°F) Demonstration Motor No. 2 . . . . .	121
77	Heat Sterilization Cycle No. 3 at 125°C (257°F) Demonstration Motor No. 2 . . . . .	122
78	Heat Sterilization Cycle No. 9 at 125°C (257°F) Demonstration Motor No. 2 . . . . .	123
79	Heat Sterilization Cycle No. 5 at 125°C (257°F) Demonstration Motor No. 2 . . . . .	124
80	Heat Sterilization Cycle No. 6 at 125°C (257°F) Demonstration Motor No. 2 . . . . .	125
81	Heat Sterilization Cycle No. 7 at 125°C (257°F) Demonstration Motor No. 2 . . . . .	126
82	Heat Sterilization Cycle No. 8 at 125°C (257°F) Demonstration Motor No. 2 . . . . .	127
83	Effect of Heat Sterilization at 125°C (257°F) on Motor Grain Dimensions . . . . .	128
84	Effect of Heat Sterilization on ANB-3438 Propellant-to-Liner Bond Strength . . . . .	130
85	Effect of Heat Sterilization on ANB-3438 Mechanical Properties . . . . .	131
86	Initial Solid Strand Burning Rates of ANB-3438 Propellant, Batch 73-30-201 . . . . .	133
87	Solid Strand Burning Rates of ANB-3438 Propellant after One Heat Sterilization Cycle, Batch 73-30-201 . . . . .	134
88	Solid Strand Burning Rate of ANB-3438 Propellant after Six Heat Sterilization Cycles, Batch 73-20-201 . . . . .	135
89	Effect of Heat Sterilization on Weight and Dimensional Stability of ANB-3438 Propellant . . . . .	137
90	Burning Rates of ANB-3438 Propellant Fired in Solid Strands and 454 g (1-lb) Motors . . . . .	139
91	Ballistic Analysis Summary . . . . .	140
92	Pressure and Thrust vs Time for Static Test Firing of Heat Sterilized Motor . . . . .	143



# LIST OF FIGURES (cont)

<u>Figure</u>		<u>Page</u>
93	Sterilizable Motor Ignition Transient . . . . .	144
94	Sterilizable Motor Ballistic Performance . . . . .	145
95	Sterilizable Motor Throat Area as a Function of Time, $K_f = 0.915$ . . . . .	146
96	Sterilizable Motor Demonstration - Burning Rates Used in Ballistic Performance Predictions . . . . .	147
97	Performance Summary . . . . .	148
98	External Case Temperature During Test Firing of Demonstra- tion Motor No. 2 . . . . .	151
99	Sterilizable Motor SN 2, Pretest . . . . .	152
100	Sterilizable Motor SN 2, Pretest . . . . .	153
101	Sterilizable Motor SN 2, Posttest . . . . .	154

## GLOSSARY

ASPC	Aerojet Solid Propulsion Company
BPN	Igniter material composed of boron and potassium nitrate
C*	Characteristic exhaust velocity
Castorwax	Saturated castor oil manufactured by the Baker Castor Oil Company
Chemlok 202	Rubber to metal adhesives manufactured by the Hughson Chemical Company
Chemlok 234	
Chemlok 304	
Chemlok 205	A metal primer for use with Chemlok metal-to-rubber adhesives
DDI	See dimeryl diisocyanate
Dimeryl Diisocyanate	A hindred isocyanate curing agent manufactured by General Mills, Inc.
DPT	Double plate tensile specimens, rectangular in cross section
DTA	Differential thermal analysis
EC-2216	A rubber to metal adhesive manufactured by Emerson Cummings, Inc.
Epon-901 Epon-923	Epoxy adhesives prepared by Shell Chemical Co.
FC-154	Bonding agent, Aerojet proprietary item
FC-169	Oxidizer stabilizing agent, Aerojet proprietary item
FC-171	Oxidizer stabilizing agent, Aerojet proprietary item
FC-217	Bonding agent, Aerojet proprietary item
GenGard V-4030	An ethylene propylene rubber insulation manufactured by Kirkhill Rubber Company
GTR0	Glyceryl triricinoleate crosslinking agent manufactured by the Baker Castor Oil Co.
HSMP Oxidizer	High speed Mikro Pulverizer-ground ammonium perchlorate oxidizer, average particle size 26 $\mu$

## GLOSSARY (cont)

ITEM-120	An ethylene propylene diene modified rubber insulation developed by the Aerojet Solid Propulsion Company
Isophorone Diisocyanate	Isocyanate curing agent manufactured by Thorson Chemical Company
IPDI	See isophorone diisocyanate
$I_s$	Specific impulse
Kaowool Fibers	Fibrous aluminum silicate, Babcock and Wilcox Company
LHT-240	Crosslinking agent which is an adduct of hexane triol and polypropylene glycol
PBAN	Carboxyl-terminated terpolymer composed of butadiene, acrylic acid, and acrylonitrile
Telagen-S	Secondary hydroxyl terminated saturated polybutadiene polymer manufactured by General Tire and Rubber Company
TMP	Trimethylolpropane crosslinking agent manufactured by Celanese Corp.
Unground Oxidizer	Ammonium perchlorate oxidizer, average particle size, $180\mu$
$\sigma_m$	Maximum stress
$\epsilon_m$	Strain at maximum stress
$\epsilon_b$	Strain at Failure
$E_0$	Instantaneous modulus
$\mu$	Micron

# DEMONSTRATION OF A STERILIZABLE SOLID ROCKET MOTOR SYSTEM

E. J. Mastrolia, G. M. Santerre, W. L. Lambert  
Aerojet Solid Propulsion Company  
Sacramento, California

## I. INTRODUCTION

This is the Final Report submitted in fulfillment of the requirements of the National Aeronautics and Space Administration Contract NAS1-10861.

Heat-sterilizable solid propellant rocket motors have considerable potential for use in space missions where entry into a biologically quarantined area is required. Sterilizable solid rockets could find application in deorbiting operations, gas generators, and booster operations for recoverable space probes. In a previous contract\* the Aerojet Solid Propulsion Company had demonstrated that subscale motors comprising the total rocket motor system, i.e., case, insulation, liner and propellant could successfully survive the required six heat sterilization cycles without adversely affecting motor integrity. The primary objective of the present program (Contract NAS1-10861) was to demonstrate that a full-scale solid propellant rocket motor, exclusive of nozzle and igniter, could successfully and reliably function following exposure to dry heat sterilization. Also, the propellant should exhibit reasonable performance and the materials exhibit acceptable physical properties following the required period of heat sterilization. Two 45.7 cm (18-in.)-dia spherical motors (SVM-3 test chambers) were to be prepared and heat sterilized, and one was to be static test fired.

The approach taken in the present program was, therefore, to prepare and heat sterilize larger diameter grains of the propellant developed in the previous program and, if needed, to improve the propellant properties to assure heat sterilizability of full-size motor grains. Also a motor design was to be developed so that a stress-relieving grain retention system could be employed which would eliminate the high bond stresses due to the shift in stress-free temperature caused by exposure to the high sterilization temperature.

During the course of the program, special technical assistance was provided by M. H. Lucy (NASA/Langley), D. O. DePree (ASPC), and J. D. McConnell (ASPC).

---

\* D.O. DePree "Demonstration of a Sterilizable Solid Rocket Motor System", Final Report, NASA CR-111889, Contract NAS1-10086, January 1971.

## II. SUMMARY

The concept of a heat sterilizable solid propellant rocket motor was demonstrated by the successful static test firing of a prototype motor during the present program. This motor, using SVM-3 hardware, contained 60.9 Kg (134-lb) of propellant, and had been subjected to eight heat sterilization cycles (three 54-hour cycles plus five 40-hour cycles) at 125°C (257°F) prior to test firing. The propellant used in the motor was ANB-3438, an 84 wt% solids system containing 18 wt% aluminum powder and 66 wt% stabilized ammonium perchlorate oxidizer. The binder was composed of Telagen-S saturated HTPB prepolymer, glyceryl triricinoleate (GTR0) cross-linker, isophorone diisocyanate (IPDI) curing agent, and FC-217 bonding agent. The motor was insulated with GenGard V-4030, an EPR material containing low levels of mobile species.

A very large shift in stress-free temperature required the use of a stress relieving insulation system. This was provided by a boot composed of GenGard V-4030 rubber insulation which was tab-bonded to the insulated chamber wall. Analysis had indicated this design would be well within the capability of the propellant and liner system. The latter material, SD-886, is an epoxy-urethane material which provided a firm bond between the propellant and insulation. Both the propellant and bond tensile strength increased during the course of heat sterilization.

Test firing of nominal 454 g (1-lb) burning rate motors indicated a scale-up between solid strand and internal burning motor firings. To accommodate this increase, the throat area of the SVM-3 nozzle was enlarged so that the expected pressure would still be within the analytical envelope generated for adequate structural performance. Ignition of the heat-sterilized demonstration motor was effected through the use of 50g BPN pellets. The ignition interval lasted just under 70 msec. The motor pressure/time relationship was within the range of expected performance, with the motor burning rate, 0.48 cm/sec (0.19 in./sec) at 438 N/cm<sup>2</sup> (635 psia), being approximately 3% lower than predicted on the basis of 454g (1-lb) motor firings. Total burn time for the motor was 25.12 seconds. The delivered

specific impulse was 1964.9 N-sec/Kg (200.8 lbf-sec/lbm), which calculated to a vacuum specific impulse of 2573.6 N-sec/Kg (263.0 lbf-sec/lbm). The high expansion ratio (40/1) of the nozzle designed for space application resulted in separated flow which caused some loss of performance,

Post-firing examination of the motor components revealed satisfactory performance of the chamber and nozzle. Aft chamber insulation thickness reduction was typically about 0.25 cm (0.1 in.), normal for the SVM-3, indicating acceptable performance of the sterilized GenGard V-4030 material. The boot was essentially intact and still firmly bonded to the retention disks in the aft end. No charring was noted under the boot and only a slight amount of soot was present.

### III. TECHNICAL DISCUSSION

#### A. SUMMARY OF PREVIOUS WORK

Successful heat-sterilization performance was demonstrated in small-scale component testing under Contract NAS1-10086. Results of these tests were presented in NASA-CR-111889 and NASA-CR-111889-A reports published in January 1971 and December 1971, respectively. The components tested were: propellant raw materials (oxidizer and prepolymer), propellant, liner, insulation, and composites of liner/insulation and propellant/liner/insulation.

The approach taken by ASPC was that all components of the solid rocket motor: the case, the insulation, the liner and the propellant must not only be stable independently to heat sterilization, but also not react with each other in such a manner as to degrade other components. Thus, the chemical stability of each of the composite components was the first consideration because thermal degradation is essentially a chemical process and the reactions involved have a direct bearing not only on the composite themselves but, through migratory processes, on the neighboring materials.

The stability of the ammonium perchlorate was increased through double-recrystallization and the addition of 0.5 wt% FC-169, a proprietary stabilizing agent. To minimize oxidative attack on the prepolymer backbone

during heat sterilization, a saturated hydroxy-terminated polybutadiene (HTPB) was employed. The purity of the prepolymer was further enhanced by vacuum stripping at 200°C to remove volatile components. Iron and silicon, contaminants which are known to catalyze propellant (and particularly AP) decomposition, were kept at low concentrations (a few parts per million).

As a result of the component testing performed during Contract NAS1-10086, the propellant, liner and insulation materials were selected for use in the full-scale motor demonstration program (Contract NAS1-10861).

The initial propellant selected for use in the demonstration program contained 84 wt% total solids, 18 wt% aluminum powder and 66 wt% of purified and stabilized ammonium perchlorate oxidizer. The binder (unplasticized) was composed of saturated HTPB prepolymer (vacuum stripped at 200°C) crosslinked with trimethylol propane and cured with dimethyl diisocyanate. The binder for this propellant was later modified to improve the physical properties and the new propellant was designated ANB-3438.

The liner selected for use was SD-886, a low-solids loaded epoxy-polyurethane material. The cured liner was subjected to 24-hr heat sterilization cycle before propellant was cast against it.

GenGard V-4030, a commercially available ethylene-propylene rubber, was selected for insulating the motor. This material contains a low level of volatile components which was decreased further by subjecting the insulation to a 24-hour heat sterilization cycle prior to liner application.

These components, either singly or as composites, were able to survive the heat sterilization requirements of the program, namely; six cycles of 53 hours each at 135°F (275°F). The component and composite properties after heat sterilization were well within the program requirements.

In analyzing the data obtained under Contract NAS1-10086 it was observed that an unexpectedly high degree of stress relaxation, or plastic

flow, occurred under the compressive stress conditions encountered with a cast-in-case grain. This resulted in a nearly complete shift of the stress-free state from the cure temperature of 57°C (135°F) to the 135°C (275°F) sterilization temperature.

Although the propellant-liner-insulation system could withstand the heat sterilization conditions without degradation, the increase in bond tensile stress due to the shift in stress-free temperature resulted in negative safety margins for the case-bonded grain concept in all designs with web thicknesses greater than 5.1 cm (2.0 in.) for the 45.0 cm (17.7 in.) dia. SVM-3 test motor.

Several approaches were evaluated to reduce the bond stress levels in the sterilized motor. The most promising appeared to be a stress-relieving system in which the insulation was attached to the case by means of flexible tabs. This approach was selected for further development in Contract NAS1-10861.

## B. MOTOR DESIGN

### 1. Requirements

The motor design was required to be a functional product of the sterilizable propellant system developed under Contract NAS1-10086 and the existing motor components used in the 46 cm (18 in.)-dia Aerojet SVM-3 motor. The initial sterilizable propellant system consisted of:

Propellant	ANB-3289-3 (Figure 1)
Liner	SD-886 (Figure 1)
Insulation	GenGard V-4030, a commercial product

To achieve the primary program objective, the motor had to demonstrate reliable operation after withstanding the specified heat sterilization conditions. This was to be accomplished by designing within the constraints of the SVM-3



ANB-3289-3 Propellant

	<u>Wt %</u>
Ammonium Perchlorate Oxidizer (stabilized with 0.5 wt% FC-169)	66.0
Aluminum Powder	18.0
Silicone Oil Processing Aid	0.005
Binder (composed of Telagen-S prepolymer, TMP, DDI and FC-154)	15.995
Total	<hr/> 100.000

SD-886 Liner

GTR0	53.9
Epon-828	18.1
TDI	22.9
Titanium Dioxide	2.0
Carbon Black	3.0
Triethylamine	0.1
Total	<hr/> 100.0

Formulations of Heat Sterilizable Propellant and Liner

Figure 1

hardware, which had demonstrated 100% reliability in development and production. By selecting the proper grain configuration, pressure-vs-time characteristics could be tailored within the motor case structural capability and the nozzle thermal and structural capabilities. The principal limitation would be the propellant burning rate.

In keeping with the objectives and scope of the program, no attempt was made to maximize propellant loading or to minimize inert weight.

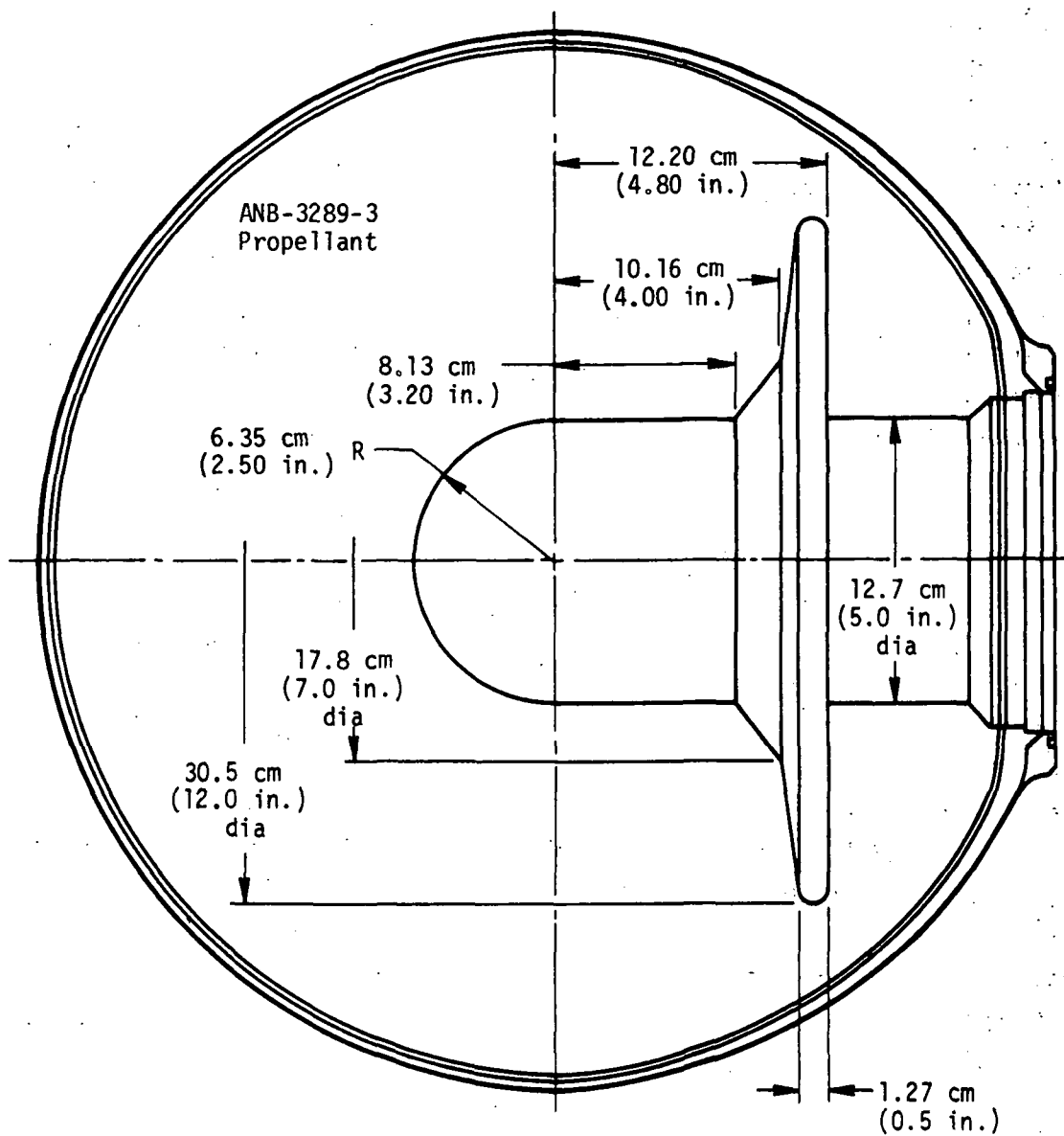
## 2. Propellant Grain and Grain Retention System

### a. Preliminary Design Approach

Work under this contract was initially predicated on grain design solutions to be provided under the preceding, but overlapping, Contract NAS1-10086. However, the only configuration which could be shown to be structurally feasible was a simple case-bonded shell with a very thin web. An alternative of a completely released grain was suggested, and subsequently adopted, for the motor demonstration.

The released grain concept was to provide flexible elements between the grain and case structures which would allow large radial separations (due to thermal shrinkage) without inducing significant interface stresses, but would be capable of providing tangential restraint for acceleration loads. This approach would allow the propellant to be formulated for optimum sterilization durability and would free the grain configuration selection from most structural limitations. There was, however, an attendant increase in inert weight, as well as the need for special design considerations.

The preliminary grain configuration selected for structural analysis, is shown in Figure 2. The configuration is representative of a flight-weight volumetric loading grain, with the advantage of being fully machinable with all surfaces of revolution.



Preliminary Grain Design - Sterilizable Motor

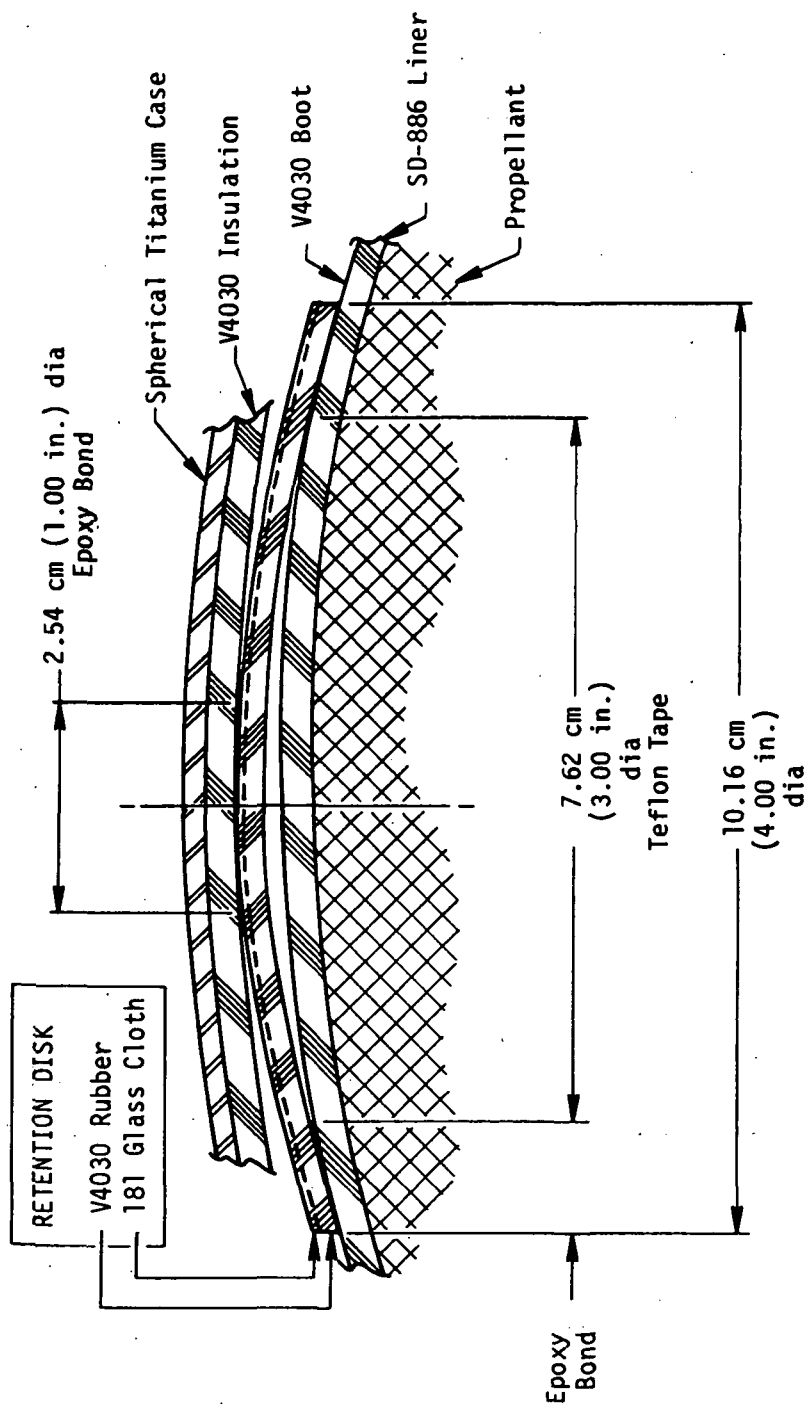
## b. Structural Analysis of Preliminary Design

### (1) Description

The preliminary grain design consisted of ANB-3289-3 propellant cast in a specially prepared 46 cm-dia SVM-3 titanium chamber. After propellant cure, the inner dimensions were to be machined to a configuration similar to the one shown in Figure 2. The special preparation of the titanium chamber consists of the installation of a SVM-3 aft insulator of V-4030 rubber and a constant thickness V-4030 rubber insulator over the forward hemisphere of the case. On the inner surface of the rubber insulators, 37 grain support disks are bonded using an epoxy adhesive. The disks are 10.16 cm (4.0 in.) in diameter with a 21.7 cm (8.55 in.) spherical radius outer surface. They are only bonded on the 2.54 cm (1.0 in.) diameter circle at their centers (see Figure 3). Teflon tape was to be used on all the inner surfaces of the insulators other than the 37 - 2.54 cm diameter spots. Each of the 37 disks have 7.62 cm (3 in.) diameter disks of Teflon tape attached concentrically on their inner surface in such a manner that the boot, when installed, could only be bonded, using epoxy adhesive, to the outer half inch annulus of each support disk. When the bonds were cured, the boot would be attached to the insulation by means of the 37 support disks so the boot has little constraint in the radial direction but considerable in the tangential direction. The 10.16 cm grain support disks were originally to be made of V-4030 rubber, but were later revised to add one ply of fiberglass cloth. The boot was then to be lined with SD-886 which was the final step in the special preparation of the titanium chamber prior to casting.

### (2) Loading Conditions

In lieu of specific mission requirements, a set of environmental conditions was arbitrarily selected as being representative of critical loads. These conditions were the basis of all structural analyses and are listed below:



Grain Retention Disk Installation

Figure 3

- . Storage at 8°C (40°F) for 3 months
- . Storage at 21°C (70°F) for 3 years
- . Static firing at 21°C (70°F)
- . Booster acceleration of 15 g's for 1 min. at 21°C (70°F)

### (3) Materials

#### (a) Propellant and Liner

The ANB-3289-3 propellant and SD-886 liner originally selected for the sterilizable motor were described previously. Mechanical and bonding properties of this propellant were reported in Reference 1.

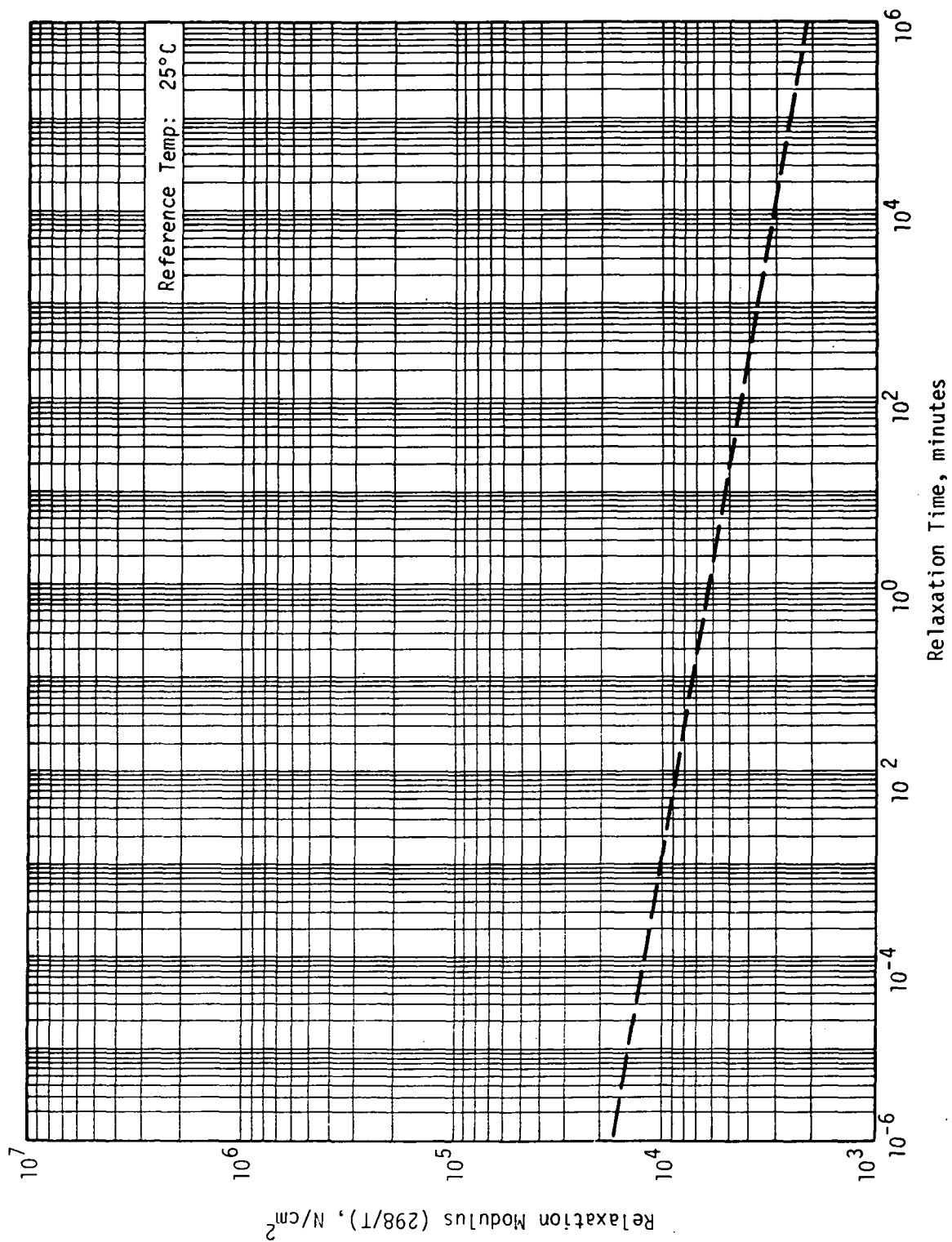
#### (b) Insulation and Boot

The insulation and boot material is GenGard V-4030. The master relaxation curve and the time-temperature shift factor for V-4030 are shown in Figures 4 and 5, respectively. The tensile stress versus time-to-failure curve for V-4030 bonded to V-4030 with EC-2216 epoxy adhesive is shown in Figure 6. The linear coefficient of thermal expansion for V-4030 is  $2.07 \times 10^{-4}$  m/m/°C.

#### (c) Motor Case

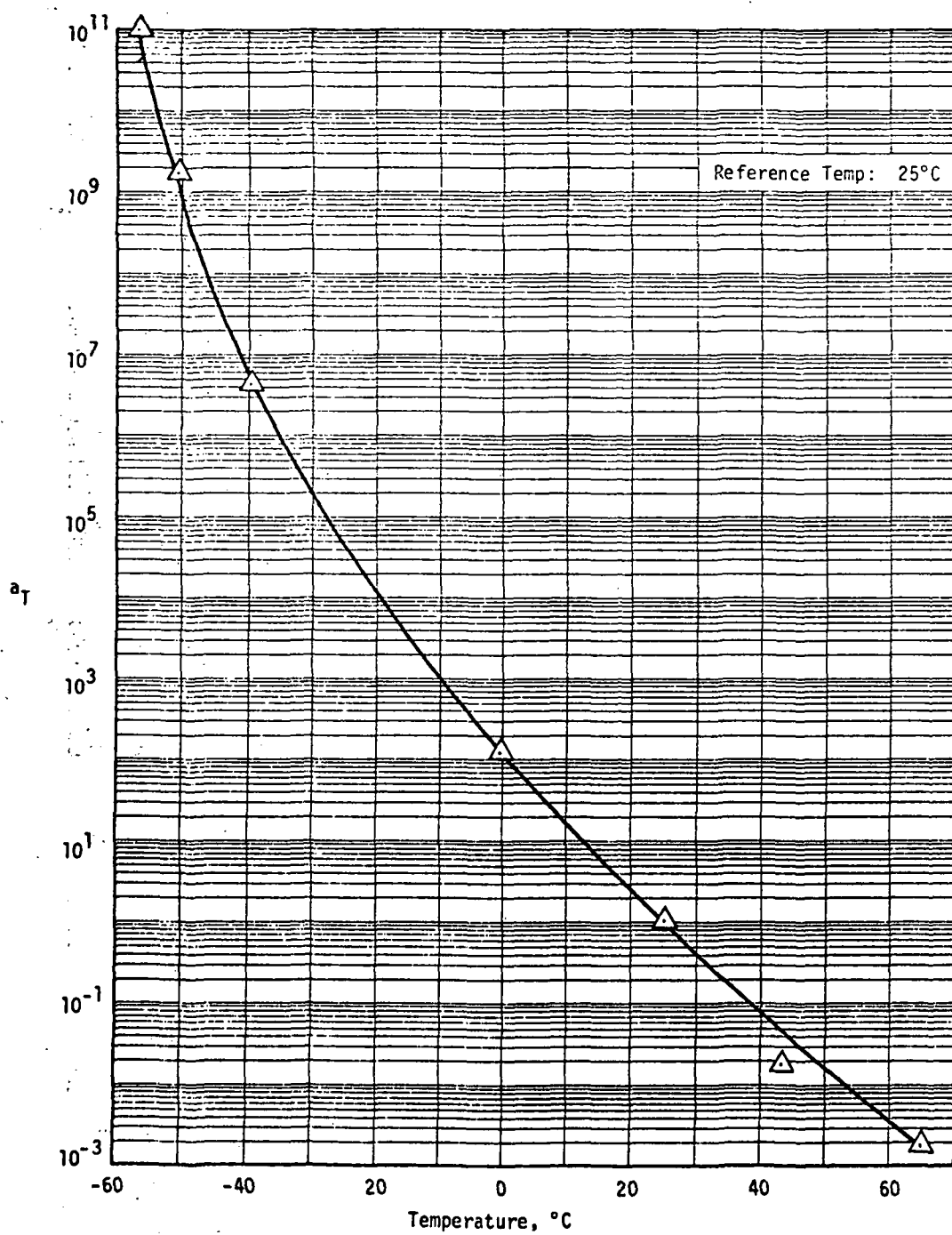
The titanium motor case was considered to have the following properties:

Modulus	$E_C = 10.3 \times 10^6 \text{ N/cm}^2$
Poisson's Ratio	$\nu_C = 0.29$
Coefficient of Linear Thermal Expansion	$\alpha_C = 8.28 \times 10^{-6} \text{ m/m/}^\circ\text{C}$



Master Relaxation Curve for V-4030 Rubber

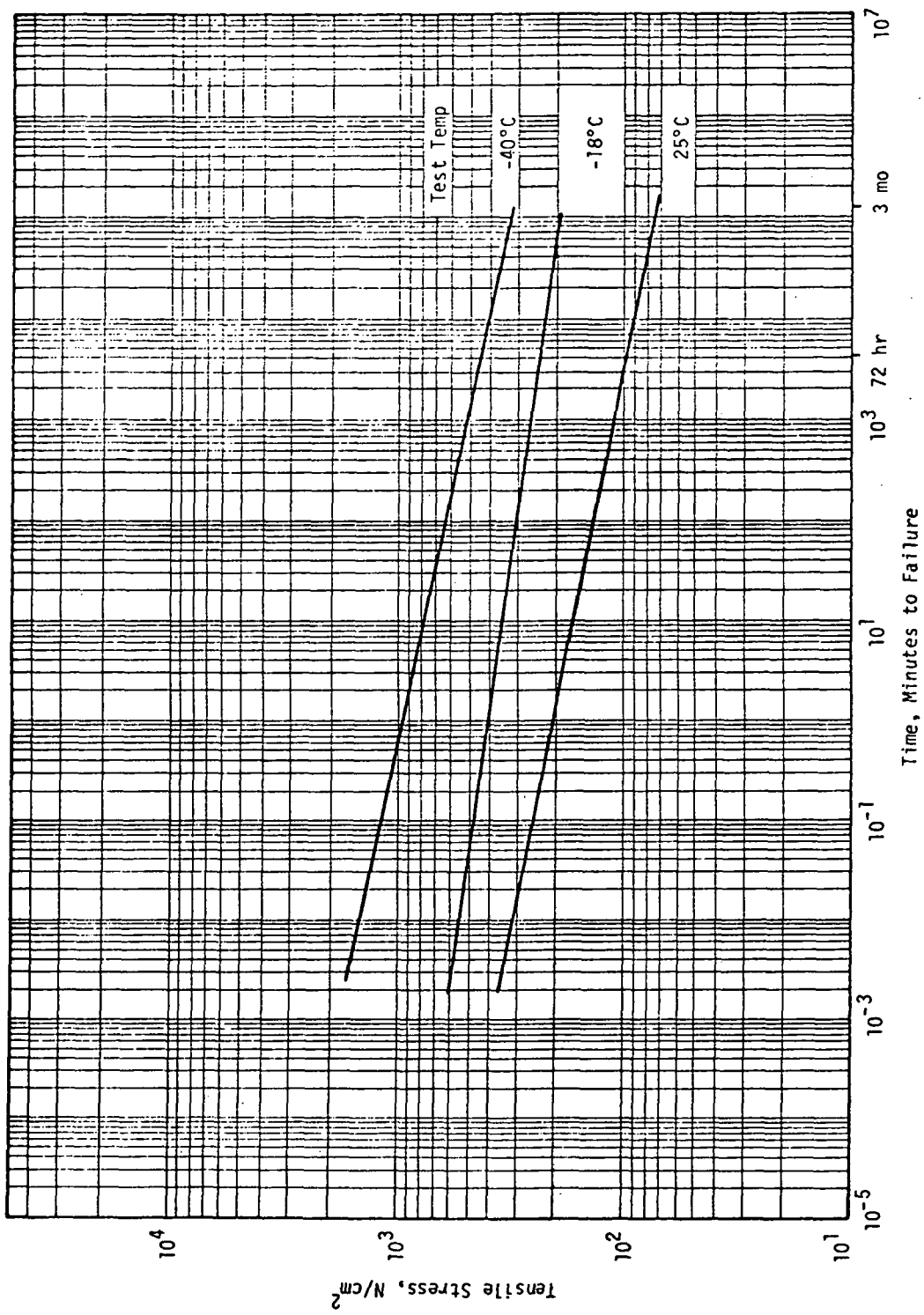
Figure 4



Time-Temperature Shift Factor for V-4030 Rubber

Figure 5





Tensile Stress vs Time to Failure for V-4030 Rubber Bonded to V-4030 Rubber with EC-2216

#### (4) Methods of Analysis

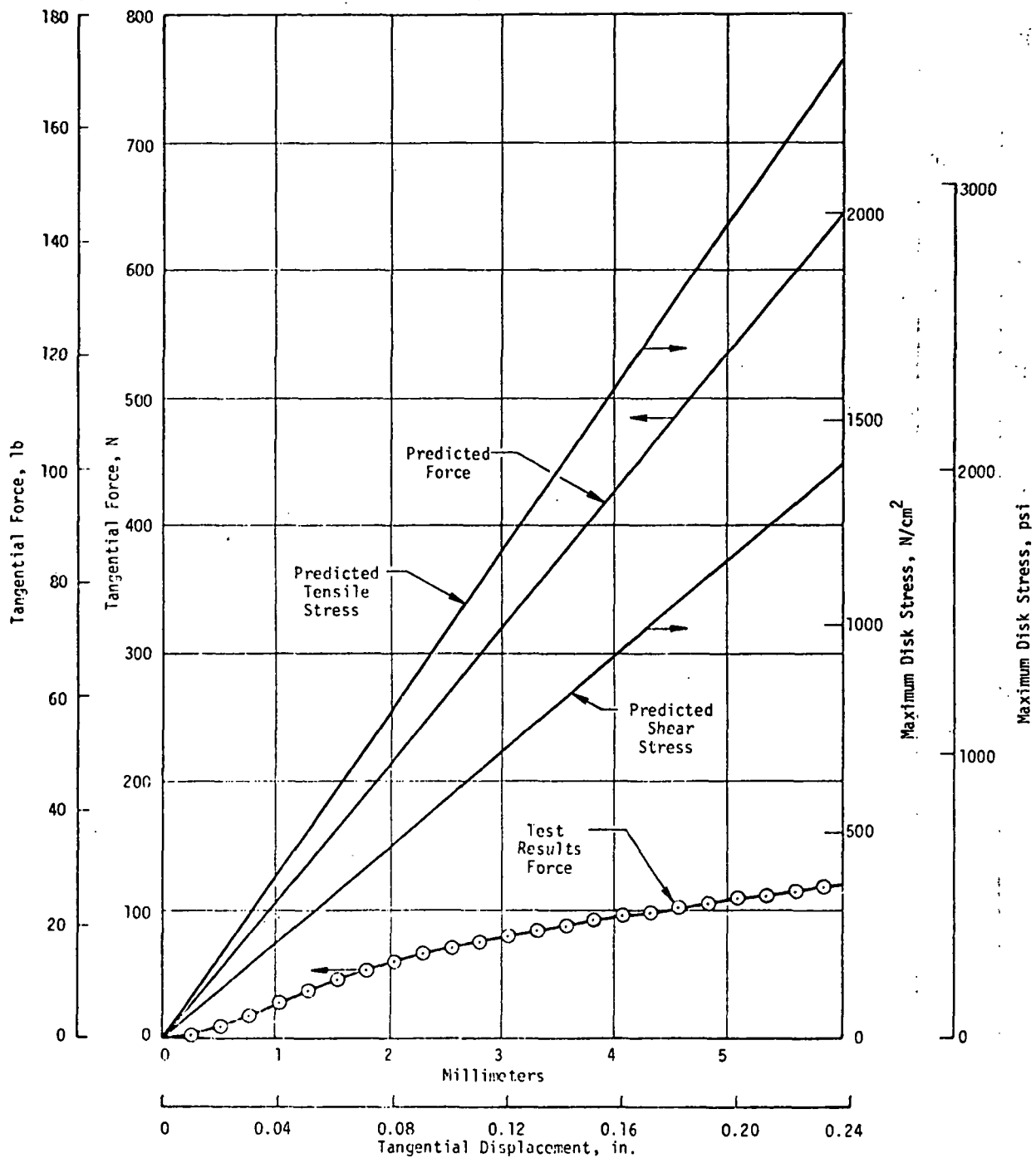
The conventional methods of analyzing propellant grains; i.e., finite element computer programs for incompressible materials in an axisymmetric or plane strain configuration (Reference 2), were used to determine the inner bore configuration at a temperature of 8°C after sterilization of the motor at a temperature of 135°C. They were also used to analyze the 15 g's axial acceleration in the event the grain "bottoms-out" against the insulation.

The analysis of the grain support disks was made using the Axisymmetric Shell Large Deflection Analysis, Computer Program No. AS8U (Reference 3), for loading normal to the surface of the disk and the NASTRAN computer program (Reference 4), for loading tangential to the surface of the disk. The NASTRAN program permits a preloading of the disk by a load applied normal to the disk surface which introduces a tension in the disk. Then applying the tangential load to the disk will increase the tension on one-half of the disk and decrease it on the other half.

#### (5) Supporting Tests

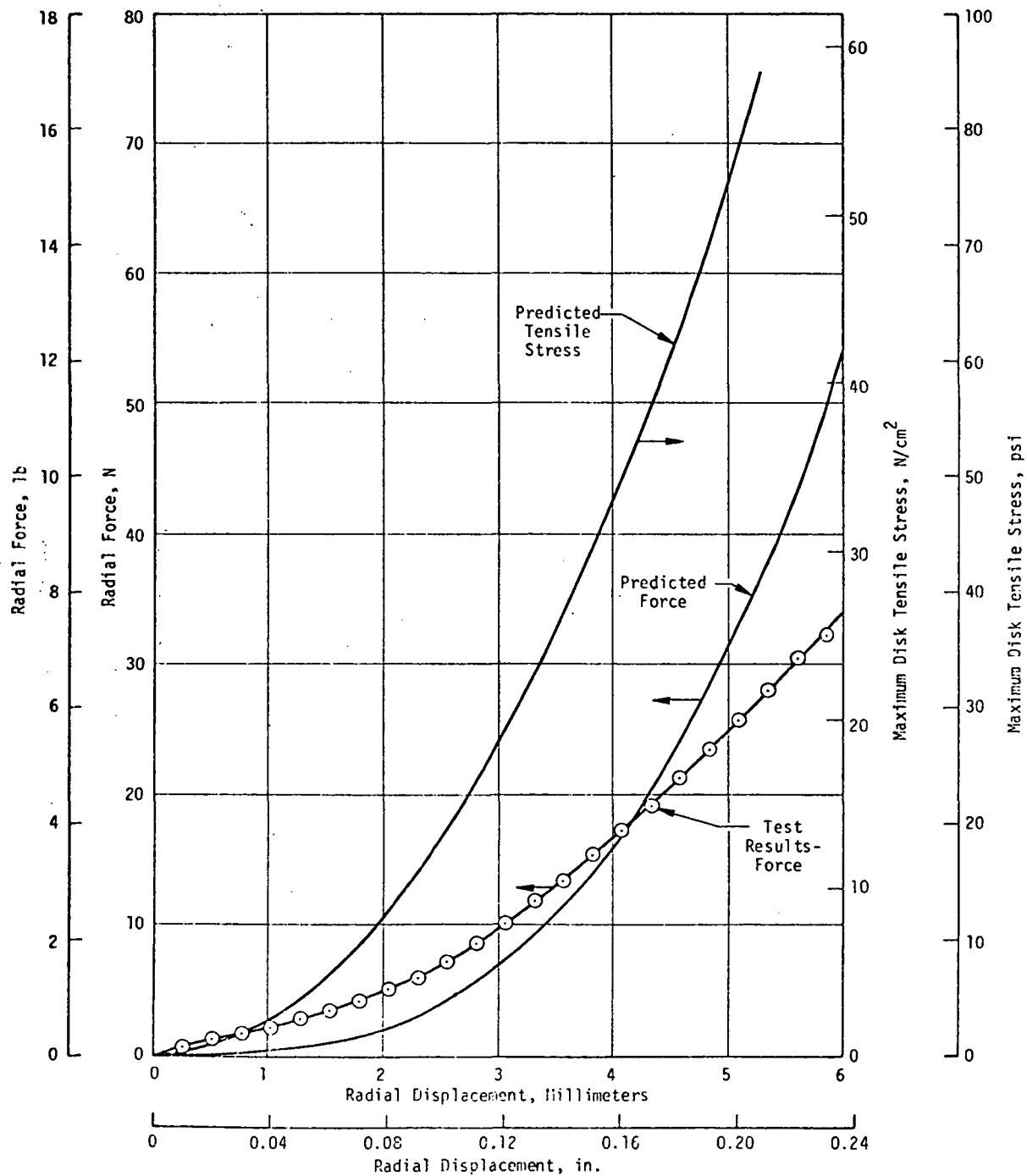
The disk model used in the structural analyses was the same as that to be used in the motor, but was fabricated in the flat condition to simplify both analysis and testing. A series of tests were performed to verify the calculated spring constants for both radial and tangential loads. A strain rate of 0.00123 m/m/sec was used in all tests.

Initial tests with non-reinforced V-4030 rubber produced three results: (a) the disks needed to be perforated to eliminate ambient pressure effects, (b) the resistance of the disks was significantly less than predicted by analysis, as shown in Figures 7 and 8; and (c) the relationship of tangential to radial resistance was essentially correct (approximately 9:1).



Comparison of Theoretical Prediction and Test Results of Disk Grain Support for Tangential Loads, V-4030 Rubber

Figure 7



Comparison of Theoretical Prediction and Test Results of Disk Grain Support for Radial Load, V-4030 Rubber

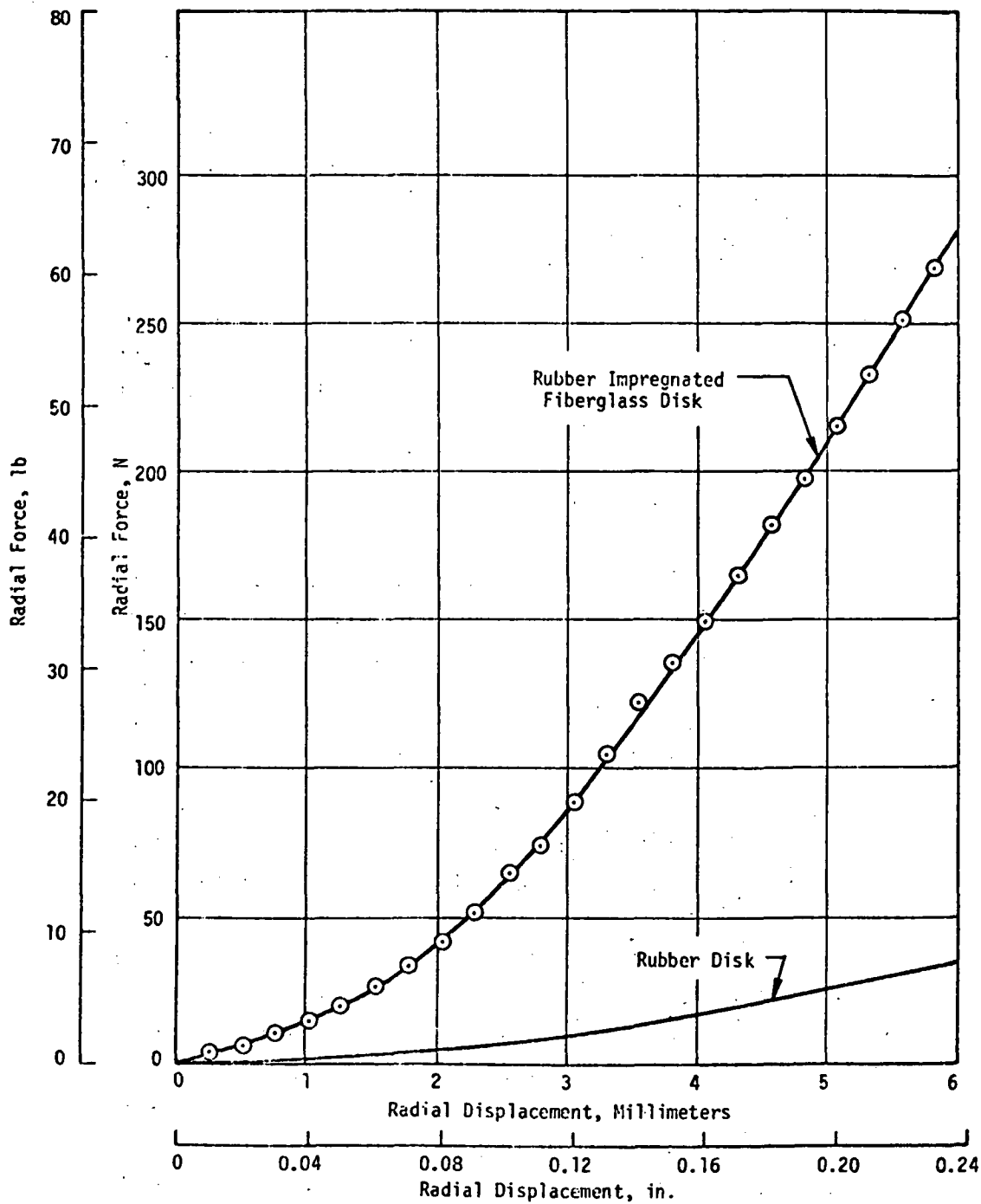
Figure 8

One of the design objectives was to restrain the grain to avoid contact with the case wall under a 15 g acceleration, since the effects of vibration were unknown. Therefore, an alternative retention disk of one ply of V-4030 rubber and one ply of 181 glass cloth was developed. The materials were compression molded in a process which assured complete penetration of the cloth by the rubber. Samples were again subjected to tangential and radial deformations.

These results indicated that both radial and tangential stiffness were increased by a factor of 10, as shown in Figures 9 and 10, thus providing all necessary stiffness against acceleration, but retaining the "soft" resistance against thermal shrinkage.

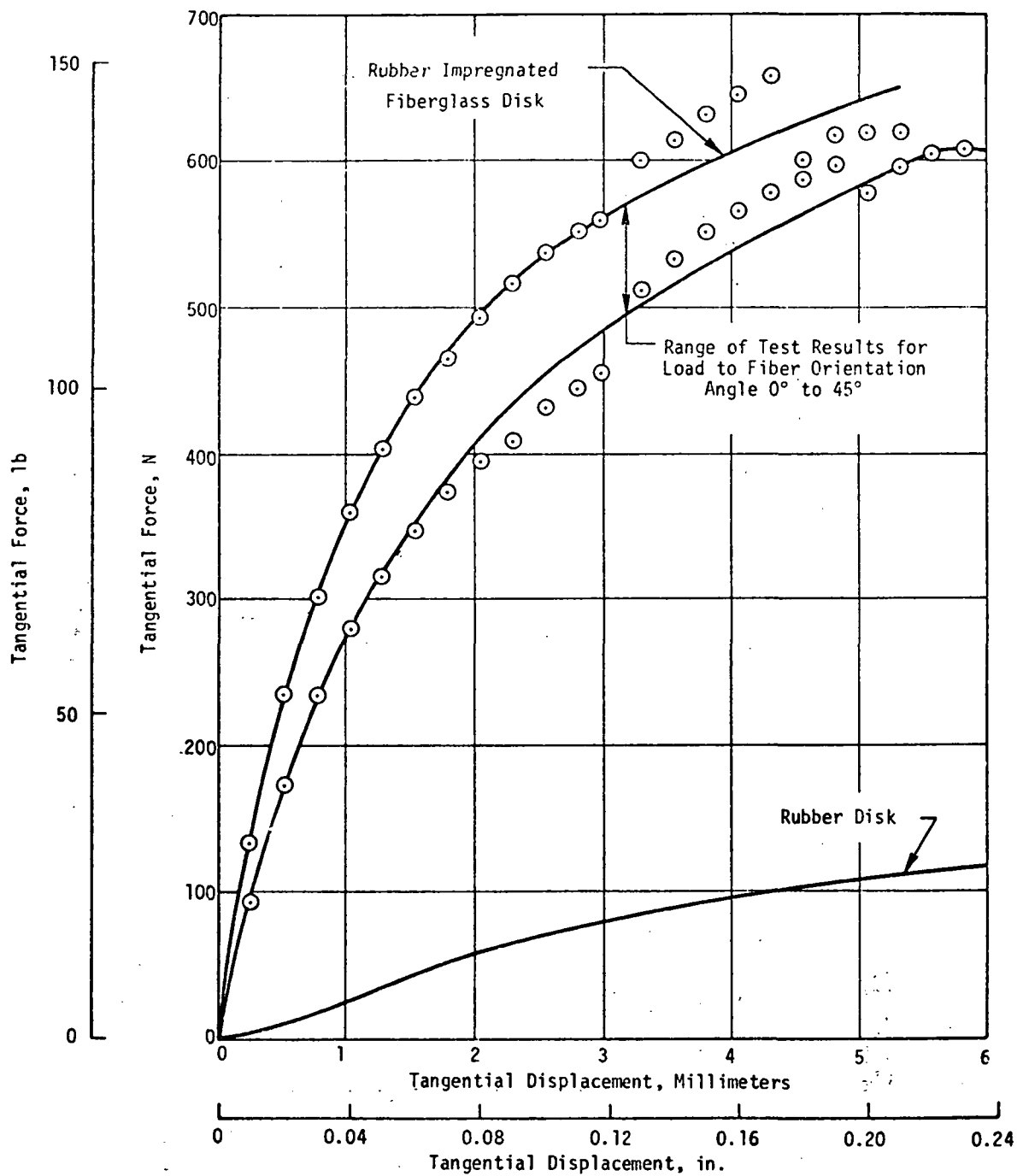
#### (6) Results of Analyses

Thermal deformation was determined using the conventional finite element computer program. The deformation as shown consists of two parts. One part, which is the largest, is attributable to heating the motor to 135°C (275°F) from the cure temperature of 60°C (140°F). The greater thermal expansion of the grain while restrained by the case results in a radially inward movement of the inner bore. The other part is that which is added (algebraically) when the motor is subsequently cooled to 8°C (40°F) conservatively assuming the grain's stress free temperature is 135°C and that the boot is completely free from the insulation and will shrink away from the case due to the thermal contraction. The thermal contraction produces a gap of 2.97 mm (0.117 in.) between the boot and insulation over all the insulation-boot interface surface. Figure 11 shows the finite-element grid of the nominal configuration, with an overlay of the grain shape at 8°C after free shrinkage from the assumed 135°C stress-free temperature. Of particular concern was the clearance with the submerged nozzle and restriction of combustion gas flow from the radial slot. Necessary alterations are indicated at Corner A (Figure 11) to reduce flow impingement on the nozzle insulation, and at Corner B to avoid interference with the nozzle and to allow venting



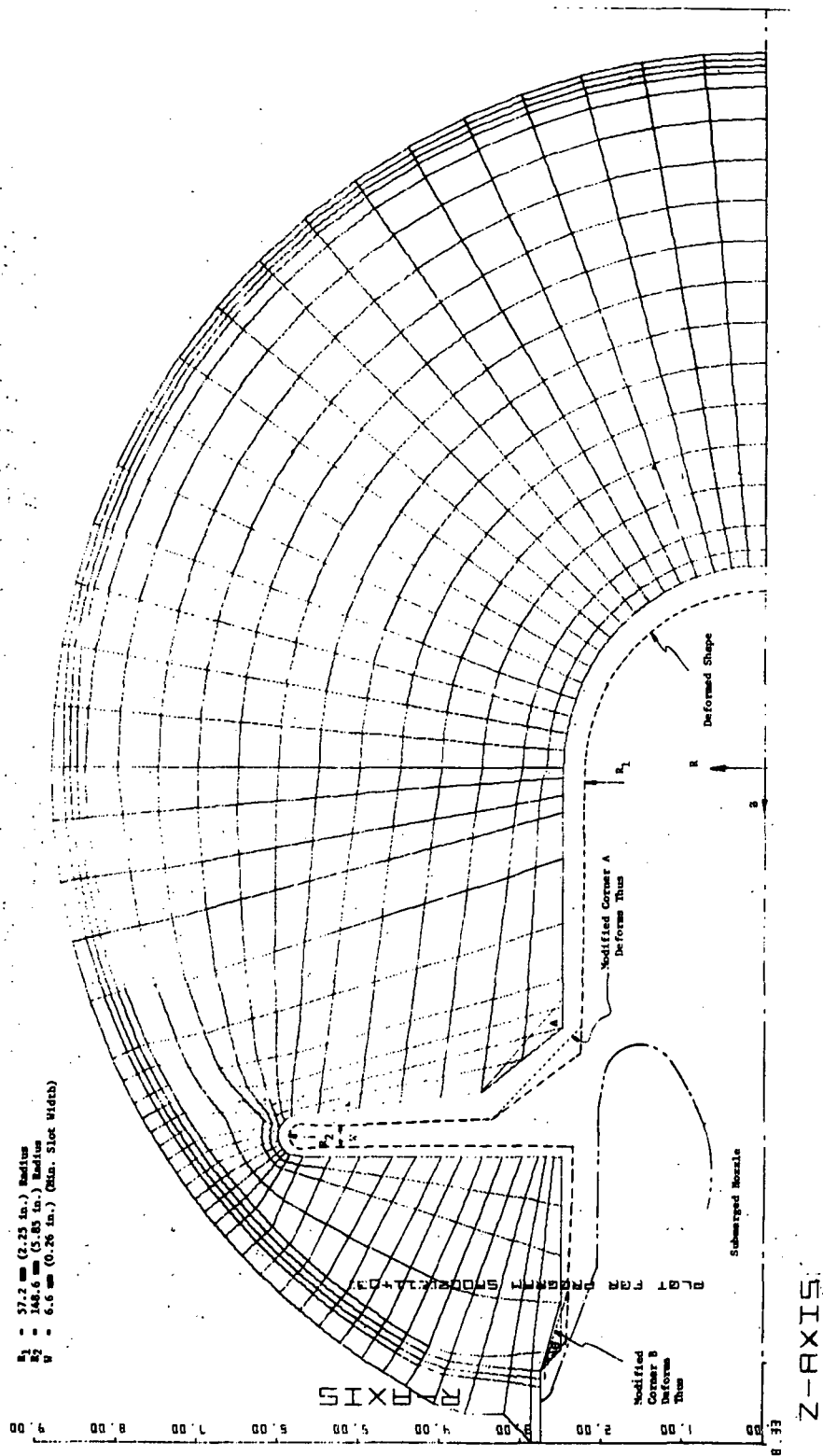
Test Results of Disk Grain Support for Radial Load

Figure 9



Test Results of Disk Grain Support for Tangential Load

Figure 10



Deformation of Motor Inner Bore at 4°C (40°F)

Figure 11

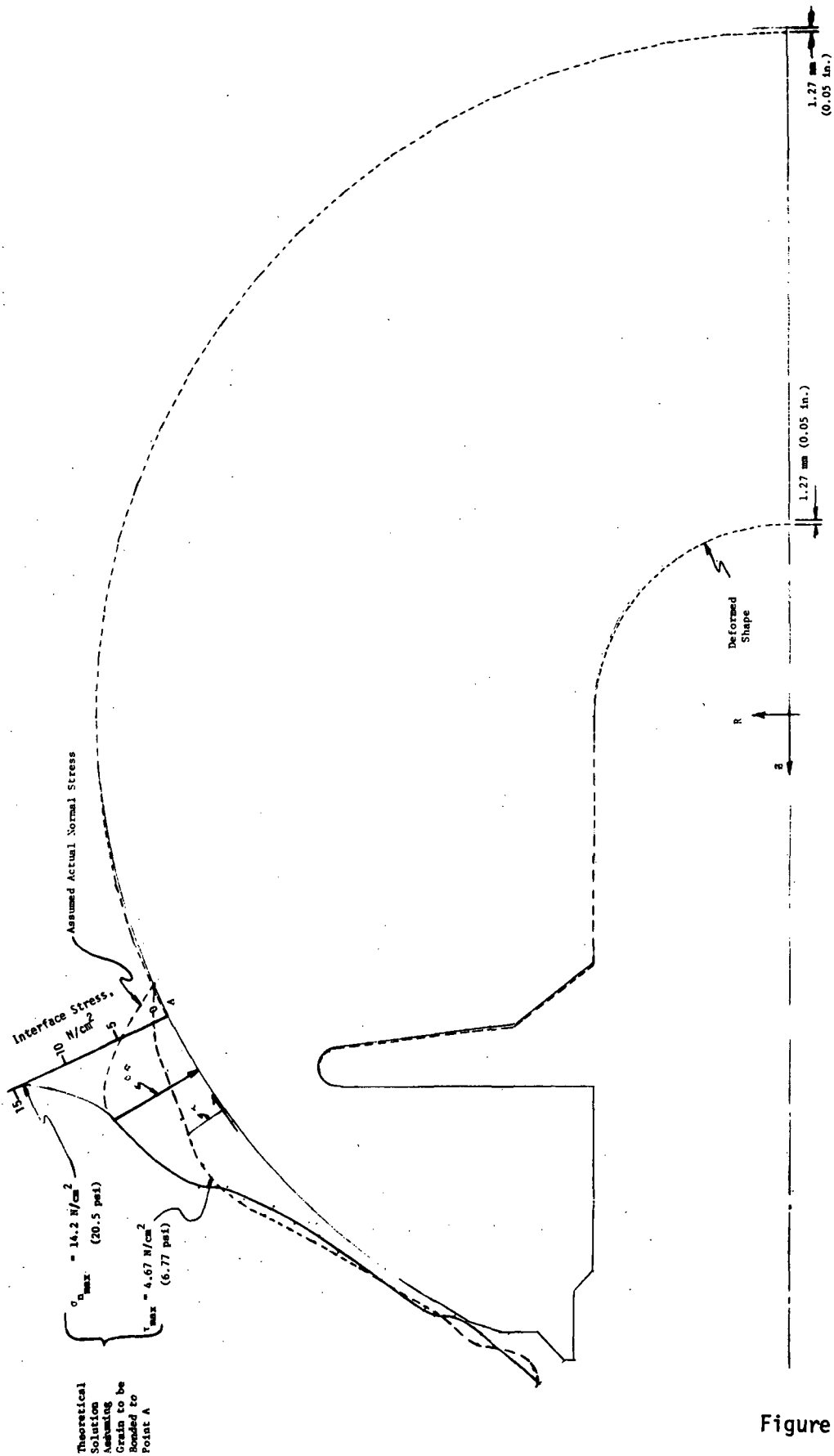


of the gap between the boot and the case insulation. The overall web thickness was predicted to be reduced by 3.3 mm.

The effect of 15 g axial acceleration on grain deformation was also investigated. To be conservative, no support was assumed from the retention system, with the grain supported in compression by the case, starting at Point A (Figure 12). The calculated maximum grain deformation is only 1.27 mm and is considered to be of insignificant magnitude.

Figures 7 and 8 show the comparison of the theoretical prediction with the test results of the load versus displacement for the circular rubber grain retention disks and the theoretical stresses in the rubber disk when subjected to radial load and tangential load, respectively. There is a discrepancy between the predictions and the results, and these discrepancies are higher at the larger displacements. This can be rationalized since the analyses performed assumed a linear stress-strain relationship of the V-4030 rubber even though the radial analysis allowed for large displacements. To obtain a better agreement between theory and test, computer programs using non-linear stress-strain properties would be required. However, as the test results confirm that (a) the grain retention system is stiffer in the tangential direction than in the radial direction, (b) that radially it can withstand a displacement of 5.95 mm (0.234 in., the maximum radial displacement when grain bottoms on the diametrically opposite surface), and (c) tangentially it can withstand a displacement of 2.97 mm (0.117 in., the maximum tangential displacement when the grain bottoms any place in the case), the circular rubber grain retention disks would work providing the "bottomed-out" propellant grain would not fail.

Figures 9 and 10 show the test results of force vs displacement for the rubber impregnated fiberglass (RIF) circular disk grain supports, the former for radial loads and the latter for tangential. These data show a ten-fold increase in stiffness over the unreinforced rubber, and allow the use of adjusted material properties to calculated interface stresses.



Interface Stresses and Inner Bore Shape of Sterilizable Motor Subjected to 15 g Axial Acceleration

Stresses calculated assuming the modulus of elasticity of RIF,  $E_{RG} = 6.9 \times 10^5 \text{ N/cm}^2$  ( $1 \times 10^6 \text{ psi}$ ) are shown in Figure 13 which summarizes the calculated stresses allowables and resulting margins of safety of RIF circular disks when subjected to the conditions listed. The design meets all objectives and has been shown to have positive margins of safety for all conditions analyzed.

From test results, the rubber disks would allow the propellant grain to "bottom-out" after two days at 1 g; whereas the RIF disks would not let the grain "bottom-out" even when the motor is subjected to 15 g's acceleration.

The grain retention system is designed to keep strains low, consequently they are not included in the summary tables. Static firing is not expected to cause any structural problems providing the volume between the grain and the insulation is adequately vented. This condition is analyzed in the subsequent section.

#### c. Grain Pressurization Study

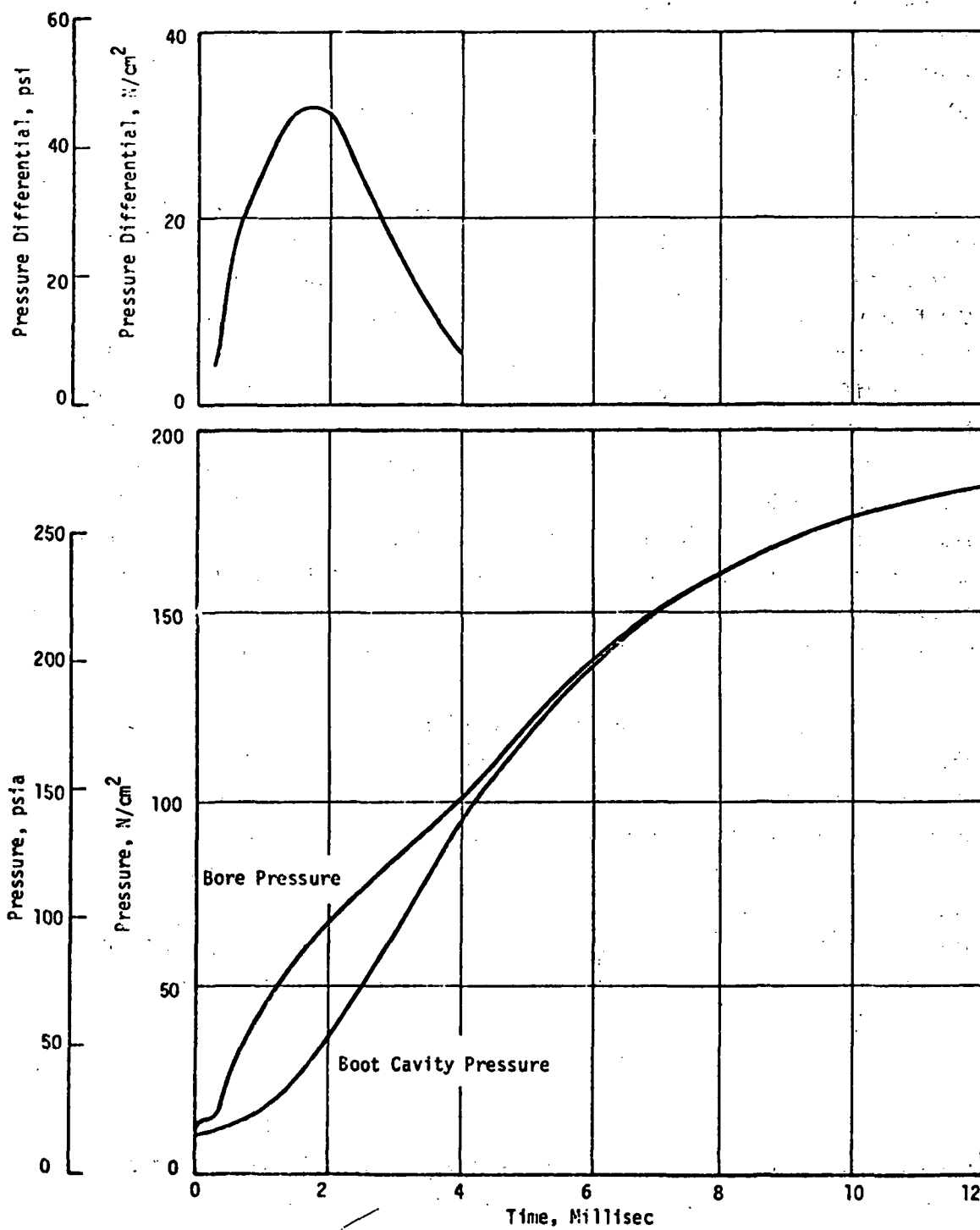
Pressurization of the cavity between the insulation and the boot resulting from grain shrinkage was potentially a problem area, since the grain could respond to ignition pressure faster than the cavity could be filled. This would force the grain toward the strained condition that would exist with a bonded grain. A preliminary ignition transient was input to a "bottle-filling" computer program, using the grain internal volume as the gas generator bottle and the cavity as the second bottle. The nozzle throat and the nominal boot gap at the aft end were input as the controlling flow areas. Figure 14 shows the two-bottle pressure transient, indicating a maximum pressure differential of  $32 \text{ N/cm}^2$  (46 psi) at 0.0017 sec. Using this data, the deflection of the cantilevered section of the grain (aft of the radial slot) was computed to be 4.32 mm (0.170 in.), or more than the nominal shrinkage gap of 2.97 mm (0.117 in.). This result, therefore, predicted a sealing of the grain cavity, resulting in a rapid deflection of the grain with attendant large bore strains. While the prediction ignored the potential forward thrust component imparted to the grain, it was considered

Condition	Interface Stresses									
	V4030 - Rubberized Cloth					Propellant - Liner				
	Tensile		Shear		M.S. (1)	Tensile		Shear		M.S. (1)
	Calc. N/cm <sup>2</sup> (psi)	Allow. N/cm <sup>2</sup> (psi)	Calc. N/cm <sup>2</sup> (psi)	Allow. N/cm <sup>2</sup> (psi)		Calc. N/cm <sup>2</sup> (psi)	Allow. N/cm <sup>2</sup> (psi)	Calc. N/cm <sup>2</sup> (psi)	Allow. N/cm <sup>2</sup> (psi)	
Storage at 8°C for 3 Months (2) E <sub>p</sub> = 965 N/cm <sup>2</sup> (1400 psi) a <sub>T</sub> = 4.84 x 10 <sup>3</sup> α <sub>p</sub> = 11 x 10 <sup>-5</sup> m/m/°C E <sub>RG</sub> = 590,000 N/cm <sup>2</sup> (1 x 10 <sup>6</sup> psi)	22.6 (32.7)	56 (81)	6.26 (9.08)	44.7 (64.7)	6.12 (8.8)	3.2 (4.7)	31 (45)	6.26 (9.08)	22.8 (33)	2.63 (3.7)
Storage at 21°C for 3 Years (2) E <sub>p</sub> = 517 N/cm <sup>2</sup> (750 psi) a <sub>T</sub> = 3.16 E <sub>RG</sub> = 690,000 N/cm <sup>2</sup> (1 x 10 <sup>6</sup> psi)	18.6 (27.0)	34 (49.3)	5.5 (8.00)	27.1 (39.3)	3.91 (5.5)	2.7 (3.9)	9.3 (13.5)	5.5 (8.00)	8.2 (11.9)	0.48 (0.68)
Boost Acceleration of 15g's for 1 Min. at 21°C E <sub>p</sub> = 1240 N/cm <sup>2</sup> (1800 psi) E <sub>RG</sub> = 690,000 N/cm <sup>2</sup> (1 x 10 <sup>6</sup> psi)	71 (103)	121 (175)	65.8 (95.3)	97 (140)	0.46 (0.66)	10.1 (14.7)	59.6 (86.4)	25.8 (37.4)	44.7 (64.8)	0.73 (1.05)

NOTES: (1) M.S. = (Allowable/Calculated) -1.

(2) Stress free temperature = 135°C (assumed)

Figure 13  
25



Motor Pressurization Using Two-Bottle Model

Figure 14

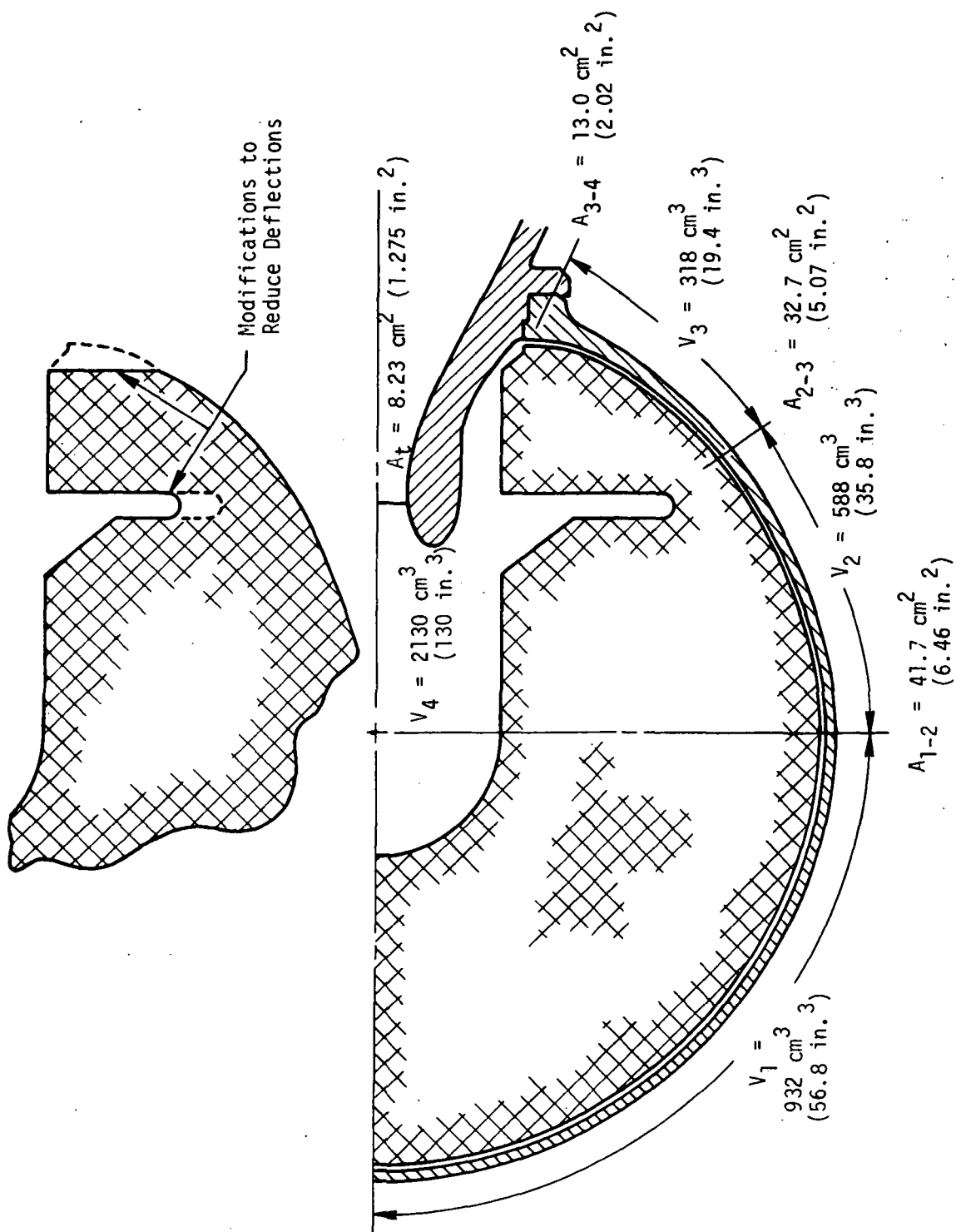
necessary to be conservative in this area, due to lack of data for the very short term propellant and rubber response characteristics. Based on the results of the analysis it was estimated that the grain would withstand the full pressurization strain, but the margin would be small.

A more accurate analysis was conducted by dividing the cavity into three bottles (Figure 15) and assuming a higher-than-ambient initial induced bore pressure. The pressure transients for the four volumes are given in Figure 16 and indicate lower peak differentials. Since the initial bore pressurization is not instantaneous, the initial differential may be ignored, so the maximum differential between the bore and the aft-most cavity is seen to be  $19 \text{ N/cm}^2$  (27 psi) at 0.0025 sec, reducing the aft grain deflection proportionately. However, the deflection of about 2.54 mm (0.100 in.) is still enough to cause concern about sealing of the cavity, although the large differential between the bore and the forward cavity, as shown in Figure 16, would probably prevent this occurrence. Again, due to uncertainties in material response characteristics, one further case was considered.

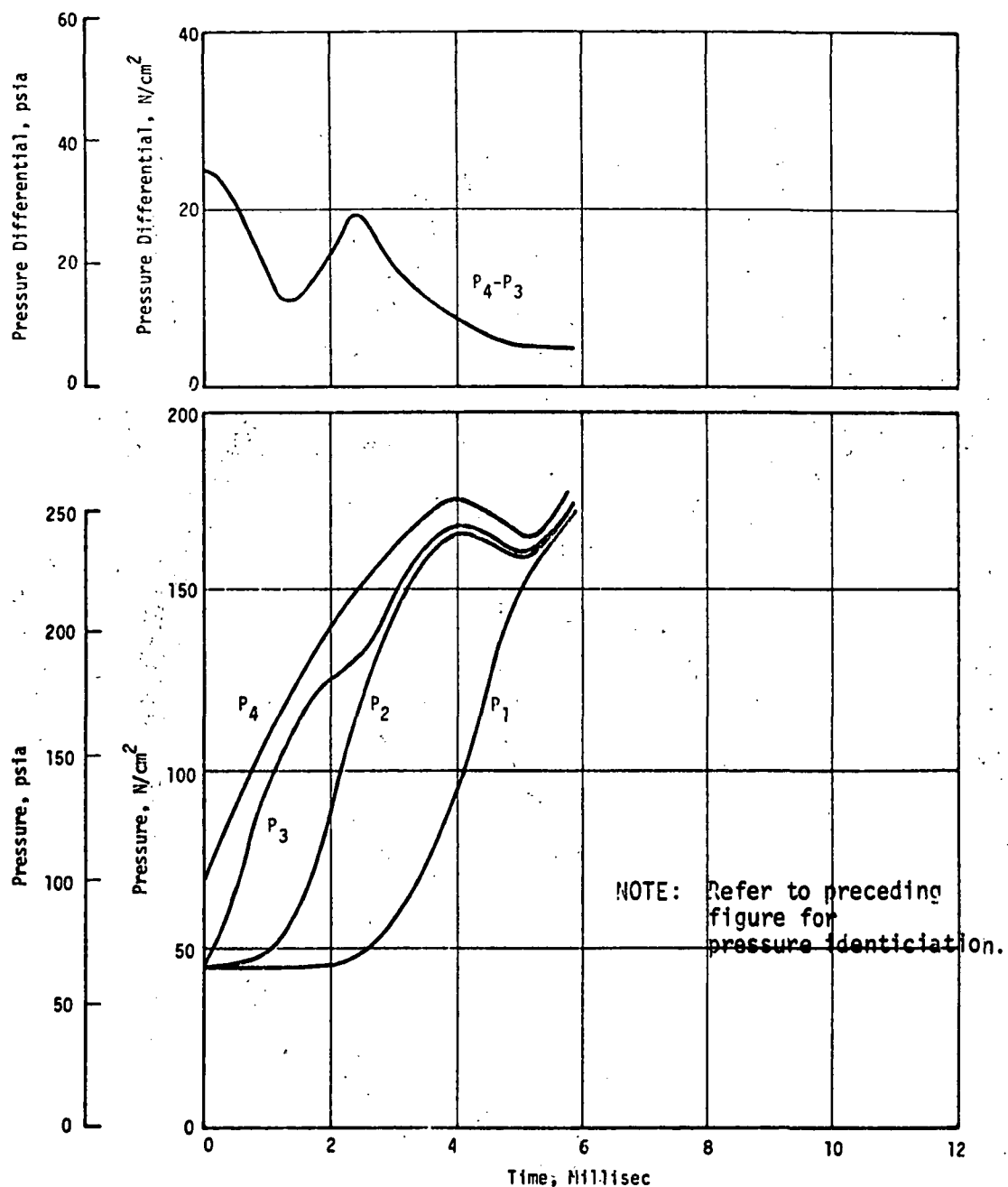
The radial slot was presumed to be reduced by 25.4 mm (1.0 in.) in radius, while part of the aft end of the grain was assumed to be fully vented to the bore volume during pressurization, such as would be the case if the boot and adjacent propellant were trimmed away radially by 39.4 mm (1.55 in.). This geometric modification would reduce the aft deflection to 0.086 mm (0.027 in.), leaving a gap of 2.30 mm (0.090 in.), which is considered to be adequate for venting. Therefore, a similar modification was incorporated in the final grain design.

#### d. Final Design

Analysis of the motor nozzle thermal and structural response as a function of burn time (Section III.B.3.c) indicated that an upper limit on burn time was needed to assure reliable nozzle operation. The preliminary design would have burned in excess of 40 sec. To comply with the recommended upper limit of 30 sec, the propellant grain was redesigned and the propellant burning rate was adjusted.



Motor Pressurization, Four-Bottle Model



Motor Pressurization Using Four-Bottle Model

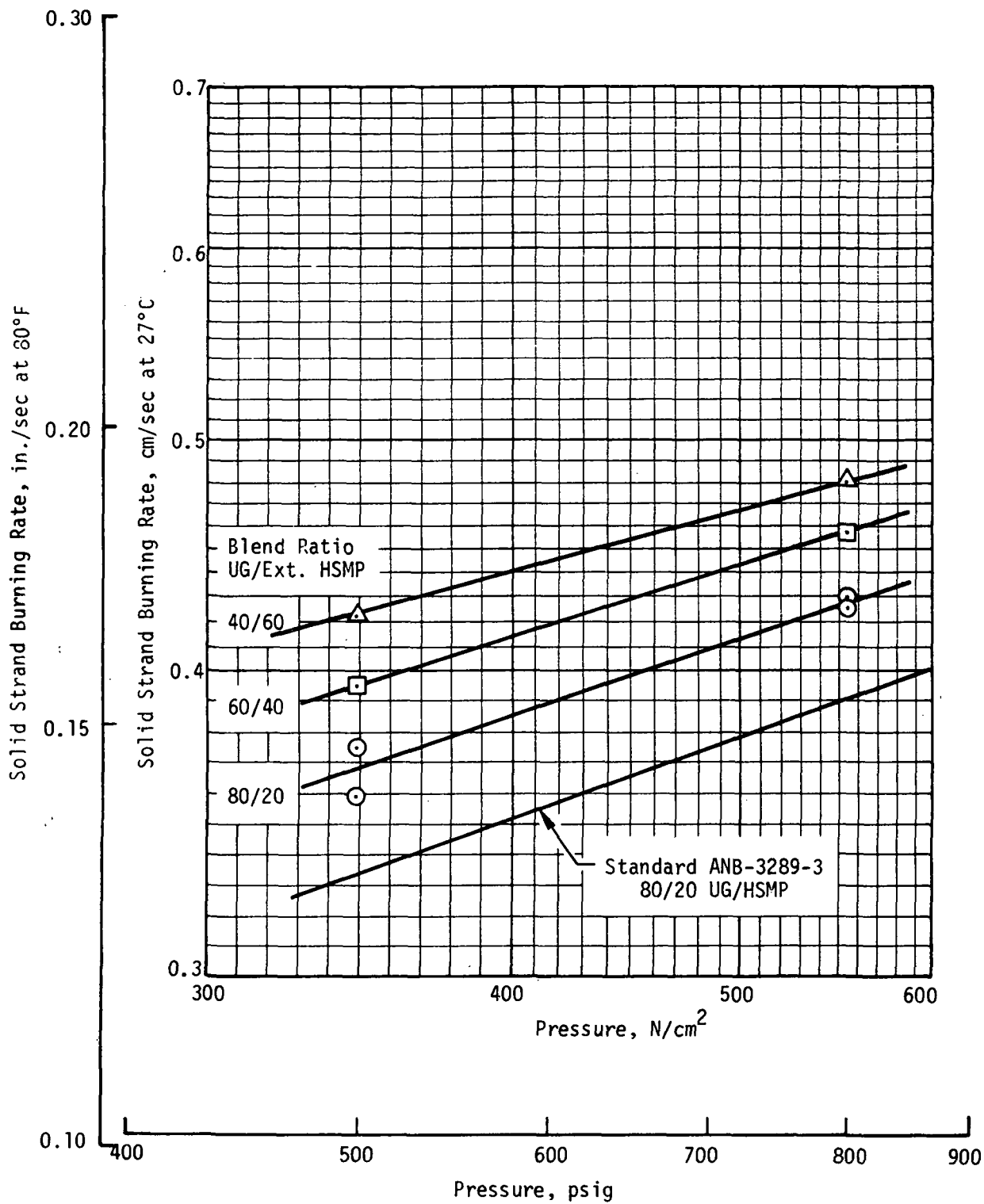


The propellant burning rate was increased from 0.33 cm/sec (0.13 in./sec) to 0.41 cm/sec (0.16 in./sec) at  $345 \text{ N/cm}^2$  (500 psig) in solid strands by modification of the oxidizer blend. Figure 17 shows the effect of blend ratios from 80/20 to 40/60 unground ( $180\mu$ )/HSMP ( $28\mu$ ) on solid strand burning rate. The HSMP fraction also was ground for an extended time period to increase the burning rate. All blends except the 40/60 were found to process satisfactorily. On this basis, the 60 Ung/40 HSMP blend with the extended HSMP was incorporated into the baseline propellant.

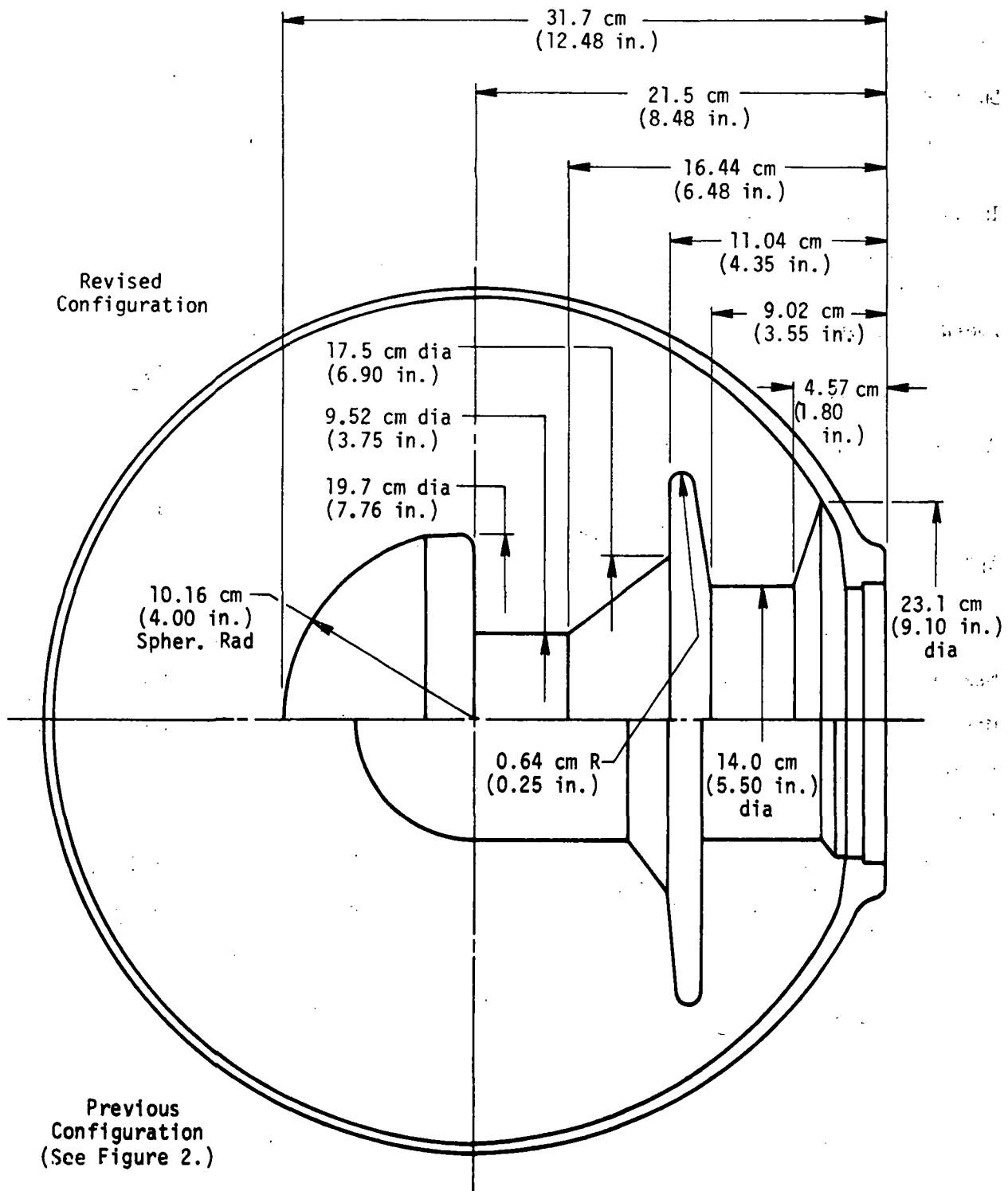
The increased burning rate was insufficient to meet the target burn time. The propellant grain was redesigned to decrease the web from 15.7 cm (6.2 in.) to 11.9 cm (4.7 in.), as shown in Figure 18. The recommendations from the grain pressurization study (Section III.B.2.c) for reducing deflections at the aft end of the grain were included in the new design. These changes resulted in a reduction of 2.2 Kg (5-lb) in propellant weight to 62.2 Kg (137-lb), approximately the same as the flightweight SVM-3. The validity of the preceding stress analyses remained intact, if somewhat conservative. Because of the larger diameter aft grain face, four of the grain retention disks would have been exposed and were therefore eliminated from the design, leaving a total of 33.

Ballistic performance was calculated for the final design using the updated ANB-3289-3 propellant ballistic properties. Parameters of interest are listed in Figure 19. The predicted chamber pressure and sea level thrust-vs-time curves are given in Figure 20. The predicted maximum pressure of  $500 \text{ N/cm}^2$  (725 psia) was well below the case proof pressure of  $648 \text{ N/cm}^2$  (939 psig). The action time of 26.7 sec meets the nozzle integrity criterion of 30 sec maximum.

Subsequently, the propellant was modified to improve sterilization durability, resulting in the ANB-3438 formulation, Figure 21. This propellant has a slightly higher solid strand burning rate, 0.43 cm/sec (0.17 in./sec) vs 0.41 cm/sec (0.16 in./sec) at  $345 \text{ N/cm}^2$  (500 psig), and exhibited a burning rate scale-up in 0.45 Kg (1-lb) motors. This resulted



Effect of Oxidizer Blend on ANB-3289-3 Burning Rate



Revised Grain Configuration

Figure 18

Duration, sec

Web Time	25.5	
Action Time (1)	26.7	

Impulse, Kg-sec (lbf-sec)

Web Time	126,537	(28448)
Action Time	126,079	(28480)

Average Thrust, Kg (lbf)

Web Time	4,759	(1070)
Action Time	4,737	(1065)

Average Pressure, N/cm<sup>2</sup> (psia)

Web Time	438	(635)
Action Time	436	(631)

Specific Impulse, N-sec/Kg (lbf-sec/lbm)

Web Time	2,025	(207.0)
Action Time	2,025	(207.0)

Max Pressure, N/cm<sup>2</sup> (psia)

500	(725)
-----	-------

Max Thrust, N (lbf)

5,526	(1242)
-------	--------

Propellant Weight, Kg (lbm)

62.5	(137.7)
------	---------

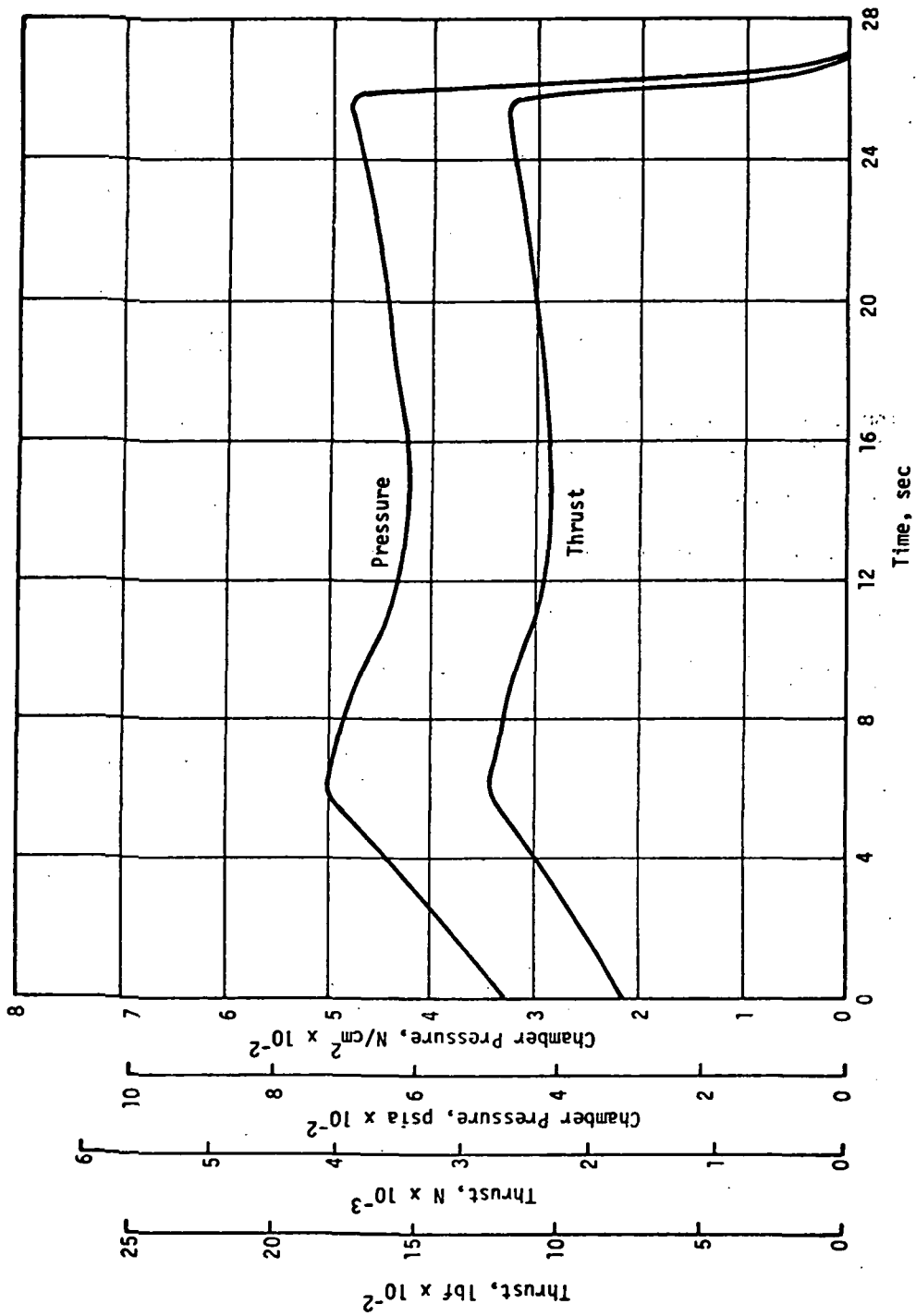
Propellant Data

Density, gm/cm <sup>3</sup> (lb/cu in.)	1.717	(0.062)
I <sub>std</sub> , N-sec/Kg (lbf-sec/lbm)	2360	(241.1)
Burn Rate, cm/sec (in./sec) at 345 N/cm <sup>2</sup> (500 psia)	0.406	(0.160)
Exponent, n		0.32

(1) Action Time = 10% p<sub>max</sub>.

Predicted Ballistic Performance Summary - Sterilizable Motor  
at 21°C (70°F), Sea Level

Figure 19



Sterilization Motor Predicted Ballistic Performance at 21°C (70°F), Sea Level

Figure 20

	<u>Wt %</u>
Ammonium Perchlorate Oxidizer (stabilized with 0.5 wt% FC-169)	66.00
Aluminum Powder	18.00
Silicone Oil Processing Aid	0.005
FC-217	0.15
Binder (composed of Telagen-S prepolymer, GTRO and IPDI)	15.845
	<hr/>
Total	100.000

Formulation of ANB-3438 Propellant

Figure 21

in a calculated increase in motor operating pressure, as shown in Figure 22. Since the full-scale motors were committed at that time, the propellant oxidizer blend and grain configuration could not be modified. Therefore, the nozzle throat diameter was increased from 3.24 cm (1.274 in.) to 3.31 cm (1.342 in.), as described in the subsequent section, resulting in the compromise pressure profile, also shown in Figure 23. Further investigation of the burning rates in small motors revealed significant differences in burning rates between batches, which was not evident in the solid strand data. These data, along with the final motor predictions, are described in Section III.E. of this report.

### 3. Hardware Components

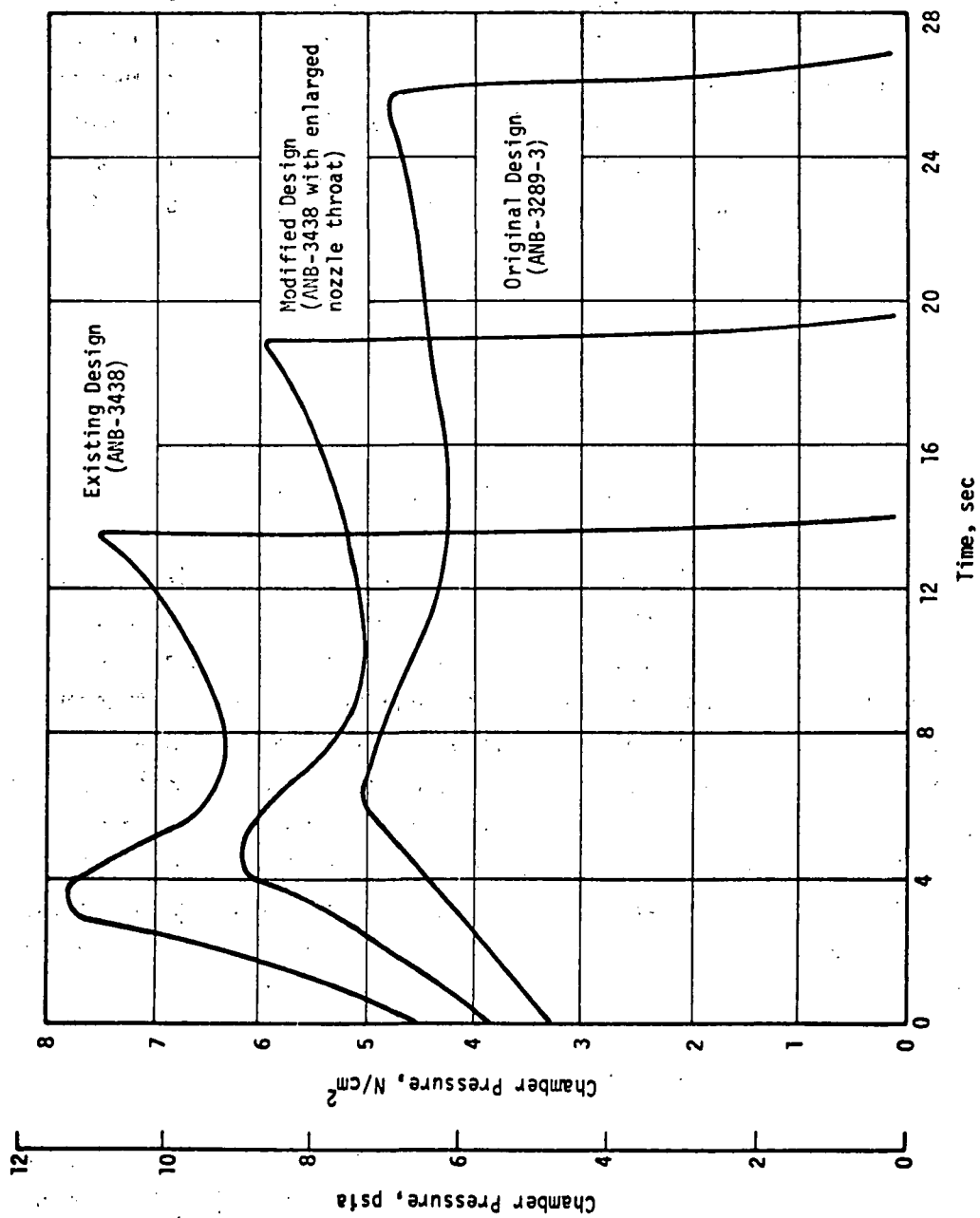
#### a. Nozzle

##### (1) Preliminary Structural Analysis

When used with the preliminary grain design, the low range of propellant burn rates available with ANB-3289-3 propellant tended to extend the motor burn time beyond that for which the existing SVM-3 nozzle was designed and developed. Consequently, a limited structural analysis of critical components was undertaken to select a burn time at which adequate structural margins could be expected. Using the heat transfer analysis results, the throat insert, throat backup and nozzle housing were analyzed as summarized below. A motor chamber pressure time integral of  $11,720 \text{ N-sec/cm}^2$  (17,000 psi-sec) was used with a factor of 1.2 to determine MEOP as a function of total burn time. The nozzle cross-section is shown in Figure 23.

##### (a) Throat Insert

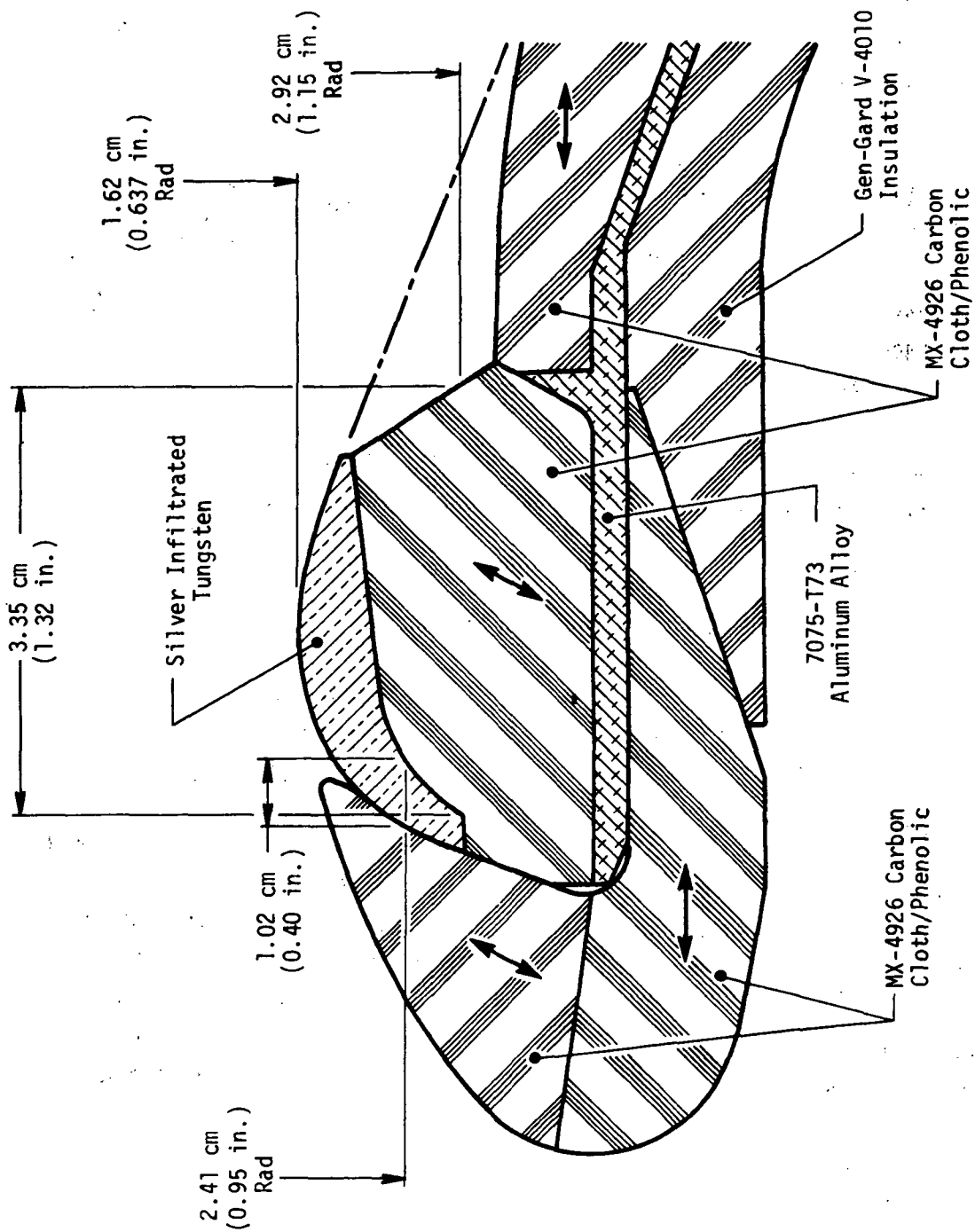
The silver-infiltrated tungsten throat insert was checked for shear stress at selected values of burn time (and MEOP) and compared to the material shear strength at the temperature calculated for



Ballistic Performance Comparison

Figure 22





SVM-3 Nozzle Cross Section

Figure 23

each time. In each case the margin of safety was large (approximately 2 to 5) at burn times up to 52 sec. The radial stress in the throat insert and interface pressure between the insert and backup were calculated for firing times of 20, 32 and 48 sec.

Total Burn Time, sec	Interface Pressure N/cm <sup>2</sup> (psi)	Radial Compressive Stress N/cm <sup>2</sup> (psi)	Insert Temperature, °C (°F)	Backup Temperatures, °C (°F)		
				Max.	Min.	Avg.
20	3690(5201)	12,770(18,500)	2750(4984)	2218(4025)	29(85)	582(1080)
32	3490(5053)	12,900(18,676)	2783(5047)	2372(4304)	60(140)	738(1360)
48	3394(4917)	12,910(18,710)	2800(5075)	2460(4459)	120(249)	900(1652)

Since the stresses do not vary significantly with total burn time, and the nozzle performs satisfactorily at the nominal burn time of 23 sec, this condition was considered structurally adequate.

#### (b) Throat Backup

The throat backup is MX-4926 carbon cloth phenolic molded at 60 degrees with respect to the nozzle centerline. The condition of axial ejection was considered, using the interface with the throat insert leading edge as the shear plane radius. Shear stress was calculated as a function of total burn time. Interlaminar shear strength properties were used to be conservative. Curves of maximum shear stress and average shear strength as a function of total burn time were plotted. The curves crossed at a time of 48 sec, where the margin of safety is zero. Very large margins (greater than 3.0) exist at burn times less than 40 sec. Shear planes at larger radii would be expected to give roughly similar results because the higher strengths at the lower temperatures offset the greater ejection area.

### (c) Nozzle Housing

The 7075-T73 aluminum alloy nozzle housing was checked for buckling at one total burn time, 36 sec. Thermal calculations indicated that a rapid decline in material properties could be expected after this time. For the computed temperature gradient, a critical pressure differential of  $1131 \text{ N/cm}^2$  (1639 psi) was calculated. For the MEOP of  $392 \text{ N/cm}^2$  (567 psia) corresponding to the burn time, the differential pressure to the throat is  $170 \text{ N/cm}^2$  (247 psi), leaving a large margin of safety. The hoop compressive stress was also checked, indicating a margin of safety of nearly 3.0.

### (d) Conclusions

For the structural conditions considered, it was apparent that significant margins of safety could be reasonably expected for burn times in the neighborhood of 40 sec, however, it was recognized that (1) the analysis was somewhat cursory in order to remain within the program scope, (2) high temperature material properties tend to be somewhat uncertain, and (3) no factors of safety were built into the calculations. Therefore, it was concluded that the target motor burn time should be approximately 30 sec to provide assurance of nozzle integrity, which was not a component of interest within the program objectives. As indicated in the preceding section, this burn time was accomplished by increasing the propellant burn rate and reducing the grain web.

### (2) Analysis of Nozzle Throat Modification

The enlargement of the nozzle throat to accommodate the increased burning rate for the ANB-3438 propellant formulation was described previously. Because of the increase in throat diameter, the structural analysis of the nozzle was repeated to assure that the nozzle reliability would not be significantly impaired. Conditions of compressive hoop stress at ignition, shear stress from ejection at burnout, and compressive

hoop stress at web burnout for the rework silver-infiltrated tungsten throat insert were evaluated at the higher MEOP and the new material thicknesses. Although there were reductions in the margins of safety, as shown in Figure 24, no significant degradation of reliability could be shown.

## b. Insulation System

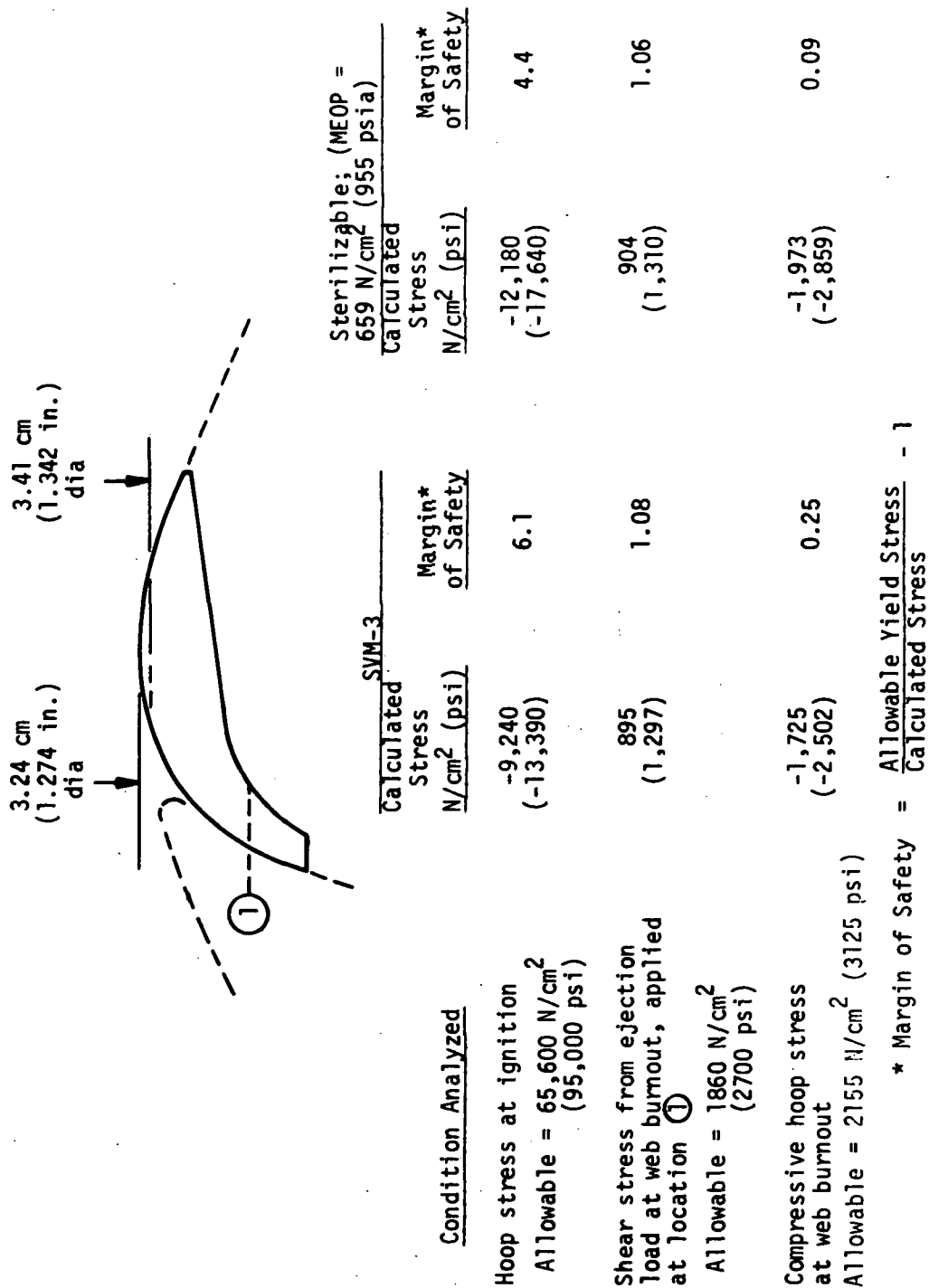
### (1) Design Description

The chamber insulation system was comprised of four types of components: (a) the aft insulator, (b) the forward insulator, (c) the 33 grain retention disks, and (d) the boot, including a casting extension. These details are defined on Aerojet Drawings 1150643 and 1150642, given in Figures 25 and 26.

The aft insulator is the same as that used on the SVM-3, except for the substitution of GenGard V-4030 for V-4010, a similar ethylene-propylene rubber (V-4030 is compatible with isocyanate curing systems and had been qualified previously for the sterilizable motor). The grain design (and insulation exposure) was sufficiently similar to the SVM-3 to justify the same design thicknesses.

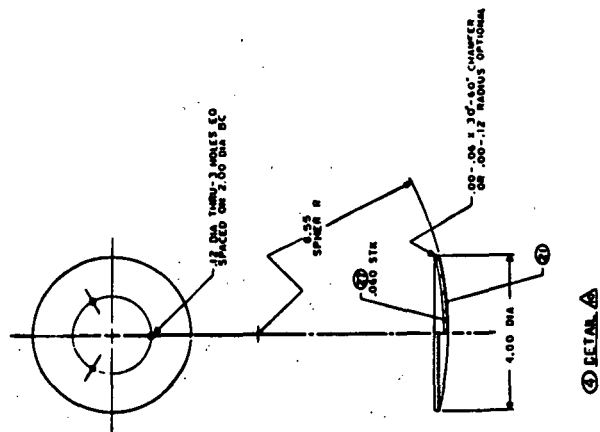
The forward insulator, a single 2 mm (0.080 in.) layer of V-4030, was used in place of the SVM-3 sprayable PBAN insulation/liner. Although the case would not normally be exposed to the flame when using the full boot of this design, this was added to assure a safe, conservative design.

The 33 retention disks were molded to the spherical shape from a single layer of 1.5 mm (0.060 in.) V-4030 rubber and a single layer of 181 glass cloth, approximately 0.25 mm (0.010 in.) thick. Three venting holes of 3.2 mm (0.125 in.) dia were used to assure proper functioning of the retention elements.



Nozzle Throat Structural Analysis

Figure 24

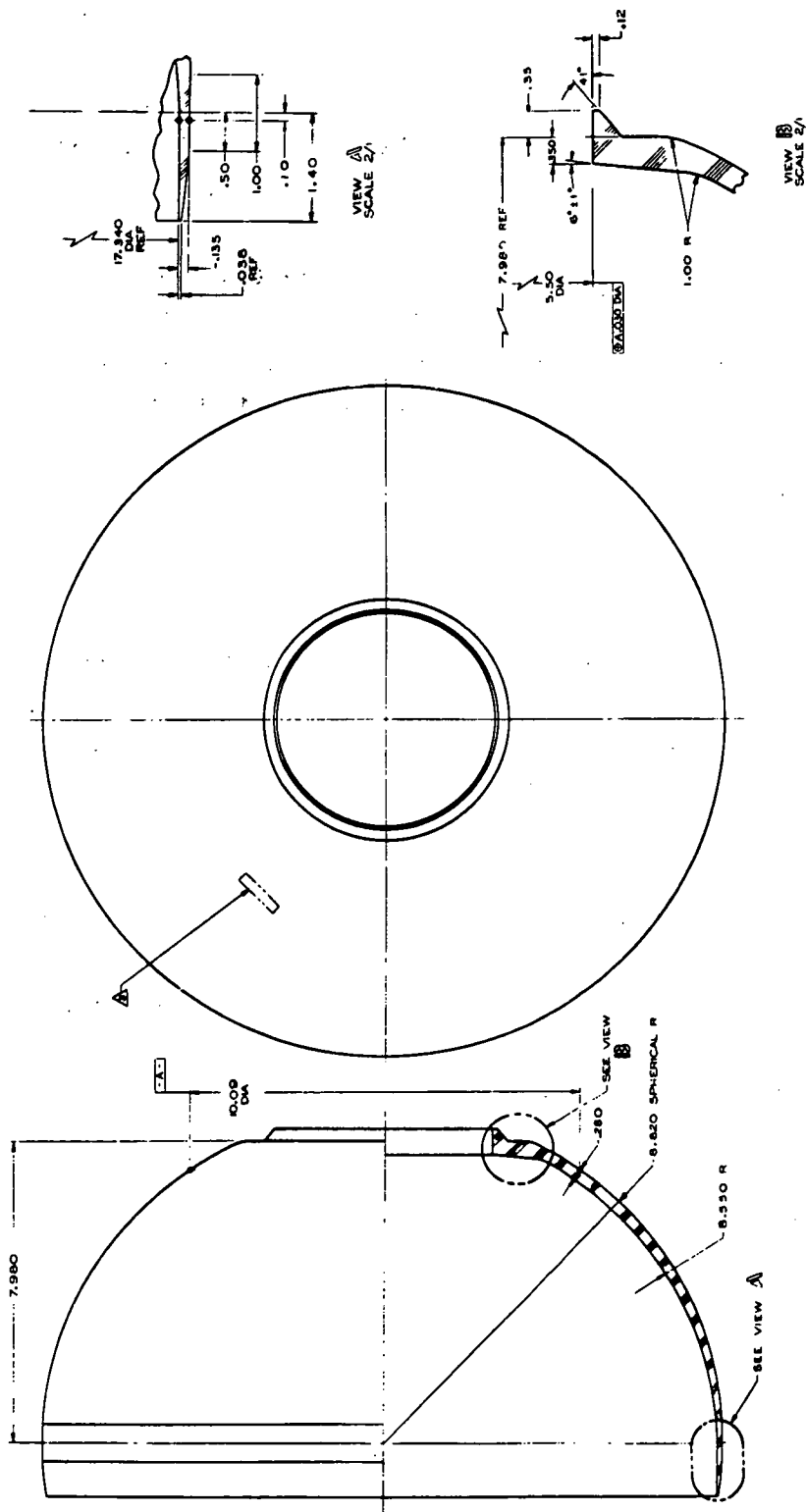


Grain Retention Disk, Aerojet Drawing 1150643 (Sheet 1 of 3)









V-4030 Rubber Insulator Construction, Aerojet Drawing 1150642

Figure 26

The boot is a layer of 2 mm (0.080 in.) V-4030 rubber molded to the insulation contour with a short cylindrical collar added at the nozzle closure opening to provide retention during propellant casting. The boot was trimmed back to the grain contour after grain machining.

The Chemlok 205 primer and Chemlok 234 rubber adhesive system was specified for bonding the forward and aft insulators to the case. Chemlok 304 epoxy adhesive was specified for bonding the retention disks to the insulation and the boot. Teflon tape was used to prevent bonding of surfaces other than those required by the design and were left in place.

## (2) Adhesive Evaluation

Previous studies to qualify the sterilizable motor system used Chemlok 220 rubber adhesive for bonding the V-4030 rubber to the case wall. In this program, this was replaced with Chemlok 234 adhesive, because of the unavailability of Chemlok 220 and extensive experience in bonding ethylene-propylene rubbers with Chemlok 234. In addition, the assembly of the insulation components necessitated the use of secondary bonds. Therefore, both rubber adhesives and two epoxy adhesives, Chemlok 304 and EC2216, were used in preparing bond samples which were subjected to the complete motor processing and sterilization cycles. The sterilized samples were then fabricated into double-plate tensile test specimens which were constructed as follows: Steel plate/Epon-901 adhesive/V-4030: test adhesive: V-4030/SD-886/propellant/Epon-923 adhesive/steel plate. Samples so constructed were tested before and after the six heat sterilization cycles with the results shown below:

### Effect of Heat Sterilization on Adhesive/Insulation Bond Strength

<u>Adhesive/ Insulation</u>	<u>Before Heat Sterilization</u>		<u>After Heat Sterilization</u>	
	<u>N/cm<sup>2</sup> (psi)</u>	<u>Break Type</u>	<u>N/cm<sup>2</sup> (psi)</u>	<u>Break Type</u>
EC2216/V-4030	88 (128)	Propellant-metal plate glue line	79 (114)	Propellant-metal plate glue line
Chemlok-234/V-4030	101 (147)	"	72 (104)	"
Chemlok-220/V-4030	115 (167)	"	84 (122)	"
Chemlok-304/V-4030	77 (112)	50% CP, 50% CPI*	118 (171)	"
Chemlok-234/V-4030- glass cloth laminate	98 (142)	Propellant-metal plate glue line		

\* CP - Cohesive failure in propellant.  
CPI - Cohesive in propellant at interface.

All failure modes but one occurred adjacent to the glue line between propellant and the steel plate used to prepare the test specimen, indicating that the bond strength of the test specimen was at least higher than 72 N/cm<sup>2</sup> (104 psi) and in some cases greater than 117 N/cm<sup>2</sup> (170 psi) after sterilization. The lone exception to the failure mode described above was the unsterilized specimen containing the Chemlok-304 rubber-to-rubber adhesive in which the failure partially occurred in the propellant/liner bond area. However, when subjected to the six heat sterilization cycles, this system failed in the glue line between the propellant and plate at a tensile strength of 118 N/cm<sup>2</sup> (171 psi). In view of these test data it was concluded that no adverse effects on liner/propellant bond occurs during heat sterilization, and that each of the rubber-to-rubber adhesives would be acceptable for use in the full-scale motor.

### (3) Effects of Sterilization on Performance

The V-4030 insulation was qualified on the basis of compatibility with the liner and propellant and on its relative resistance to mechanical properties degradation during heat sterilization. However, ablation performance after sterilization had not previously been assessed.

Tubular sections of V-4030 insulation were molded for testing with the 5 cm (2 in.) dia end-burning LITE motor. Two specimens were sterilized at 135°C (six 53 hr cycles) and two specimens were used for a control. The motors were fired at 435 N/cm<sup>2</sup> (500 psia) for 20 sec. The sterilized insulation had loss rates of 0.086 and 0.091 mm/sec (0.0034 and 0.0036 in./sec) as compared with 0.074 and 0.076 mm/sec (0.0024 and 0.0030 in./sec) for the control. Although the rates are up to 20% higher in the sterilized condition, the motor insulation is designed to a factor of 2.0, so that no design changes were required.

c. Ignition System

(1) Arc-Image Ignitability Tests

Arc-Image ignition tests were conducted with sterilized ANB-3289-3 propellant to provide data for the igniter design. Parameters obtained in the tests are the Threshold Ignition Energy Requirement (TIER) and the low pressure ignition limit, p\*.

The TIER is defined as the radiant energy required to ignite the propellant with a 0.50 probability as determined by observation of consecutive fire and no-fire tests which have the narrowest possible range of exposure time allowed by the ignition characteristics of the propellant.

The low pressure ignition limit, p\*, is defined as the pressure below which sustained ignition and combustion does not occur. This is done at a constant, arbitrarily chosen exposure time of 300 milliseconds, which was selected because it exceeds the action time of most igniters by a wide margin and yet is short enough to preclude total ablation of the sample in the event of a no-fire test. The ignitability measurements were made at a flux level ( $\dot{Q}$ ) of 80 cal/cm<sup>2</sup>-sec and pressure levels of 1, 3, 5 and 7 atmospheres of nitrogen gas.

Data are presented in Figures 27 and 28. The TIER is the product of the flux ( $\dot{Q}$ ) and exposure time at a given pressure because the radiant energy pulse-time profile is essentially a square wave. The  $p^*$  value of  $8.6 \text{ N/cm}^2$  (12.5 psia) indicates the propellant possesses no unusual ignitability problems. The pressure asymptote of ANB-3289-3 propellant is in excess of 7 atmospheres.

## (2) Design Description

The SVM-3 ignition system consists of two external igniters mounted to the aft head of the chamber, requiring access to the grain surface for the igniter gases. However, the sterilizable grain configuration would interfere with this function. Therefore, the igniter housings were used only for chamber pressure measurement. A paper wrapped igniter was designed and built for direct placement in the grain bore after motor assembly. The pyrotechnics consisted of the following components:

Main Charge	50 gm Boron Potassium Nitrate, Type 2L Pellets
Initiator Charge	2 gm Alclo/Boron Barium Chromate
Squib	Hercules Mark 2

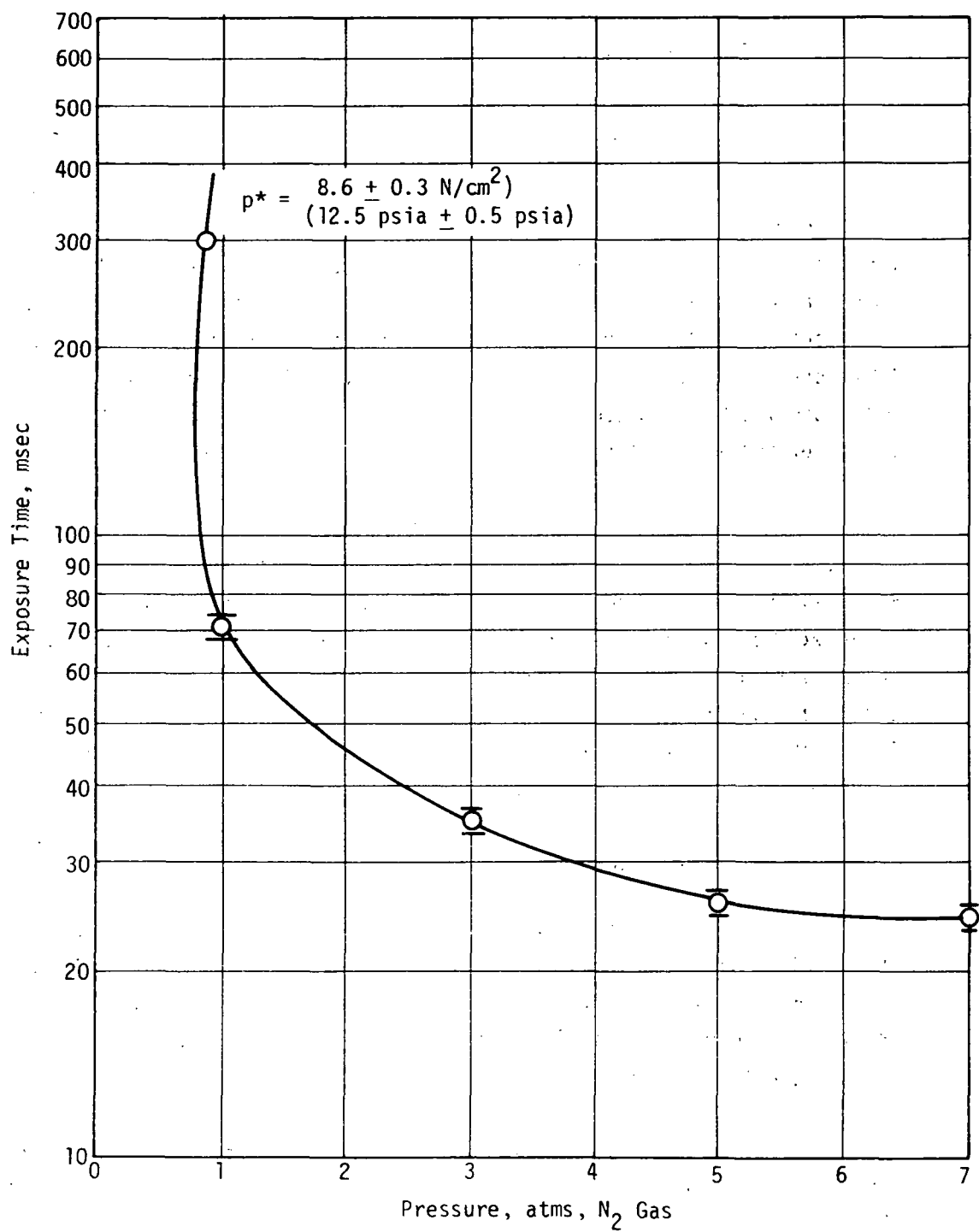
$$\dot{Q} = 80 \text{ Cal/cm}^2 - \text{sec}$$

<u>TIER, cal/cm<sup>2</sup></u>	<u>Exposure Time, msec</u>	<u>Press. Atms</u>
5.8	72 ± 2	1
2.9	36 ± 1	3
2.1	26 ± 1	5
2.0	24.5 ± 0.5	7

$$p^* = \begin{matrix} 8.6 \pm 0.3 \text{ N/cm}^2 \\ (12.5 \pm 0.5 \text{ psia}) \end{matrix}$$

Arc Image Furnace Data - ANB-3289-3 Propellant

Figure 27



Ignition Time as a Function of Pressure, ANB-3289-3 Propellant, Batch 72-92

Figure 28

## C. PROPELLANT VERIFICATION

### 1. Raw Materials

The requirements for the successful heat sterilization of solid propellant grains had been established prior to the start of this program. The most important requirements were shown to be (1) thermally stable ammonium perchlorate, (2) the use of stable, non-volatile polymeric components and (3) adequate propellant strength. During this program, therefore, principal emphasis was placed on verification of propellant properties, bonding properties and confirmation of the sterilizability of the propellant in larger grains.

During the course of work in this program, it was found that the propellant strength was marginal. This led to the development of a new propellant formulation (ANB-3438) which incorporated the use of a new oxidizer binder bonding agent, crosslinker and curing agent. This new propellant formulation showed improved mechanical behavior, met all sterilization criteria and exhibited improved processing characteristics. This latter formulation was successfully sterilized and test fired in the SVM-3 motor.

#### a. Telagen-S Prepolymer

The Telagen-S, a secondary hydroxyl-terminated saturated polybutadiene prepolymer used on this program was obtained in three lots. Each lot was purified by vacuum stripping at 200°C in a wiped film still. Pertinent analyses for each of the three lots used before and after stripping are shown in Figure 29.

Most of the 400 to 4000-g size batch mixes were prepared with prepolymer from Lot 316AM-5 and 316 AM-11/12. The first 91 Kg (200 lb) mix (batch 72-92) prepared for casting the first large diameter



		Analyses			
		<u>Fe</u>	<u>Si</u>	<u>H<sub>2</sub>O</u>	<u>Eq. Wt.</u>
Lot 316AM-5					
	Unstripped	8	150	-	1120
	Stripped	<2 ppm	4 ppm	-	1036
Lot 316AM-11/12					
	Unstripped	<2 ppm	<3 ppm	0.031	1212
	Stripped	<1 ppm	50 ppm*	0.003	1089
Lot 3HPL-228/239					
	Unstripped	<10 ppm	<10 ppm	0.009	1139
	Stripped	-	-	-	1148

---

\*Possible contamination from silicone grease used on ground glass fittings.

#### Analyses of Telagen-S HTPB Prepolymers

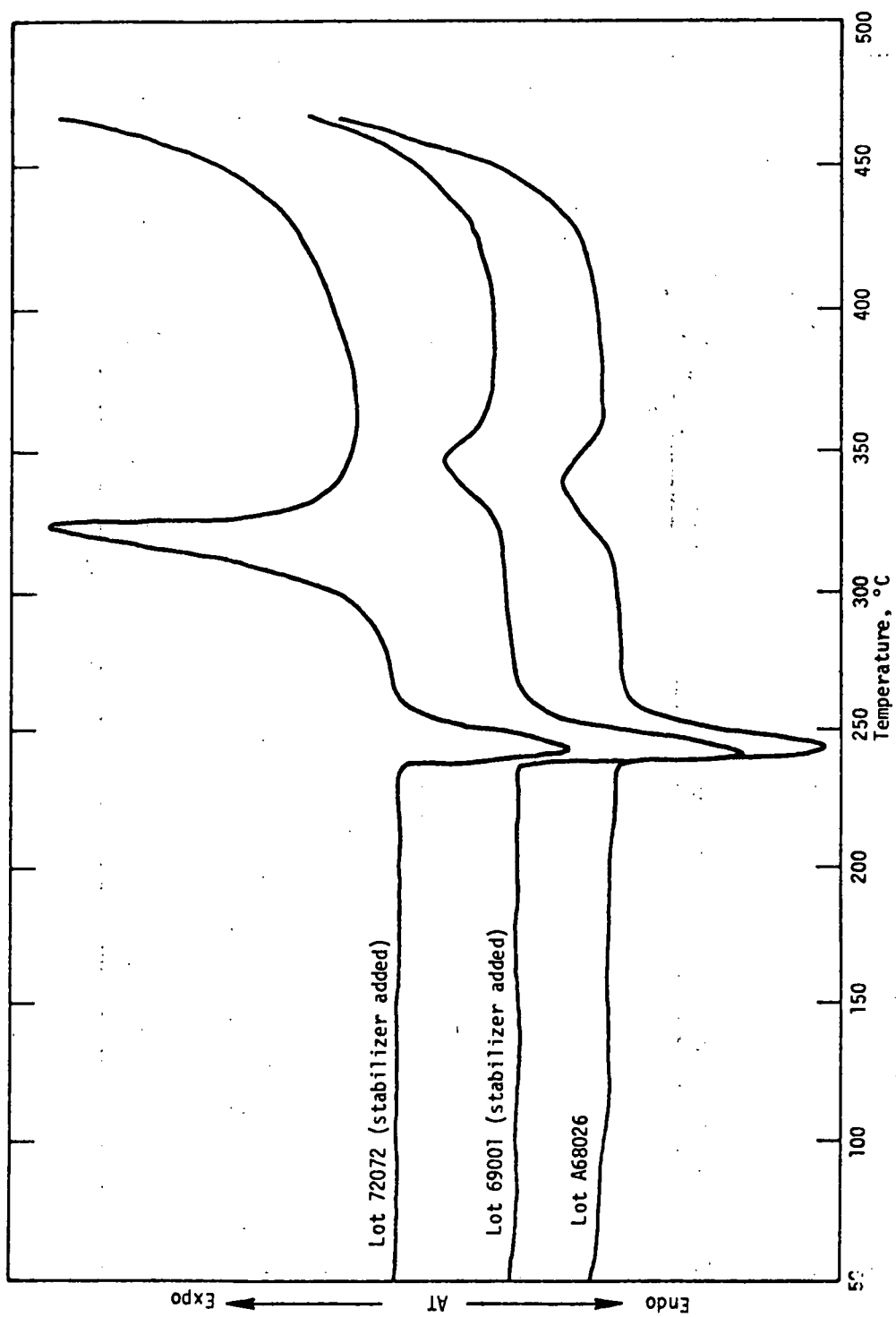
Figure 29

grains also utilized Lot 316 AM-11/12. Subsequent large-diameter grains and the demonstration motors were made from a master blend of Telagen-S prepared from Lots 316 AM-5, 316 AM-11/12 and 3HPL-228/239. The equivalent weight of this master blend of material was 1067.

b. Oxidizer

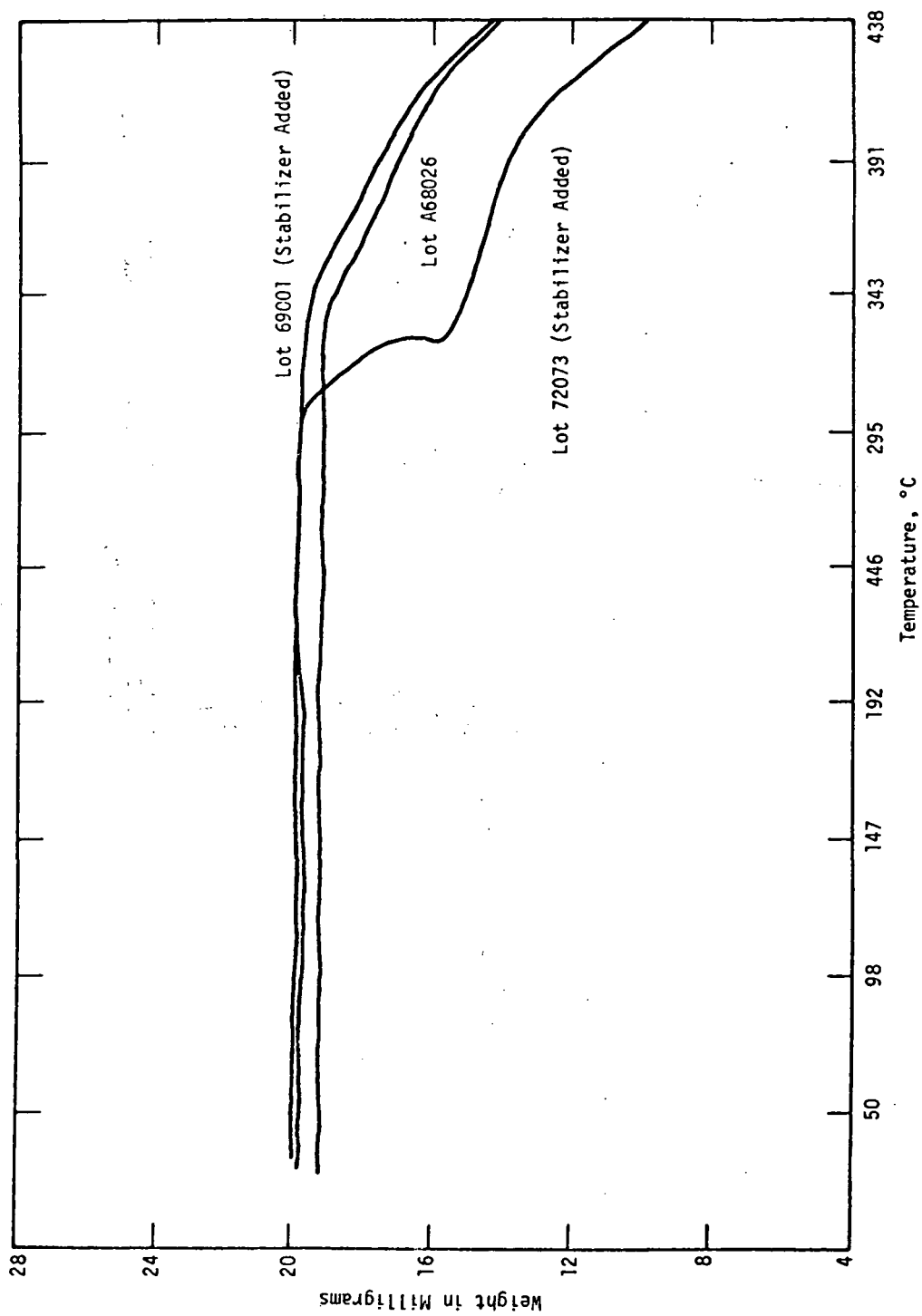
Approximately 454 Kg (1000 lbs) of recrystallized stabilized ammonium perchlorate, prepared by the Pacific Engineering Company of Nevada (PEPCON), had been kept in stock for one year before the inception of the program. This material, Lot PE 69001, had been stored in sealed drums with desiccant bags and possessed a very low moisture level (surface moisture - 0.004 wt%, total moisture 0.010 wt%). This material met all the requirements for the AP and was later used during the demonstration phase.

A second lot of similar size (Lot No. 72073) was also prepared at PEPCON during the course of the present program. The procedure employed to apply the stabilizer and dry the oxidizer was essentially identical for both AP lots. However, analysis of samples taken from Lot No. 72073 revealed that the concentration of stabilizing agent (FC-169) ranged between 0.065 to 0.076 wt%, whereas 0.5 wt% had been added. Differential thermal analysis (DTA) and thermogravimetric analysis (TGA) of Lot No. 72073 were obtained and are shown in Figures 30 and 31. Also included are the analyses of Lot No. 69001 (recrystallized and stabilized) and Lot No. A68026, a high-purity lot of oxidizer which does not contain a stabilizing agent. The analyses of Lots 69001 and A68026 show these materials to be similar in behavior and quite heat stable. The exotherm peaks in the DTA's are considerably reduced in height and occur at a higher temperature than that obtained with Lot No. 72073 (Figure 30). Similar behavior for these three lots of material is shown in the TGA's (Figure 31). The weight losses of Lots 69001 and A68026 are insignificant until 343°C, whereas Lot No. 73026



DTA Thermograms of PEPCON Produced Oxidizer

Figure 30



TGA Thermograms of PEPCON Produced Oxidizer

Figure 31

material was 20% decomposed at this temperature. As a result of these analyses, Lot No. 72073 was considered unsatisfactory for use in sterilizable propellants and deleted from the program.

To confirm the acceptability of Lot A68026 AP, 0.5 wt% of FC-169 stabilizer was added to the oxidizer and a 3500 gram batch of ANB-3289-3 propellant was made. The effects of heat sterilization on this propellant batch as well as those prepared with other oxidizer lots shown below were determined in 7.6 cm x 7.6 cm x 12.7 cm (3 in. x 3 in. x 5 in.) blocks subjected to six 53 hr cycles at 135°F).

<u>Batch Number</u>	<u>Oxidizer Lot</u>	<u>Treatment</u>
10GP-8074	72073	Stabilized with FC-169
10GP-7949	A68026 (high purity)	Untreated
10GP-7950	69001	Stabilized with FC-169

The propellant containing Lot 72073 oxidizer was badly fissured after the heat sterilization. The performance of the propellant prepared with Lot A68026 oxidizer was similar to that of the control (Lot 69001) in that the two propellants both survived heat sterilization but experienced some loss in propellant modulus (Figure 32). The propellant containing Lot A68026 oxidizer which was dry-surface treated with the stabilizer, FC-169, had several fine-line cracks after sterilization. This indicates that the addition of the stabilizer to the dry oxidizer is not a satisfactory method of applying FC-169. This stabilizer is somewhat basic, and, during the dry application to the oxidizer surface, ammonia gas was evolved. The oxidizer treated in this manner was stored for several hours at 57°C (135°F) to remove the ammonia prior to batch mixing. However, it is apparent that the evolution of ammonia continued during heat sterilization and caused the cracks to form. Since this lot of oxidizer (A68026) performed adequately without added stabilizer, it was later used, untreated, in the preparation of the large grains for heat sterilization tests.

Mechanical Properties at 25°C (77°F)											
Batch No.	Oxidizer Lot	Surface Treatment	Before Sterilization				After Sterilization (1)				
			$\sigma_m$ , N/cm <sup>2</sup> (psi)	$\epsilon_m$ , %	$\epsilon_b$ , %	$E^0$ , N/cm <sup>2</sup> (psi)	$\sigma_m$ , N/cm <sup>2</sup> (psi)	$\epsilon_m$ , %	$\epsilon_b$ , %	$E^0$ , N/cm <sup>2</sup> (psi)	
10GP-7950	69001	FC-169 (control)	87 (126)	7	7	1688 (2446)	92 (133)	12	19	1210 (1753)	
10GP-7949	A68026 (high purity)	Untreated	75 (109)	7	8	1434 (2078)	71 (103)	9	22	1172 (1698)	
10GP-8074	72073(2)	FC-169	93 (135)	10	12	1339 (1940)	Decomposed				
10GP-8079	A68026 (high purity)	FC-169 (added dry to dry AP surface)	104 (150)	13	18	1172 (1698)	Fine line cracks observed in the propellant				

(1) Six 53-hour cycles at 135°C (275°F)

(2) Most recent lot from PEPCON

Effect of Heat Sterilization on Mechanical Properties of  
ANB-3289-3 Propellant Prepared with Different Oxidizer Lots

Figure 32

c. Curing Agents

Two diisocyanates were used as curing agents for the heat sterilizable propellants, one was dimethyl diisocyanate (DDI) obtained from General Mills, Inc., the other was isophorone diisocyanate (IPDI), purchased from Thorson Chemical Corp. DDI was used as the curative in ANB-3289-3 propellant and IPDI in ANB-3438. The diisocyanate assays of the two lots of each material used in this program are shown in the following table.

DIISOCYANATE ASSAYS OF CURING AGENTS

DDI				IPDI			
Lot No.	Meq/g NCO		Assay, %	Lot No.	Meq/g NCO		Assay, %
	Theo	Analysis			Theo	Analysis	
8L-306	3.27	3.10	95	1975-126	8.93	8.91	99.8
2A-10445	3.27	3.31	101	VCP-07	8.93	8.94	100.1

d. Crosslinking Agents

The crosslinker, trimethylolpropane (TMP), used as the crosslinker in ANB-3289-3 propellant, is a very pure commercial product obtained from Celanese Corp. It is used in several propellants at the Aerojet Solid Propulsion Company. A sufficient amount remained (Lot 6710) from the previous contract to prepare all the ANB-3289-3 required in the present program. Glyceryl triricinoleate (GTRO) from the Baker Castor Oil Co. was used as the crosslinker in ANB-3838 propellant. Again, a single lot sufficed for the program. The analysis of this material, Lot 692, was as follows:

ANALYSIS OF GTRO CROSSLINKER

Eq wt: 344 (350 nominal)  
H<sub>2</sub>O: 0.026 wt%  
Acid No.: 0.52

e. Aluminum Powder

H-5 aluminum (spheroidal, particle size 8-14 $\mu$ ) purchased from Valley Metallurgical Company was used in all propellant formulations.

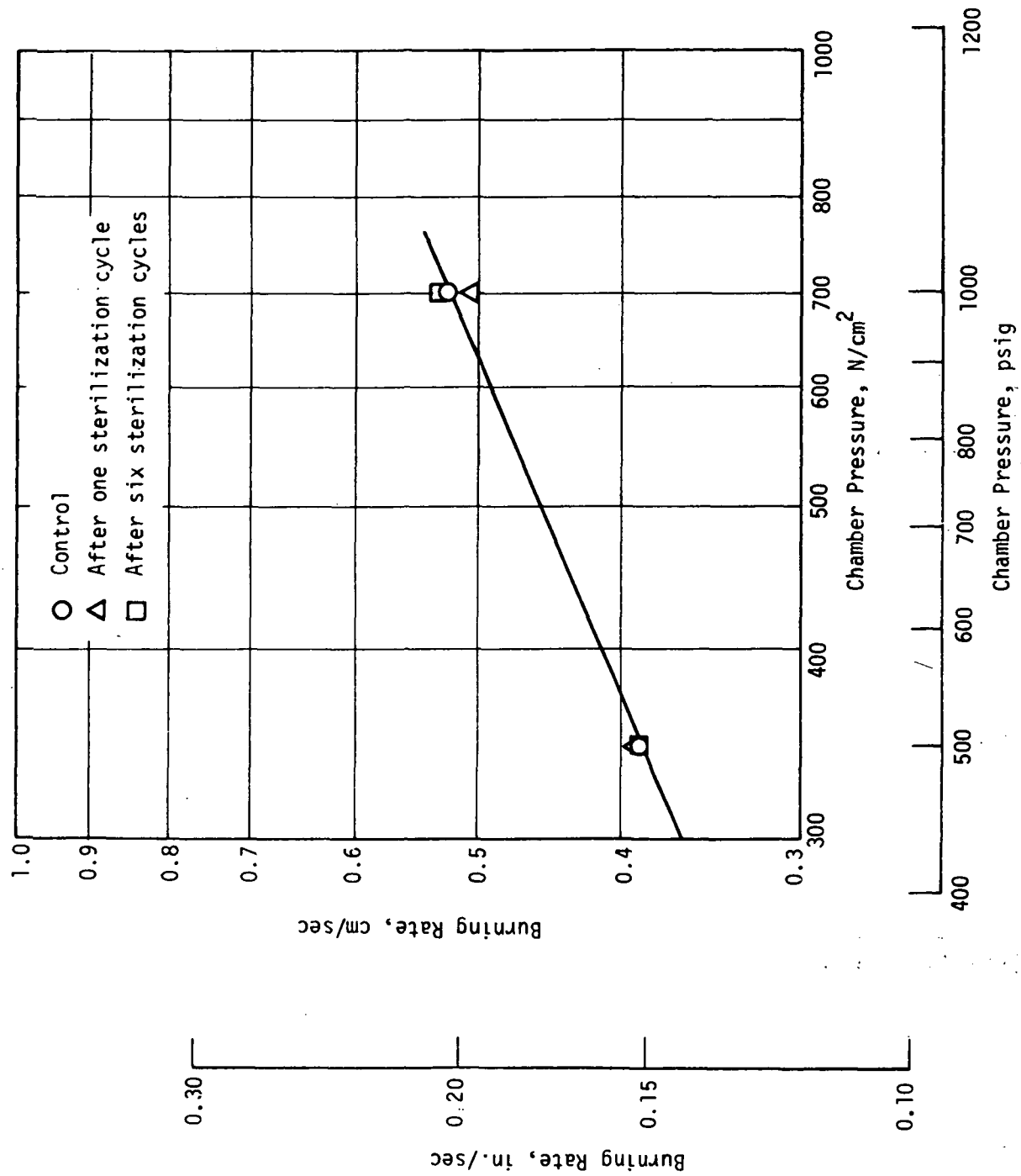
2. Heat Sterilization of Small Grains

The propellant grain size used for screening the heat sterilizability of propellants was a block 7.6 cm x 7.6 cm x 12.7 cm (3 in. x 3 in. x 5 in.). These dimensions were selected from the subscale testing of propellant developed during Contract NAS1-10086. The propellant blocks were wrapped in aluminum foil and exposed to six cycles of 53 hours each at 135°C (275°F). Weight losses, dimensional changes and mechanical property variations were the test parameters used to evaluate the effects of sterilization. In certain cases, the effects of heat sterilization on the solid strand burning rates were also determined.

a. ANB-3289-3 Propellant

Propellant ANB-3289-3 was prepared in a 90 Kg (200-lb) process confirmation mix (Batch 72-92) and cast into a 38 cm (15-in.) dia. grain. Preliminary testing of the heat sterilizability of the batch involved the testing of 7.6 cm x 7.6 cm x 12.7 cm (3 in. x 3 in. x 5 in.) blocks of propellant. No significant dimensional or weight changes were observed after the six heat sterilization cycles (53 hours each at 135°C (275°F)). Solid strand burning rates were measured after the first and sixth cycles, and showed no change as indicated in Figure 33. Mechanical property measurements are presented in Figure 34 and indicate a loss of 27% in the modulus value measured at 25°C (77°F) after the sixth heat sterilization cycle. Also shown in Figure 34 are similar data obtained from the heat sterilization of ANB-3289-3 propellant prepared in a 75 Kg





Solid Strand Burning Rates for Batch 72-92, ANB-3289-3 Propellant

Figure 33

Batch No. and Size	Test Temp. °C (°F)	No. of 53-hr Cycles at 135°C (275°F)	Uniaxial Tensile Properties at .74 min <sup>-1</sup> Strain Rate			
			$\sigma_m$ , N/cm <sup>2</sup> (psi)	$\epsilon_m$ , %	$\epsilon_b$ , %	$E_o$ , N/cm <sup>2</sup> (psi)
72-92 90 Kg (200 lb)	25 (77)	0	116 (168)	16	18	1121 (1625)
		1	117 (169)	18	20	1044 (1513)
		6	90 (131)	21	31	819 (1187)
	135 (275)	0	43 ( 63)	7	8	734 (1064)
		1	39 ( 57)	7	9	647 ( 937)
		6	25 ( 36)	10	16	368 ( 534)
71-63 <sup>(1)</sup> 75 Kg (165 lbs)	25 (77)	0	106 (154)	14	20	1138 (1650)
		1	114 (165)	13	14	1344 (1950)
		6	102 (148)	15	20	1117 (1620)

(1) Data obtained under contract NAS 1-10086

Effect of Heat Sterilization on Mechanical Properties  
of ANB-3289-3 Propellant

Figure 34

(165 lb) batch prepared during the previous contract, NAS1-10086. In this latter batch, the propellant experienced an increase in modulus after the first cycle followed by a decrease of 17% at the end of the sixth cycle. Both batches also experienced some loss in tensile strength as a result of the heat sterilization. This loss in mechanical properties was not considered prohibitive in view of the severe environment imposed on the propellants. Further heat sterilization testing of ANB-3289-3 propellants containing various binder modifications is discussed in Appendix A of this report.

b. ANB-3438 Propellant

Propellant ANB-3438 is a heat sterilizable system developed during the binder improvement portion of the present program (see Appendix A). The binder of this propellant is composed of Telagen-S prepolymer, glyceryl triricinoleate (GTR0) crosslinker, isophorone diisocyanate (IPDI) curing agent, and FC-217 bonding agent. The solids composition is identical to ANB-3289-3. As discussed in Appendix A, small scale batches (3500g size) of this propellant exhibited mechanical properties, processing and heat sterilization characteristics that were superior to ANP-3289-3 propellant. The results of heat sterilization of small-size grains of ANB-3438 propellant prepared in a 73 Kg (160 lb) mix (Batch 73-30-70) are shown below.

EFFECT OF HEAT STERILIZATION ON THE MECHANICAL PROPERTIES OF  
ANB-3438 PROPELLANT

No. of Heat Sterilization Cycles (53 hr ea at 135°C (275°F))	Uniaxial Tensile Properties @ 25°C (77°F)			
	$\sigma_m$ , N/cm <sup>2</sup> (psi)	$\epsilon_m$ , %	$\epsilon_b$ , %	$E_o$ , N/cm <sup>2</sup> (psi)
0	115 (166)	30	46	1196 (1734)
6	204 (296)	21	27	1984 (2875)

Sample dimensions 7.6 cm x 7.6 cm x 12.7 cm (3 in. x 3 in. x 5 in.)

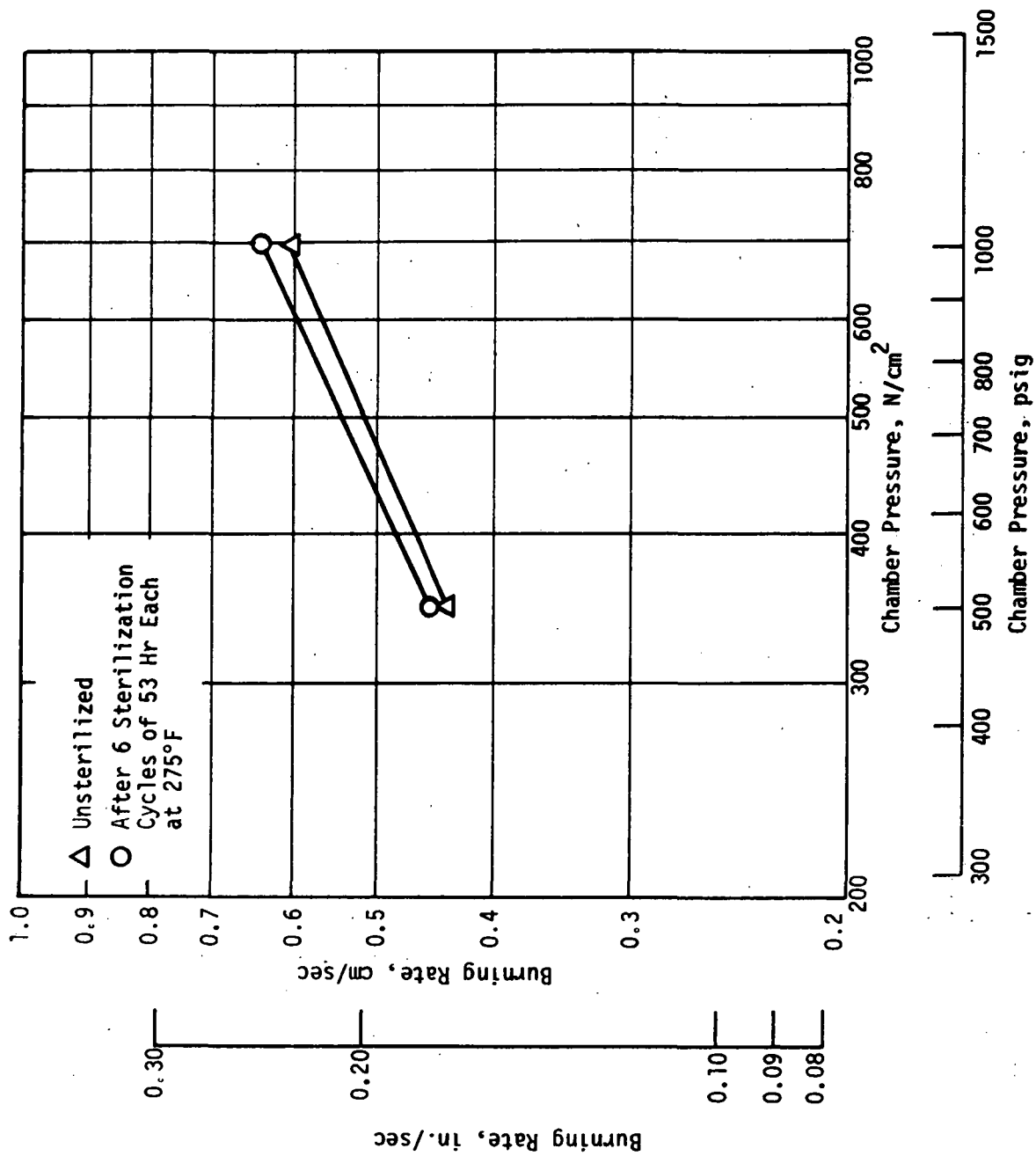
A sizeable increase in tensile strength and modulus with some loss in elongation occurred after the six sterilization cycles. Solid strand burning rate data shown in Figure 35 indicate only a minor increase in burning rate after the six sterilization cycles.

### 3. Heat Sterilization of Large Grains

Large cylindrical propellant grains varying in diameter from 23 cm (9 in.) to 38 cm (15 in.) were prepared in order to obtain heat sterilization data that would be more representative of the propellant mass in the demonstration motors. Additionally, processing characteristics of large batches were obtained which were of value in establishing the casting method to be employed in loading the demonstration motors. Finally, heat sterilization of the large grains would enable the oven heating characteristics and time/temperature profiles to be established for the full-scale motor tests.

#### a. Batch Preparation and Process Characteristics

Propellant ANB-3289-3 was prepared in a 90 Kg (200-lb) mix (Batch 72-92) using a 0.11 m<sup>3</sup> (30 gal) Baker Perkins Vertical Blade mixer. Propellant from the batch was used to cast a 38 cm (15 in.) diameter grain and various small size samples. All batches of ANB-3289-3 propellant were prepared in a similar manner. A submix was prepared which contained the Telagen-S prepolymer, TMP crosslinker and FC-154 bonding agent. Temperature of the submix was maintained at 66 - 82°C (150 - 180°F) to insure that the TMP remained molten. The premix was then prepared by adding aluminum under high-shear agitation by means of a Cowles Dissolver at a temperature of 66-82°C (150-180°F). The premix was stored overnight at 82°C (180°F) and reagitated under high shear before transferring to the mixer bowl (also at 66°C (150°F)). The batch mix temperature was maintained at 66°C (150°F) until all oxidizer and the curing agent, DDI, was added. This was to maintain the TMP in a finely-divided molten state until it could react with the DDI, thereby forming an intermediate product which is compatible with the



Solid Strand Burning Rate for Batch 73-30-70, ANB-3438 Propellant

Figure 35

Telagen-S prepolymer. At this time the temperature was lowered to 57°C (135°F) to complete the mix cycle. Analyses of the submix, premix, and uncured propellant are presented in Figure 36. The viscosity build-up properties of the first mix of ANB-3289-3 are shown in Figure 37; the uncured and solid strand burning rates are presented in Figure 38.

Four other batches were made in the 0.11 m<sup>3</sup> (30 gal) size mixer from which large grains were cast. Three involved modifications of ANB-3289-3 and the fourth was a batch of ANB-3438 propellant. A fifth smaller batch, 27 Kg (60 lbs) of ANB-3438 was prepared in the 0.02 m<sup>3</sup> (5 gal) size verticle blade mixer. The identification and propellant variables associated with the batches are shown in Figure 39.

The preparation of the ANB-3438 propellant batches was altered to the extent that high processing temperatures were not needed, since the GTR0 crosslinker (unlike TMP) is a liquid and is miscible with the Telagen-S prepolymer. The bonding agent used, FC-217, was added to the batch just prior to oxidizer addition. Submix, premix, oxidizer and uncured propellant analyses of the ANB-3289-3 batches are detailed in Figure 40. Similar data for the ANB-3438 batches are in Figure 41.

Viscosity build-up properties for Batches 73-30-70, -75, -81 and -82 are shown in Figures 42 through 45. All batches were quite processable up to 5 hours or more after curative addition. ANB-3289-3 propellant prepared without bonding agent (Batch 73-30-82) showed the fastest viscosity increase. ANB-3438 (Batch 73-30-70) had excellent processing properties, with a useable casting time (pot-life) in excess of 15 hours at 57°C (135°F). The low-shear stress viscosities of this propellant are also quite attractive, exhibiting Newtonian flow characteristics up to seven hours after curing agent addition.

SUBMIX

H <sub>2</sub> O, Wt%	0.006
Acid No.	0.15
OH No.	96.98
Refractive Index, 15°C	1.4802
Density, g/cc	0.879

PREMIX

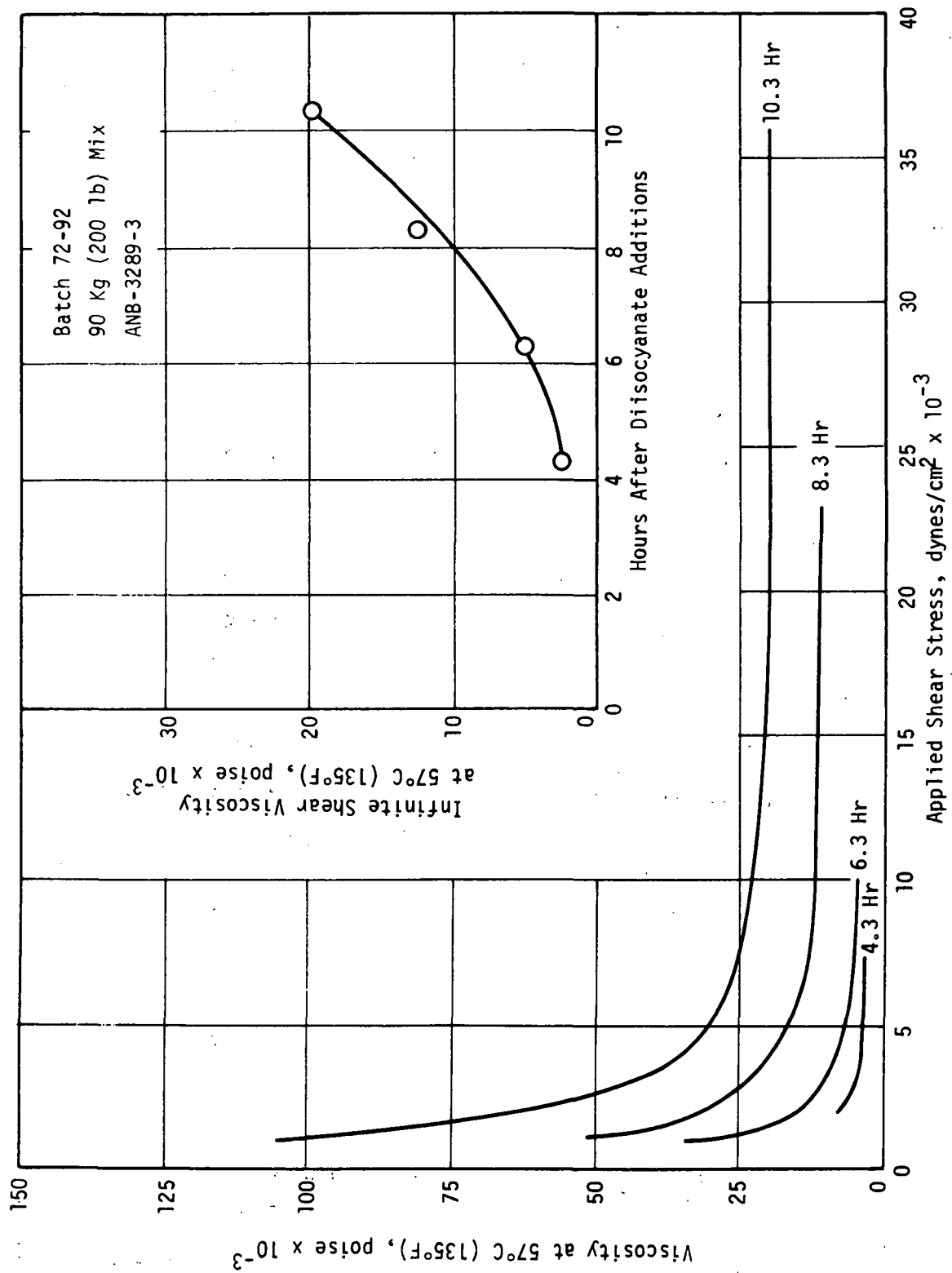
H <sub>2</sub> O, Wt%	0.018
Density, g/cc	1.544

UNCURED PROPELLANT

Density, g/cc	1.716
Solids, Wt%	84.18 (Theo. 84.00)

Analytical Data from 0.11 m<sup>3</sup> (30 Gal) Size  
Mix of ANB-3289-3, Batch 72-92

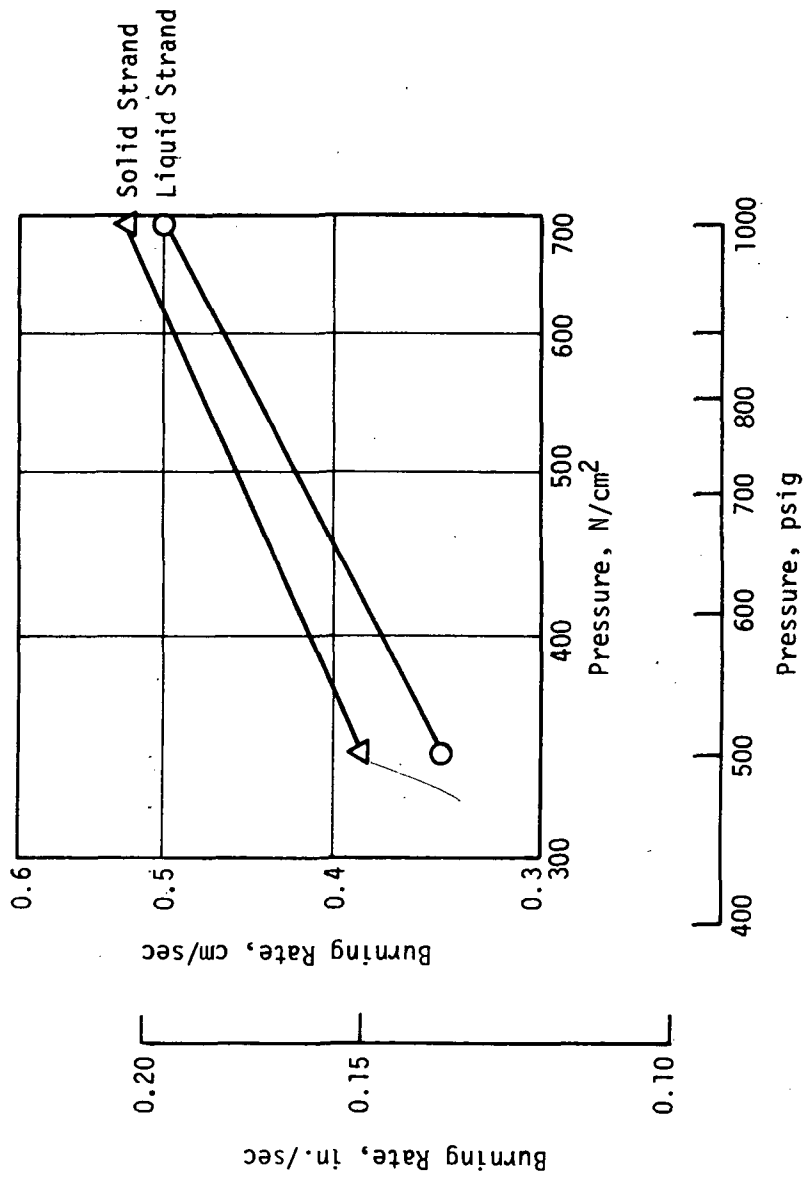
Figure 36



Propellant Viscosity as a Function of Shear Stress and Time from Curing Agent Addition

Figure 37





Burning Rates of Solid and Liquid Strands for ANB-3289-3 Batch 72-92

Figure 38

<u>Batch No.</u>	<u>Batch Size</u> <u>Kg (lb)</u>	<u>Telagen Lot</u>	<u>Crosslinker</u>	<u>Curative</u>	<u>Bonding Agent</u>	<u>Oxidizer (1)</u> <u>Treatment</u>	
						<u>Unground</u>	<u>Ground</u>
72-92	90 (200)	316AM-11/12	TMP	DDI	FC-154	Stab.	Stab.
73-30-70	54.5 (120)	Master Blend	GTR0	IPDI	FC-217	Purified	Stab.
73-30-75	73 (160)	Master Blend	TMP	DDI	FC-154	Purified	Stab.
73-30-81	54.5 (120)	Master Blend	TMP	DDI	FC-154	Purified	Stab.
73-30-82	54.5 (120)	Master Blend	TMP	DDI	-	Purified	Stab.
73-05-121	27 (60)	Master Blend	GTR0	IPDI	FC-217	Stab.	Stab.

(1) Stabilized oxidizer was recrystallized and treated with a stabilizing agent; purified oxidizer was recrystallized only. Oxidizer blend was 60/40 180 $\mu$ /28 $\mu$  material.

Propellant Compositions of Scale-Up Batches

Figure 39

<u>BATCH</u>	73-30-75	73-30-81	73-30-82
<u>SUBMIX</u>			
H <sub>2</sub> O, Wt%	0.052	0.008	0.012
Acid No.	0.17	0.24	0.21
OH No.	74.21	62.48	70.14
Refractive Index, 15°C	1.4796	1.4795	1.4787
Density, g/cc	0.873	0.872	0.872
<u>PREMIX</u>			
H <sub>2</sub> O, Wt%	0.040	0.014	0.022
Density, g/cc	1.544	1.512	1.492
<u>OXIDIZER MOISTURE, WT%</u>	- - - - - 0.009 - - - - -		
<u>UNCURED PROPELLANT</u>			
Density, g/cc	1.714	1.708	1.712

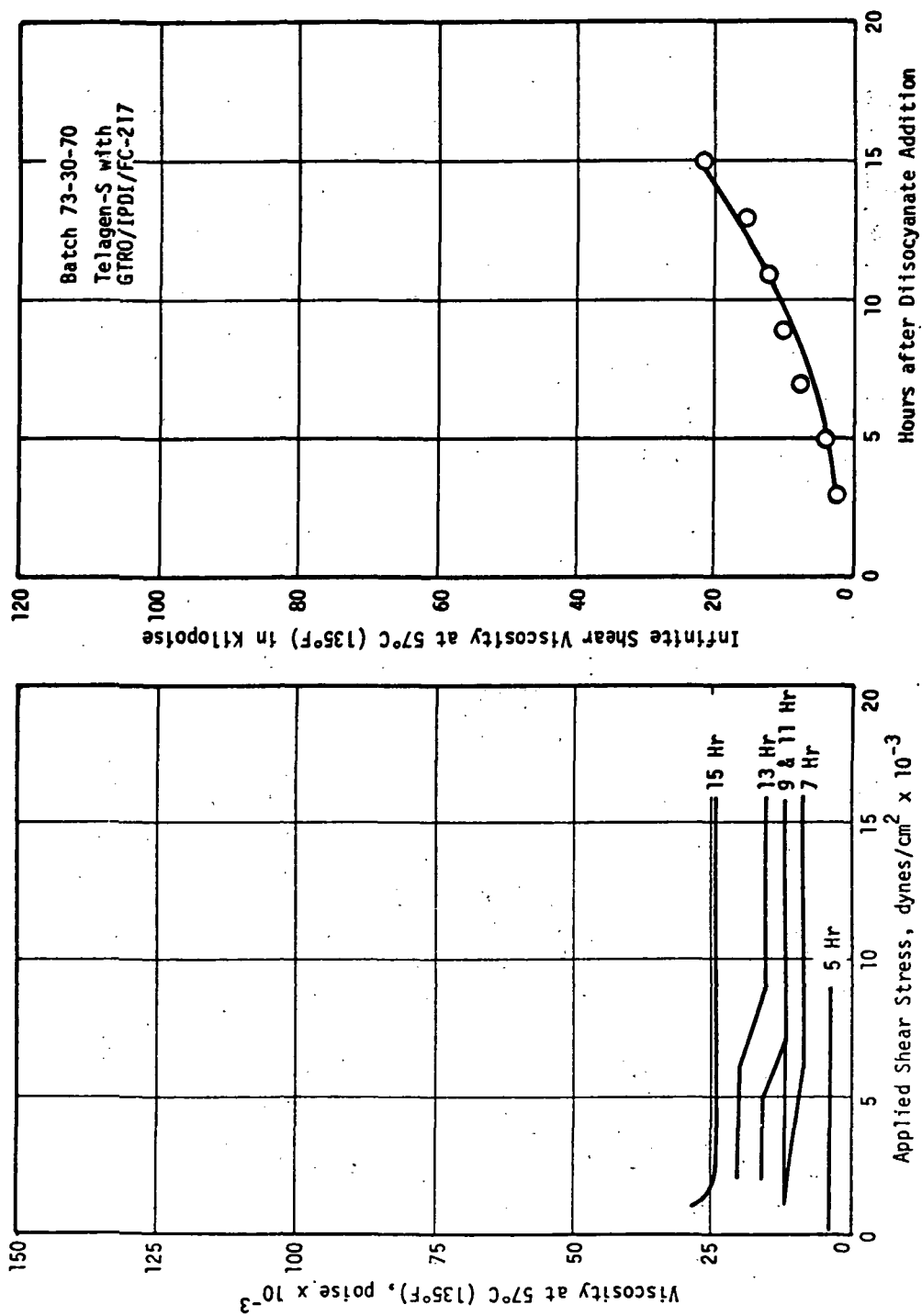
Analytical Data from 0.11 m<sup>3</sup> (30 gal) Size  
Batch Mixes of ANB-3289-3 Type Propellants

Figure 40

<u>BATCH</u>	73-05-121	73-30-70
<u>BATCH SIZE</u>	27 Kg (60-15)	73 Kg (160-1b)
<u>SUBMIX</u>		
Moisture, Wt%	0.017	0.021
OH No.	72.46	71.90
Refractive Index	-	1.4792
Density, g/cc	-	0.882
<u>PREMIX</u>		
Moisture, Wt%	0.016	0.019
Density, g/cc	1.429	1.426
Solids, Wt%	-	-
<u>OXIDIZER</u>		
Moisture, Wt%	-	0.009
<u>UNCURED PROPELLANT</u>		
Density, g/cc	-	1.719

Analytical Data from ANB-3438 Propellant Prepared  
in 0.02 m<sup>3</sup> (5 gal) and 0.11 m<sup>3</sup> (30 gal) Batches

Figure 41



Propellant Viscosity as a Function of Shear Stress and Time from Curing Agent Addition

Figure 42

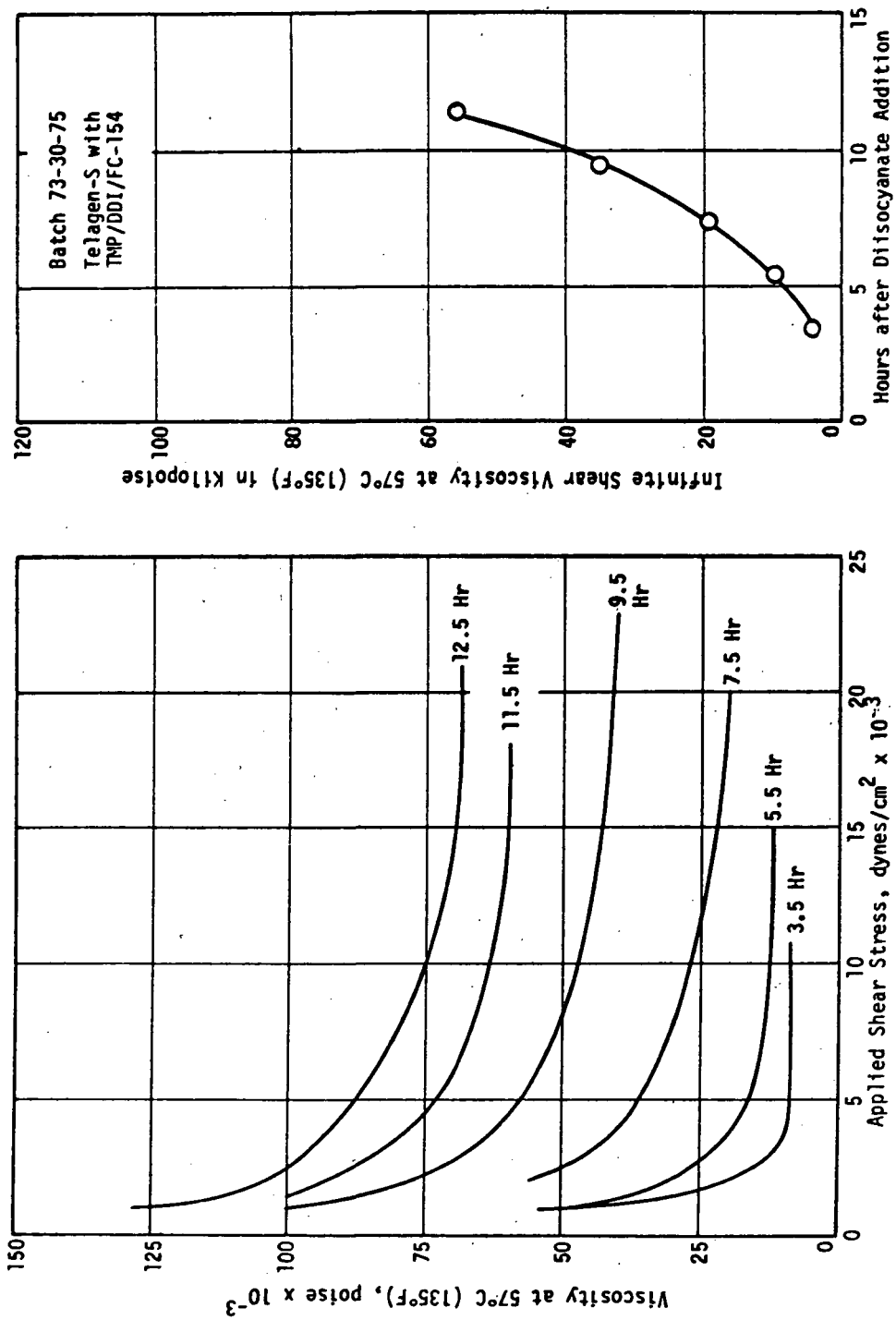
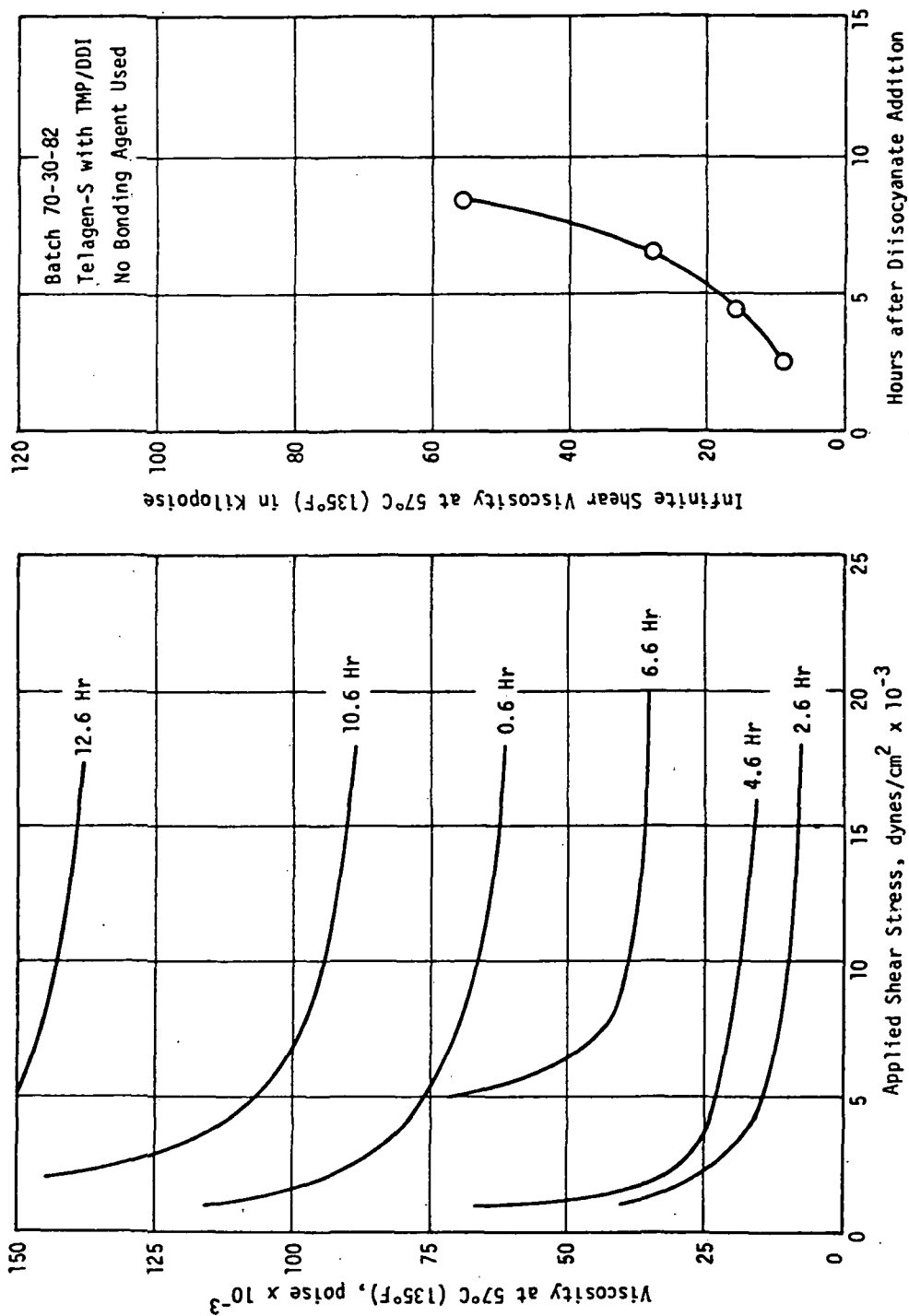
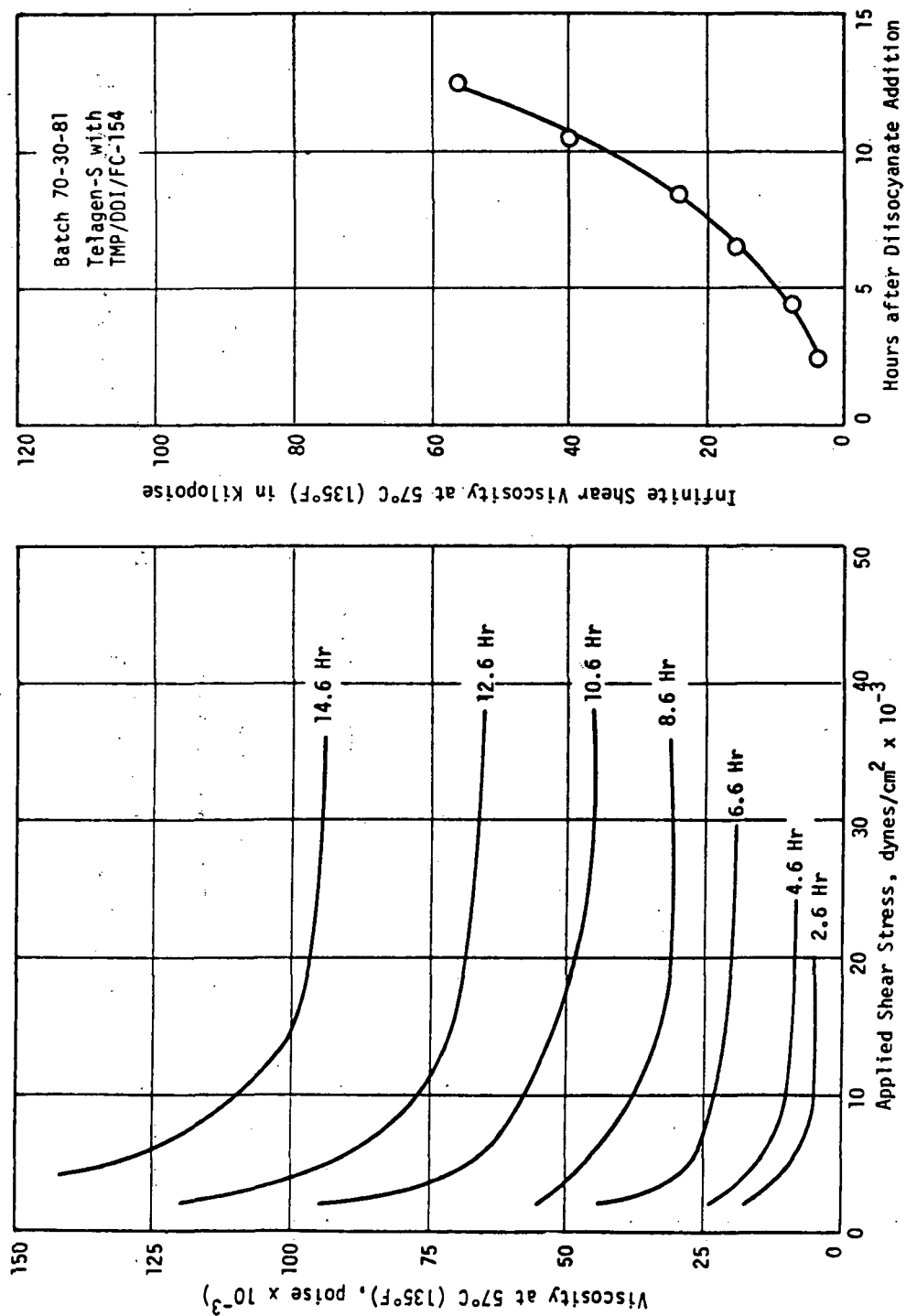


Figure 43

Propellant Viscosity as a Function of Shear Stress and Time from Curing Agent Addition



Propellant Viscosity as a Function of Shear Stress and Time from Curing Agent Addition



Propellant Viscosity as a function of Shear Stress and Time from Curing Agent Addition

Figure 45



#### b. Heat Sterilization of 38 cm (15 in.) Diameter Grain

The first large grain was 38 cm (15 in.) in diameter and was cast from a 90 Kg (200 lb) mix (Batch No. 72-92) of ANB-3289-3 propellant. The configuration is shown in Figure 46. Five thermocouples were inserted into the grain at selected positions so that the heating profile of the grain could be obtained. The 10 cm (4 in.) well was placed in the grain to simulate the web thickness of the motor. Heat sterilization was performed in a BEMCO walk-in oven.

In addition to sterilization, other objectives were to define the oven and grain heating characteristics and establish procedures for the motor sterilization cycles. The time-temperature history of the 38 cm (15 in.) grain were taken throughout the five cycles and, as a result of these tests, a nominal heating profile for the grain and oven was established (Figure 47).

X-ray examination of the grain after the fifth cycle to 135°C (+275°F) revealed several horizontal fissures. No X-rays were taken other than prior to the cycling tests, therefore, it is not known during which of the five cycles the grain cracked. Since the smaller blocks from the same propellant batch successfully passed the sterilization cycle, (see Section III.C.2 above), the problem apparently was one of scale-up in sample size and not one of batch size or propellant ingredients.

#### c. Analysis of Grain Failure

One of the possible causes of grain failure could be related to the thermal stresses induced in the grain due to the large temperature differential between the surface and center during heat-up. A thermal stress analysis was performed which estimated the maximum thermal stresses occurring in the grain (Figure 46) when undergoing the heat

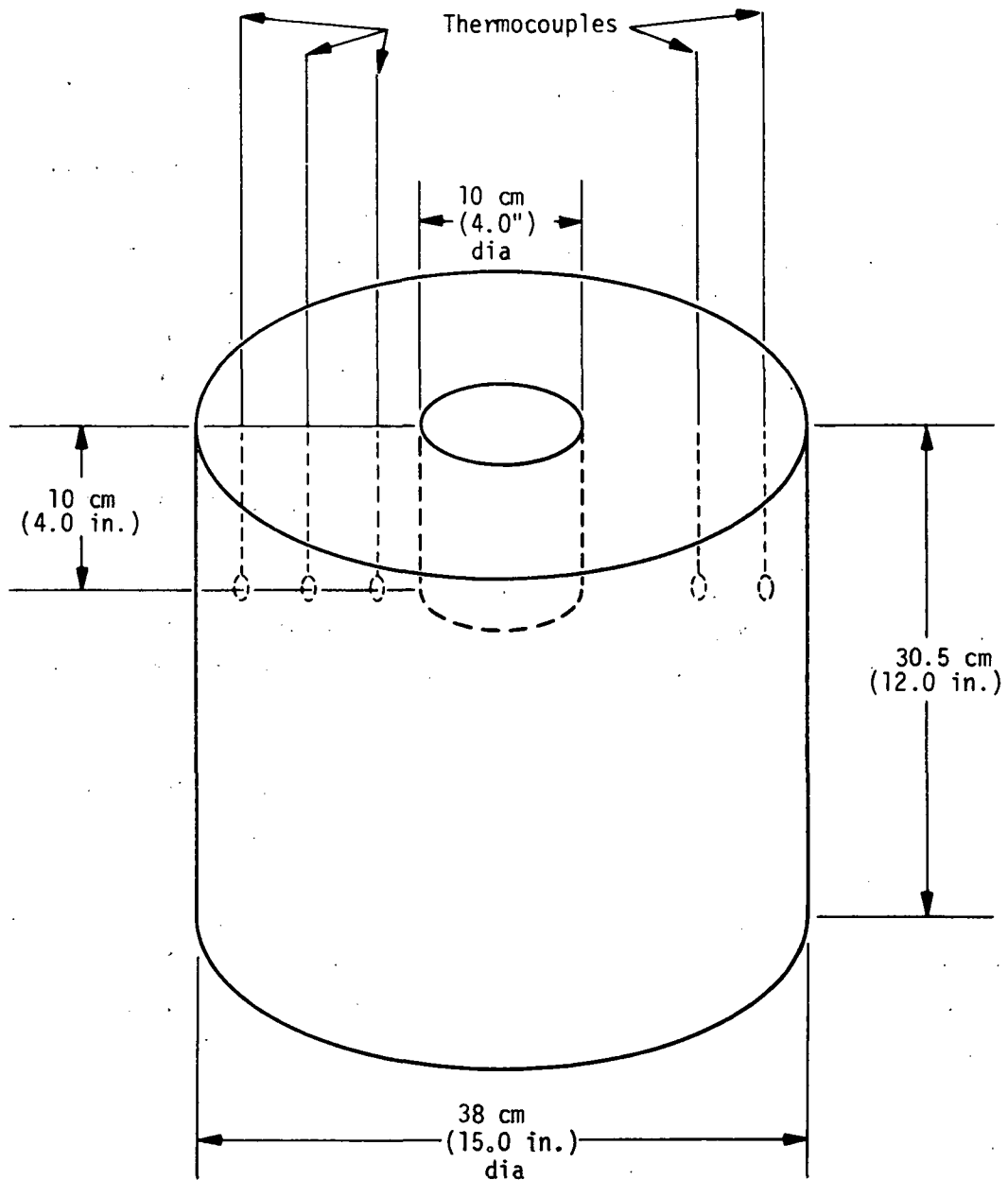
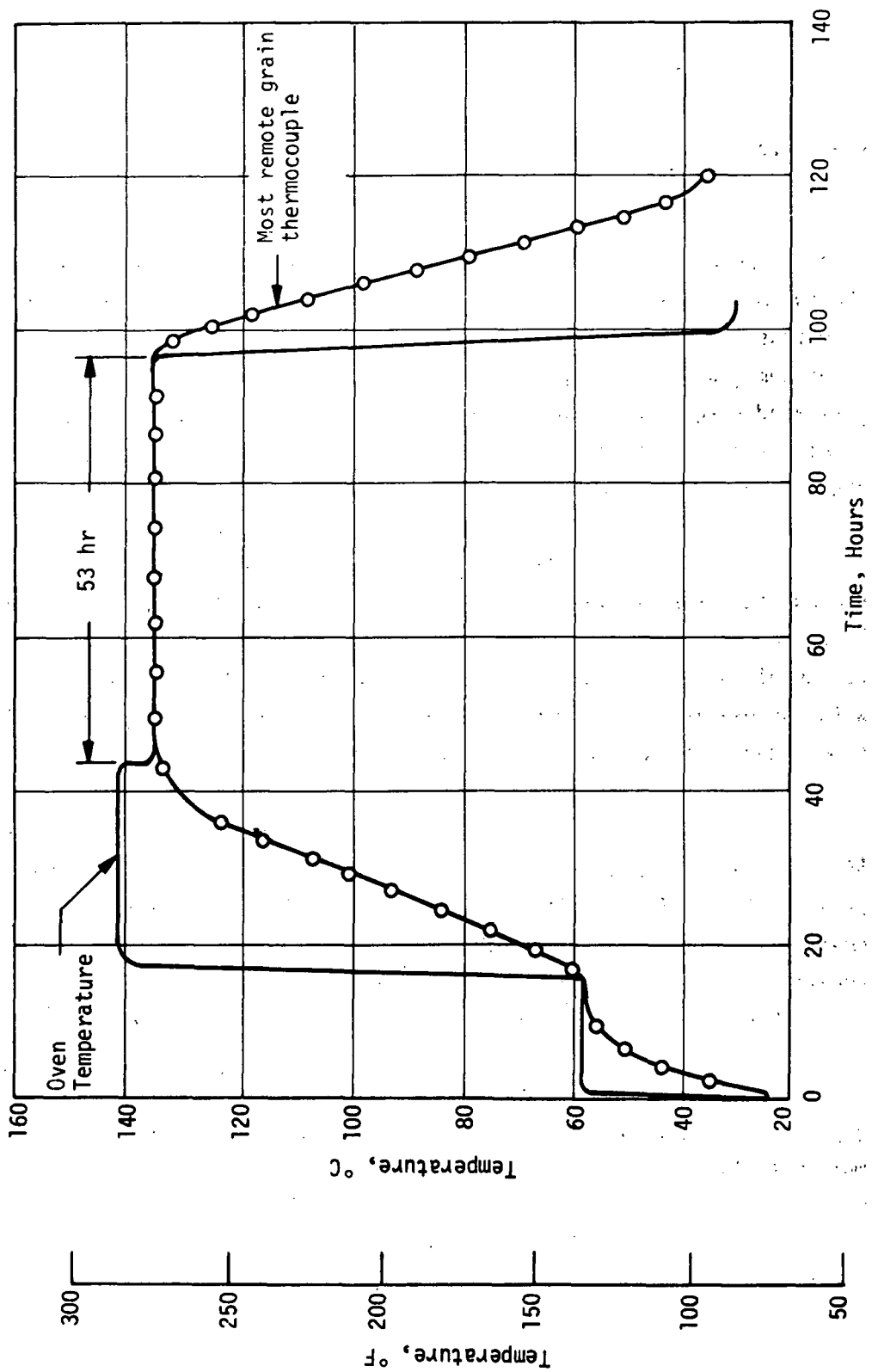


Diagram of 38 cm (15-in.) Diameter Propellant Grain  
Used in Heat Sterilization Tests

Figure 46



Nominal Grain Sterilization Conditions

Figure 47

sterilization cycle defined in Figure 47.

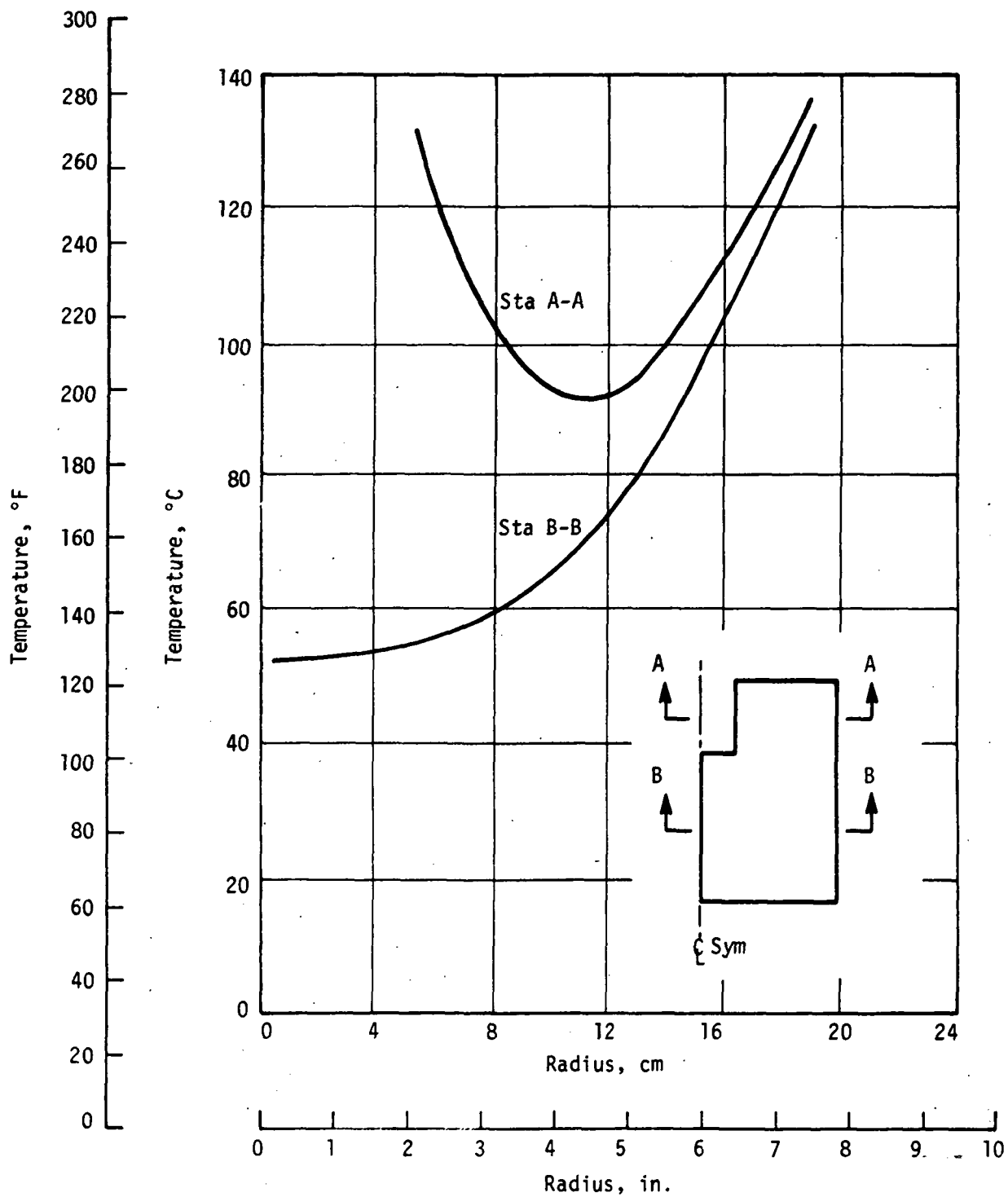
In making this evaluation, the temperature distribution in the actual sample was estimated from one-dimensional analyses of the two different cross sections of the grain. Results of these thermal solutions indicated the maximum gradient occurs at 20 hours and the calculated temperature distribution for that time is shown in Figure 48. The estimated gradients in the actual sample, along with the resultant maximum tensile stresses obtained from a finite element elasticity solution, are shown in Figure 49.

As indicated in Figure 49 the maximum calculated thermal stress anywhere in the sample is  $5.2 \text{ N/cm}^2$  (7.5) psi and occurs near the center where the temperature was taken as  $54^\circ\text{C}$  ( $130^\circ\text{F}$ ). Maximum values of thermal stress occurring at the various temperature regions, along with the estimated equivalent capability of the ANB-2389-3 propellant, are summarized in Figure 50.

On the basis of the above results it does not appear that thermal stresses alone could have caused the cracking observed in the sample. It should be noted however, that the maximum stress values for the heat up cycle does occur in the area where the cracks occurred. If the capability of the propellant were reduced due to gas generation, the thermal stresses could have contributed significantly to the observed failures.

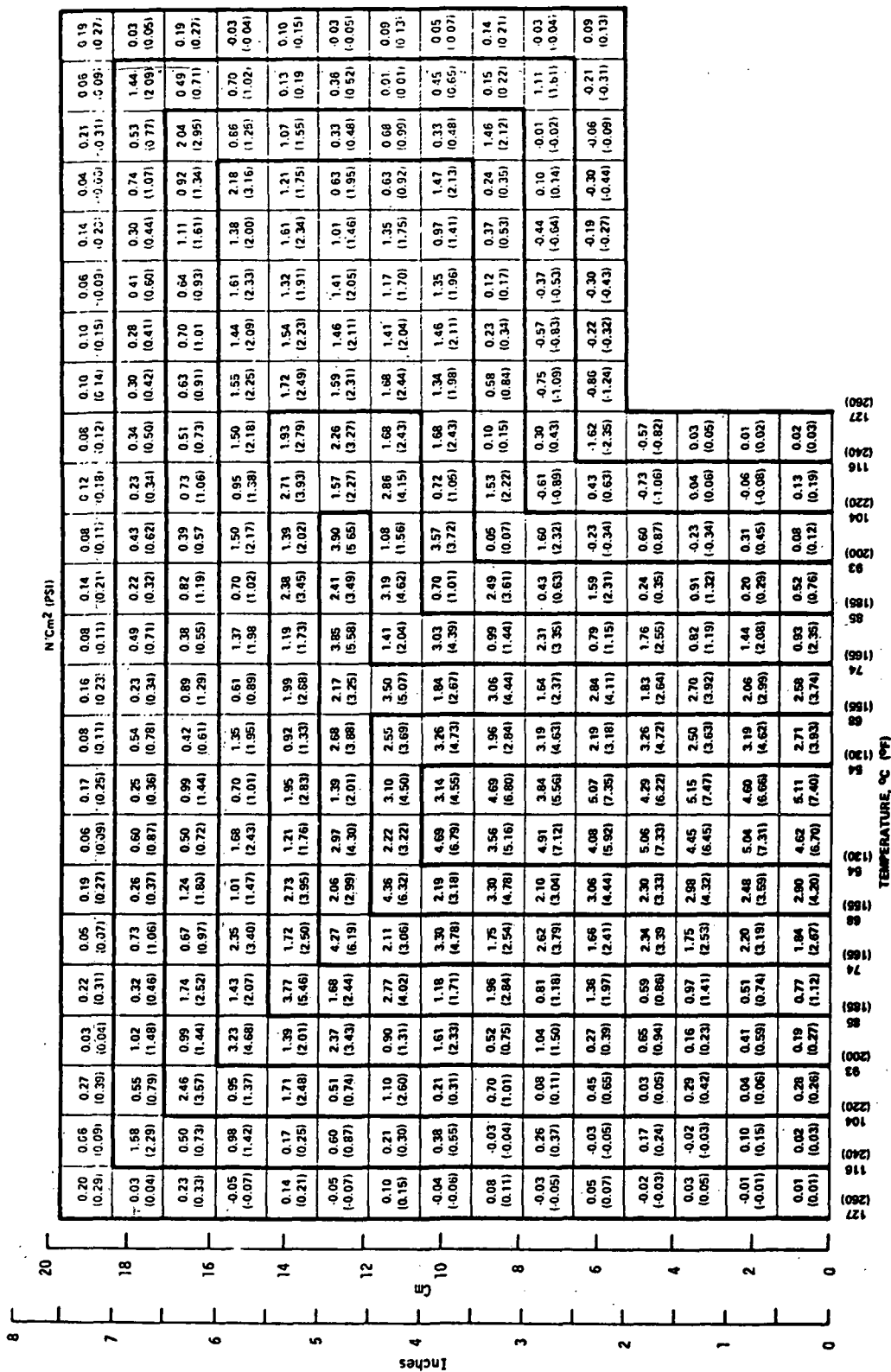
As a result of the stress analysis presented above, a recovery program was designed to evaluate means of preventing crack formation in the large grains. These methods consisted of:

- (1) Increasing propellant tensile strength (and modulus) so as to resist internal stresses generated by thermal gradients



Calculated Thermal Gradients in Sample Cross Sections

Figure 48



Assumed Thermal Gradients and Calculated Maximum Tensile Stresses  
in 38.5 cm (15 in.) Dia. Grain

Temperature Regions in Grain @ t = 20 hrs °C (°F)	Propellant Modulus @ t = 20 hrs N/cm <sup>2</sup> (psi)	Max. Tensile Stress, N/cm <sup>2</sup> (psi)	Estimated Allowable Stress for 5 Cycles, N/cm <sup>2</sup> (psi)	M. S.
54 (130)	607 (880)	5.2 (7.5)	11.9 (17.2)	1.29
68 (155)	552 (800)	4.3 (6.3)	10.4 (15.0)	1.38
74 (165)	545 (790)	4.3 (6.2)	9.9 (14.4)	1.32
85 (185)	518 (750)	3.8 (5.5)	9.0 (13.0)	1.36
93 (200)	483 (700)	3.2 (4.7)	8.5 (12.3)	1.62
104 (220)	476 (690)	2.5 (3.6)	7.7 (11.1)	2.08
116 (240)	448 (650)	1.6 (2.3)	7.1 (10.3)	3.48
127 (260)	428 (620)			

Calculated Thermal Stresses Occurring During Heat Sterilization of Propellant Grain

Figure 50

and/or gas formation. This would include the use of ANB-3438 propellant which increases in tensile strength and modulus during heat sterilization.

(2) Minimize gas formation by eliminating the oxidizer bonding agent, FC-154. This material contains a tertiary amine group which could conceivably react with the oxidizer surface at the sterilization temperature to generate gases.

(3) Lower the rate of heat-up and cool-down of the propellant grain during sterilization. This would minimize the thermal gradients and hence lower the thermal stresses in the grain.

The experimental design selected to evaluate these parameters was as follows:

<u>Heating and Cooling Rate</u>	<u>ANB-3289-3, Low Modulus</u>	<u>ANB-3438</u>	<u>ANB-3289-3, High Modulus</u>
1	X, []		0
2	0	0	0
3	0, []	0	0

X Completed 38 cm (15 in.) grain which cracked

0 To be tested

[] Contained no bonding agent

#### d. Selection of Binder Compositions

A master blend of Telagen-S prepolymers was prepared from three different lots of stripped material (see Section III.C.1). The lots used were: 316 AM-11/12 (~4.5 Kg (10 lbs)), 316 AM-5 (~27 Kg (60 lbs)) and ~36 Kg (80 lbs)) of blended lot (3HPL - 229/235).



454 g (1-lb) batch mixes of ANB-3289-3 propellant were prepared at TMP crosslinker levels ranging from 35 to 50 equivalents using Telagen-S prepolymer from the master blend. In addition, a 454 g (1-lb) batch was mixed using Lot 3HPL - 229/235. The uniaxial tensile properties measured at 25°C (77°F) are shown in Figure 51. The modulus as a function of TMP content is illustrated in Figure 52. Also shown in Figure 52 is the modulus/TMP level relationship for ANB-3289-3 propellant prepared with Lot Lot 316 AM-11/12 Telagen-S prepolymer. The moduli obtained at a given TMP level were considerably higher using the Telagen-S prepolymer master blend. Still higher was the modulus obtained with Lot 3HPL - 229/235 (Batch 7567-62-1). This increase in modulus was due to the higher concentration of difunctional species in Lot 3HPL - 229/235 (77% difunctional as opposed to 72% for Lot 316 AM-11/12).

A similar effect was noted in the propellants prepared with the ANB-3438 binder system composed of Telagen-S/GTRO/IPDI/FC-217. The moduli values from uniaxial tensile data at 25°C (77°F) (Figure 51) are shown graphically as a function of the GTRO crosslinker level in Figure 53. As with the TMP crosslinked systems (Figure 52) there is a considerable increase in modulus at a given crosslinker level with the master blend of Telagen-S over that obtained with Lot 316 AM-11/12 prepolymer.

As a result of the increased modulus levels obtained with the master blend of Telagen-S prepolymers, it was necessary to incorporate lower crosslinker levels than those originally selected for use with prepolymer Lot 316 AM-11/12. The large grains of ANB-3289-3 to be prepared for heat sterilization tests, therefore, contained the following concentration of crosslinker:

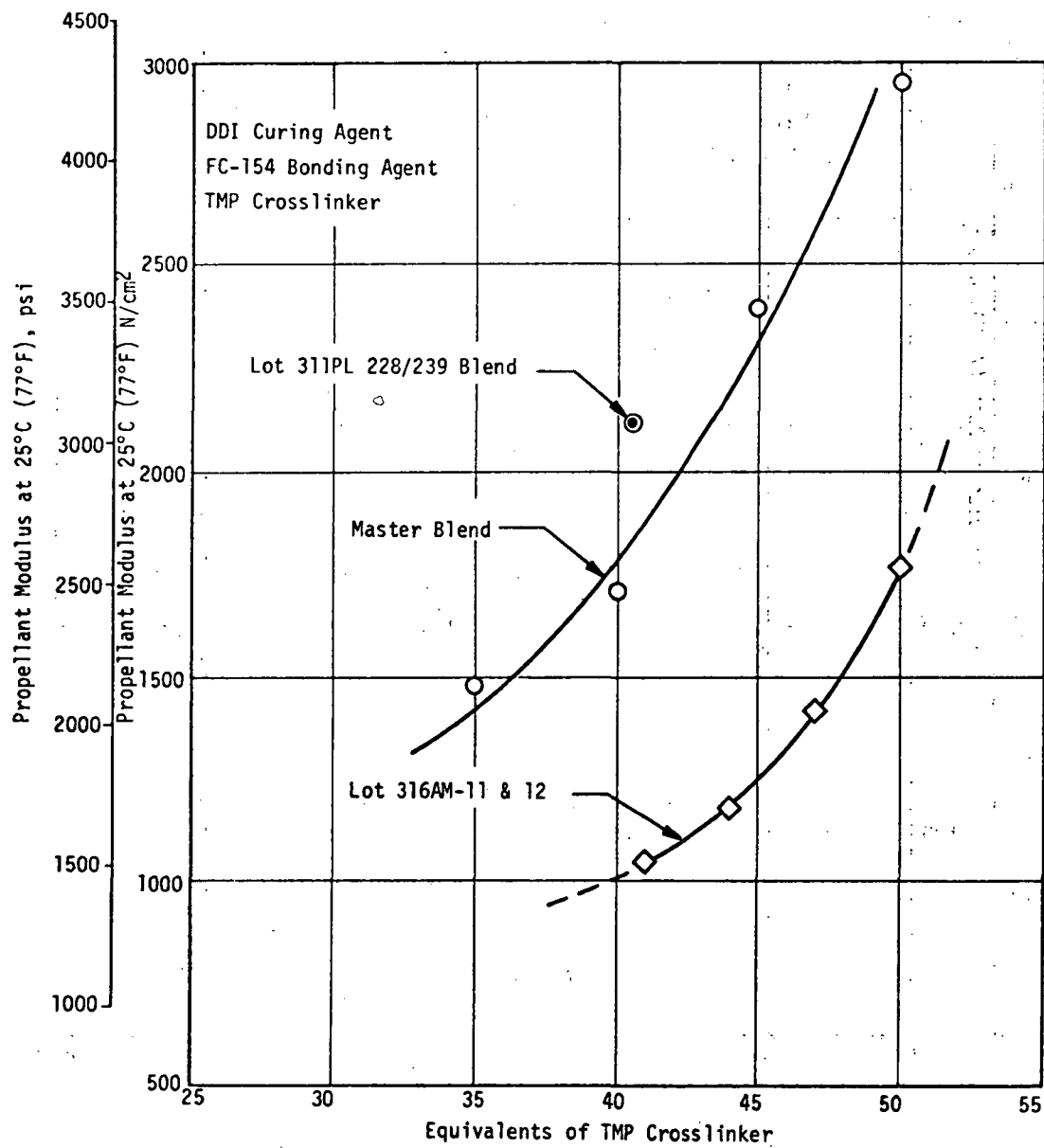
Low Modulus ( $E_0 \sim 1173 \text{ N/cm}^2$  (1700 psi)) Propellant  
 with and without FC-154 Bonding Agent: 30 equiv. TMP

Batch	Equivalents of Crosslinker	Bonding Agent Used	Uniaxial Mechanical Properties At 25°C (77°F)			
			$\sigma_m$ , N/cm <sup>2</sup> (psi)	$\epsilon_m$ , %	$\epsilon_b$ , %	$E_o$ , N/cm <sup>2</sup> (psi)
ANB-3289-3	TMP <sup>(2)</sup>					
SAN-1	35	FC-154	137 (199)	17	22	1472 (2133)
SAN-2	40	↕	137 (199)	15	20	1703 (2468)
SAN-3	45		150 (217)	10	11	2389 (3463)
SAN-4	50		157 (228)	7	8	2943 (4265)
7567-62-1 <sup>(3)</sup>	51	FC-154	140 (203)	10	11	2113 (3062)
ANB-3438	GTR <sup>(4)</sup>					
GMS-64-4	35	FC-217	79 (114)	45	78	626 (907)
GMS-64-3	40	↕	95 (138)	35	65	842 (1220)
GMS-64-2	45		118 (171)	16	35	1779 (2578)
GMS-64-1	50	FC-217	124 (180)	11	28	2363 (3424)

- (1) Blend of Lots: 316AM-11/12, 316AM-5, 3HPL-229/235  
 (2) Binder composed of Telagen-S/TMP/DDI/FC-154  
 (3) Contains Lot 3HPL-229/235 Telagen-S prepolymer  
 (4) Binder composed of Telagen-S/GTR/IPDI/FC-217

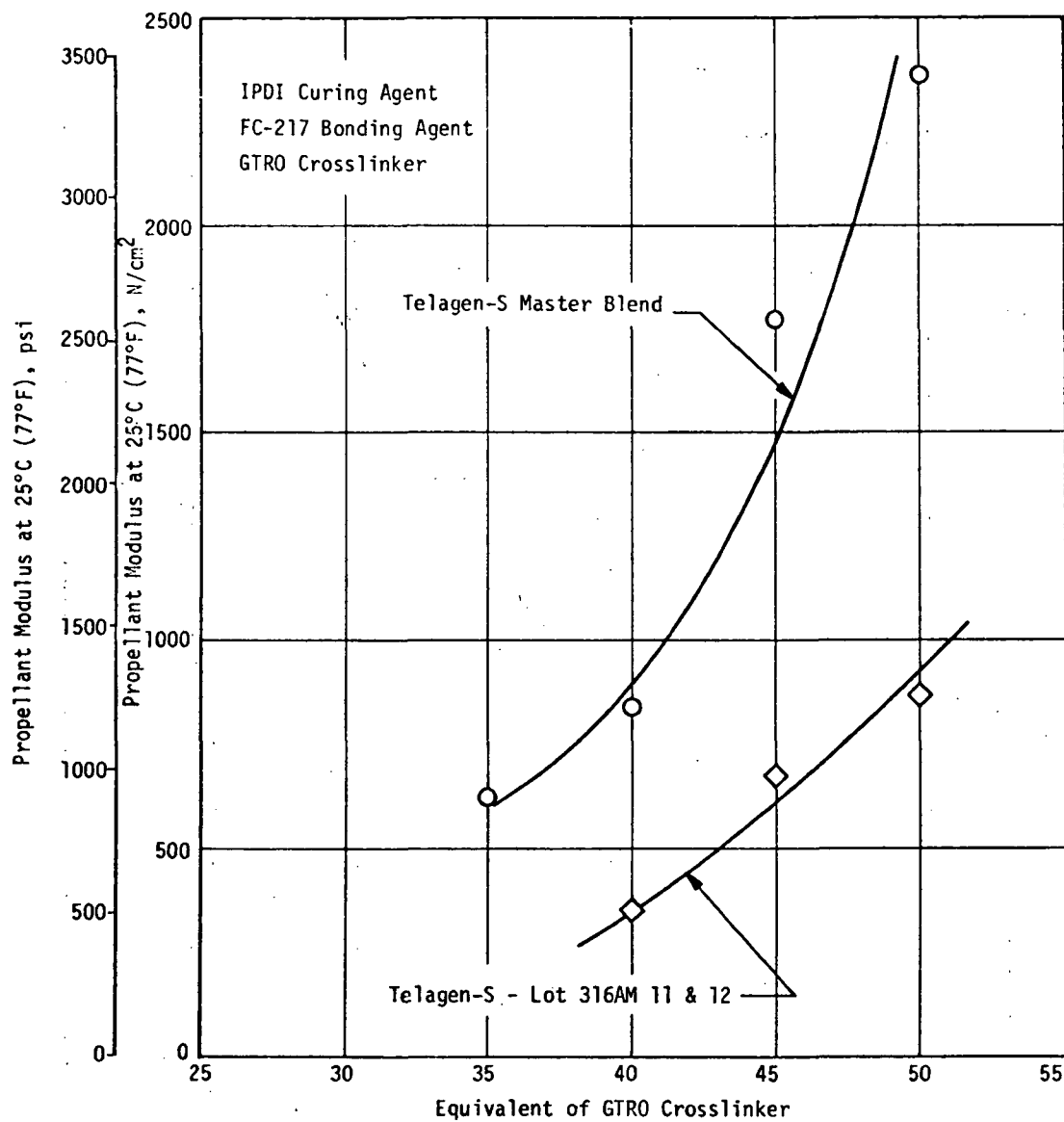
Effect of Crosslinker Level on Mechanical Properties of ANB-3289-3 and ANB-3438  
 Propellant Prepared with Telagen-S Prepolymer Master Blend(1)

Figure 51



Effect of Telagen-S Prepolymer Lot on Modulus/Crosslinker Level  
Relationship of ANB-3289-3 Propellant

Figure 52



Effect of Telagen-S Prepolymer Lot on Modulus/Crosslinker Level  
Relationship of ANB-3438 Propellant

Figure 53

High Modulus ( $E_0 \sim 1725 \text{ N/cm}^2$  (2500 psi)) Propellant  
with FC-154 Bonding Agent:

40 equiv. TMP

Propellant with FC-217 bonding Agent  
( $E_0 \sim 828 \text{ N/cm}^2$  (1200 psi)):

40 equiv. GTRO.

A lower initial modulus was selected for the ANB-3438 propellant because the modulus and tensile strength tend to increase during heat sterilization.

e. Preparation of Grains for Sterilization Tests

Four  $0.11 \text{ m}^3$  (30-gal) size batches of propellant were mixed and cast into 30.5 cm (12-in.) -dia. by 20 cm (8-in.) long grains. Two thermocouples were placed in each grain, one in the center and the other 1.3 cm (1/2-in.) from the periphery. Compositions of the batches are shown below.

<u>Propellant</u>	<u>Batch</u>	<u>Crosslinker</u>	<u>Bonding Agent</u>	<u>Curing Agent</u>
ANB-3438	73-30-70	GTRO (40 eq.)	FC-217	IPDI
ANB-3289-3	73-30-75	TMP (40 eq.)	FC-154	DDI
ANB-3289-3	73-30-81	TMP (30 eq.)	FC-154	DDI
ANB-3289-3	77-30-82	TMP (30 eq.)	None	DDI

The oxidizer blend used in these batches was 60/40 unground ( $180\mu$ )/HSMP ( $26\mu$ ) ammonium perchlorate. Lot 69001, a recrystallized and stabilized material from PEPCON, was used to prepare the ground portion of the oxidizer blend. The unground fraction was the high-purity (but unstabilized) Lot A68026, also purchased from PEPCON. This selection was based on the results of a test in which a 7.6 cm x 7.6 cm x 12.7 cm (3 in. x 3 in. x 5 in.) block of ANB-3289-3 propellant prepared with

unground Lot A68026 oxidizer successfully passed six heat sterilization cycles of 53 hours each at 135°C (275°F), as described in Section III.C.2.

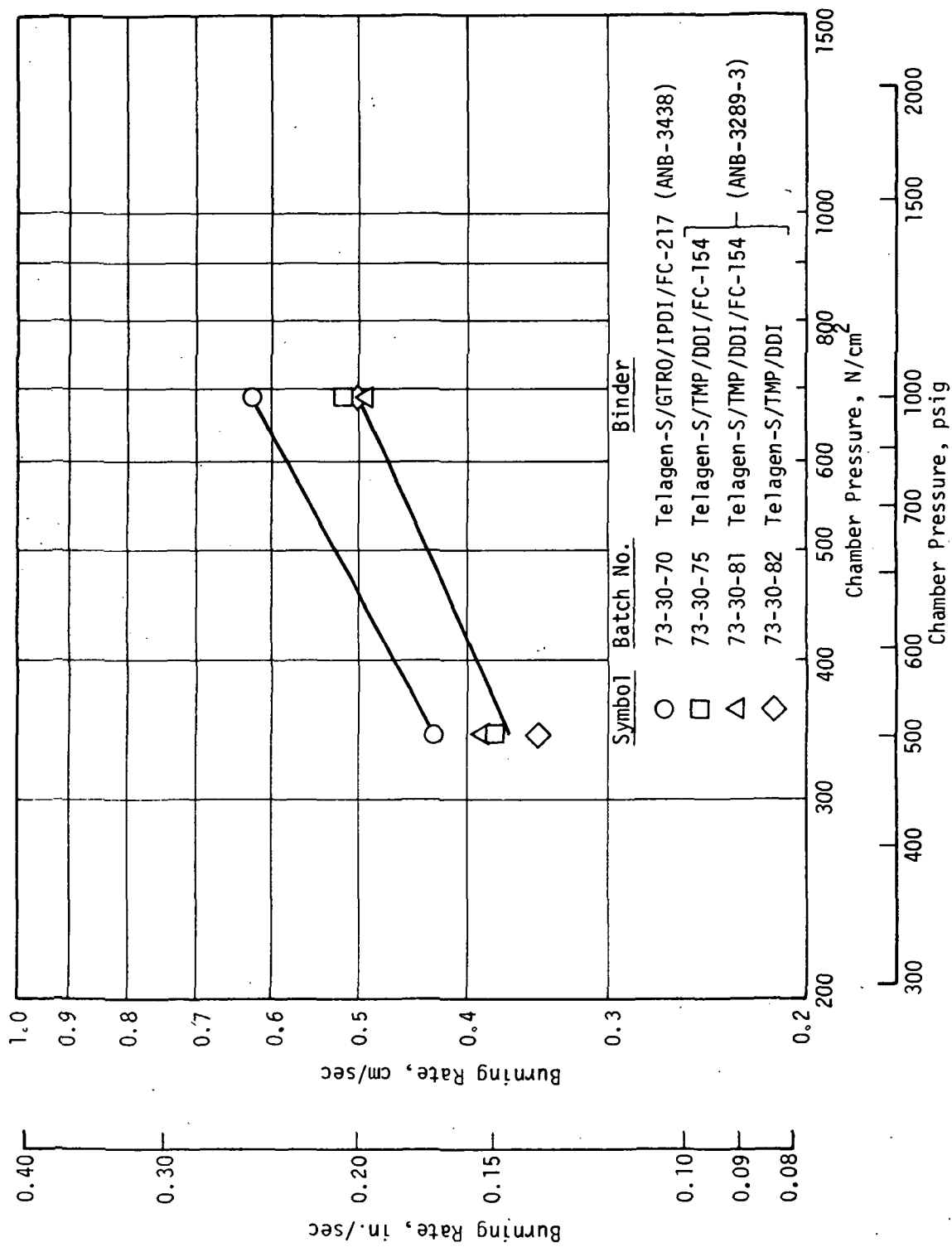
The processing characteristics of the propellants were described previously. It was apparent that any of the formulations could be readily cast into the demonstration motors, but that the excellent processability of ANB-3438 propellant would provide the best grains.

Uncured strand burning rates of the batches were measured at 345 (500) and 690 N/cm<sup>2</sup> (1000 psi). The data are shown in Figure 54. Burning rates of the three batches containing the TMP/DDI system (ANB-3289-3) appear to be the same; however, those from the batch containing GTR0/IPDI (ANB-3438, Batch 73-30-70) are somewhat higher. This difference in burning rate was verified in solid strand firings of the cured propellant (Figure 55).

Uniaxial tensile properties at 25°C (77°F) are listed in Figure 56. The modulus level of the ANB-3289-3 propellants are slightly lower than those obtained in 400-gram size batches, whereas the tensile and modulus values of ANB-3438 are higher.

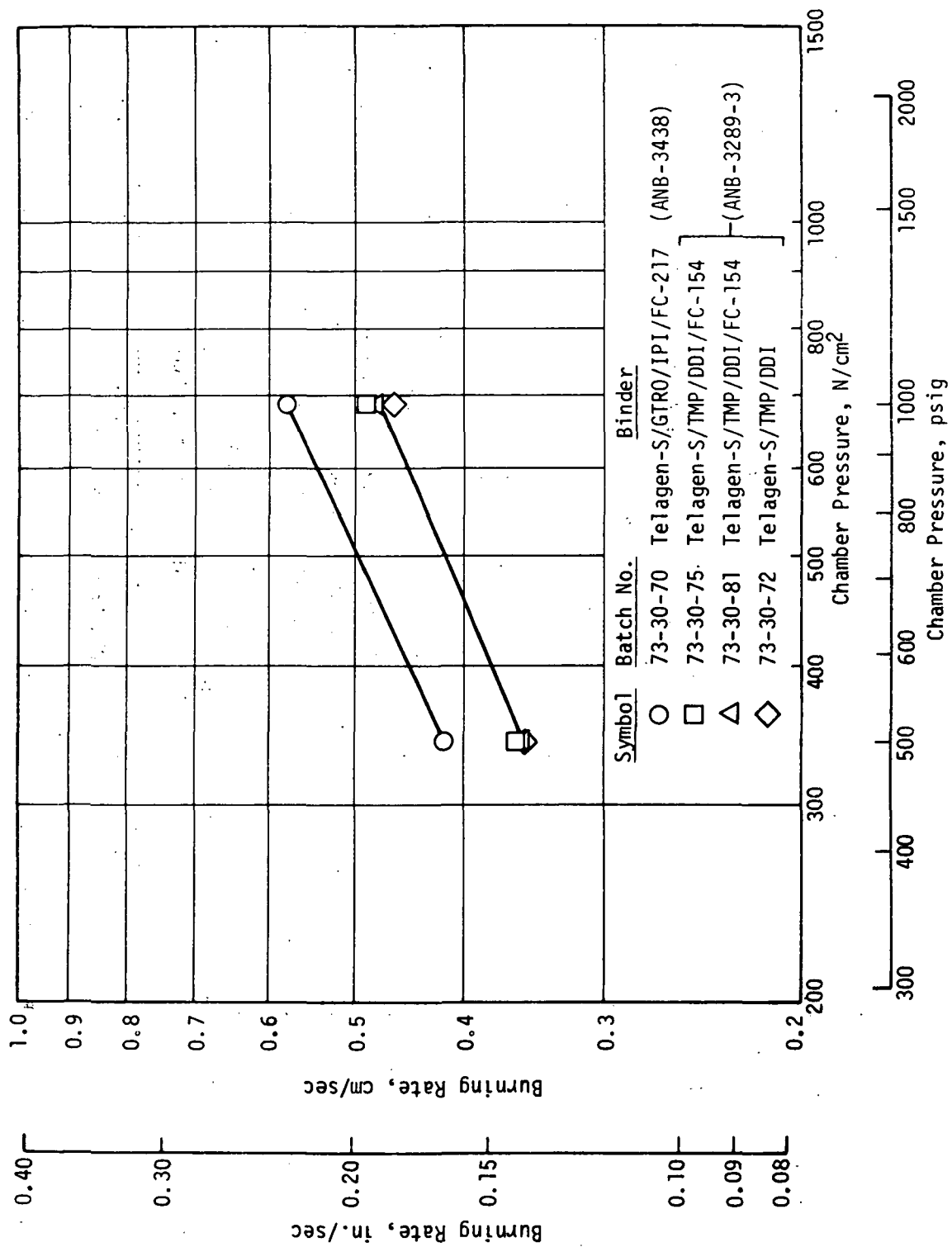
#### f. Heating Profiles Selected for Sterilization Tests

Three heating profiles were selected for the sterilization tests and are shown in Figure 57 through 59. The first (Figure 57) was the two-step temperature increment used in the earlier sterilization tests which resulted in a cracked grain (Batch 72-92). This heating cycle was selected to evaluate the effects of formulation modifications with respect to the performance of the original grain. A four-step temperature increment was chosen for the second heating profile (Figure 58) in order to lower the thermal stresses in the grains. The third heating profile (Figure 59) was that selected by JPL for the Capsule System Advanced



Liquid Strand Burning Rate (LSBR) of Propellant Prepared in 0.11 m³ (30-Gal) Vertical Mixer Batches

Figure 54



Solid Strand Burning Rate (SSBR) of Propellant Prepared in 0.11 in.<sup>3</sup> (30-Gallon) Vertical Mixer Batches.

Figure 55

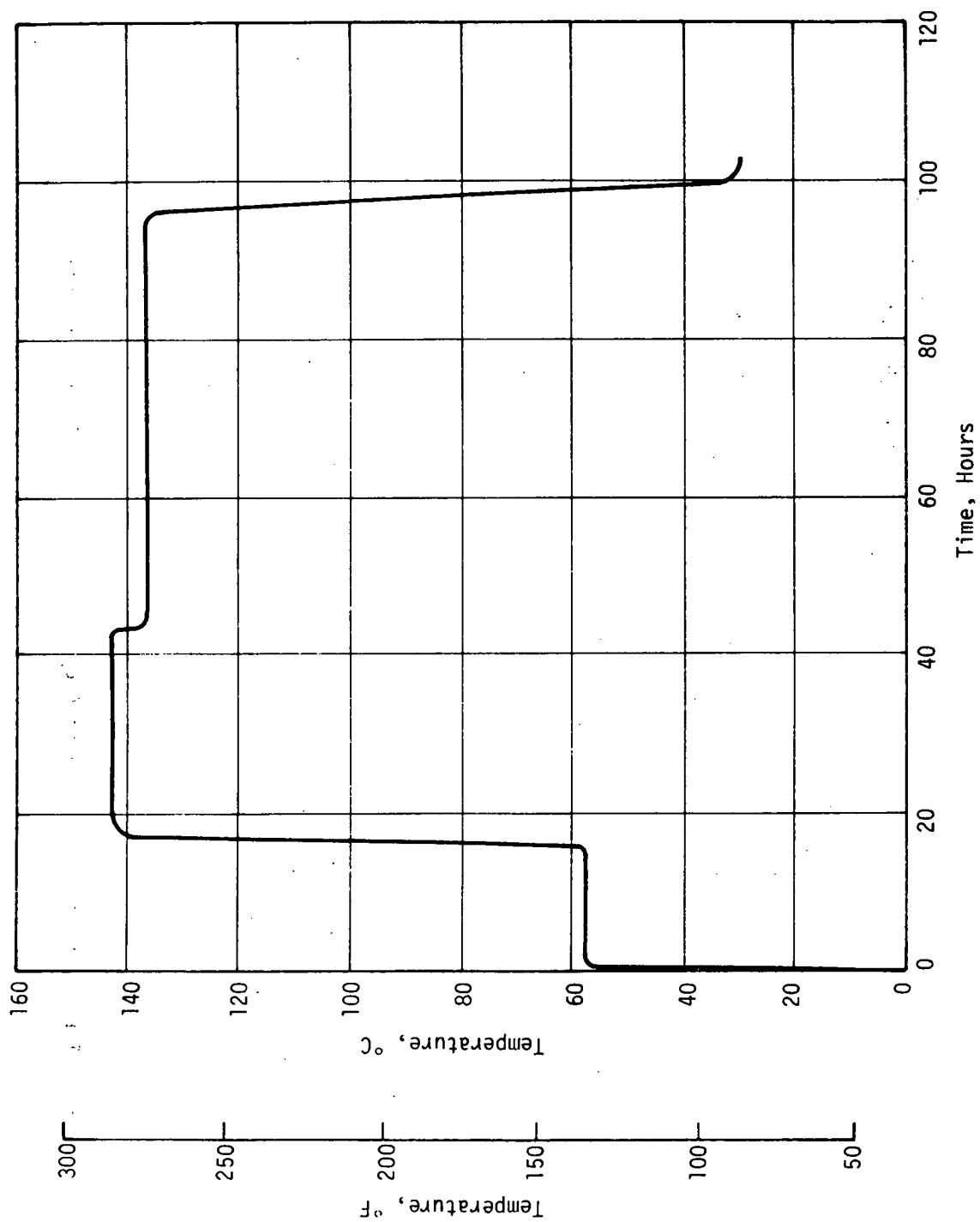


Batch	Equivalents of Crosslinker	Bonding Agent Used	Uniaxial Mechanical Properties At 25°C (77°F)			
			$\sigma_m$ , N/cm <sup>2</sup> (psi)		$\epsilon_m$ , %	$\epsilon_b$ , %
			$E_o$ , N/cm <sup>2</sup> (psi)			
73-30-70 <sup>(1)</sup>	TMP - 40	FC-217	115 (166)	30	46	1196 (1734)
73-30-75	40 -	FC-154	121 (176)	13	18	1452 (2105)
73-30-81	30 -	FC-154	106 (153)	20	28	1028 (1490)
73-80-82	30 -	-	97 (141)	24	38	914 (1325)

(1) Binder composed of Telagen-S, GTR0 and IPDI; the binders of the remaining batches contained Telagen-S, TMP, and DDI.

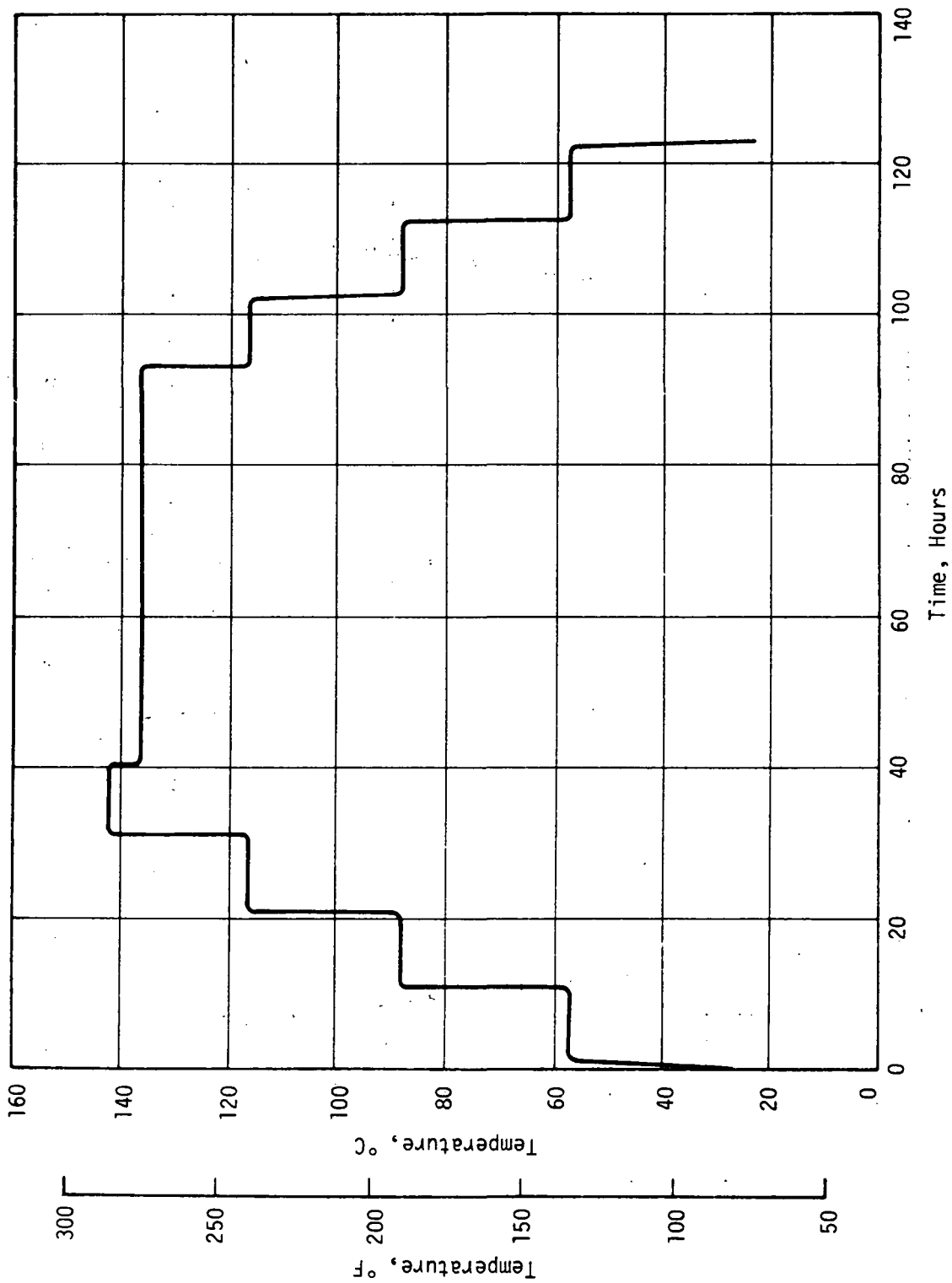
Mechanical Properties of Propellants Prepared in 0.11 m<sup>3</sup> (30 gal) Vertical Mixer

Figure 56

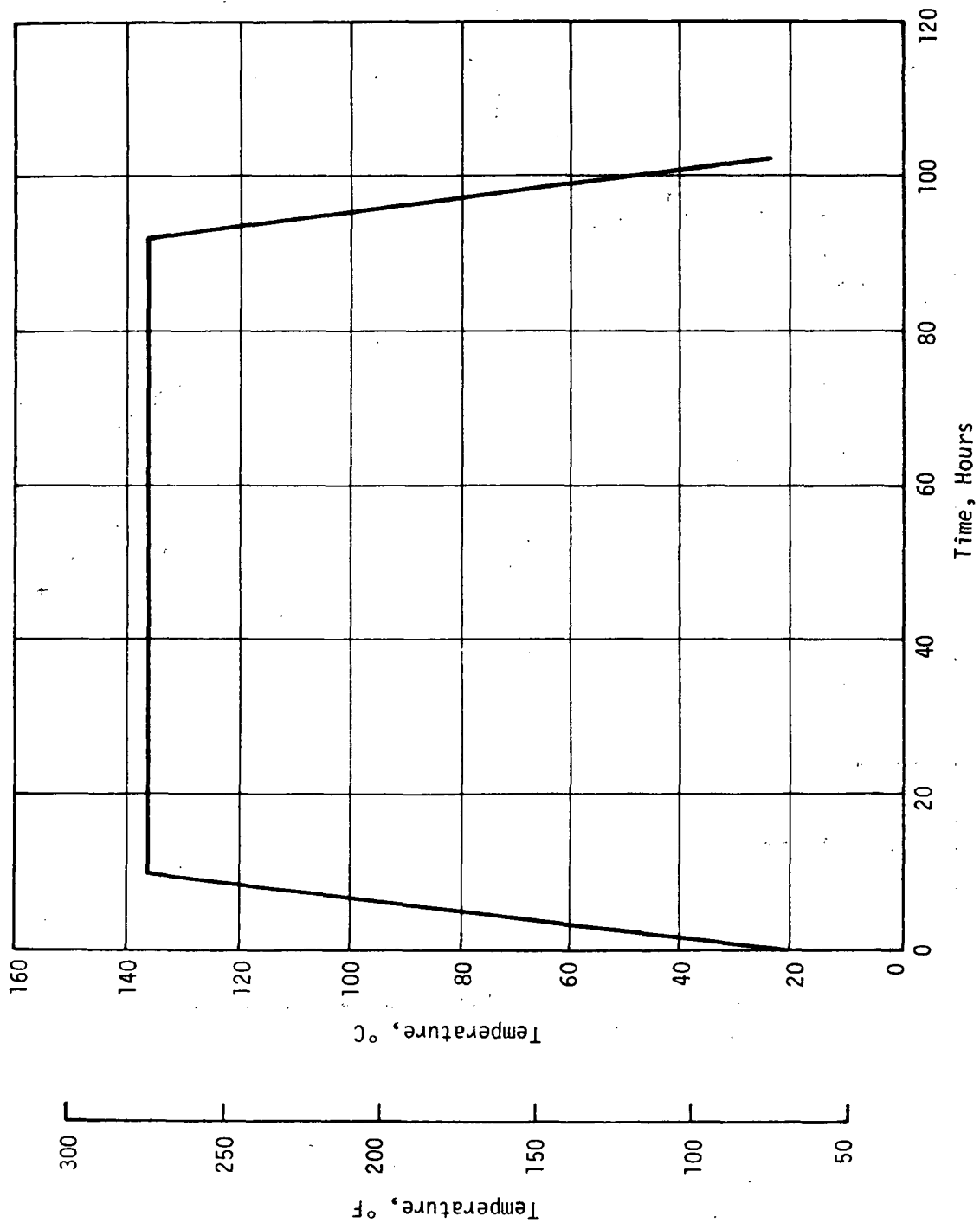


Oven Temperature Profile, Two-Step Heating Rate

Figure 57



Oven Temperature Profile, 4-Step Heating Rate



Oven Temperature Profile, Heating Rate of 11°C/hr (~20°F/Hr)

Figure 59

Development Sterilizable Program\*. The heating profiles associated with the grains of the different propellant batches are shown in Figure 60.

X-ray analysis indicated that the grains were void-free except for a few surface voids in Grains #1 and #2 of Batch 73-30-81 and a total of 8 voids ( $\leq 0.3$  cm (0.12-in.)-dia) in Grain #2 of Batch 73-30-82.

g. Heat Sterilization of 30.5 cm (12 in.)  
Diameter Grains

Representative oven and grain heating profiles for the different heating rates are shown in Figures 61 through 63. The results obtained from each test are tabulated in Figure 64. All the ANB-3289-3 grains prepared with the Telagen-S/TMP/DDI binder showed evidence of fissure when X-rayed after the second heat sterilization cycle. ANB-3438 propellant prepared with the Telagen-S/GTRO/IPDI/FC-217 binder (Batch 73-30-70) survived two sterilization cycles of the four-step heating/cooling sequence, but showed fissure formation when X-rayed after the fourth cycle.

The relative degree of severity of the fissuring observed in the large grains (Figure 64) indicate that the ANB-3438 (Batch 73-30-70) is far superior to the ANB-3289-3 propellants. Increasing the propellant modulus (Batch 73-30-75) reduced the severity of fissuring over that of the reference Batch (73-30-81), whereas eliminating the bonding agent (73-30-82) tended to increase the fissure content. With respect to heating rate, the two-step heat-up cycle was more severe than the four-step cycle. The  $11^{\circ}\text{C}$  ( $20^{\circ}\text{F}$ )/hour NASA heating cycle appeared to be slightly less severe than the four-step heating path.

---

\*A. R. Hoffman, J. T. Wang and M. R. Christensen, "Capsule System Advanced Development Sterilization Program," Technical Report 32-1320, Jet Propulsion Laboratory, Pasadena, California, October 15, 1969.

Propellant Batch and Grain Number	
73-30-81	73-30-82
73-30-70	73-30-75

Grain #C

### Heating Profile

Grain #1

Grain #B

2-Step

Grain #2

Grain #2

4-Step

Grain #1

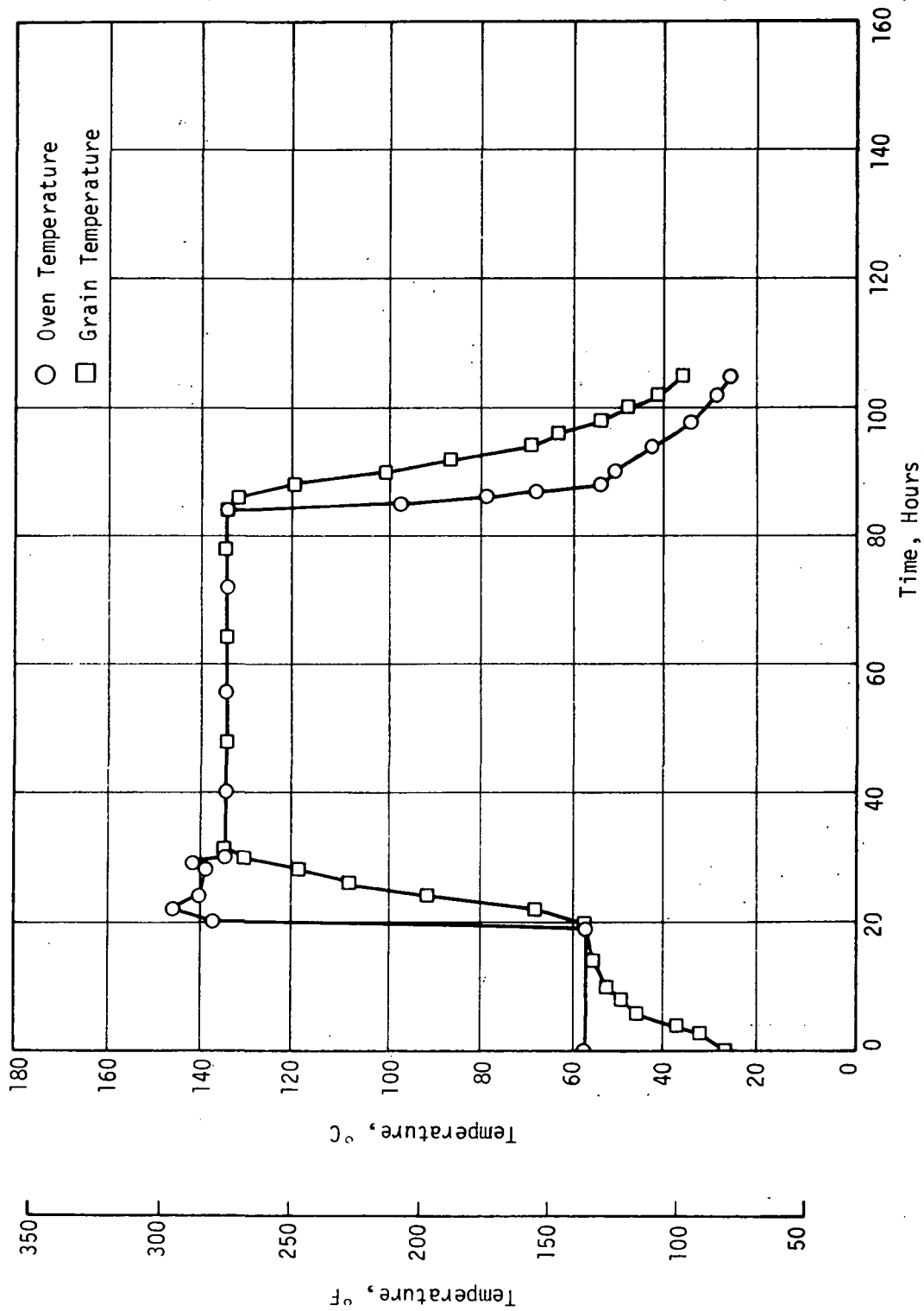
Grain #2

Grain #1

Grain #A

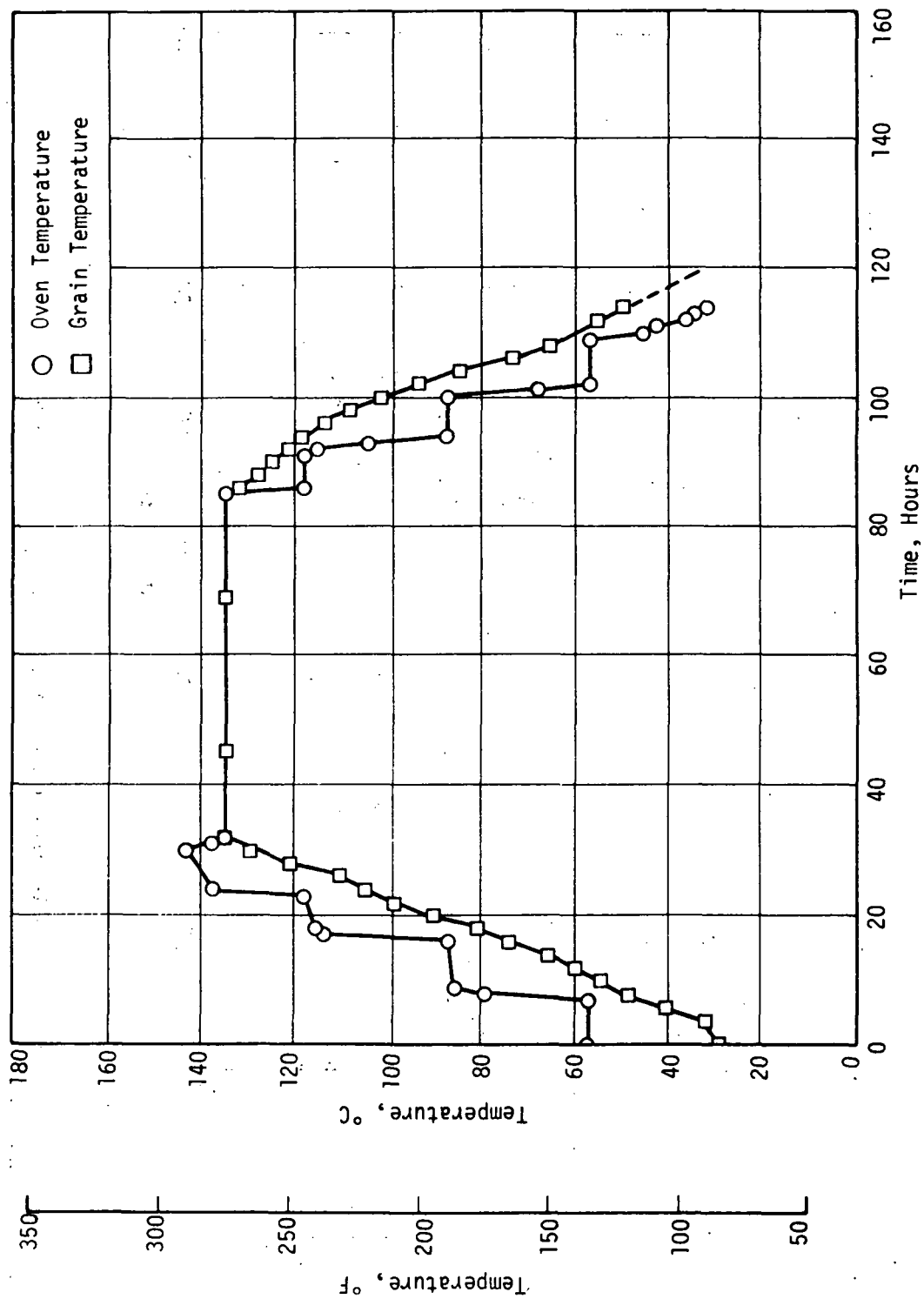
JPL Cycle ( $11 \pm 4^\circ\text{C/hr.}$ )

Large Grain Heat Sterilization Schedule



Oven and Grain Temperature Profile, Two-Step Heating Rate

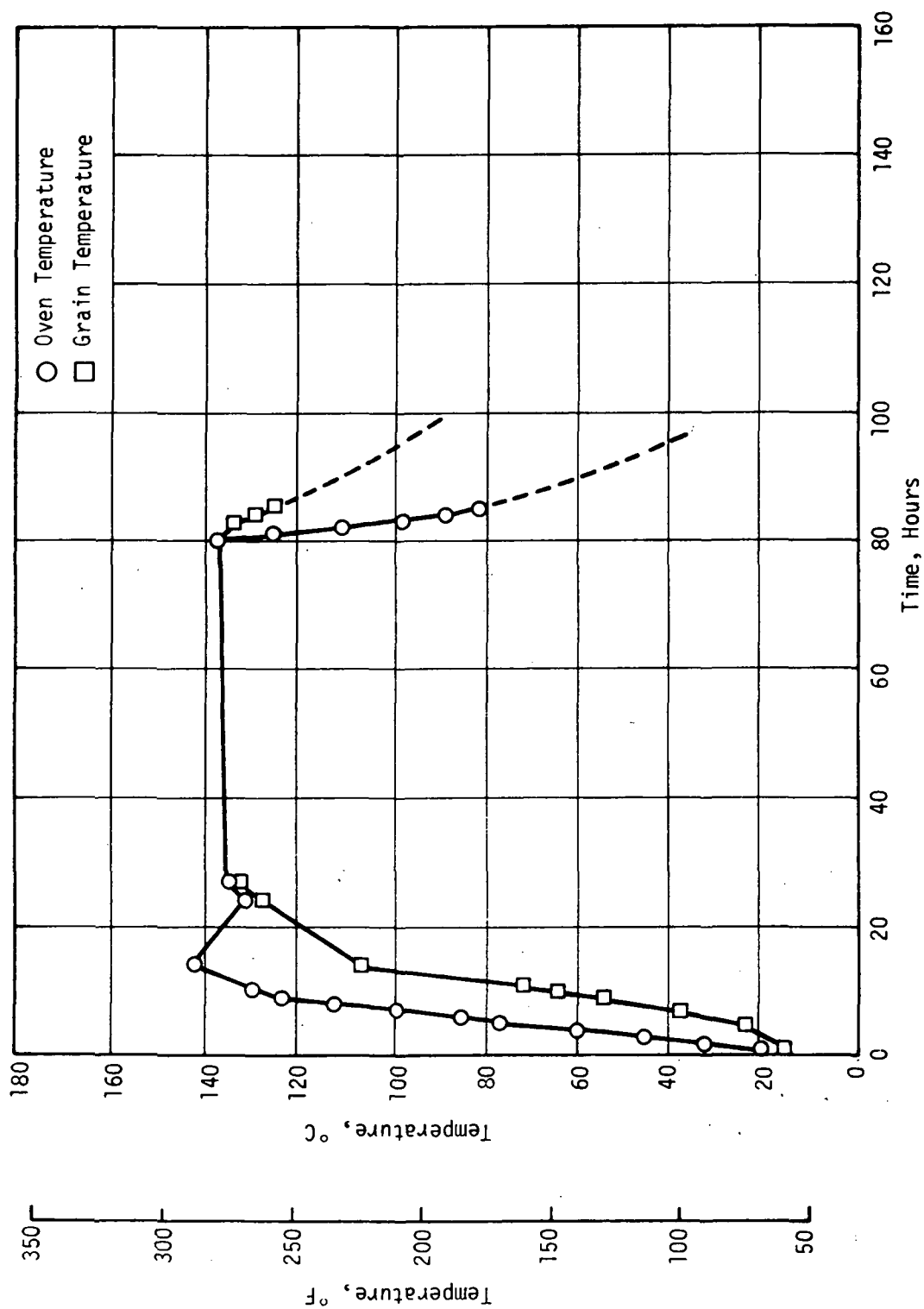
Figure 61



Oven and Grain Temperature Profile, 4-Step Heating Rate

Figure 62





Grain Temperature Profile at Oven Heating Rate of 11°C/hr (20°F/hr)

Figure 63

Batch	Grain No.	Grain Size	Oven Heating Rate	Cycle Number at Which Cracks Observed						Relative Severity of Fissure Occurrence (1)
				2	4	5	6			
72-92	1	15	2 step (2)	-	-	-	(3)	-	-	-
73-30-75	C	12	2 step	x	-	-	-	-	-	3
73-30-82	1	12	2 step	x	-	-	-	-	-	7
73-30-70	2	12	4 step	-	x	-	-	-	-	1
73-30-75	B	12	4 step	x	-	-	-	-	-	2
73-30-81	2	12	4 step	x	-	-	-	-	-	5
73-30-75	A	12	11°C (20°F)/Hr	x	-	-	-	-	-	2
73-30-81	1	12	11°C (20°F)/Hr	x	-	-	-	-	-	4
73-30-82	2	12	11°C (20°F)/Hr	x	-	-	-	-	-	6

(1) Based on a rating of 1 for least severe to 7 for most severe.

(2) 2 step: 27° to 57°C (80° to 135°F), then 57° to 135°C (135° to 275°F).

4 step: 27° to 57°C (80° to 135°F), 57° to 88°C (135° to 190°F), 80° to 116°C (190° to 240°F), 116° to 135°C (240° to 275°F).

(3) Grain was not X-rayed until 5th cycle, at which time it was badly fissured.

Results of Heat Sterilization Tests of Large Grains

Figure 64

h. Heat Sterilization of 24 cm (9.25 in.) Diameter Grains

One of the two grains of ANB-3438 propellant, which had successfully passed two cycles utilizing the 11°C (20°F)/hour oven heating rate, was reduced in diameter from 30.5 (12 in.) to 24 cm (9.25 in.). This was done to more closely duplicate the design web thickness of the demonstration motor (11.745 cm (4.625 in.)). Reducing the grain diameter also lowered the thermal stresses during heat-up. This reduced-diameter grain was then subjected to five more heat sterilization cycles (11°C (20°F)/hour heat-up rate) to a total of seven cycles without indication of fissure formation.

In order to provide greater confidence that the demonstration motor would successfully survive heat sterilization, an additional 24 cm (9.25 in.) dia. by 24 cm (9.25 in.) long grain of ANB-3438 propellant was prepared from a 27 Kg (60-lb) batch (73-05-121) using 100% stabilized oxidizer. All ingredients employed were from the same lot to be used in preparing propellant for the full-scale motors. The GTR0 level was increased slightly to yield a higher initial modulus (1380 N/cm<sup>2</sup> (~2000 psi), since the sterilization tests discussed above indicated that the high-modulus propellant fissured less than those with lower moduli. This grain was subjected to eight heat sterilization cycles (53 hours each at 135°C (275°F)) before failure was detected through X-ray analysis.

Mechanical properties were also measured on propellant taken from this large 24 cm (9.25 in.) -dia. grain after the eight sterilization cycles, but well removed from the cracked area. The properties are compared to those obtained from the small propellant grains in Figure 65. There was a sizeable increase in tensile and modulus values after the six sterilization cycles performed with the 7.6 cm x 7.6 cm x 12.7 cm (3 in. x 3 in. x 5 in.) block. This was consistent with the previously

Sample Dimensions	No. of Heat Sterilization Cycles (53 hrs ea at 135°C (275°F))	Uniaxial Tensile Properties at 25°C (77°F)				
		$\sigma_m$ , N/cm <sup>2</sup>	$\epsilon_m$ , %	$\epsilon_b$ , %	$E_o$ , N/cm <sup>2</sup>	
		(psi)				(psi)
-	0	115 (166)	30	46	1196	(1734)
7.6 cm x 7.6 cm x 12.7 cm (3-in. x 3-in. x 5-in.)	6	204 (296)	21	27	1984	(2875)
23 cm (9-in.) x 23 cm (9-in.) Cylinder	8	104 (150)	26	29	823	(1193)

(1) Batch 73-30-70

Effect of Heat Sterilization on Mechanical Properties of ANB-3438 Propellant<sup>(1)</sup>

Figure 65

observed behavior of ANB-3438. In the large grain, however, there was a decrease in tensile properties after eight cycles, compared to the initial unsterilized values. This decrease in properties is approximately equal to 50% of those observed after the six sterilization cycles using the small size block. It appears unlikely that the tensile properties would degrade so extensively due to the two additional heating cycles alone. In addition to the heat exposure a sizeable contribution to the degradation of the propellant properties undoubtedly arises from the thermal stresses and the associated cumulative damage effects which arise during the heat sterilization of the larger grain. This behavior emphasizes the need for using sample sizes which are representative of the test motor dimensions in order to obtain meaningful heat sterilization data.

#### D. DEMONSTRATION MOTOR PROCESSING AND HEAT STERILIZATION

##### 1. Demonstration Motor Processing

The two SVM-3 insulated motor chambers were heat sterilized, lined with SD-886, resterilized, and cast with ANB-3438 propellant prepared in a 198 Kg (435-lb) batch mix. Details are presented in the following paragraphs.

##### a. Processing of Insulated SVM-3 Chambers

The two SVM-3 motor chambers which had been previously insulated with V-4030 were subjected to final preparation prior to propellant casting. This consisted of the following sequential operations.

(1) Abrading the surface of the V-4030 rubber to remove surface contaminants which might interfere with liner/rubber bonding.

(2) Heat sterilizing the insulated motor cases for 24 hours at 135°C (275°F) to remove volatiles in the V-4030.

(3) Wiping the surface of the V-4030 with chlorothene to remove adhering volatiles driven out during sterilization.

(4) Drying the chambers at 57°C (135°F) to remove chlorothene solvent.

After the completion of the above operations, the motor was lined with SD-886, applied in two coats to give a liner thickness of 0.038 cm (15 mils). The first coat was cured at 57°C (135°F) prior to the application of the second coat. After cure of the second coat, the lined chamber was again heat sterilized at

135°C (275°F) for 24 hours prior to loading with propellant.

b. Propellant Mixing

A 198 kg (435-lb) batch of ANB-3438 propellant was mixed for loading the motors and preparing samples for additional tests. This batch contained 100% stabilized oxidizer. Submix and premix analyses are compared with previous batches of ANB-3438 propellant in Figure 66. The viscosity buildup at both low and high shear stress levels is shown in Figure 67. The excellent processability that is typical of this propellant is evidenced in the low initial viscosities vs shear-stress curves (Newtonian viscosity) and long potlife (>15 hours at 57°C (135°F)).

The uncured strand burning rate curve of the propellant is presented in Figure 68. The rates are essentially identical to those obtained in a previously prepared 73-Kg (160-lb) batch of ANB-3438 propellant (batch 73-30-70).

The propellant was cast into the two SD-886-lined SVM-3 motors using the standard vacuum casting method with vibration applied to the vacuum bell.

2. Heat Sterilization of Demonstration Motors

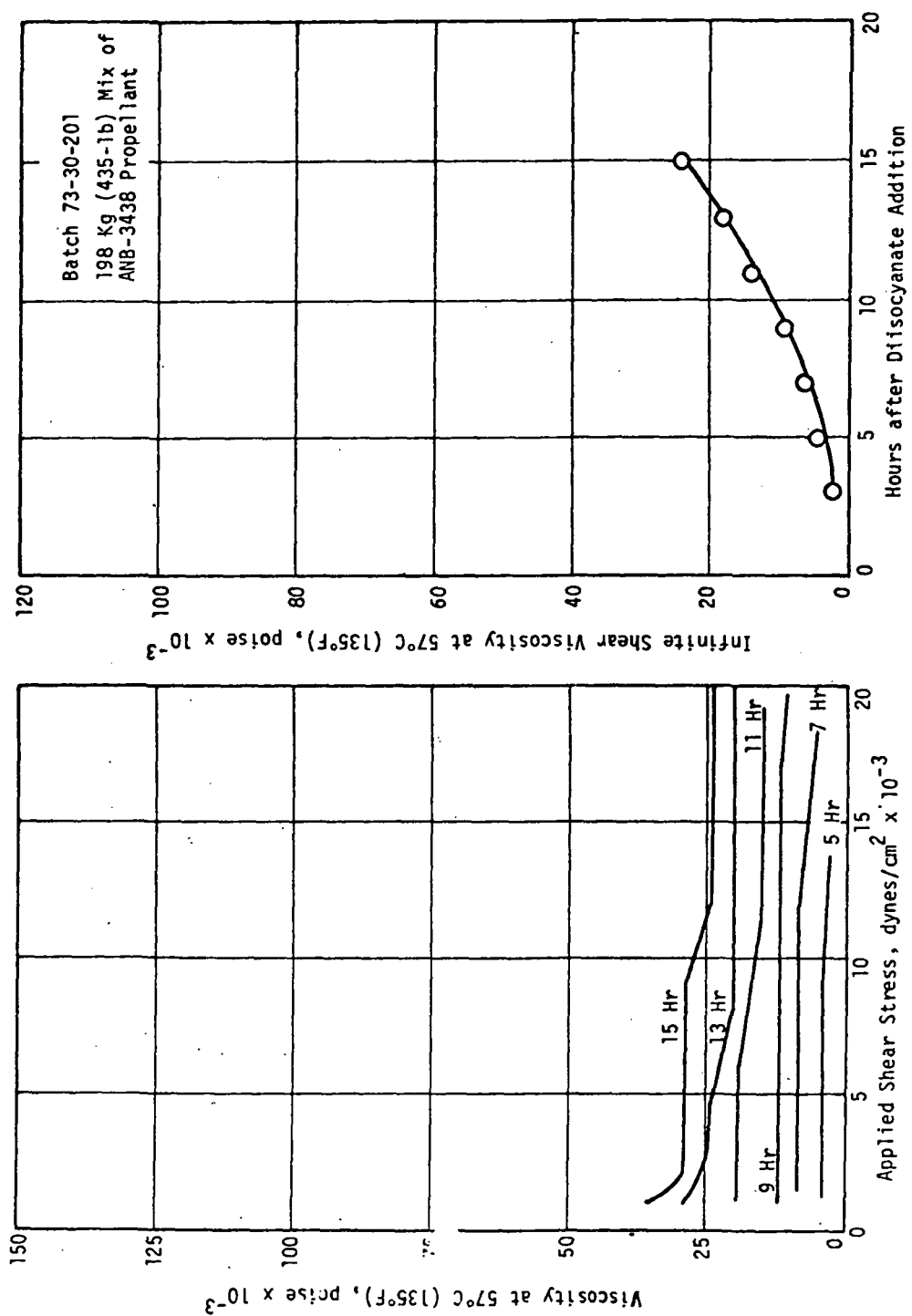
Upon direction from the Program Office (JPL) the heat sterilization procedure was modified as follows: the first motor SVM-3 No. 1 was heat sterilized by exposure to six cycles of 53 hours each at 135°C (275°F). The second motor, SVM-3 No. 2 received three cycles at 125°C (257°F) of 54 hours each, followed by five cycles of 40 hours each at 125°C (257°F). The first motor was x-rayed after each cycle at 135°C (275°F), and the second motor was x-rayed after the 3rd, 6th and 8th cycle at 125°C (257°F).

<u>BATCH</u>	73-05-121	73-30-70	73-30-201
<u>BATCH SIZE</u>	27 Kg (60-1b)	73 Kg (160-1b)	198 Kg (435-1b)
<u>SUBMIX</u>			
Moisture, Wt%	0.017	0.021	0.022
OH Number	72.46	71.90	71.48
Refractive Index	-	1.4792	1.4780
Density, g/cc	-	0.882	0.882
<u>PREMIX</u>			
Moisture, Wt%	0.016	0.019	0.016
Density, g/cc	1.429	1.426	1.429
Solids, Wt%	-	-	56.80
<u>OXIDIZER</u>			
Moisture, Wt%	-	0.009	0.01
<u>UNCURED PROPELLANT</u>			
Density, g/cc	-	1.719	1.719
Solids, Wt%	-	-	84.07 (84.00 Theo)

Analytical Data from ANB-3438 Propellant Prepared  
in 0.02 m<sup>3</sup> (5-gal) and 0.11 m<sup>3</sup> (30-gal) Batches

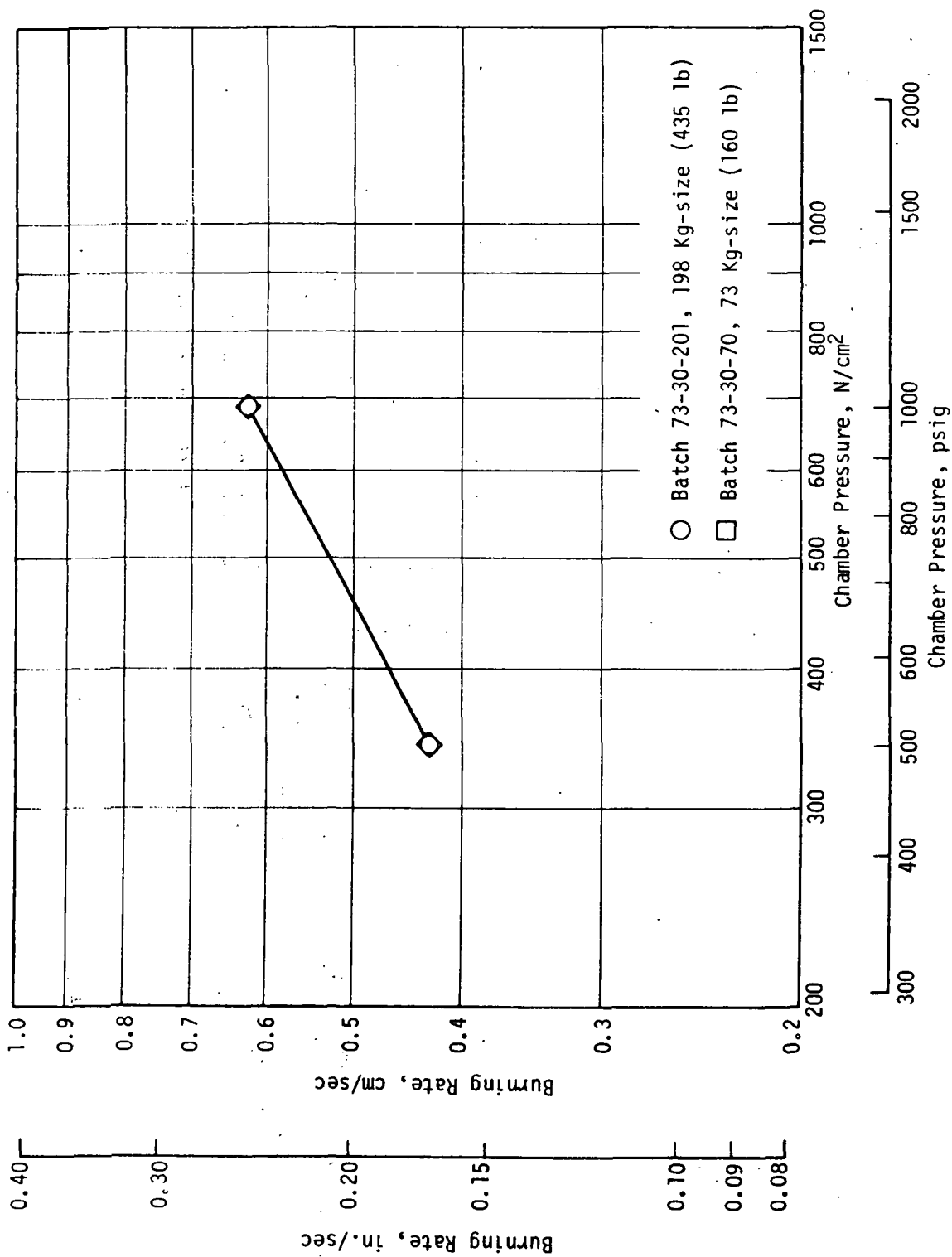
Figure 66





Propellant Viscosity as a Function of Shear Stress and Time from Curing Agent Addition

Figure 67



Liquid Strand Burning Rates of ANB-3438 Propellant

Figure 68

a. X-ray and Machining

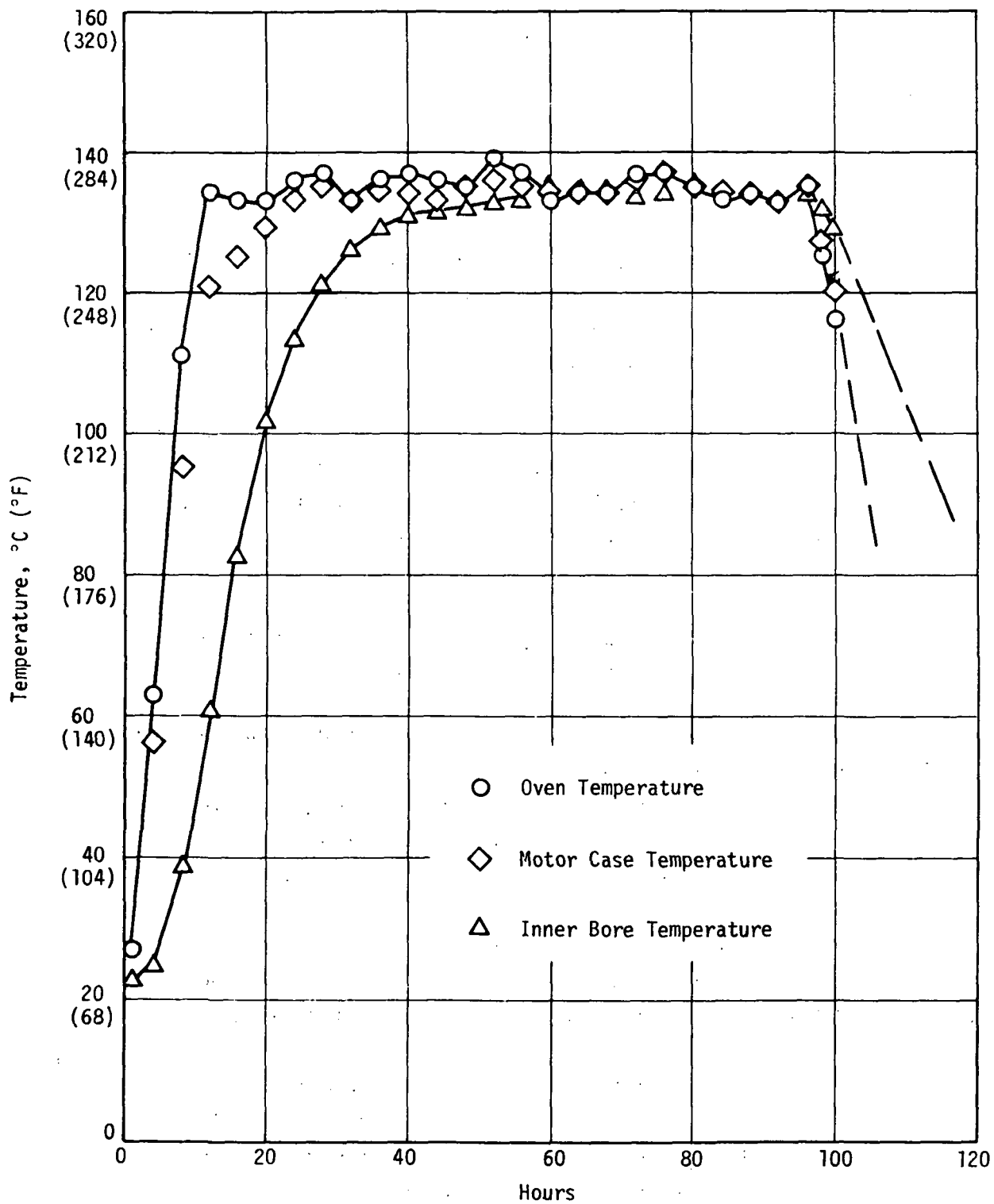
The two SVM-3 motors containing ANB-3438 propellant were cured at 135°F. After cure the motors were x-rayed at 0°, 30°, 60°, 90°, 120°, 150° and 180° rotation; 0° and 90° at the head end and also through the motor along the thrust axis. No voids or liner/propellant separations were observed. The bore configuration shown in Figure 18 was machined and the internal dimensions were taken prior to starting the heat sterilization tests.

The motor temperatures during sterilization were monitored by placing thermocouples on the outer case wall and at the inner bore surface of the propellant grain. The zero start time for the heat sterilization cycle was taken at the time when the inner bore surface came within 2°C of the sterilization temperature.

b. Heat Sterilization of Demonstration Motor No. 1  
at 135°C (275°F)

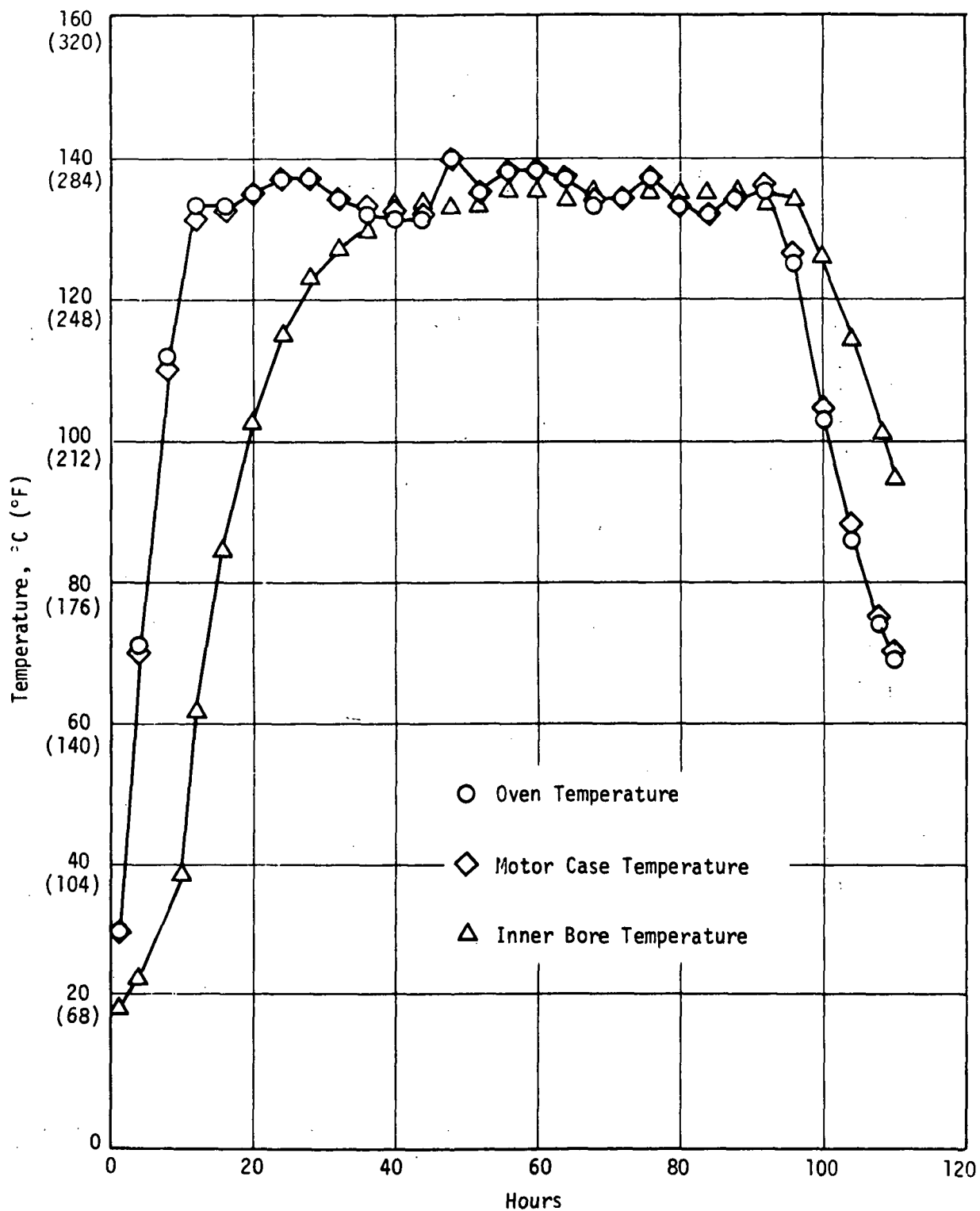
The time/temperature heating profiles of the oven, external motor case, and grain inner bore are shown in Figures 69 through 74 for the six heat sterilization cycles (53 hours each) conducted at 135°C (275°F). The cyclic nature of the oven heating curve is due to the Chromolox heater controlling unit which operates in an intermittent manner. Oven heat-up was accomplished in approximately 10 hours and the total motor exposure time is about 80 hours/cycle at 135°C (275°F). A recorder malfunction during the third cycle (Figure 71) prevented a complete temperature profile being taken of the grain inner bore.

After the fourth heat sterilization cycle at 135°C (275°F), a small crack, ~1 inch long, was observed near the center at the inner bore. The appearance and location of the fissure indicate it was not due to heat degradation of the propellant. Close reinspection of X-rays taken after the third cycle revealed a slight cloudiness in the



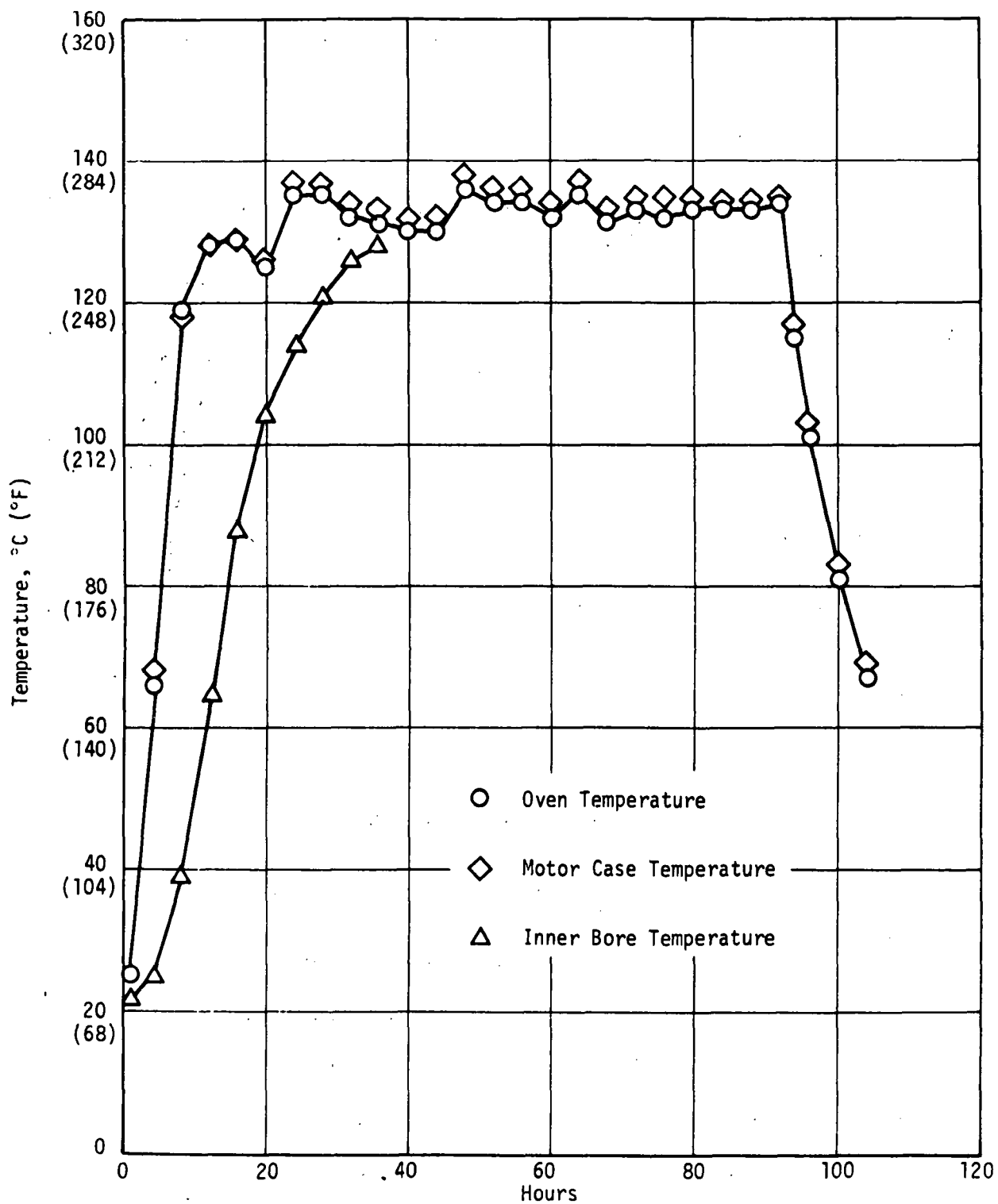
Heat Sterilization Cycle No. 1 at 135°C (275°F) Demonstration Motor No. 1

Figure 69



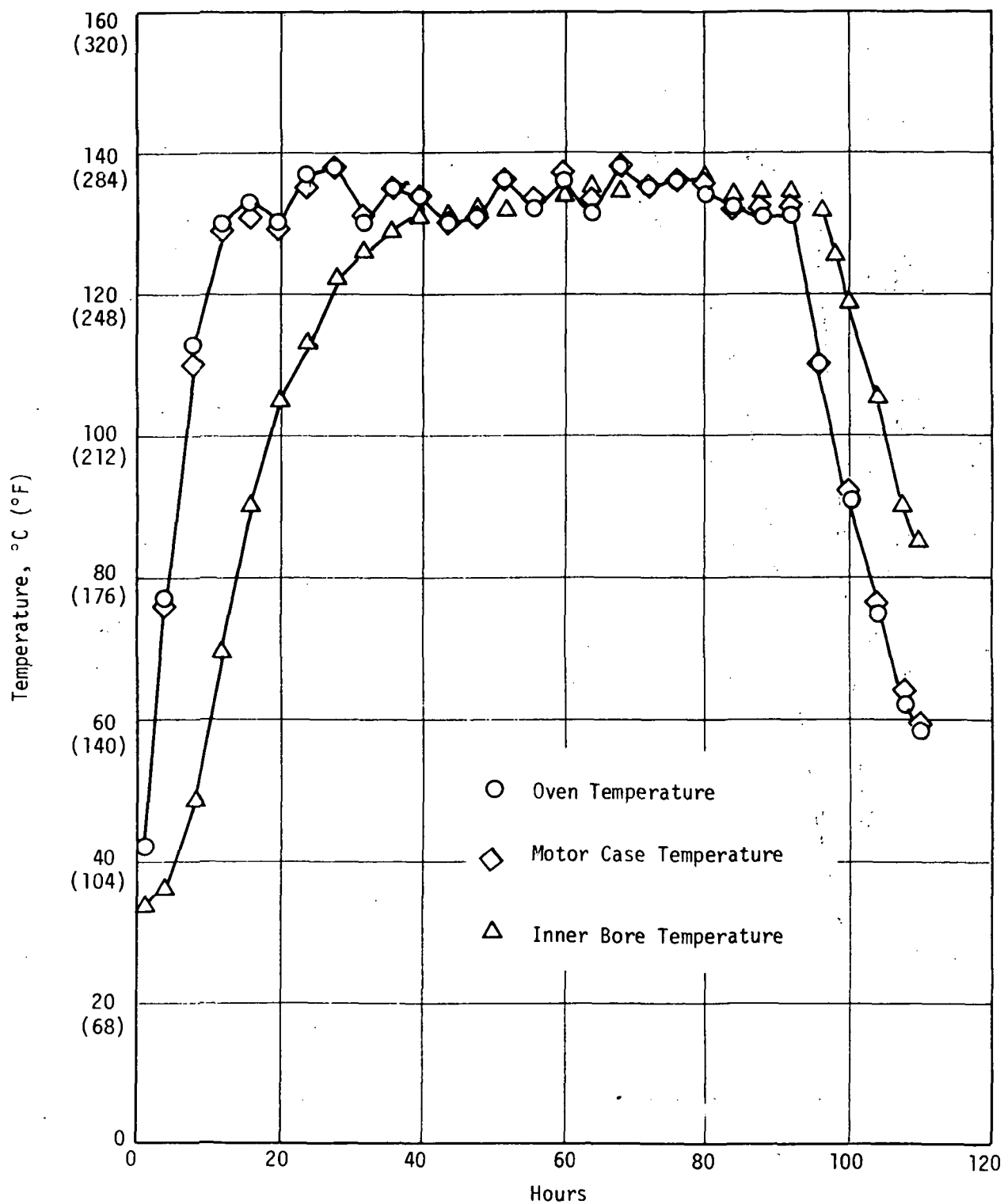
Heat Sterilization Cycle No. 2 at 135°C (275°F) Demonstration Motor No. 1

Figure 70



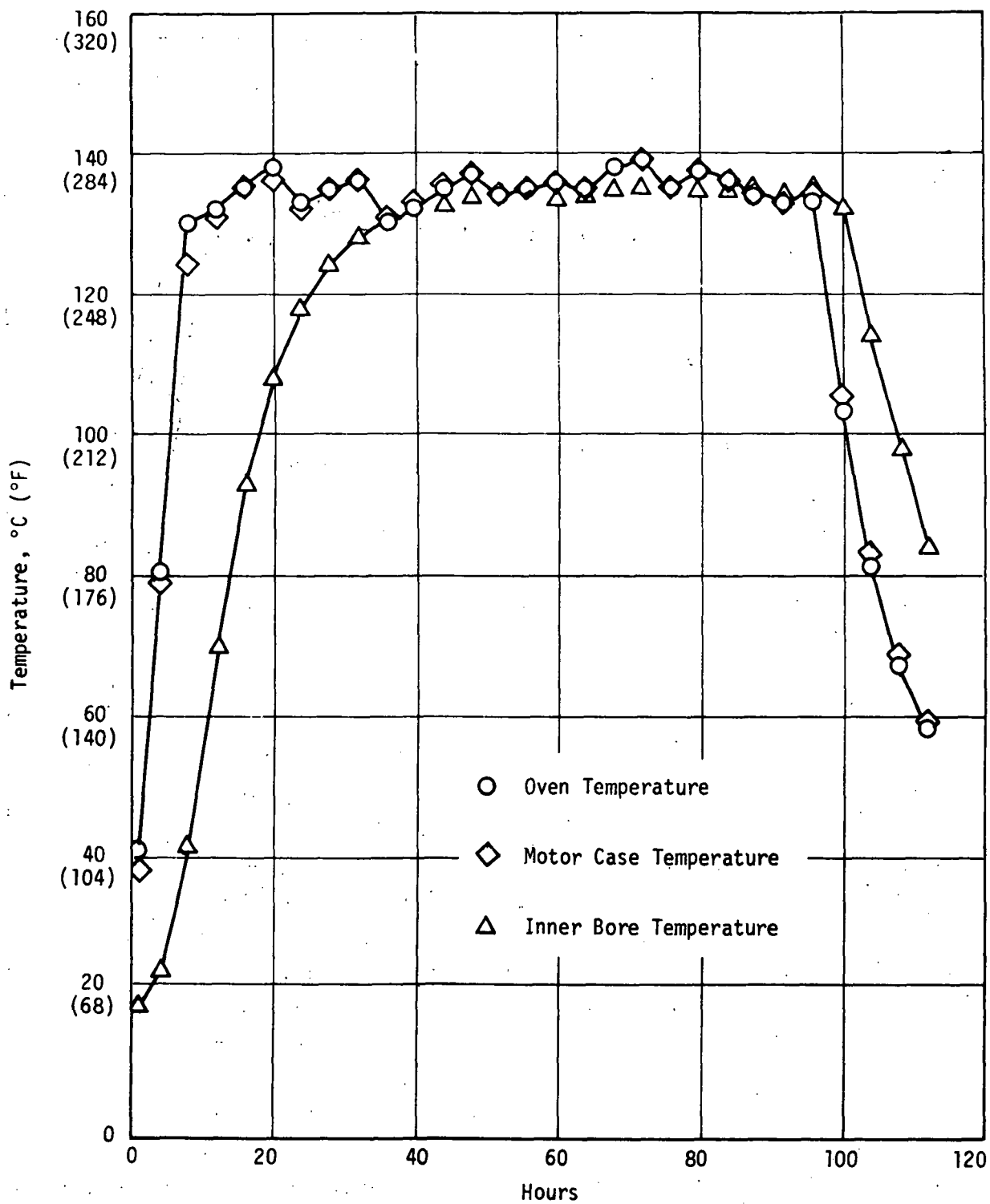
Heat Sterilization Cycle No. 3 at 135°C (275°F) Demonstration Motor No. 1

Figure 71



Heat Sterilization Cycle No. 4 at 135°C (275°F) Demonstration Motor No. 1

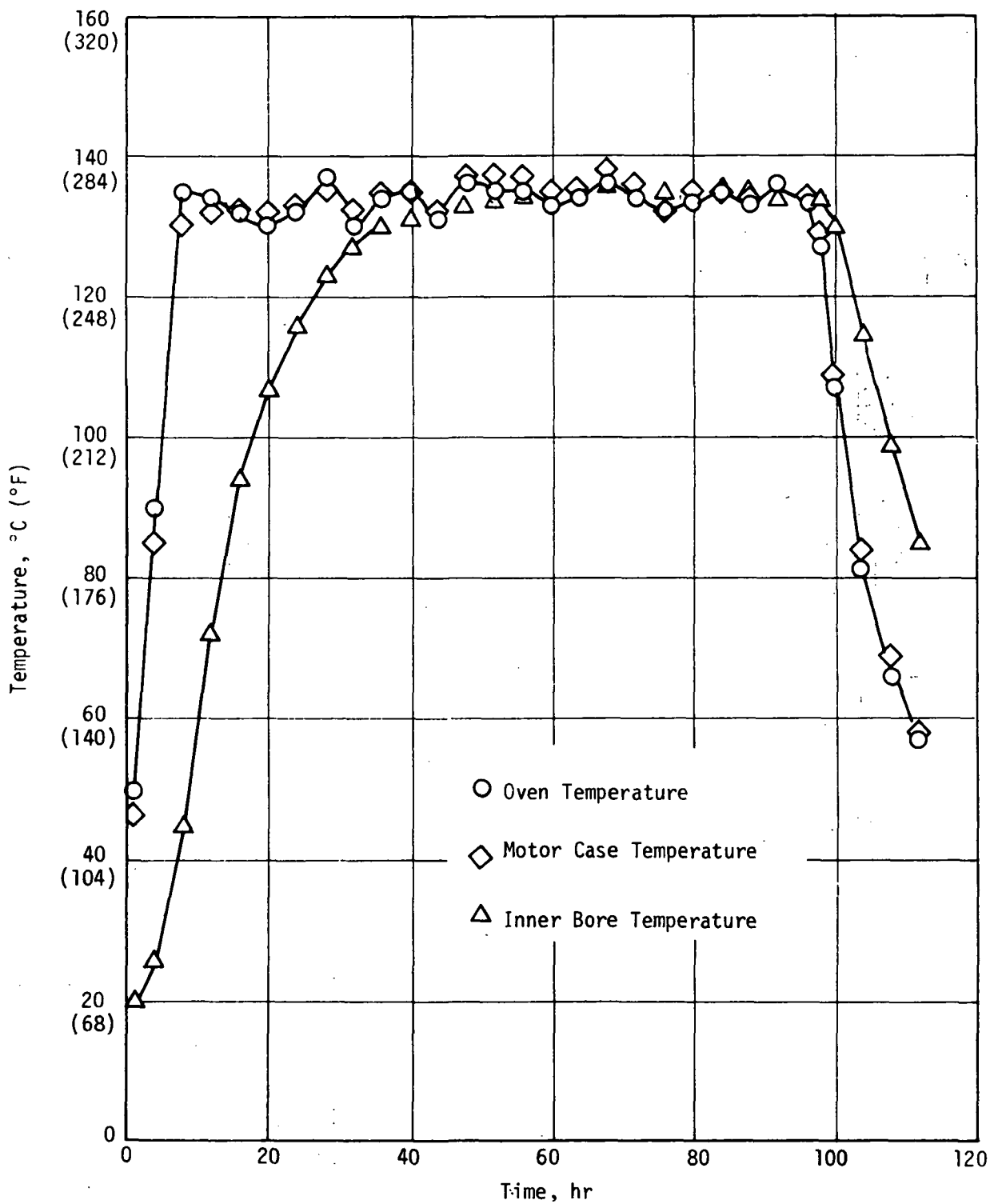
Figure 72



Heat Sterilization Cycle No. 5 at 135°C (275°F) Demonstration Motor No. 1

Figure 73





Heat Sterilization Cycle No. 6 at 135°C (275°F) Demonstration Motor No. 1

Figure 74

same area. The crack broke through the surface during the fifth cycle and remained unchanged during the sixth. No other defects or grain separations could be observed in the X-rays.

c. Heat Sterilization of Demonstration Motor No. 2  
at 125°C (257°F)

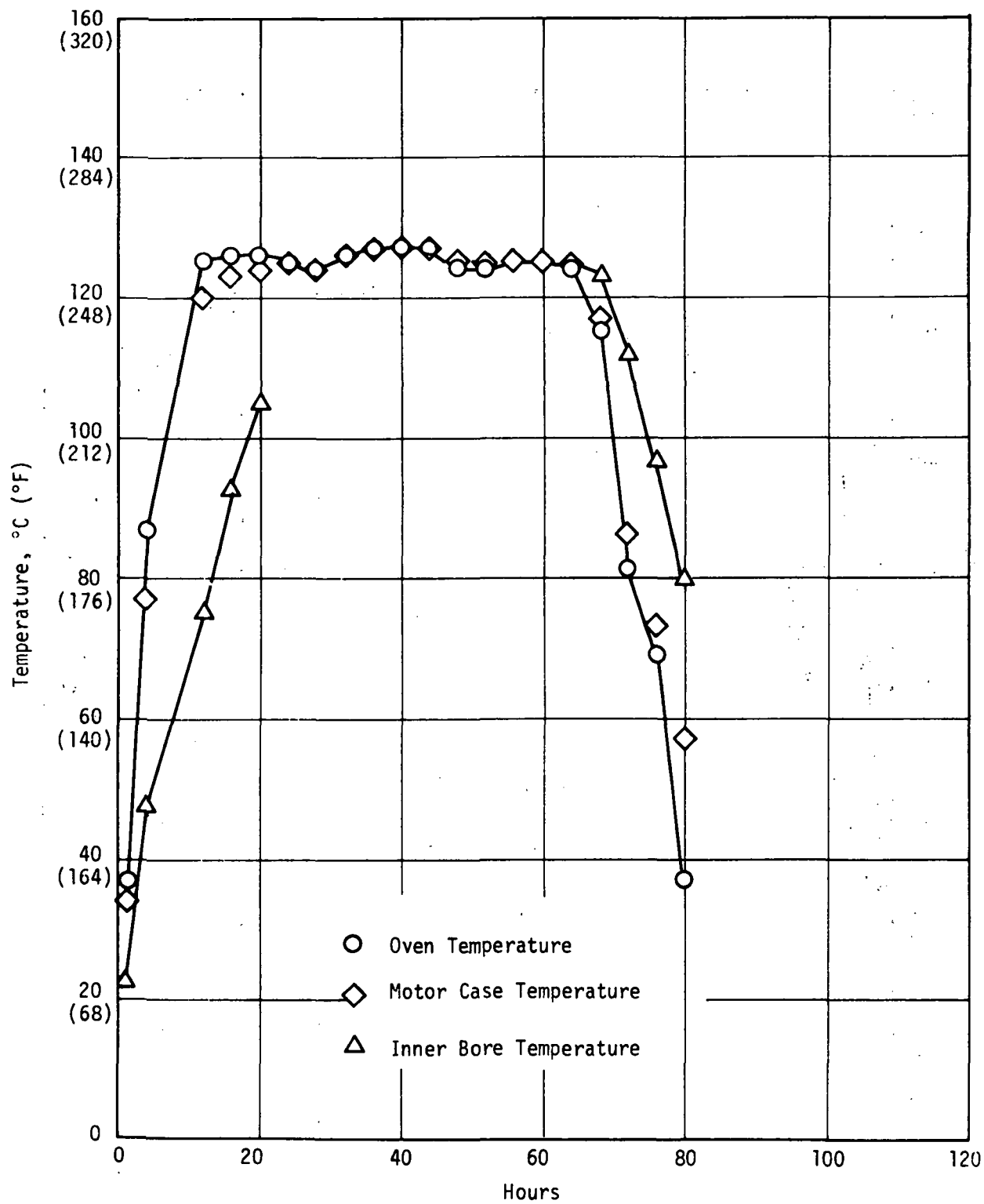
The heat sterilization requirements for Demonstration Motor No. 2 were three 54-hr cycles at 125°C (257°F) followed by five 40-hr cycles at 125°C (257°F). The time/temperature profiles for the oven, external case and inner grain bore are shown in Figures 75 through 82. A temperature recorder malfunction resulted in the first cycle being terminated approximately 30 hours too soon (Figure 75). To compensate for this loss of time, the motor was subjected to 20 extra hours heat exposure during the second cycle (Figure 76). The motor was X-rayed after the 3rd, 6th and 8th heat sterilization cycles and was found to be free of voids and fissures with no indication of propellant-to-liner separation. The effect of the heat sterilization on the grain dimensions of the motor were minimal as shown in Figure 83. The greatest change was in the slot diameter, approximately 1% shrinkage.

3. Selection of Motor for Static Test Firing

With the concurrence of the JPL it was decided to test fire Demonstration Motor No. 2. Demonstration Motor No. 1 will be used in another program to determine environmental effects on a heat sterilized motor and propellant.

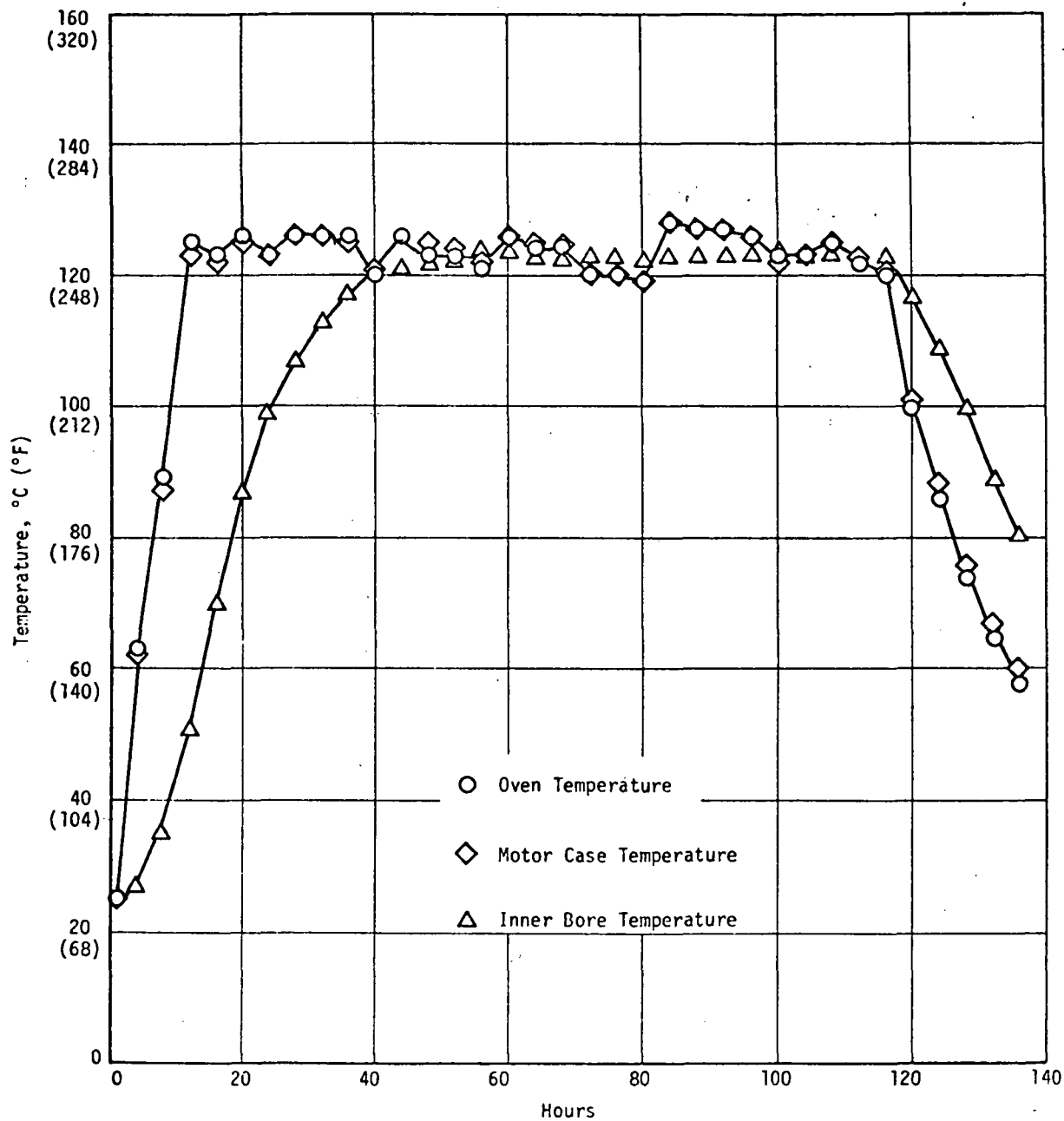
4. Testing of Small-Size Samples

Supportive testing was performed on samples prepared from the propellant batch (73-30-201) used to cast the demonstration motors. Details are presented in the following paragraphs.



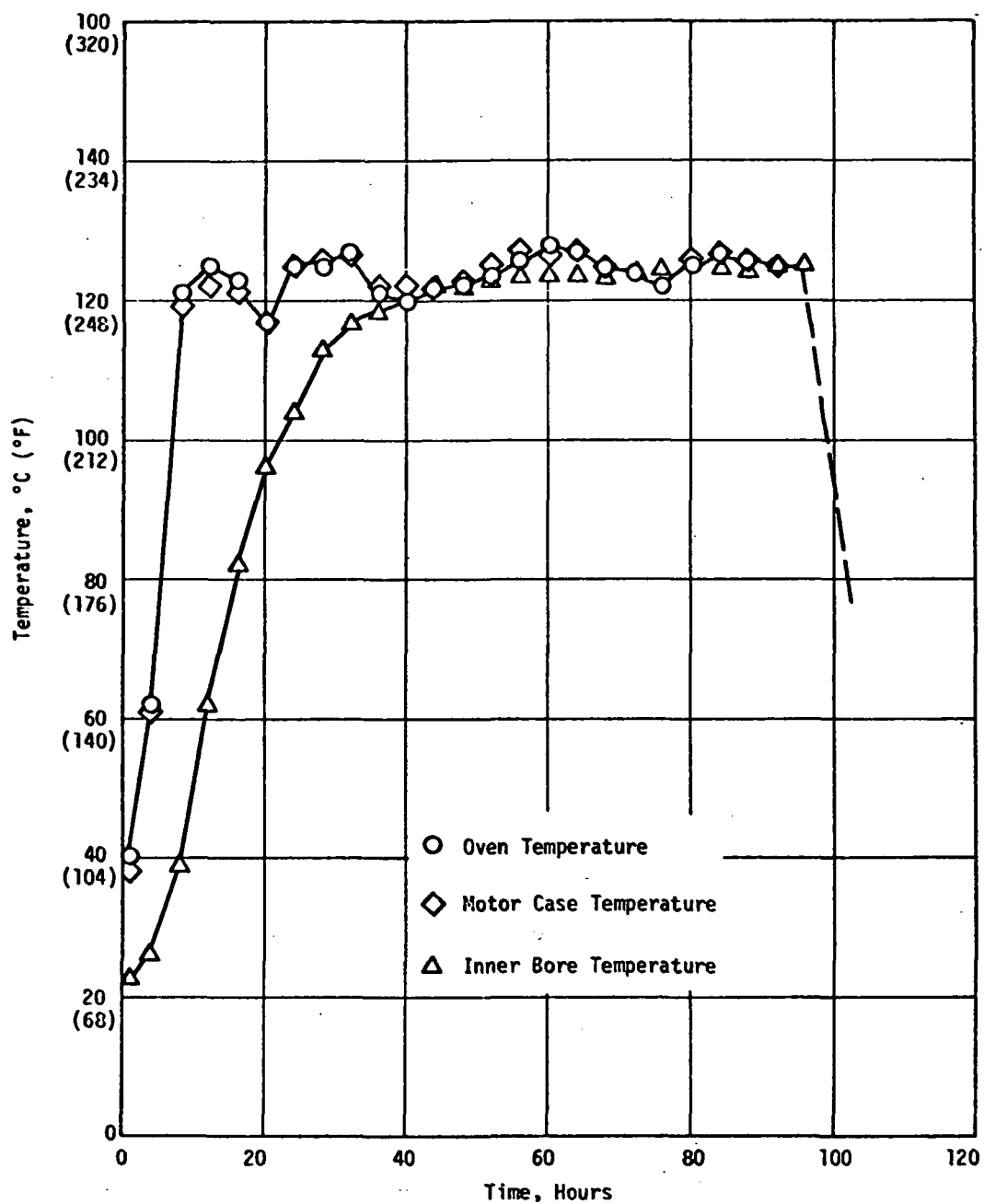
Heat Sterilization Cycle No. 1 at 125°C (257°F) Demonstration Motor No. 2

Figure 75



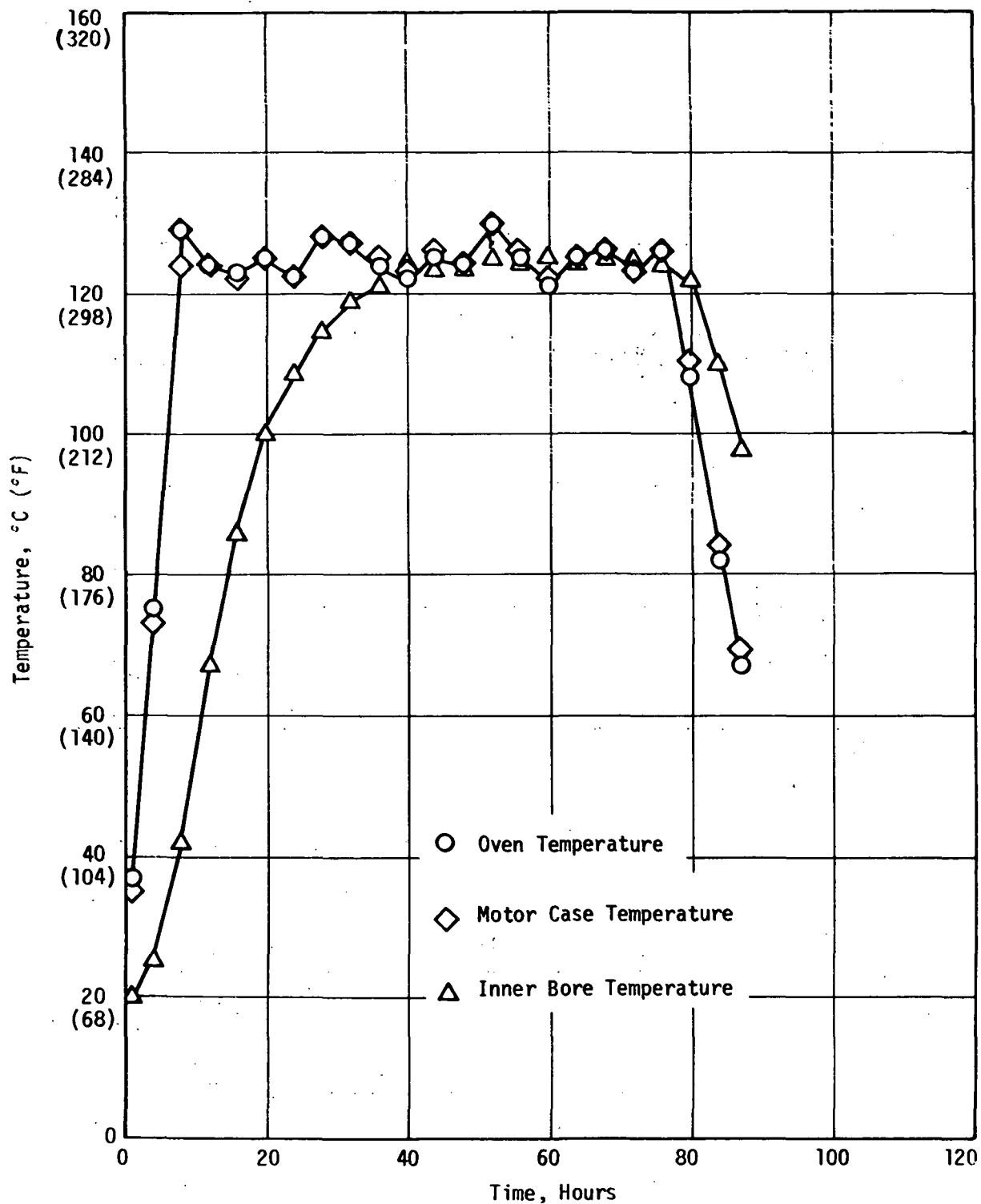
Heat Sterilization Cycle No. 2 at 125°C (257°F) Demonstration Motor No. 2.

Figure 76



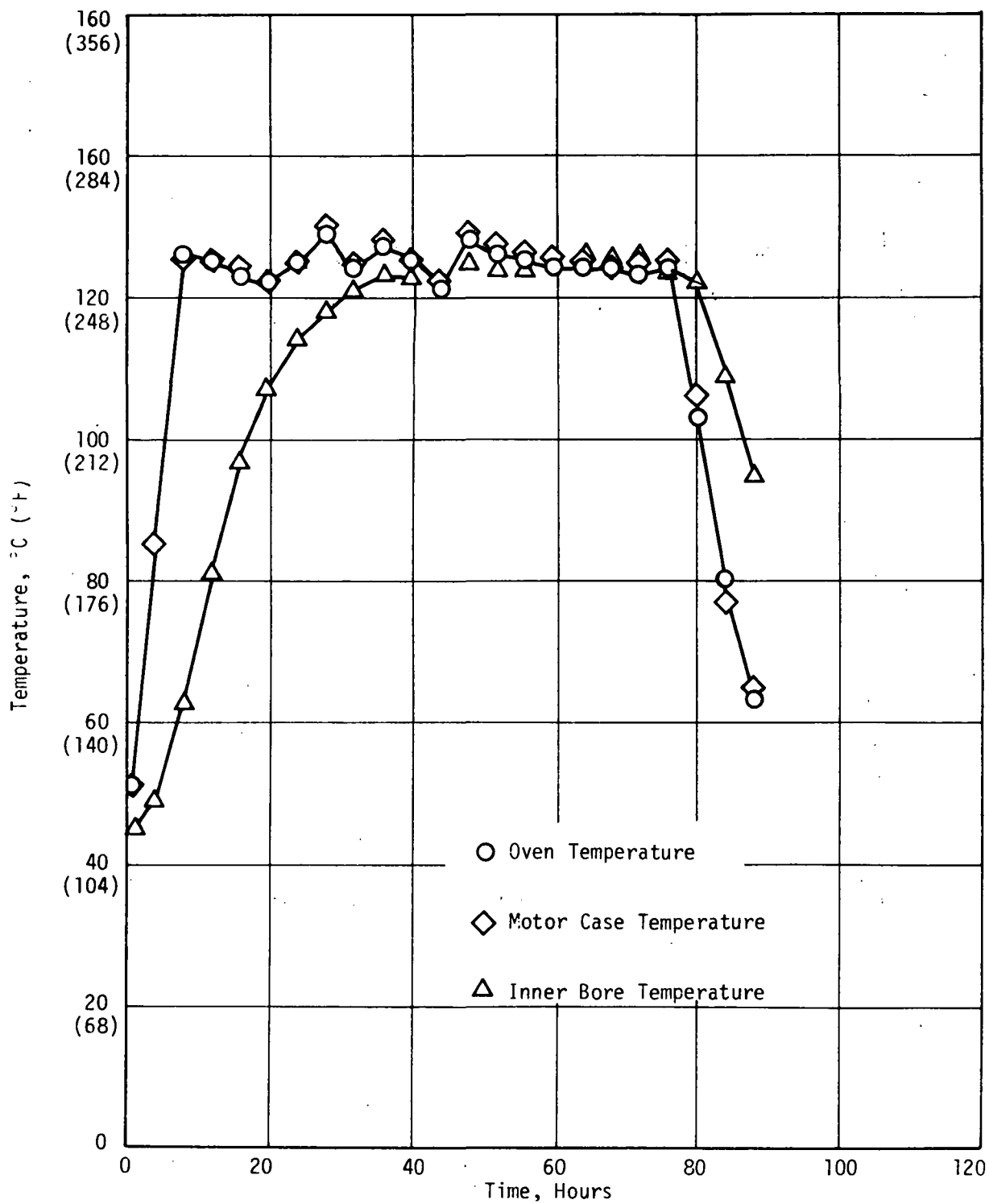
Heat Sterilization Cycle No. 3 at 125°C (257°F) Demonstration Motor No. 2

Figure 77



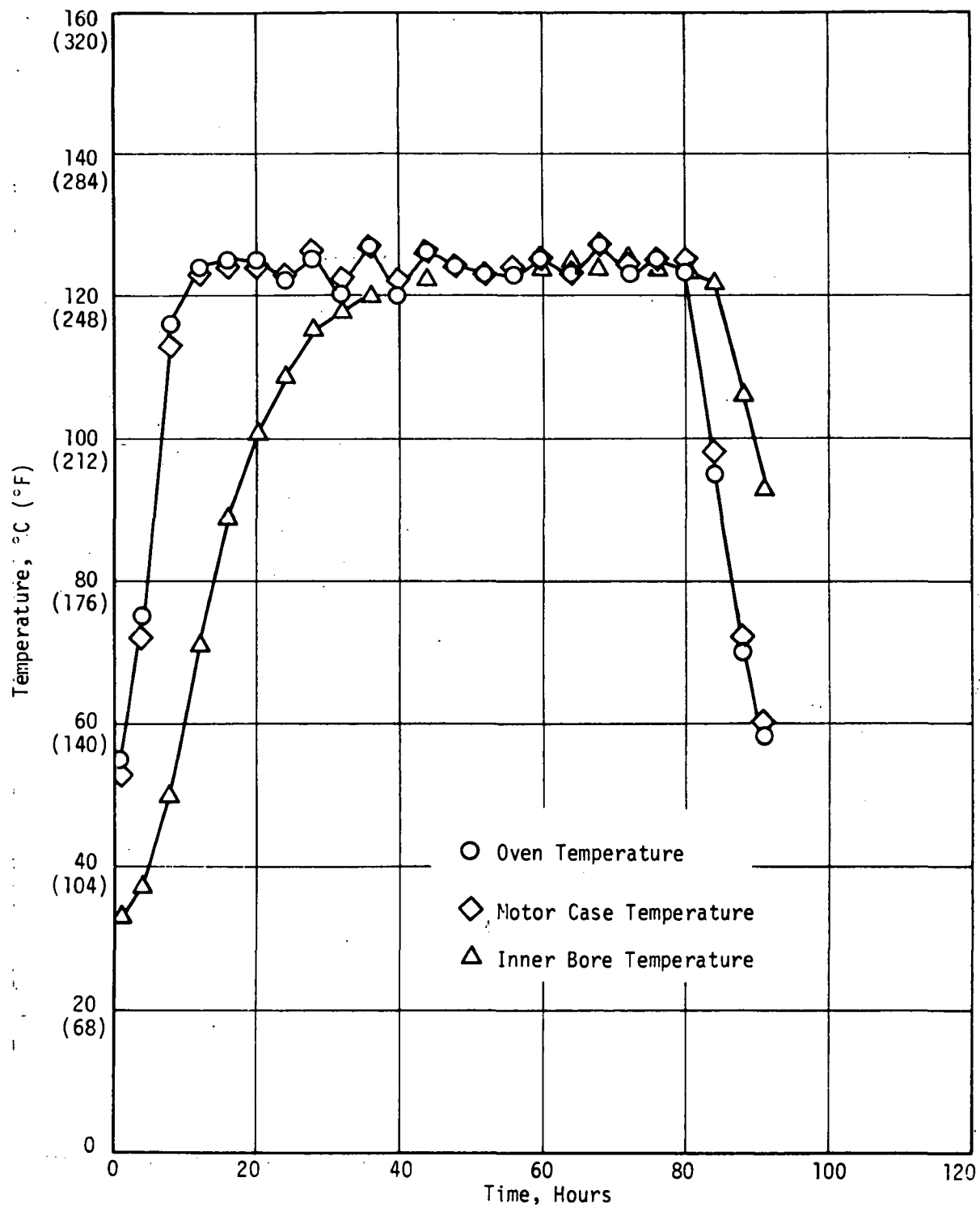
Heat Sterilization Cycle No. 4 at 125°C (257°F) Demonstration Motor No. 2

Figure 78



Heat Sterilization Cycle No. 5 at 125°C (257°F) Demonstration Motor No. 2

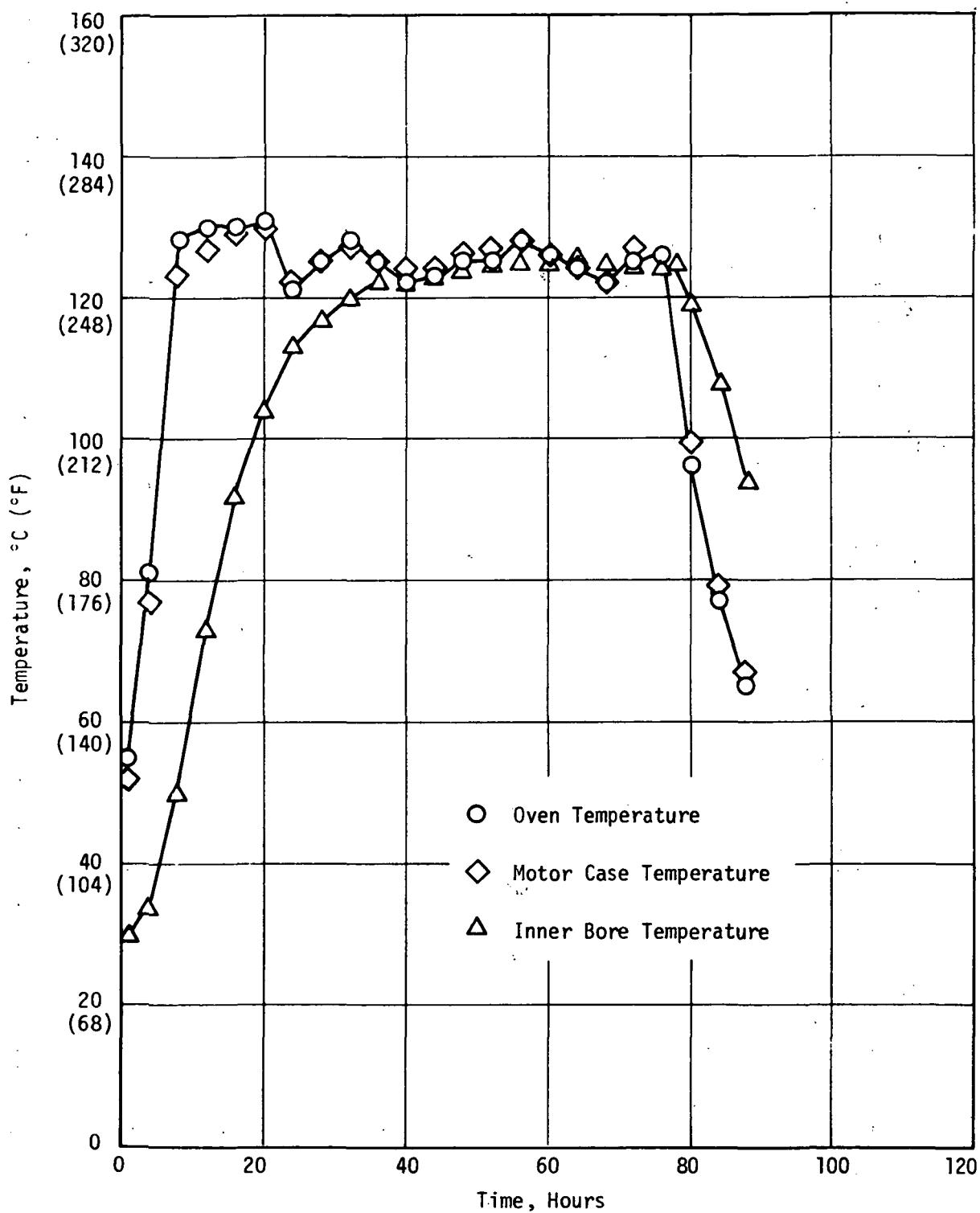
Figure 79



Heat Sterilization Cycle No. 6 at 125°C (257°F) Demonstration Motor No. 2

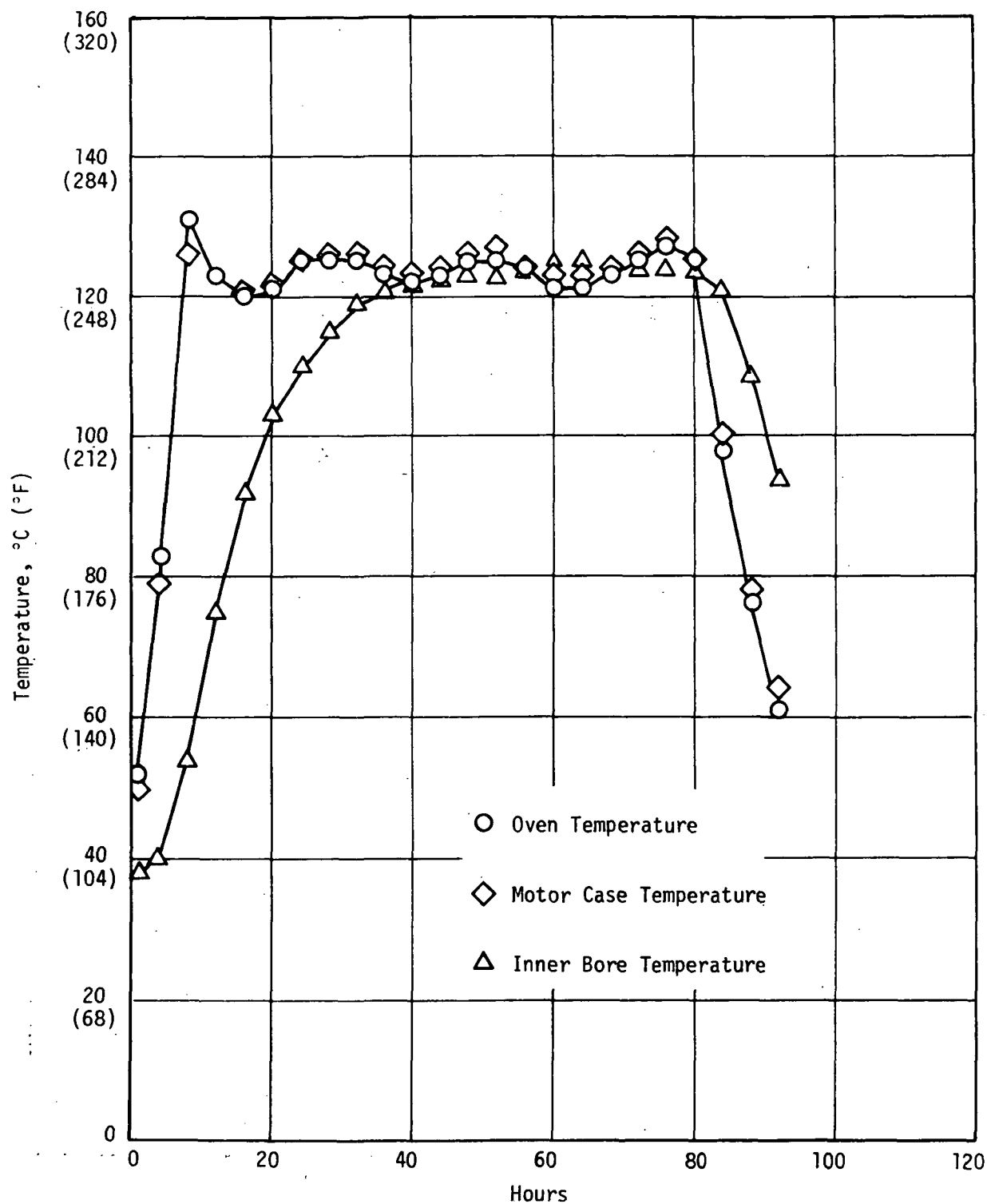
Figure 80





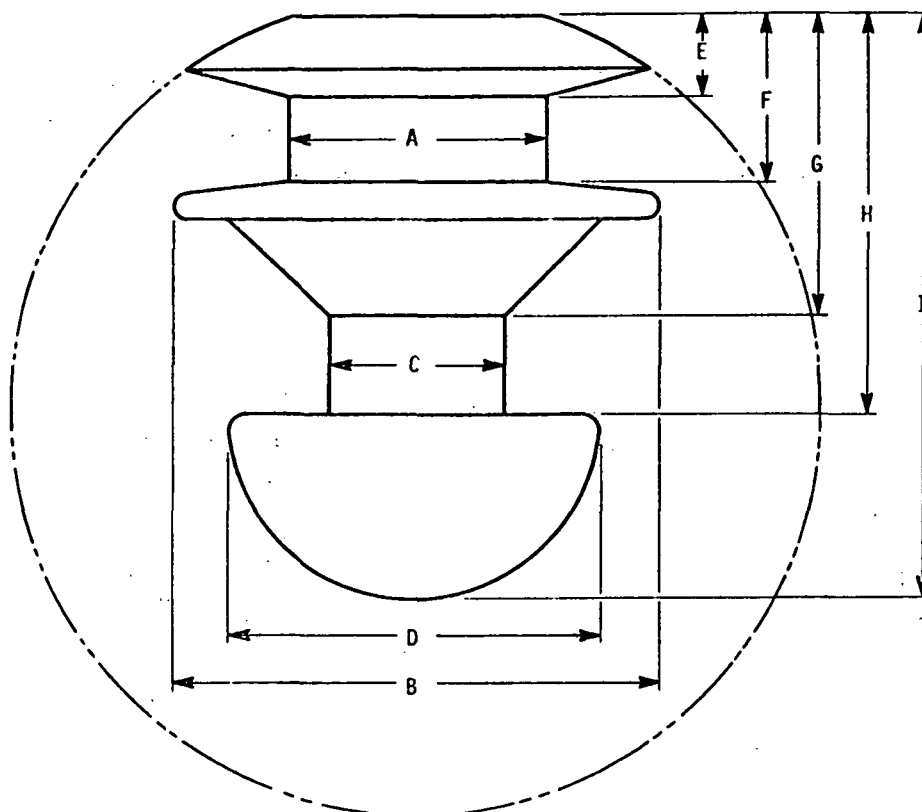
Heat Sterilization Cycle No. 7 at 125°C (257°F) Demonstration Motor No. 2

Figure 81



Heat Sterilization Cycle No. 8 at 125°C (257°F) Demonstration Motor No. 2

Figure 82



SERIAL NUMBER 2				
	Pre		Post	
	cm	(in.)	cm	(in.)
A	13.93	(5.486)	13.93	(5.486)
B	26.38	(10.386)	26.12	(10.282)
C	9.40	(3.701)	9.39	(3.697)
D	19.43	(7.648)	19.34	(7.614)
E	4.40	(1.732)	4.35	(1.714)
F	9.07	(3.572)	9.00	(3.542)
G	16.26	(6.400)	16.27	(6.404)
H	21.51	(8.470)	21.56	(8.490)
I	31.57	(12.430)	31.65	(12.460)

Effect of Heat Sterilization at 125°C (257°F) on Motor Grain Dimensions

Figure 83

a. Propellant Density and Coefficient of Thermal Expansion

The cured density of ANB-3438 propellant from Batch 73-30-201 (motor batch) was determined to be 1.722 g/cc (0.0622 lb/in.<sup>3</sup>). The coefficient of thermal expansion over the range of (0° to 275°F) was  $10.8054 \times 10^{-5}$  m/m/°C.

b. Liner-to-Propellant Bond

Tensile and peel bond tests were measured initially and after six heat sterilization cycles (53 hrs each at 135°C (275°F)). Data are shown in Figure 84. The initial tensile bond strength of 125 N/cm<sup>2</sup> (179 psi) increased to 172 N/cm<sup>2</sup> (249 psi) after the six heat sterilization cycles. Peel strength at 25°C (77°F) increased from 164 to 264 Kg/m (9.2 to 14.8 lb/in.) after sterilization. A decrease in peel strength was observed when tested at 135°C (275°F) after sterilization, 28.6 to 17.9 Kg/m (1.6 to 1.0 lb/in.). However, the compressive state of the grain at 135°C (275°F) results in essentially no bond strength requirement.

c. Mechanical Properties

Uniaxial tensile tests were performed at 25°C (77°F) on ANB-3438 propellant initially and after each of the six sterilization cycles. Testing at 135°C (275°F) was done initially and after the first and the sixth cycle. The data are shown in Figure 85. Typical of this formulation, a sizable increase in tensile strength and modulus occurred during heat sterilization: from 109 (158) to 181 N/cm<sup>2</sup> (263 psi) for tensile strength and from 1506 (2182) to 2499 N/cm<sup>2</sup> (3622 psi) for modulus after 0 and 6 sterilization cycles, respectively.

<u>No. of Heat Ster. Cycles</u>	<u>Test Temp., C° (°F)</u>	<u>Peel Strength, Kg/m (lb/in)</u>	<u>Double-Plate Tensile Strength, N/cm<sup>2</sup> (psi)</u>
0	25 (77)	164 ( 9.2)	124 (179)
6	25 (77)	264 (14.8)	172 (249)
0	135 (275)	28.6 ( 1.6)	--
6	135 (275)	17.9 ( 1.0)	--

---

(1) SD-886 liner applied to GenGard V-4030 rubber insulation.

Effect of Heat Sterilization on ANB-3438  
Propellant-to-Liner(1) Bond Strength

Figure 84

Batch No.	Test Temp. °C (°F)	No. of Heat Ster. Cycles	Uniaxial Mechanical Properties			
			$\sigma_m$ , N/cm <sup>2</sup> (psi)	$\epsilon_m$ , %	$\epsilon_b$ , %	$E_o$ , N/cm <sup>2</sup> (psi)
73-30-201	25 (77) <sup>(1)</sup>	0	109 (158)	28	42	1506 (2182)
		1	150 (218)	17	21	2207 (3199)
		2	172 (249)	14	18	2670 (3870)
		3	177 (256)	13	16	2841 (4117)
		4	164 (237)	13	16	2632 (3815)
		5	166 (241)	14	16	2651 (3842)
		6	181 (263)	17	21	2499 (3622)
	135 (275) <sup>(2)</sup>	0	43 (62)	14	15	466 (675)
		1	65 (94)	8	7	1074 (1557)
		6	68 (99)	7	8	1123 (1627)

- (1) Average of 5 test specimens.  
(2) Average of 2-3 test specimens.

Figure 85

Small samples were also subjected to heat sterilization at 125°C (257°F) in order to simulate the sterilization conditions of Demonstration Motor No. 2. Mechanical properties were measured after 3 and 8 cycles and are shown below:

EFFECT OF 125°C (257°F) STERILIZATION ON MECHANICAL PROPERTIES

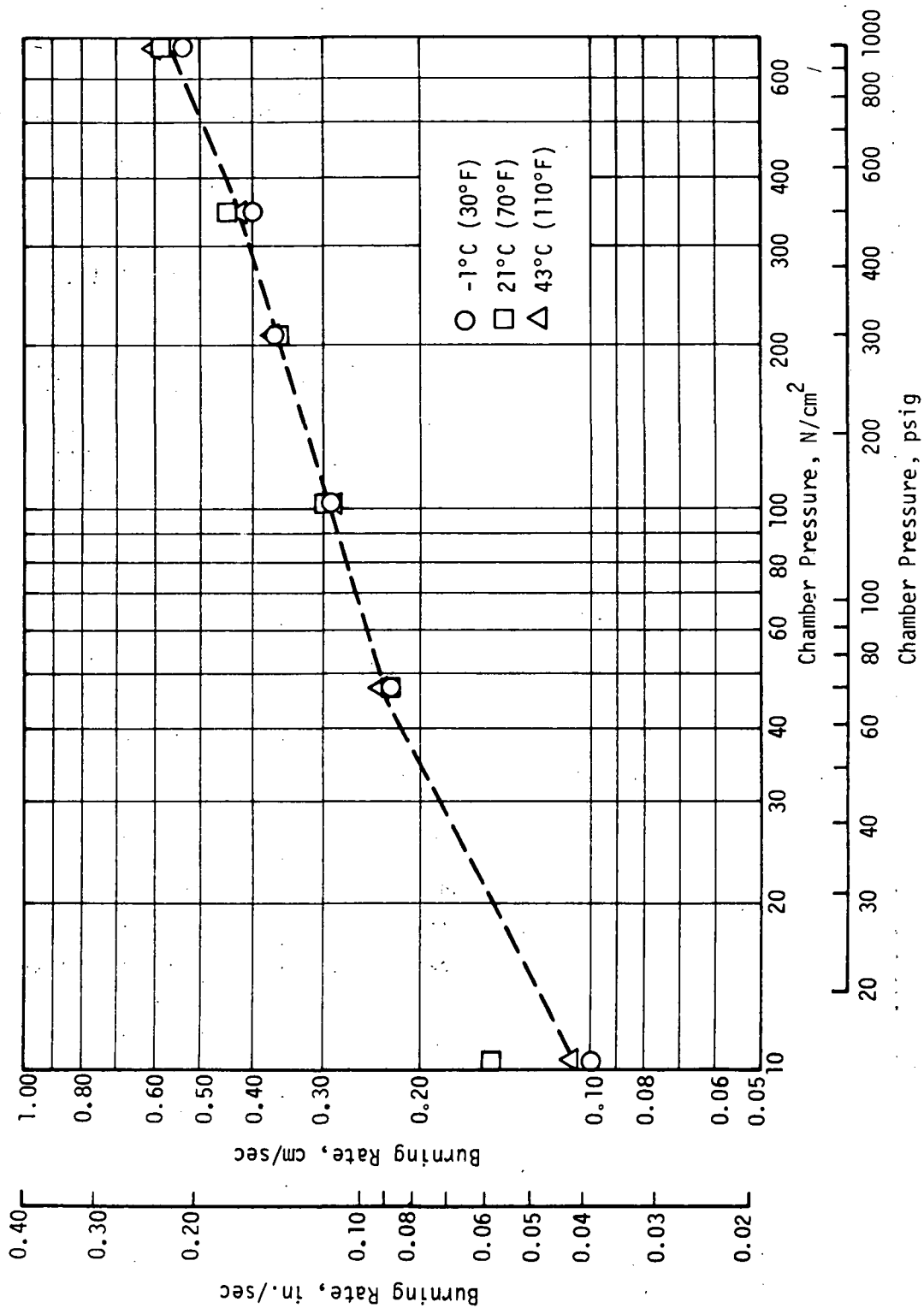
Batch No.	Cycles at 125°C (257°F)	Mechanical Properties at 25°C (77°F)			
		$\sigma_m$ , N/cm <sup>2</sup> (psi)	$\epsilon_m$ , %	$\epsilon_b$ , %	$E_o$ , N/cm <sup>2</sup> (psi)
73-30-201	0	109 (158)	28	42	1506 (2182)
	3 (54 hrs ea)	159 (230)	15	17	2545 (3683)
	8 (3 of 54 hrs ea followed by 5 of 40 hours each)	132 (264)	16	20	2829 (4100)

d. Solid Strand Burning Rates

Solid strand burning rates were measured after 0, 1 and 6 sterilization cycles over the pressure range of 10.4 (15) to 690 (1000) N/cm<sup>2</sup> (psi) at temperatures of -1°C (30°F), 21°C (70°F) and 43°C (110°F). (Figure 86 to 88). Burning rates were essentially the same before and after heat sterilization although some decrease was noted after the sixth sterilization cycle. In general, little difference in burning rates were observed that could be attributed to the test temperature. The data point for the 21°C (70°F) firing at 10.4 N/cm<sup>2</sup> (15 psig) in Figure 86 is apparently a spurious value. There appears to be two breaks in the slope (pressure exponent) with this propellant, one occurring at or before 43 N/cm<sup>2</sup> (70 psi), the other at 345 N/cm<sup>2</sup> (500 psig).

e. Dimensional and Weight Stability

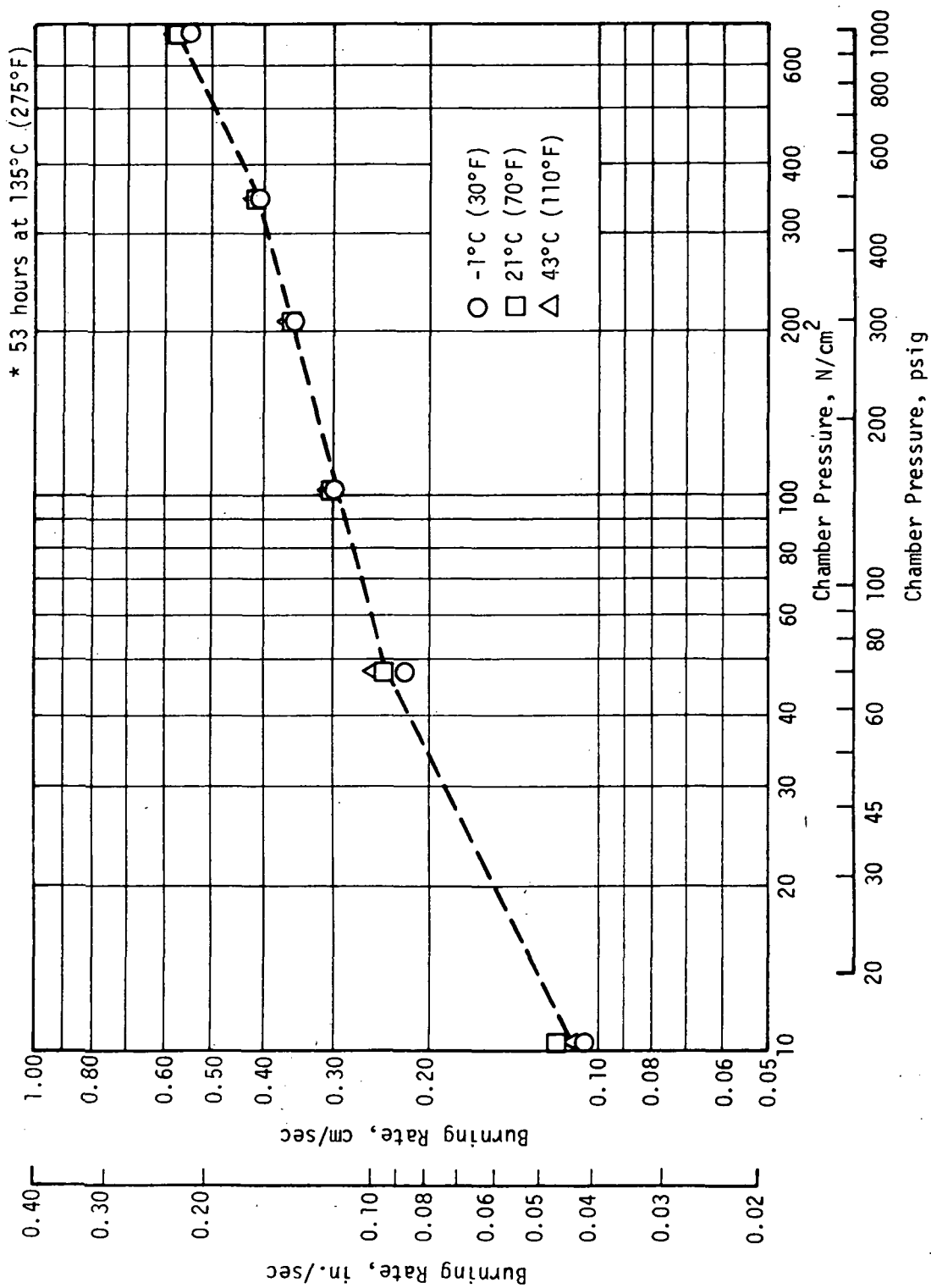
Dimensional and weight changes of the 7.6 cm x 7.6 cm x 12.7 cm (3 in. x 3 in. x 5 in.) blocks of propellant used to prepare the mechanical property specimens and burning rate strands were determined after each sterilization cycle. The dimensions of the block



Initial Solid Strand Burning Rates of ANB-3438 Propellant, Batch 73-30-201

Figure 86





Solid Strand Burning Rates of ANB-3438 Propellant After One Heat Sterilization Cycle\*, Batch 73-30-201

Figure 87

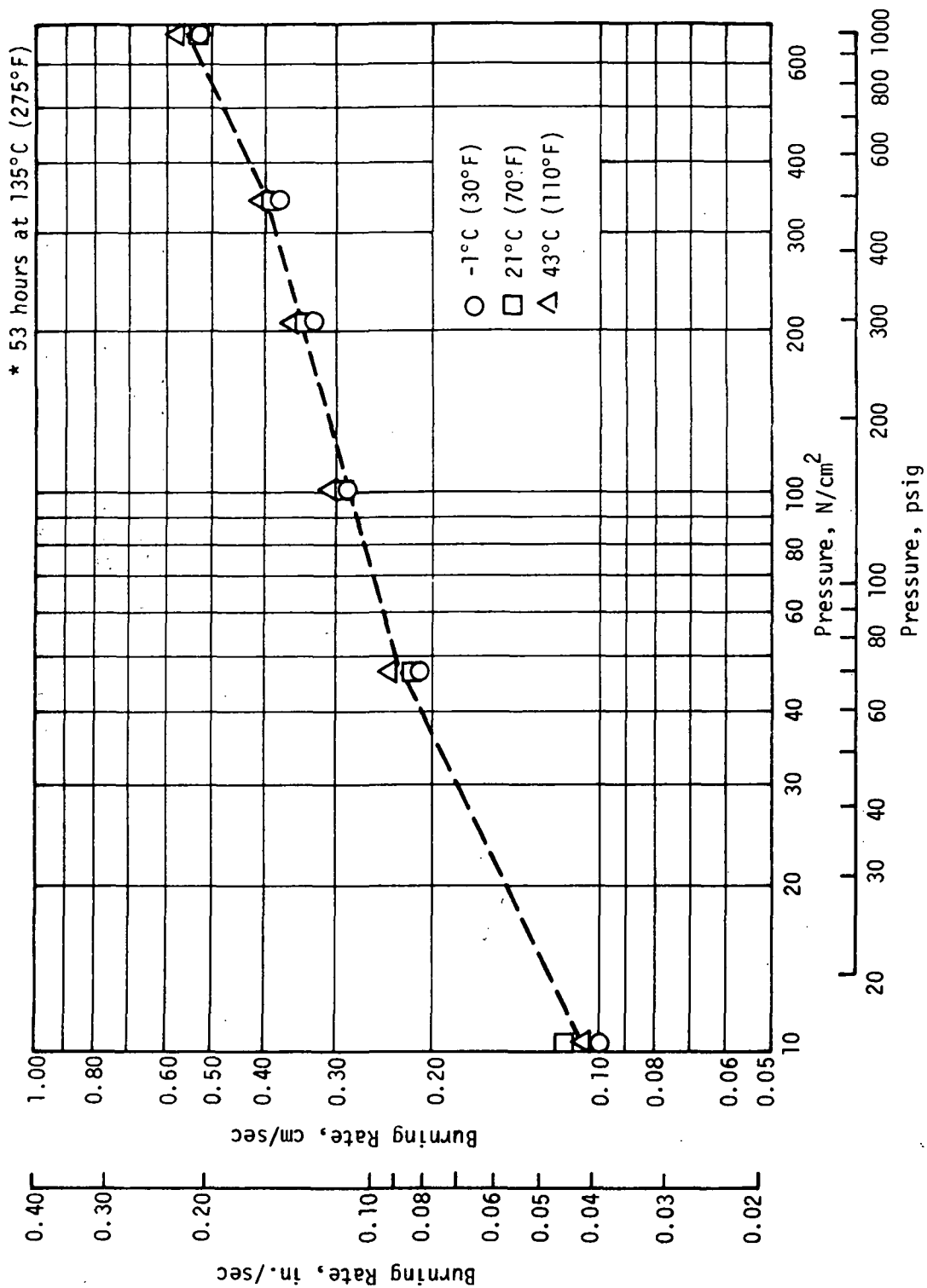
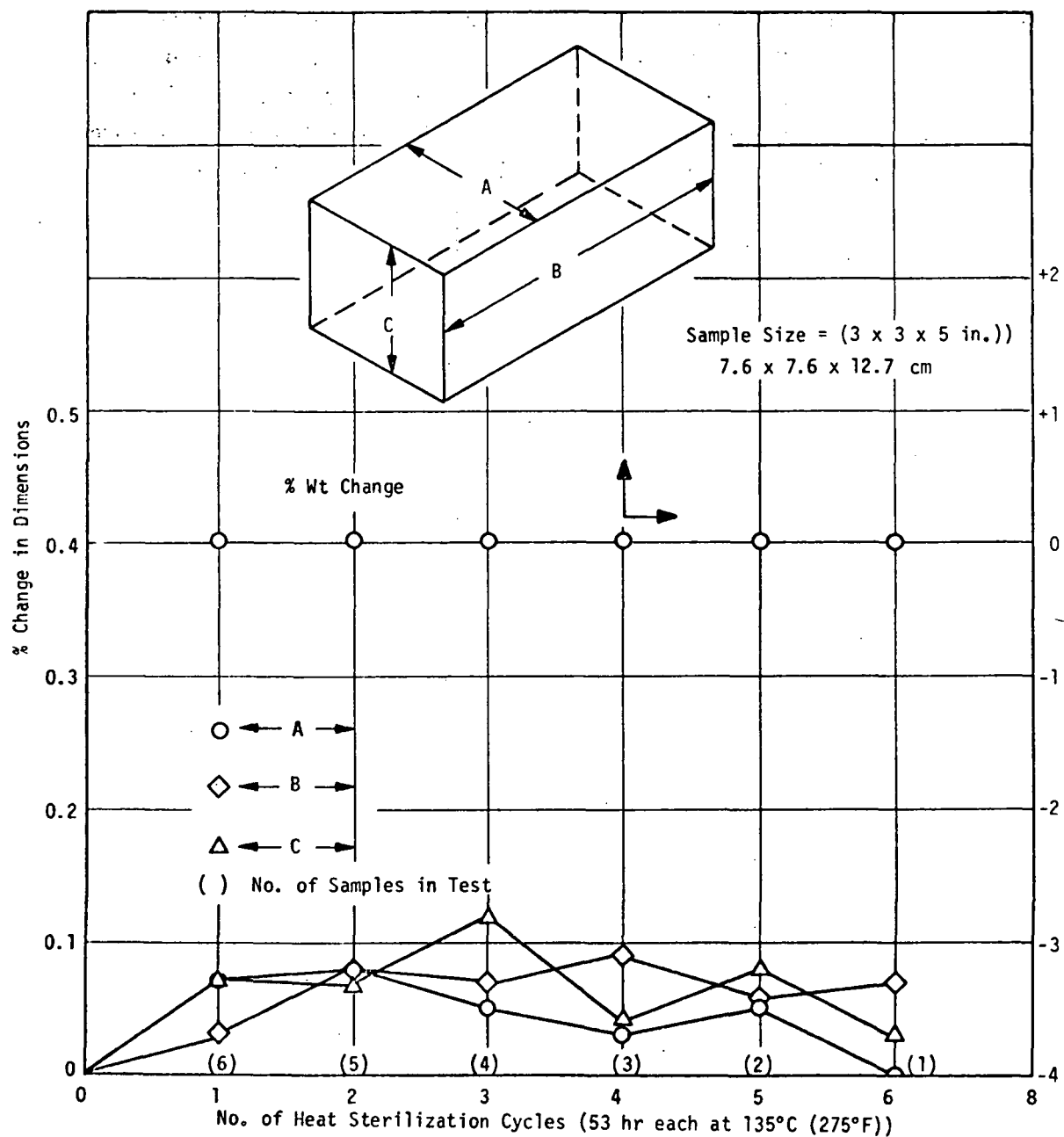


Figure 88

were measured along the three axes as illustrated in Figure 89. Also plotted in Figure 89 are the average changes in the block's dimensions and the weight changes after each sterilization cycle. No change in weight was observed through the six sterilization cycles. The dimensional changes were also minimal, averaging less than 0.1% in all but one instance.



Effect of Heat Sterilization on Weight and Dimensional Stability of ANB-3438 Propellant

Figure 89

## E. STATIC TEST FIRING OF THE HEAT STERILIZED MOTOR

Demonstration Motor No. 2 was selected for static test firing. This motor had been subjected to eight heat sterilization cycles at 125°C (257°F) (see Section III.D.). X-ray analysis of this motor after the eighth sterilization cycle showed no signs of fissures, voids or grain/liner separations. Details of the motor assembly, conditioning, test firing and data reduction are presented in the following paragraphs.

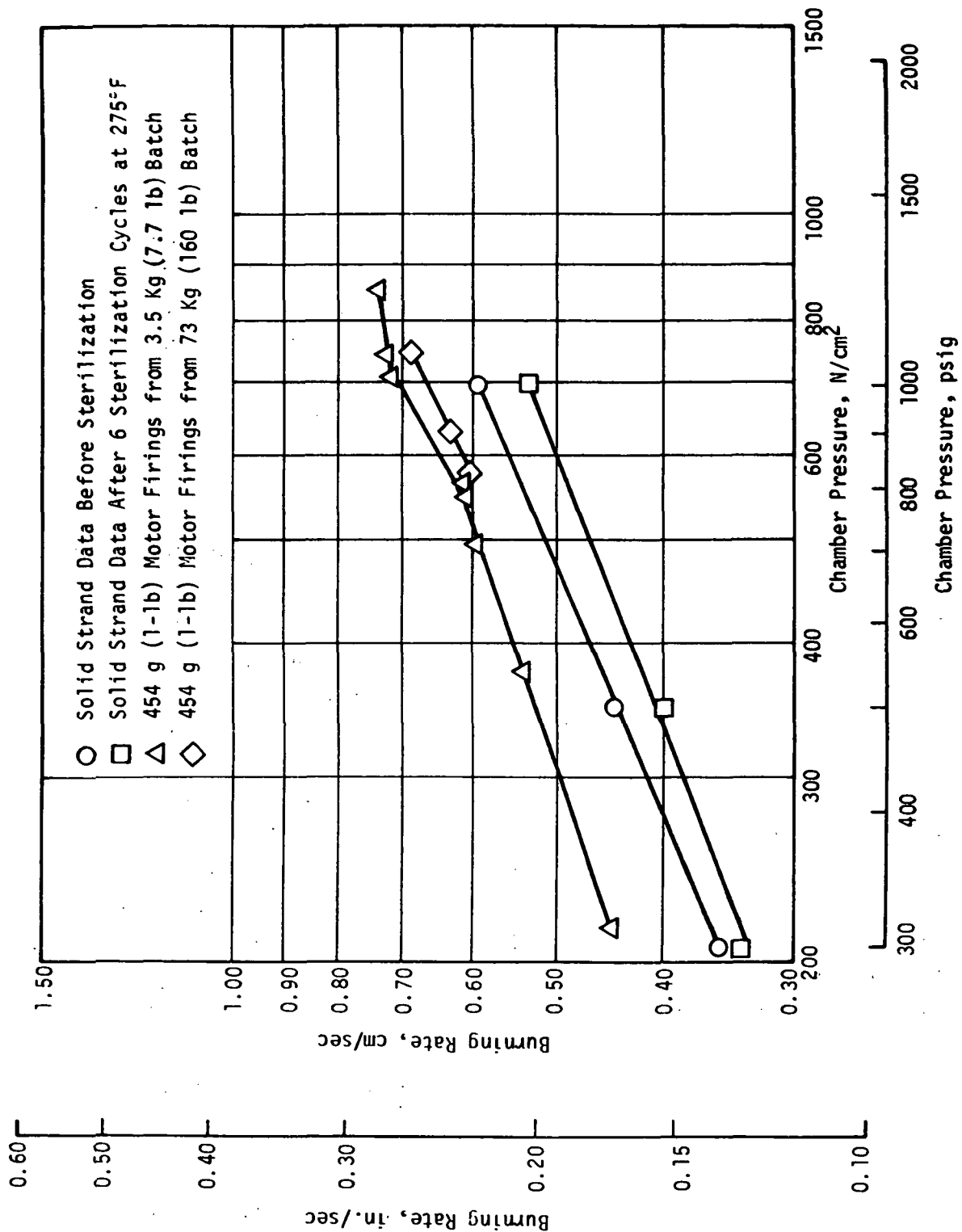
### 1. Nozzle Throat Modification

A scale-up in the burning rate was observed when internal-burning, nominal 1-lb motor firings were made with ANB-3438 propellant. This is shown in the comparison of the 454g (1-lb) motor firings and solid strand data presented in Figure 90. The effect of this burning rate increase on the expected ballistic performance of the demonstration firing was shown in Figure 22 (compare upper and lower curve). In order to reduce the chamber pressure, the nozzle throat area of the initial design was increased from 3.236 cm (1.274) to 3.409 (1.342 in.) diameter. This resulted in the expected pressure/time trace shown in the intermediate curve of Figure 23. A structural analysis of the modified nozzle (Figure 25) showed that a 9% safety margin remained after the throat area was increased. This analysis was based on the nominal 454 g (1-lb) motor firings of non-heat-sterilized propellant, and provided a conservative approach since the effect of heat sterilization tended to lower the strand burning rates for the propellant batch used to cast the demonstration motors (Figure 90).

A summary of ballistic predictions resulting from these analyses is shown in Figure 91.

### 2. Motor Assembly

The motor insulation was damaged slightly during final machining of the grain prior to heat sterilization. This damage was not



Burning Rates of ANB-3438 Propellant Fired in Solid Strands and 454 g (1-1b) Motors

Figure 90

Propellant	Original Design	With		With New Burn Rates and Larger Nozzle Throat
		New Burn Rates	ANB-3438	
ANB-3289-3			ANB-3438	ANB-3438
Burn Rate @ 345 N/cm <sup>2</sup> (500 psia), cm/sec (in./sec)				
Solid Strand	0.41 (0.16)	0.43 (0.17)	0.43 (0.17)	0.43 (0.17)
Motor	-	0.51 (0.20)	0.51 (0.20)	0.51 (0.20)
Throat Diameter, cm (in.)	3.236 (1.274)	3.236 (1.274)	3.409 (1.342)	
Maximum Pressure, N/cm <sup>2</sup> (psia)	500 (725)	773 (1120)	615 (891)	
MEOP, N/cm <sup>2</sup> (psia)	535 (775)	828 (1200)	658 (954)	
Factors of Safety (Minimum)				
*Chamber (Yield)	1.43	0.92	1.16	
*Chamber (Burst)	1.52	0.97	1.21	
Nozzle Throat (Yield)	1.25	-	1.09	
<hr/>				
*Chamber Proof Pressure (min)	939 psig			
Yield Pressure (min)	1089 psig			
Burst Pressure (min)	1156 psig - Demonstrated greater			

Ballistic Analysis Summary

Figure 91

detected until X-ray inspection after completion of the sterilization cycles. At this time the insulation was repaired by manual application of a polybutadiene potting insulation.

Final assembly operations consisted of acquiring grain dimensions and post-sterilization weights, installing the nozzle and test-weight igniter housings, and leak testing. The igniter charge of 50 gm boron/potassium nitrate (BPN) pellets was inserted just prior to installation of the motor in the test stand.

### 3. Temperature Conditioning

The motor was transported to the test facility in a protected condition and stored at 21°C (70 ± 10°F) until set up in the test stand on the morning of the firing. When the igniter was installed and motor setup was complete, a portable conditioning unit maintained the ambient temperature at 21°C (70 ± 10°F), until 17 minutes before fire switch. Ambient temperature and pressure were 11°C (52°F) and 768 mm (30.22 in.) Hg, respectively.

### 4. Test Installation

The motor was fired horizontally in the SVM-3 spin fixture, which was restrained for this test. A single 909 Kg (2000-lb) load cell with dual bridge wires was used to measure axial thrust. Two 454 Kg (1000-psi) Taber transducers measured chamber pressure through the otherwise non-functional igniter housings. Thermocouples were attached to the case exterior at locations corresponding to the minimum insulation thicknesses at the equator and at the aft end of the grain. Motion picture coverage consisted of a single 400 frame/sec Milliken camera directed at an aft quarter view of the motor.



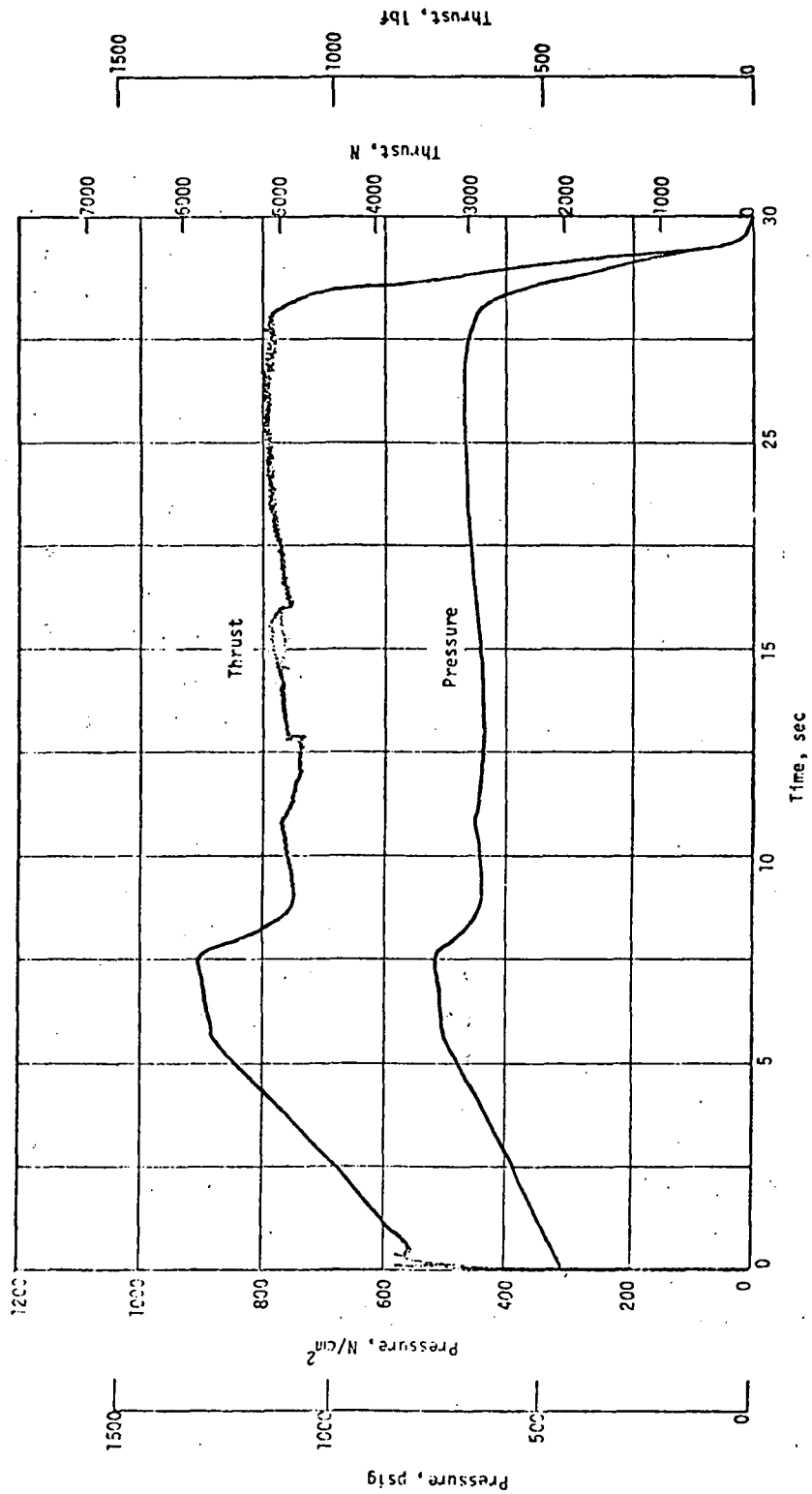
## 5. Ballistic Performance

Motor ballistic performance is shown in the pressure and thrust traces given in Figure 92. The ignition sequence, plotted in Figure 93, was smooth and entirely satisfactory, with an ignition interval of just under 70 msec.

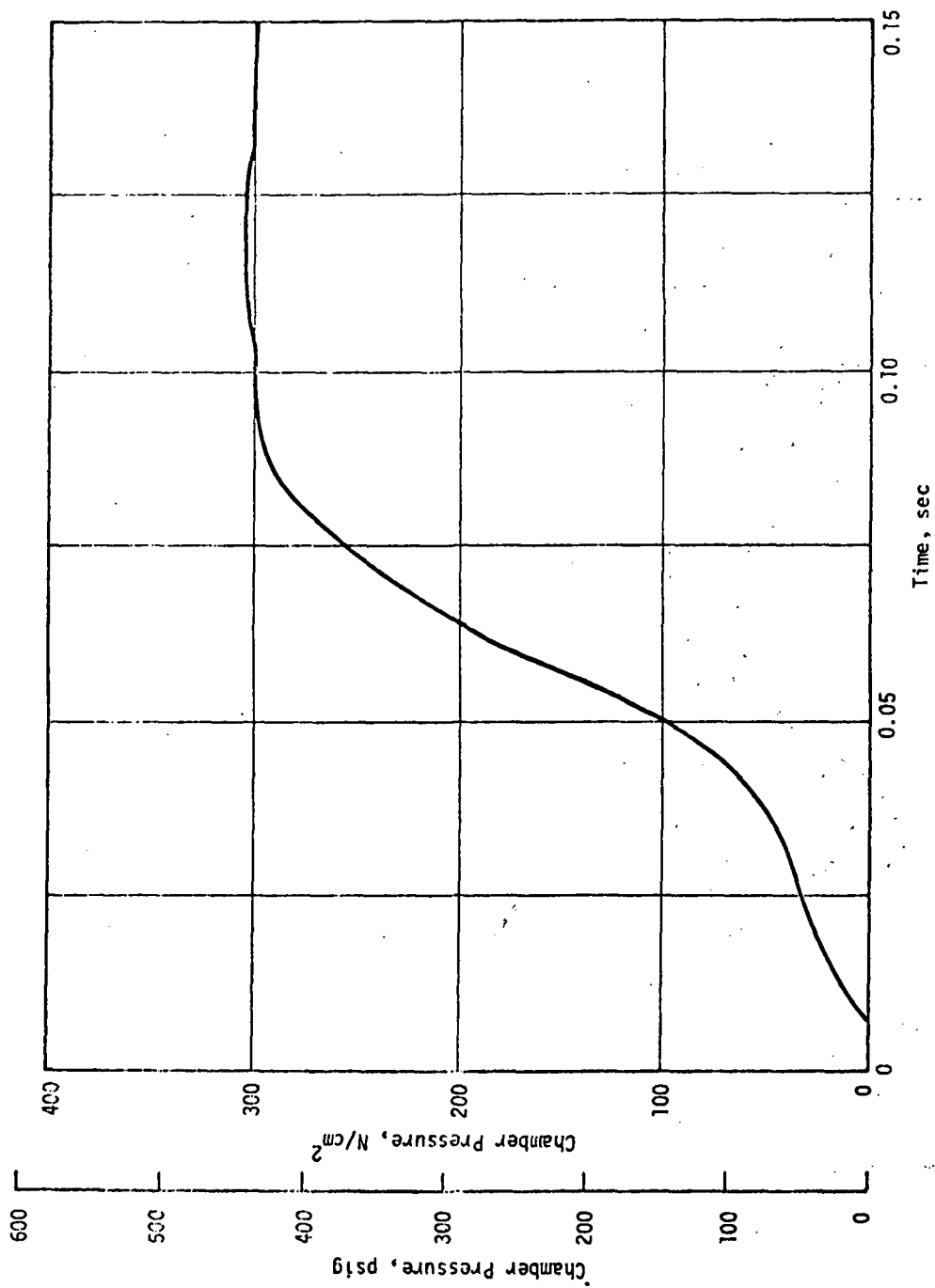
As shown in Figure 94, the measured motor pressure lies within the expected range of predicted performance. It is apparent that the motor burning rate of 0.48 cm/sec (0.190 in./sec) at  $438 \text{ N/cm}^2$  (635 psia) closely matches that measured with 454 g (1-lb) test motors taken from the full-scale motor batch (prediction curve No. 4, Figure 94). The actual pressure-time integral exceeds the predicted value because of the reduced throat area calculated from pressure and thrust data (Figure 95). The actual motor burning rate is about 3% lower than that projected from the 450 g (1-lb) motor data (Figure 96).

Deviations between the predicted and actual ballistic curves between 5 and 12 seconds (Figure 94) are apparently the result of selecting increments which were too large for the calculation of surface area progression and, hence, the individual peaks were not predicted. The slight rounding of the curve at web burnout, and subsequent slow tailoff was not unexpected and can be attributed to a combination of within grain burning rate variations, and variations in insulation contour and grain machining. The perturbations in the thrust trace, particularly between 13 and 16 sec (Figure 92) are not related to motor operation, but are more likely due to data acquisition problems. All of the described variations from predicted performance were within the normal range predictability. No anomalies due to sterilization were in evidence.

The ballistic performance of the motor is summarized in Figure 97. The delivered specific impulse of 1964.9 N-sec/Kg (200.8 lbf-

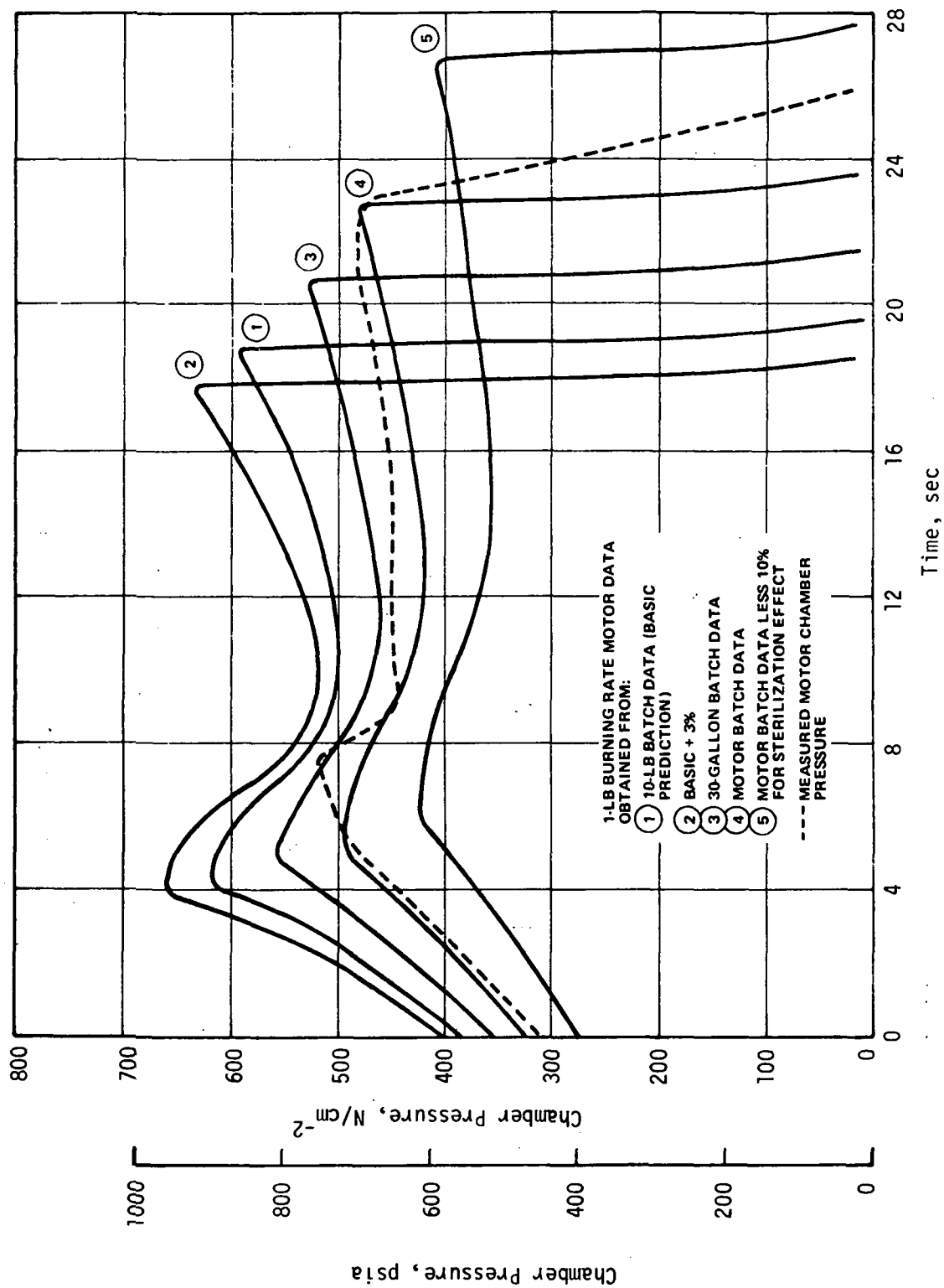


Pressure and Thrust vs Time for Static Test Firing of Heat Sterilized Motor



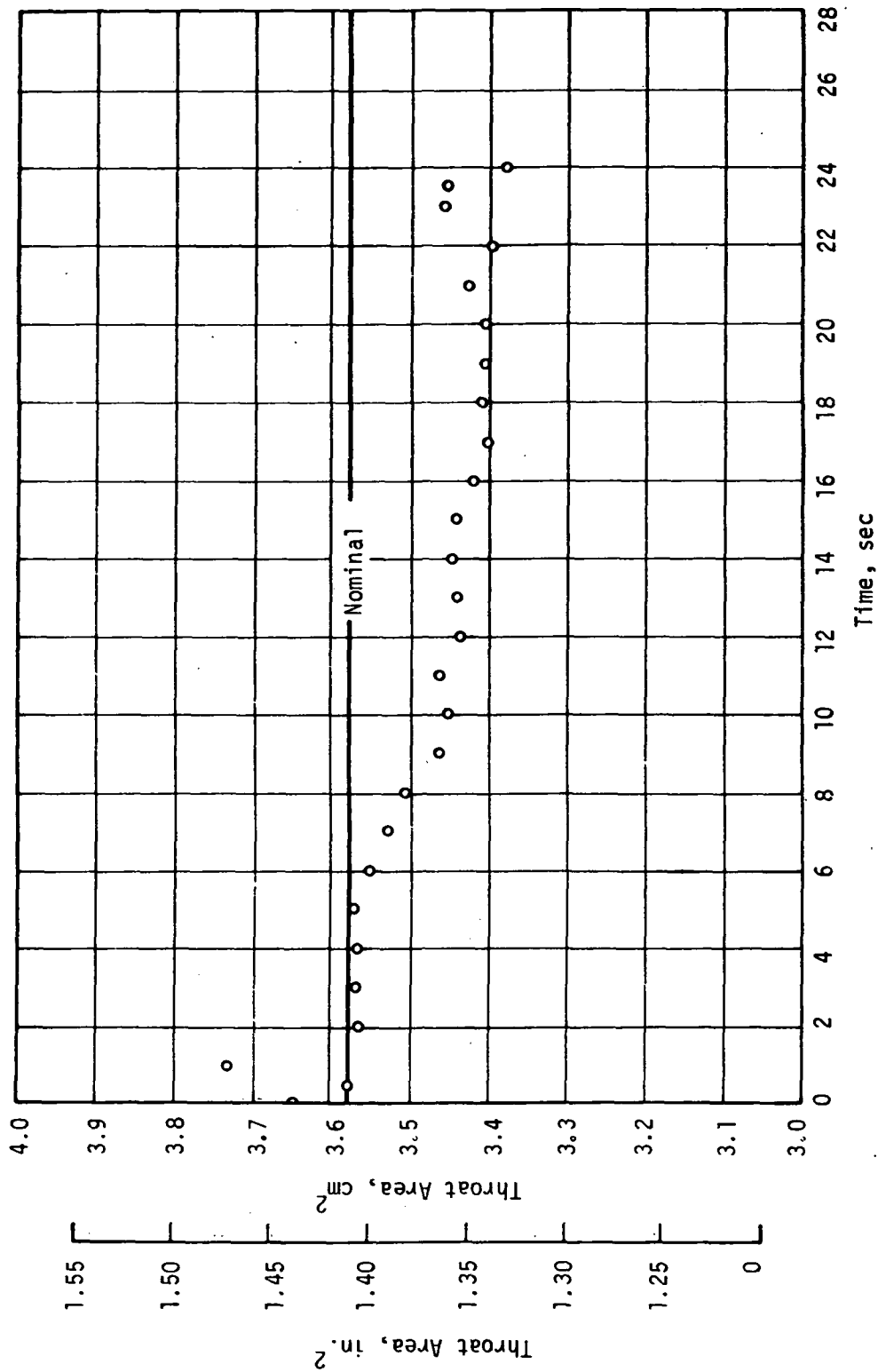
Sterilizable Motor Ignition Transient

Figure 93

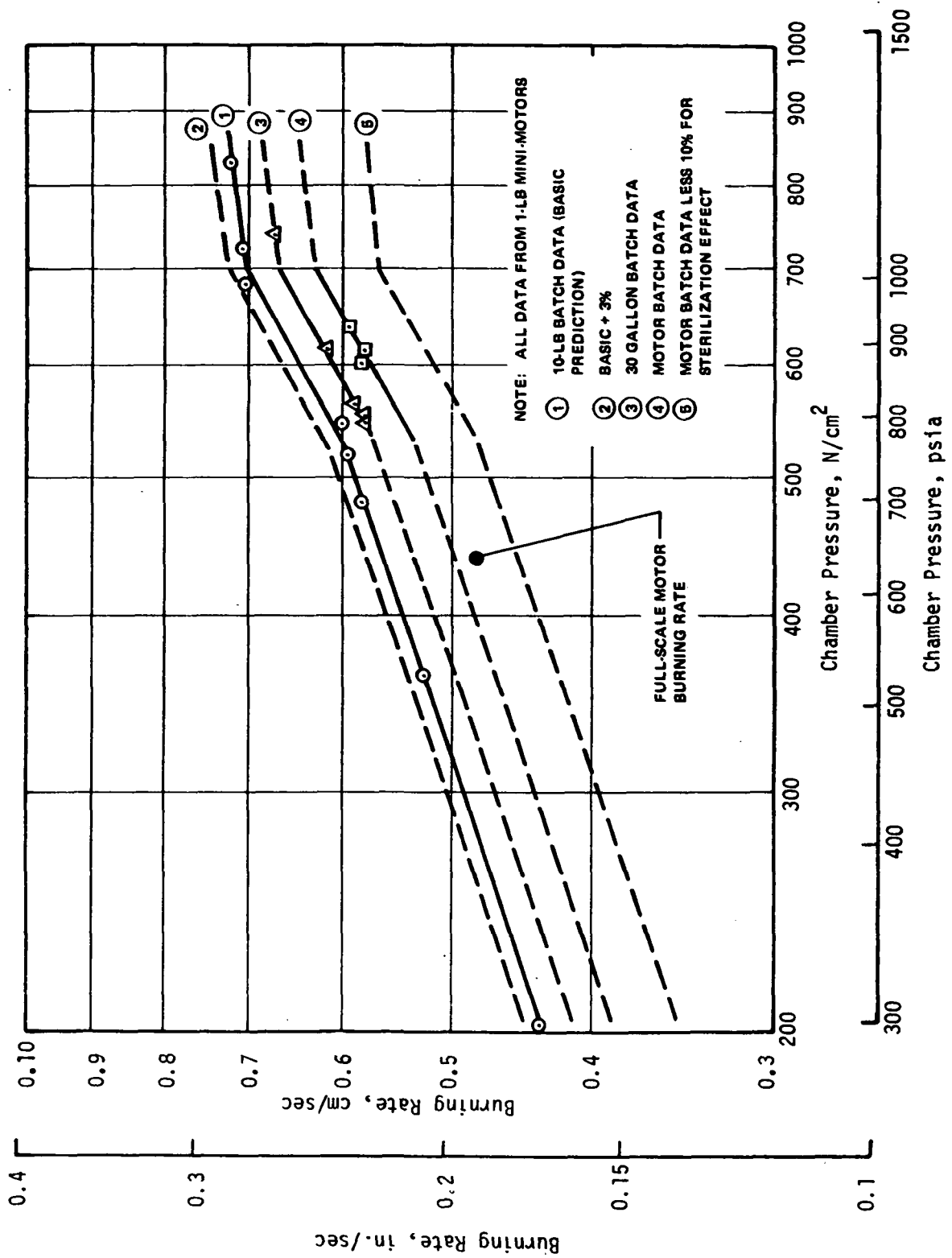


Sterilizable Motor Ballistic Performance

Figure 94



Sterilizable Motor Throat Area as a Function of Time,  $K_f = 0.915$



Sterilizabile Motor Demonstration - Burning Rates Used in Ballistic Performance Predictions

Figure 96

Web Action Time, sec	23.18
Action Time, sec	24.73
Total Burn Time, sec	25.12
Maximum Pressure, N/cm <sup>2</sup> (psia)	518 (750)
Web Average Pressure, N/cm <sup>2</sup> (psia)	438 (635)
Action Time Average Pressure, N/cm <sup>2</sup> (psia)	428 (620)
Maximum Thrust, N (lbf)	5836 (1312)
Web Average Thrust, N (lbf)	4946 (1112)
Action Time Average Thrust, N (lbf)	4839 (1088)
Average Burning Rate (Web Time), cm/sec (in./sec)	0.48 (0.19)
Initial/Final Throat Diameter, cm (in.)	3.404/3.223 (1.340/1.269)
Initial/Final Expansion Ratio	40.5/45.6
Propellant Weight, kg (lbm)	60.91 (134.00)
Total Expended Weight, kg (lbm)	61.70 (135.75)
Delivered Specific Impulse, N-sec/kg (lbf-sec/lbm)	1964.9 (200.8)
Vacuum Specific Impulse, N-sec/kg (lbf-sec/lbm)	2573.6 (263.0)

#### Sterilizable Motor Performance Summary

Figure 97

sec/lbm was corrected to a vacuum specific impulse of 2573.6 N-sec/Kg (263.0 lbf-sec/lbm), about 2.5% lower than the expected value of 2642 N-sec/Kg (270 lbf-sec/lbm). Several factors may have contributed to this low value.

a. The thrust data might be in error. Perturbations in the thrust trace have not been explained, although the calibration data did not indicate any significant error.

b. The thrust coefficient for the nozzle may be incorrect. A detailed loss analysis has never been conducted for this configuration. Comparison with SVM-3 performance is not useful, because of the large difference in propellant aluminum content. The apparent nozzle thrust coefficient is 91.5% of the theoretical and divergence loss. This is about 2.5% lower than that projected for this mass flow rate.

c. Combustion efficiency might be expected to be low for this motor size and aluminum content, but the apparent  $C^*$  efficiency is about 97.5%, slightly better than expected. This efficiency may be optimistic, if the tubular throat shape produced an effectively smaller aerodynamic throat.

d. The calculation methods are probably imprecise, because of the 40:1 expansion ratio of the nozzle, which caused separated flow. The relationships used in the computer program are probably the best available but cannot be expected to yield exact results.

No further analysis of the motor thrust performance were made since the program technical objectives were oriented toward demonstrating sterilizability followed by reliable operations which have both been confirmed.



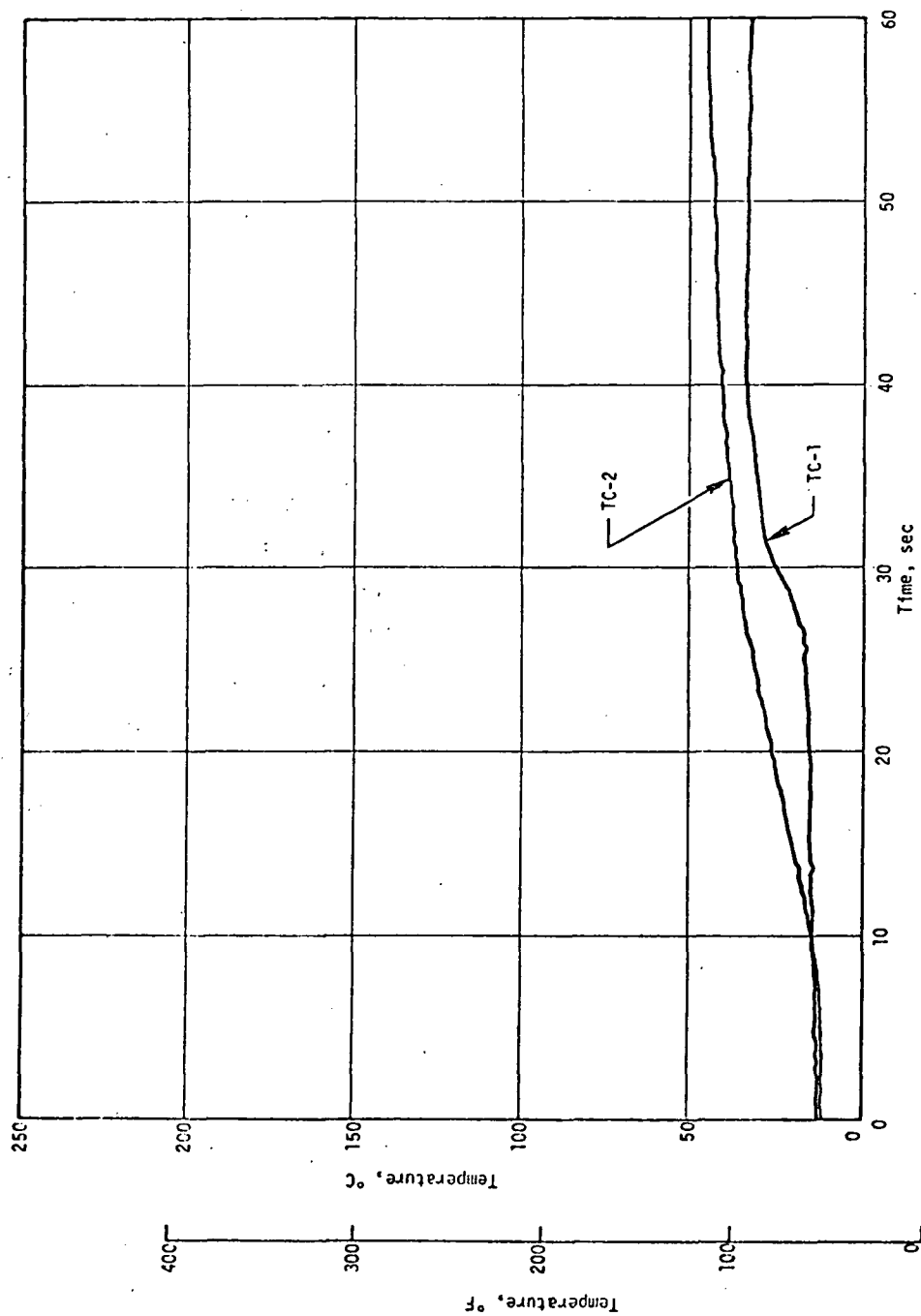
## 6. Component Performance

The performance of the chamber and nozzle were completely satisfactory, with no evidence of hot spots or leakage. The slight temperature increases indicated by the external thermocouples (Figure 98) were probably due to plume radiation and recirculation. The nozzle throat showed a shrinkage from 3.404 cm (1.340 in.) to 3.223 (1.269 in.) diameter, which is more than was indicated by ballistic data and is an expected condition when using a silver-infiltrated tungsten throat. No throat erosion was incurred. The nozzle ablative components were uniformly eroded and charred which is typical in the SVM-3 motor.

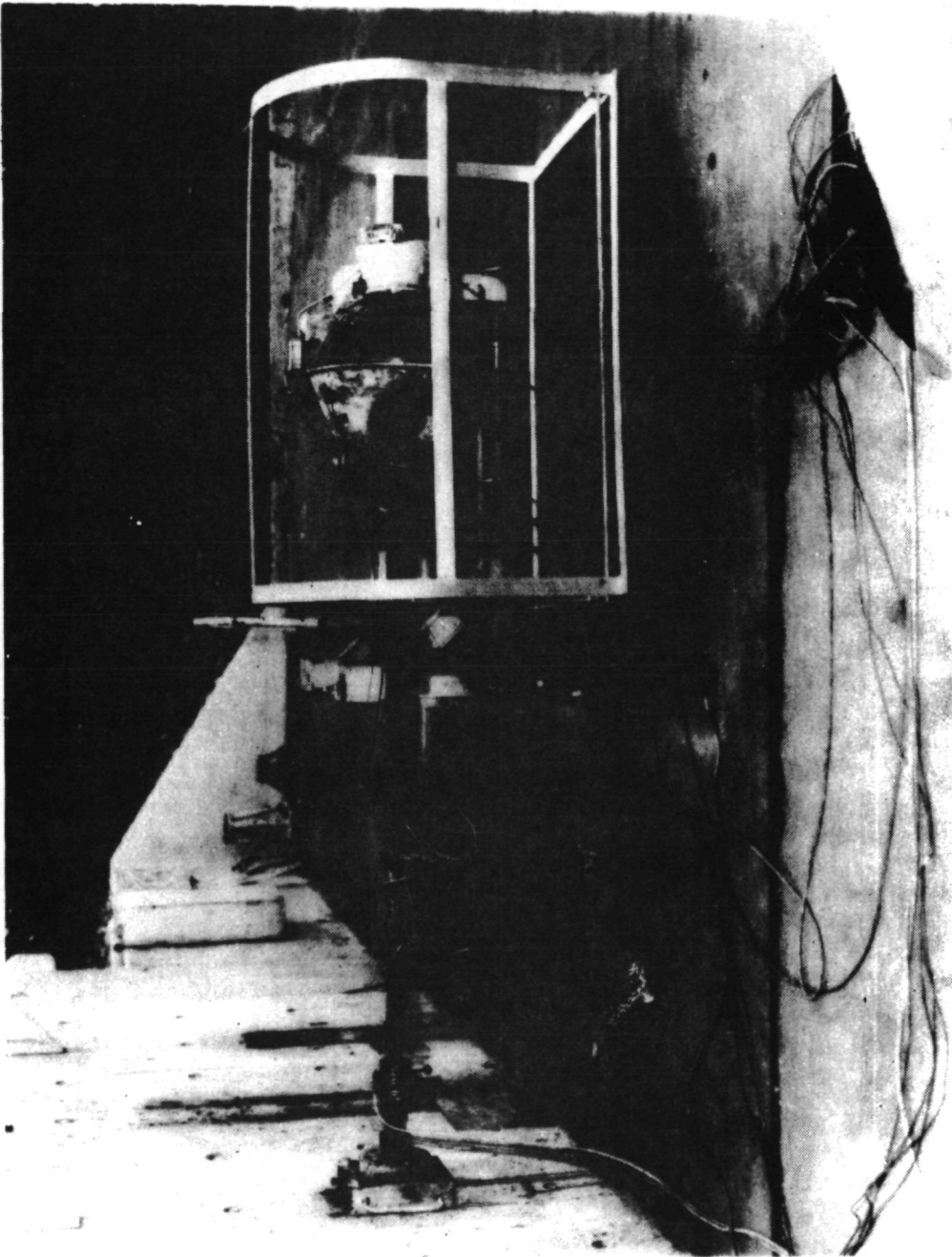
The chamber insulation performance was completely successful. Aft chamber insulation thickness reduction was typically about 0.25 cm (0.10 in.), normal for the SVM-3, indicating adequate performance of the sterilized V-4030 insulation material. The boot was essentially intact, with some feathering at the aft perimeter, and was still firmly bonded to the retention disks at the aft end. The insulation under the boot was uncharred, with only a slight amount of soot present. No significant amount of aluminum oxide slag was present in the chamber. External photographs of the motor before firing are shown in Figures 99 and 100, and after firing in Figure 101.

An attempt was made to estimate the flight-weight design requirement for this type of insulation and grain retention system. Referring back to earlier estimates of weight penalty related to the design (Section III.B.), the following adjustments can be made.

- a. The forward case insulation is unnecessary -0.73 Kg ( 1.6 lb).

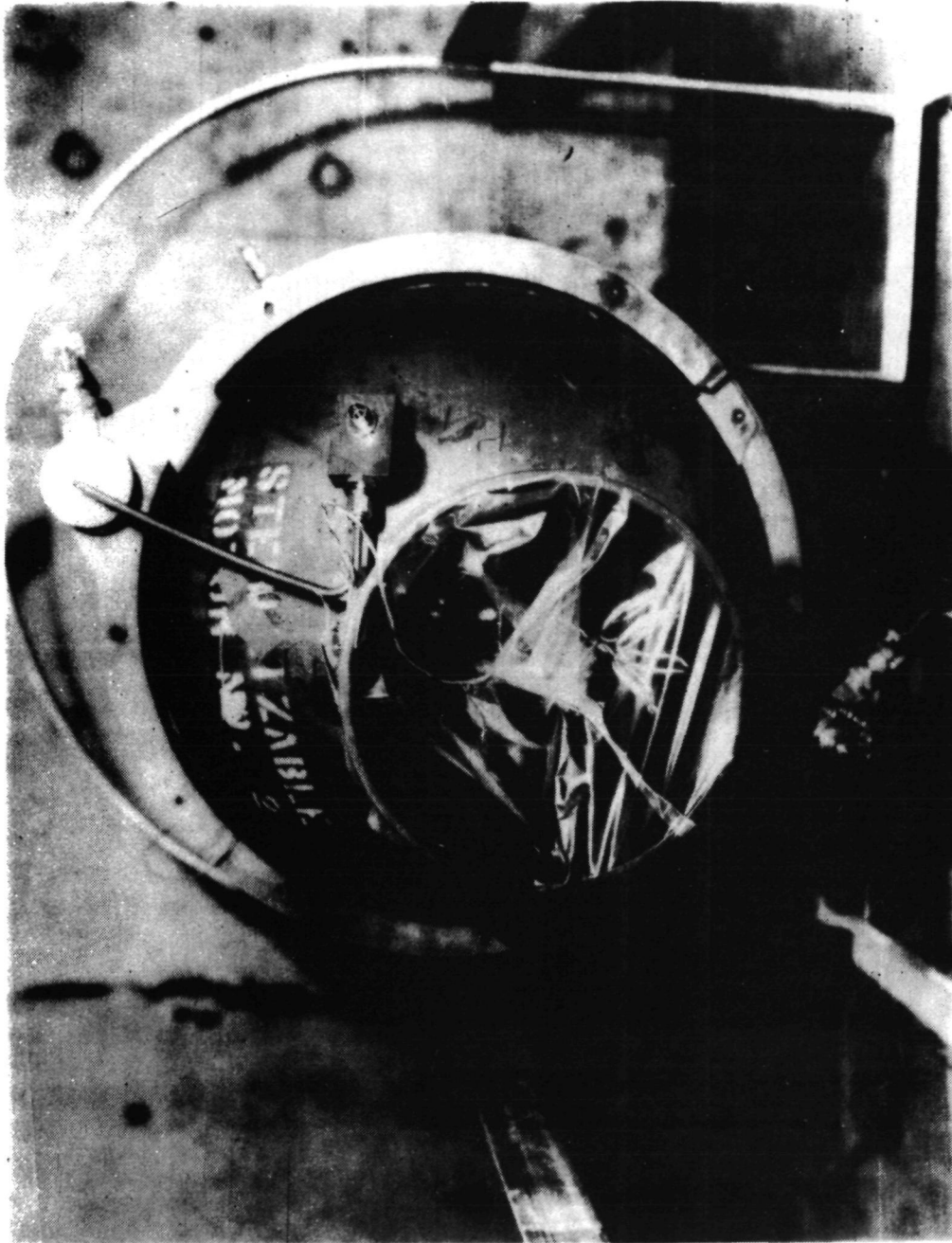


External Case Temperature During Test Firing of Demonstration Motor No. 2

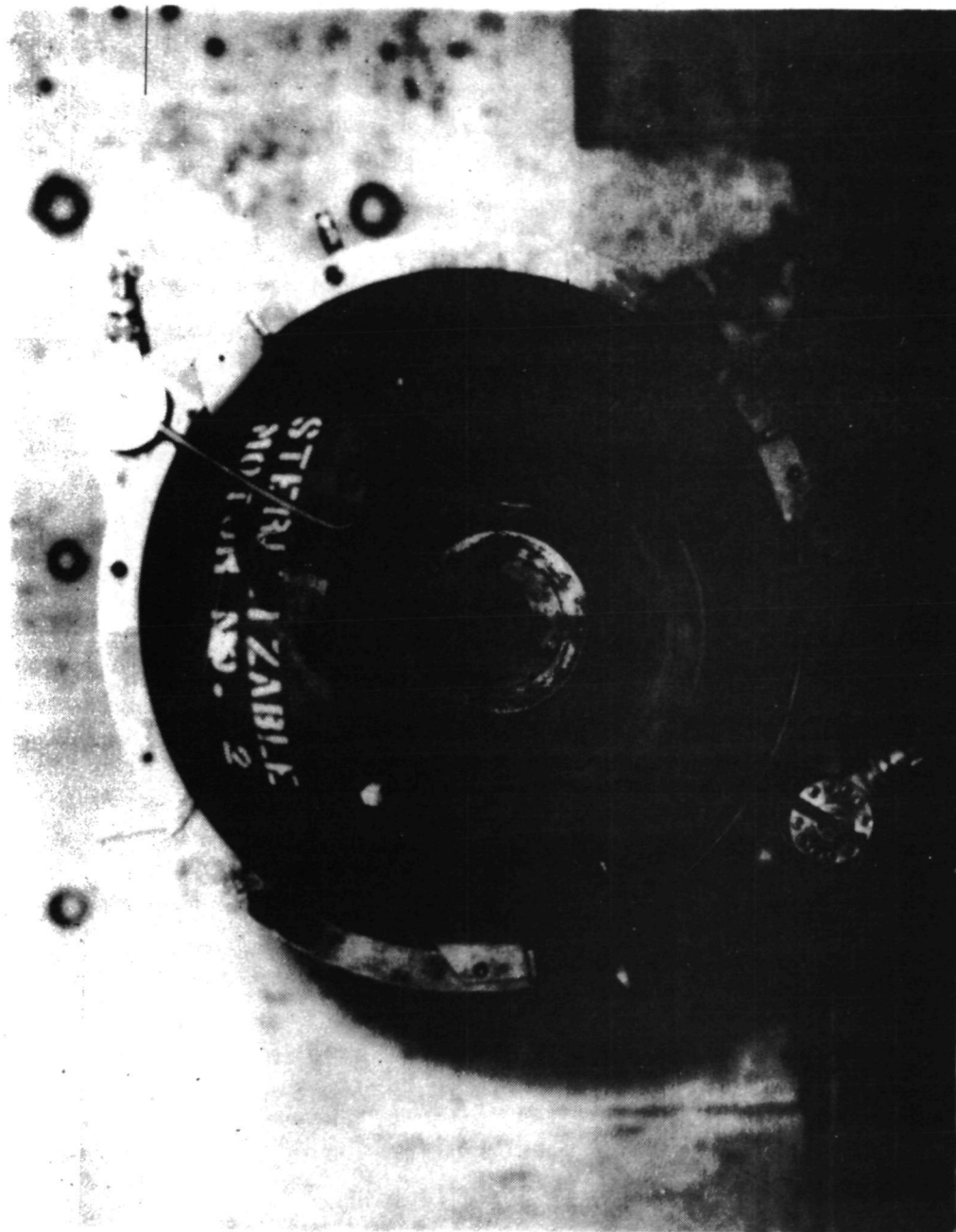


Sterilizable Motor SN 2, Pretest

Figure 99



Sterilizable Motor SN 2, Pretest



Sterilizable Motor SN 2, Posttest

Figure 101

b. The boot can be reduced in thickness by about 50% - 0.66 Kg (1.45 lb).

c. The retention disks can be reduced in thickness by about 50% and, depending on load requirements, could be reduced in quantity by about 50% - 0.34 Kg (0.75 lb).

d. The net insulation penalty would be reduced from 2.5 Kg (5.5 lb) to 0.77 Kg (1.7 lb). Under these conditions the motor mass fraction (assuming no added propellant) would increase from 0.8246 to 0.8443. With additional design effort, further increases in mass fraction would also be possible.

## APPENDIX A

### BINDER IMPROVEMENT

#### I. INTRODUCTION

The propellant initially selected for use in the Sterilizable Motor Demonstration Program was ANB-3289-3. This propellant contains a saturated HTPB binder composed of Telagen-S prepolymer crosslinked with trimethylol propane (TMP) and cured with dimeryl diisocyanate (DDI). This propellant had several undesirable features, including the crosslinker selected. In addition to being a solid material (M.P. 60°C), the crosslinker (TMP) is incompatible with the nonpolar HTPB. Therefore, great care is required during propellant processing to insure that the TMP remains in a finely divided, molten state until it reacts with the curing agent when it forms a reaction product compatible with the prepolymer. This requires that the premix containing the TMP be stored at relatively high temperatures (66°C to 82°C) and be agitated with a high-shear mixer just prior to propellant batch mixing. In addition, a 38 cm (15-in.) dia. grain of ANB-3289-3 propellant cracked during the early stages of heat sterilization at 135°C (275°F), indicating a problem in propellant strength.

A binder improvement program was, therefore, conducted to evaluate alternative approaches to eliminate these problems. These included: crosslinkers, curing agent, bonding agent, oxidizer stabilizing agent, prepolymer molecular weight and functionality, and solid particle surface treatment.

An extensive study of the above listed parameters was not possible due to a reallocation of funding to solve a grain cracking problem. However, sufficient work was conducted to permit the formulation of an improved binder system which resulted in the successful test firing of the heat sterilized demonstration motor.

## II. CROSSLINKING AND CURING AGENTS

### A. GLYCERYL TRIRICINOLEATE

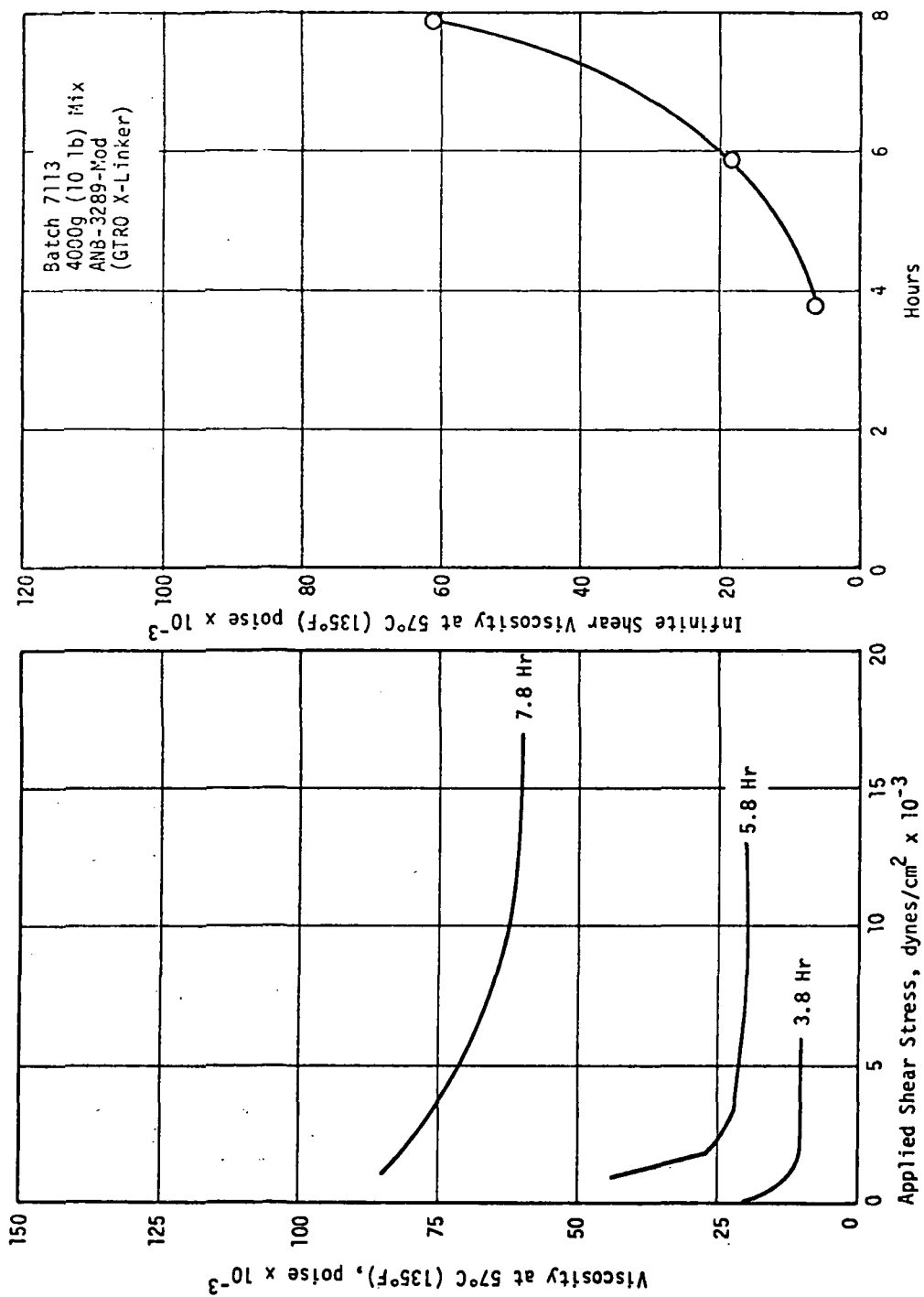
Glyceryl triricinoleate (GTRO) is a liquid crosslinking agent which is soluble in the Telagen-S prepolymer. Replacing TMP with GTRO, therefore, eliminated the need for high processing temperatures and the high shear agitation of the propellant premix. A series of 3500-gram batches of ANB-3289-3 propellant was made in which the TMP crosslinker was replaced with GTRO at the same calculated crosslink density level:

CROSSLINK DENSITIES AND COMPARATIVE EQUIVALENTS  
RATIOS OF GTRO AND TMP

<u>Crosslink Density</u> <u>Moles Branch Points/g x 10<sup>-4</sup></u>	<u>Equivalents</u> <u>GTRO</u>	<u>Equivalents</u> <u>TMP</u>
1.54	46	41
1.72	49	44
1.91	53	47
2.11	57	50

Visual observation indicated that the as-cast viscosity of the propellant containing the GTRO crosslinker was lower than that with comparable levels of TMP. However, the viscosity buildup rate was more rapid with GTRO (Figures 1-A and 2-A). Mechanical properties of the propellants are shown in Figure 3-A and a plot of the propellant modulus as a function of crosslink density of the propellants containing the two crosslinking agents is presented in Figure 4-A. Unlike the moduli of the TMP-propellants, which appears to increase continually with TMP level, the moduli of the GTRO-propellants tend to level off at the higher GTRO concentrations. In addition to the difference in the manner in which the modulus changes with crosslinker concentration, it is seen that the tensile strength and elongation of the GTRO propellants are inferior to those containing TMP (Figure 3-A).





Propellant Viscosity as a Function of Shear Stress and Time from Curing Agent Addition

Figure 1-A

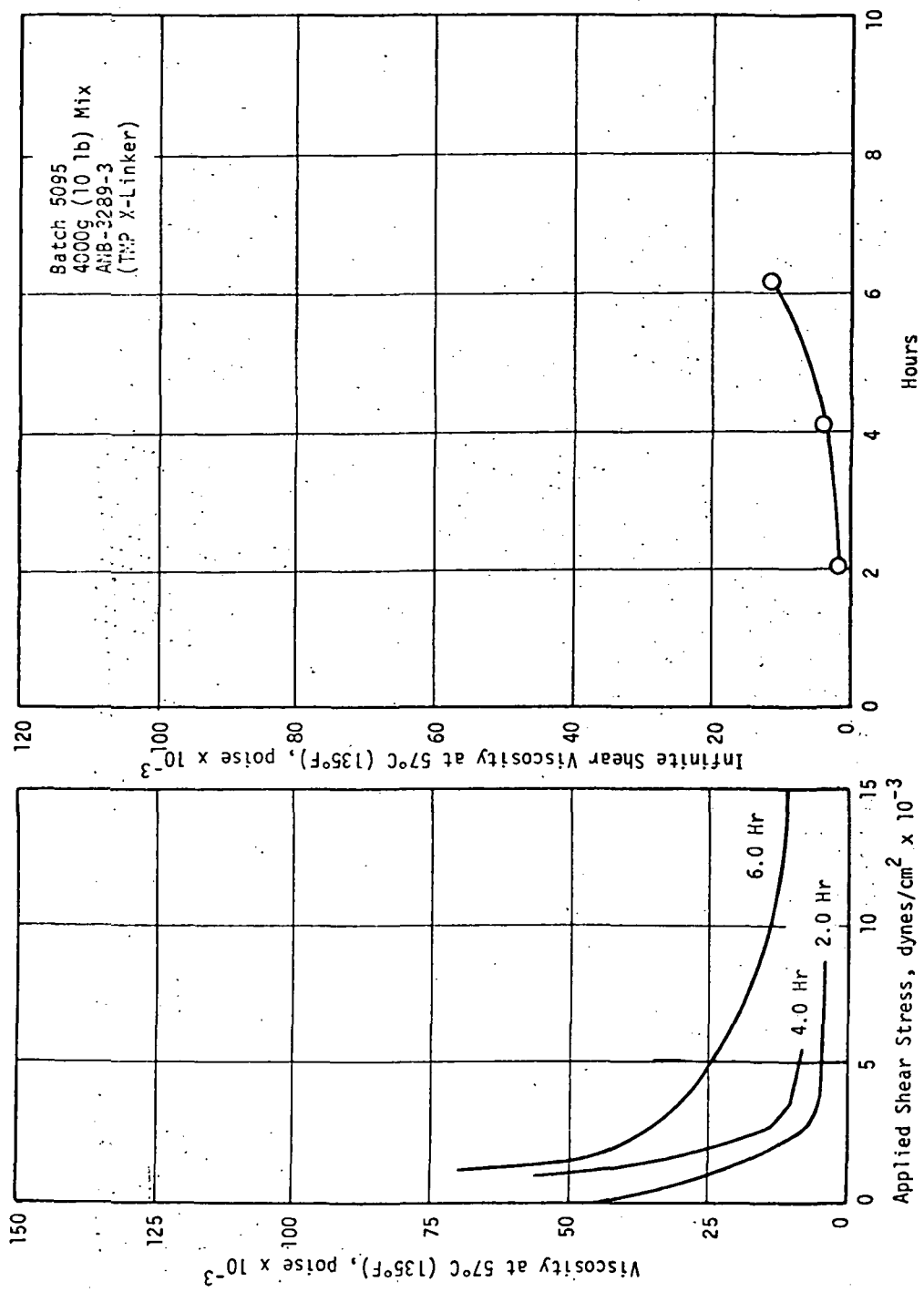


Figure 2-A

Propellant Viscosity as a Function of Shear Stress and Time from Curing Agent Addition

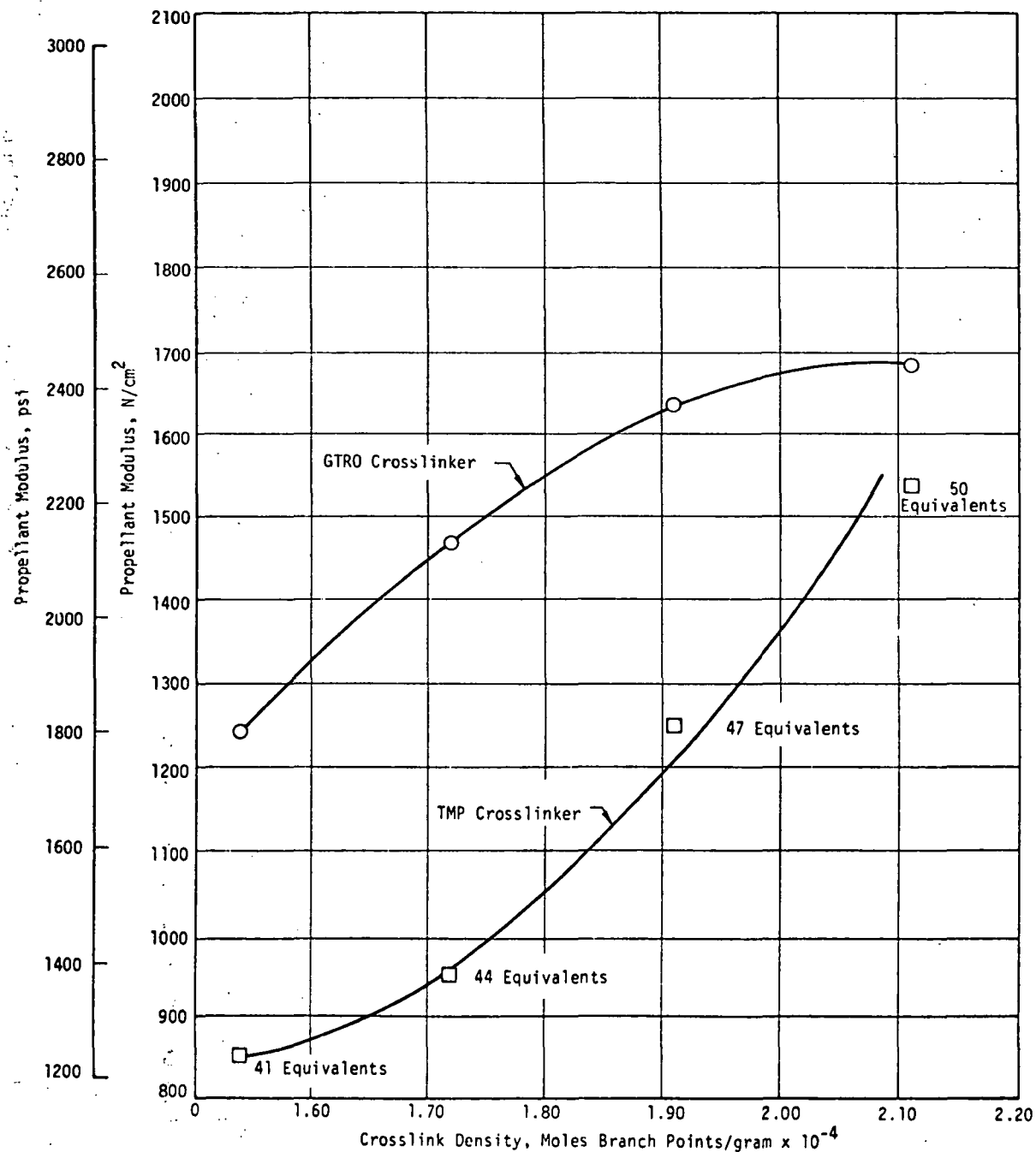
Batch Number <sup>(1)</sup>	Crosslinker Equiv. GTR	Mechanical Properties at 25°C (77°F)			
		$\sigma_m$ , N/cm <sup>2</sup> (psi)	$\epsilon_m$ , %	$\epsilon_m$ , %	$E_o$ , N/cm <sup>2</sup> (psi)
7113	46	100 (145)	12	13	1240 (1797)
7114	49	92 (133)	9	10	1472 (2133)
7152	53	86 (125)	7	8	1639 (2375)
7172	57	87 (126)	6	7	1684 (2440)
7173R <sup>(2)</sup>	49	85 (123)	7	8	1635 (2369)
<u>Equiv. TMP</u>					
6877	41	112 (163)	18	20	860 (1247)
6878	44	110 (160)	17	19	957 (1387)
6879	47	107 (155)	13	15	1252 (1814)
6880	50	115 (167)	11	12	1539 (2231)

(1) Binder composed of Telagen-S prepolymer, crosslinker, FC-154 bonding agent, and DDI curing agent.

(2) Prepared with stabilized oxidizer.

Effect of Crosslinker Level on Mechanical Properties of ANB-3289 Type Propellants

Figure 3-A



Effect of Crosslink Density on Modulus of ANB-3289-3-Type Propellant

Figure 4-A

Batch 7173R (Figure 3-A) containing the GTR0 crosslinker was prepared with stabilized oxidizer so that the propellant could be heat sterilized. A 7.6 cm x 7.6 cm x 12.7 cm (3 in. x 3 in. x 5 in.) block of this propellant was subjected to six 53-hour cycles at 135°C (275°F). No weight losses were noted and dimensional changes were minimal. Mechanical properties measured before and after heat sterilization are shown below along with data obtained from similar testing of propellant containing the TMP crosslinker prepared in a 91 Kg (200-lb) batch.

Batch	Crosslinker	Sterilization Cycles (53 hrs at 135°C (1175°F))	Mech. Prop. @ 25°C (77°F)			
			$\sigma_m$ , N/cm <sup>2</sup> (psi)	$\epsilon_m$ , %	$\epsilon_b$ , %	$E_o$ , N/cm <sup>2</sup> (psi)
7173R (3500g)	GTR0	0	85(123)	7	8	1635(2369)
		6	90(131)	11	14	1145(1660)
72-92	TMP	0	116(168)	16	18	1121(1625)
		6	90(131)	21	31	819(1187)

The loss in modulus, 29%, is similar to that experienced with propellant from the 91 Kg (200-lb) batch containing the TMP crosslinker. However, in the latter propellant there was also a corresponding drop in propellant tensile strength. The GTR0 propellant data showed a slight increase in tensile strength after heat sterilization.

#### B. ISOPHORONE DIISOCYANATE

In order to increase tensile strength and elongations of ANB-3289-3 propellant containing GTR0 crosslinker, the binder was further modified by replacing the DDI with isophorone diisocyanate (IPDI) curing agent. Also a new bonding agent, FC-217, was used instead of FC-154. A series of 400-gram batches were prepared over a range of GTR0 levels and the properties obtained are listed below:

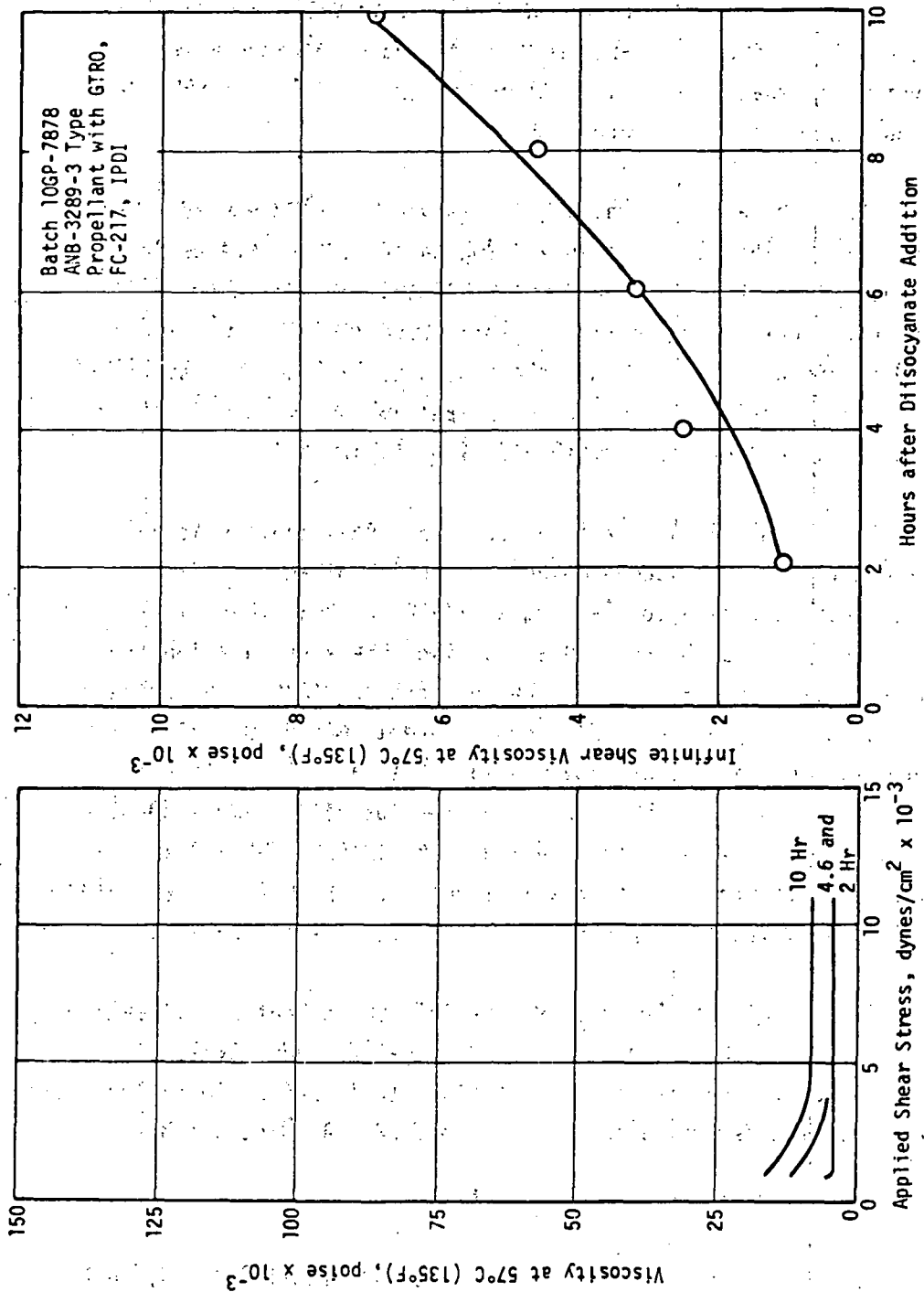
Mechanical Properties at 25°C (77°F)					
Batch	GTR0 Equiv.	$\sigma_m$ , N/cm <sup>2</sup> (psi)	$\epsilon_m$ , %	$\epsilon_b$ , %	$E_o$ , N/cm <sup>2</sup> (psi)
GMS-0-19-12-1	40	103(149)	64	87	344(499)
GMS-52-1	45	146(212)	40	51	675(978)
HMS-52-2	50	150(218)	32	43	857(1242)

The high tensile strengths obtained at the relatively low modulus levels are quite attractive for use in heat sterilizable applications, since these properties yield a system which is more resistant to failure caused by mechanical or temperature-induced stresses. (The modulus can be considered as the stress-inducing factor and the tensile strength as the stress-bearing factor in the propellant matrix).

The formulation containing FC-217 and 50 equivalents GTR0 was prepared in a 4000g batch mix with stabilized oxidizer for use in heat sterilization tests. Processability of this propellant was excellent. Viscosity buildup data are shown in Figure 5-A. The propellant was extremely fluid, reaching approximately 7000 poise at 62°C (135°F) 10 hours after diisocyanate addition. The excellent process characteristics also indicate that higher solids loadings should be readily obtainable.

The IPDI curing agent was also employed in place of DDI in the standard ANB-3289-3 propellant system, which utilizes Telagen-S, FC-154 and TMP. A 1-lb batch of this propellant was inferior in processability to that containing the DDI curative, did not flow well under vibration, and cured rapidly to a crumbly, non-uniform consistency. When IPDI was used as the curative with GTR0 replacing the TMP crosslinker the result was a propellant with excellent processability, and the following mechanical properties were obtained.

Mechanical Properties at 25°C (77°F)					
Batch	Equiv. of GTR0	$\sigma_m$ , N/cm <sup>2</sup> , (psi)	$\epsilon_m$ , %	$\epsilon_b$ , %	$E_o$ , N/cm <sup>2</sup> , (psi)
GMS-49-2	46	128(185)	20	33	1252(1814)
GMS-50-3	57	141(204)	11	16	2518(3650)



Propellant Viscosity as a Function of Shear Stress and Time from Curing Agent Addition

Figure 5-A

The initial mechanical properties of the batch containing 46 equivalents GTR0 and the IPDI curing agent are superior to those obtained with the TMP/DDI systems in that higher elongations are obtained at a given modulus level (compare with data in Figure 3-A).

The formulation containing 46 equivalents GTR0 and 105 equivalents IPDI with FC-154 was mixed in a 4000g batch (10GP-7977) using stabilized ammonium perchlorate to prepare samples for heat sterilization tests. The excellent processability of this propellant is indicated by the viscosity data shown in Figure 6-A. The viscosity buildup is just slightly faster than that described above for the propellant using FC-217 with the GTR0/IPDI crosslinker/curative combination (see Figure 5-A).

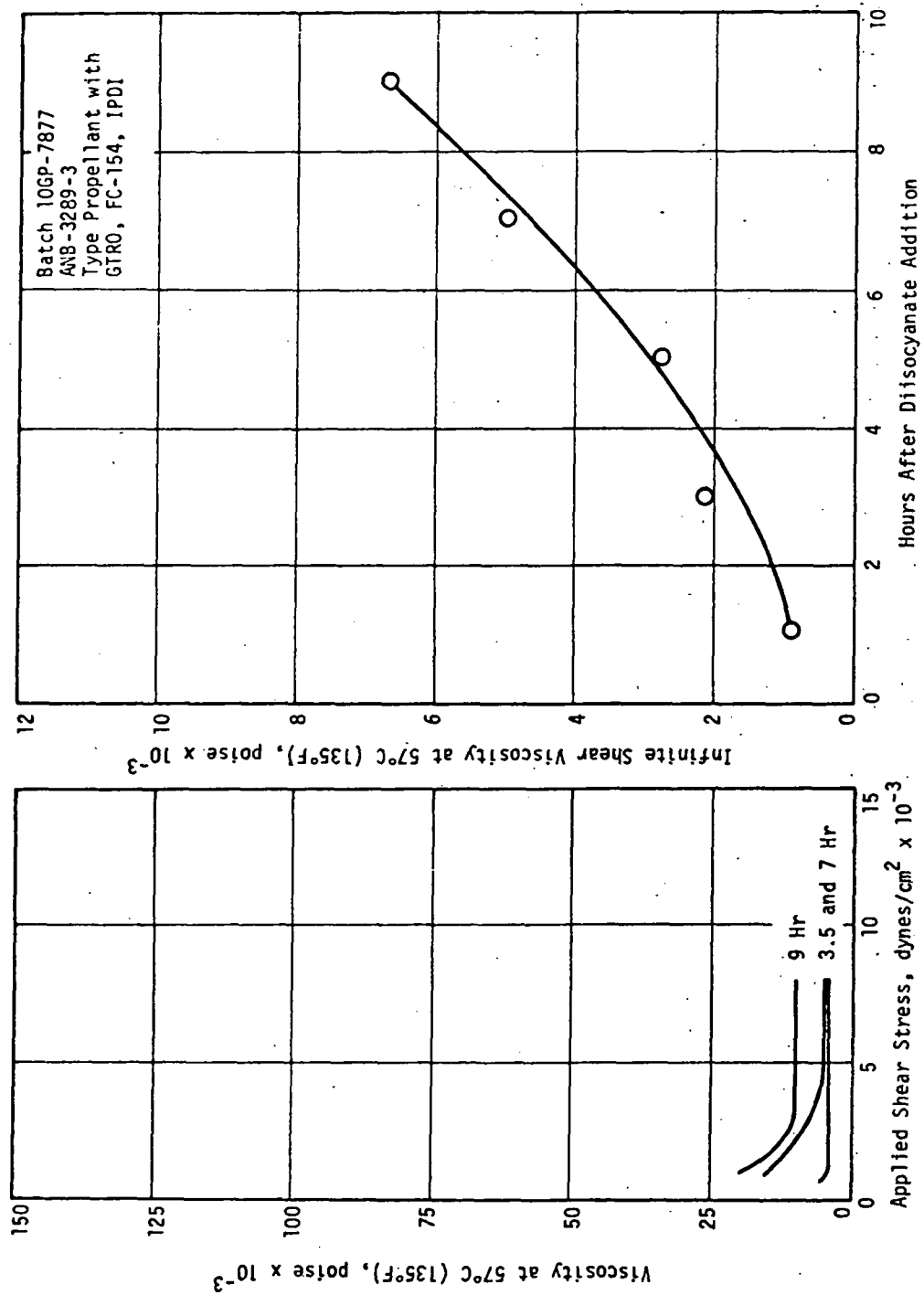
Propellant samples from the batches containing the Telagen-S/GTR0/IPDI/FC-217 and the Telagen-S/GTR0/IPDI/FC-154 binder systems were subjected to heat sterilization testing at 135°C (275°F). Results are tabulated in Figure 7-A. Both propellants survived the sterilization treatment without cracking or experiencing weight loss or dimensional changes. The propellant containing the FC-217 bonding agent (Batch 10GP-7878) increased in both tensile strength and modulus, but maintained its rather high elongation ( $\epsilon_b$  of 37%) even though the modulus value almost doubled. The propellant using FC-154 as the bonding agent (Batch 10GP-7877) also increased in tensile strength and modulus, however, in this mix experienced some loss in elongation (31%  $\epsilon_b$  down to 21%  $\epsilon_b$  after sterilization).

As a result of the excellent resistance to heat sterilization, a propellant based on the Telagen-S/GTR0/IPDI/FC-217 binder system (ANB-3438) was selected for use in large grain heat sterilization tests and later for casting into the demonstration motors (see Technical Discussion).

#### C. SATURATED GTR0 CROSSLINKING AGENTS

Propellants prepared with the Telagen-S/GTR0/IPDI/FC-217 binder systems harden considerably during the heat sterilization cycles. One





Propellant Viscosity as a Function of Shear Stress and Time from Curing Agent Addition

Figure 6-A

Mechanical Properties at 25°C (77°F)											
Batch No.	Cross-linker	Curing Agent	Bonding Agent	Before Sterilization				After Sterilization (1)			
				$\sigma_m$	$\epsilon_m$	$\epsilon_b$	$E_o$	$\sigma_m$	$\epsilon_m$	$\epsilon_b$	$E_o$
				N/cm <sup>2</sup> (psi)	%	%	N/cm <sup>2</sup> (psi)	N/cm <sup>2</sup> (psi)	%	%	N/cm <sup>2</sup> (psi)
10GP-7878	GTR0	IPDI	FC-217	147 (213)	27	38	1107 (1605)	226 (328)	28	37	2056 (2979)
10GP-7877	GTR0	IPDI	FC-154	121 (176)	20	31	1308 (1896)	159 (230)	14	21	2169 (3144)

(1) Six 53-hour cycles at 135°C (275°F), test sample size was 7.6 cm x 7.6 cm x 12.7 cm (3" x 3" x 5")

Effect of Heat Sterilization of Mechanical Properties  
of ANP-3289-3 Propellant Modifications

Figure 7-A

possible explanation of this phenomenon is that the glyceryl triricinoleate moiety of the cured binder network is undergoing oxidative cross-linking at its points of unsaturation. (There is one carbon-carbon double bond in each ricinoleic acid group).

An effort was made to eliminate this postcure hardening by using a saturated GTRO, "Castorwax", in place of the unsaturated material. The Castorwaxes are relatively high-melting materials, 70-80°C, but are compatible with the Telagen-S binders. However, propellant prepared using Castorwax as a crosslinker was quite thixotropic and exhibited very poor flow properties. Mechanical properties obtained from the Castorwax propellant are compared to those at an equivalent level of GTRO in the following table:

<u>Batch No.</u>	<u>Crosslinker</u>	<u>Uniaxial Ten. Prop. at 25°C (77°F)</u>			
		$\sigma_m, N/cm^2$ <u>(psi)</u>	$\epsilon_m, \%$ <u>%</u>	$\epsilon_b, \%$ <u>%</u>	$E_o, N/cm^2$ <u>(psi)</u>
GMS-76-A	40 eq. Castorwax	153(222)	24	34	1176(1704)
SAN-64-3	40 eq. GTRO	95(138)	35	65	842(1220)

A considerable increase in tensile strength was obtained at a relatively low increase in modulus when the Castorwax was used. Because of the deleterious effects on flow properties, the use of Castorwax as the sole crosslinking agent does not appear feasible. However, a proper blend of Castorwax and GTRO may offer a satisfactory compromise with respect to flow and mechanical properties.

#### D. LHT-240 CROSSLINKING AGENT

As part of the binder improvement program crosslinking agent, LHT-240, was evaluated with Telagen-S prepolymer utilizing IPDI curing agent and the FC-217 bonding agent. LHT-240 is an adduct of hexane triol and polypropylene glycol, and, like GTRO, is quite fluid at room temperatures.

A 400g batch of ANB-3289-3 type propellant (Batch 10GP-8615) was prepared with a binder composed of Telagen-S/LHT-240/IPDI in a 50/50/105 equivalents ratio. FC-217 was included as the bonding agent. The propellant was quite thixotropic, as indicated by the viscosity versus shear stress relationship shown in Figure A-8. Although the propellant exhibited a low viscosity and good potlife at infinite shear stress, the low-shear flow properties were quite poor and the propellant samples cast showed little tendency to flow, even under vibration. Based on these results, further work with the LHT-240 crosslinker was discontinued.

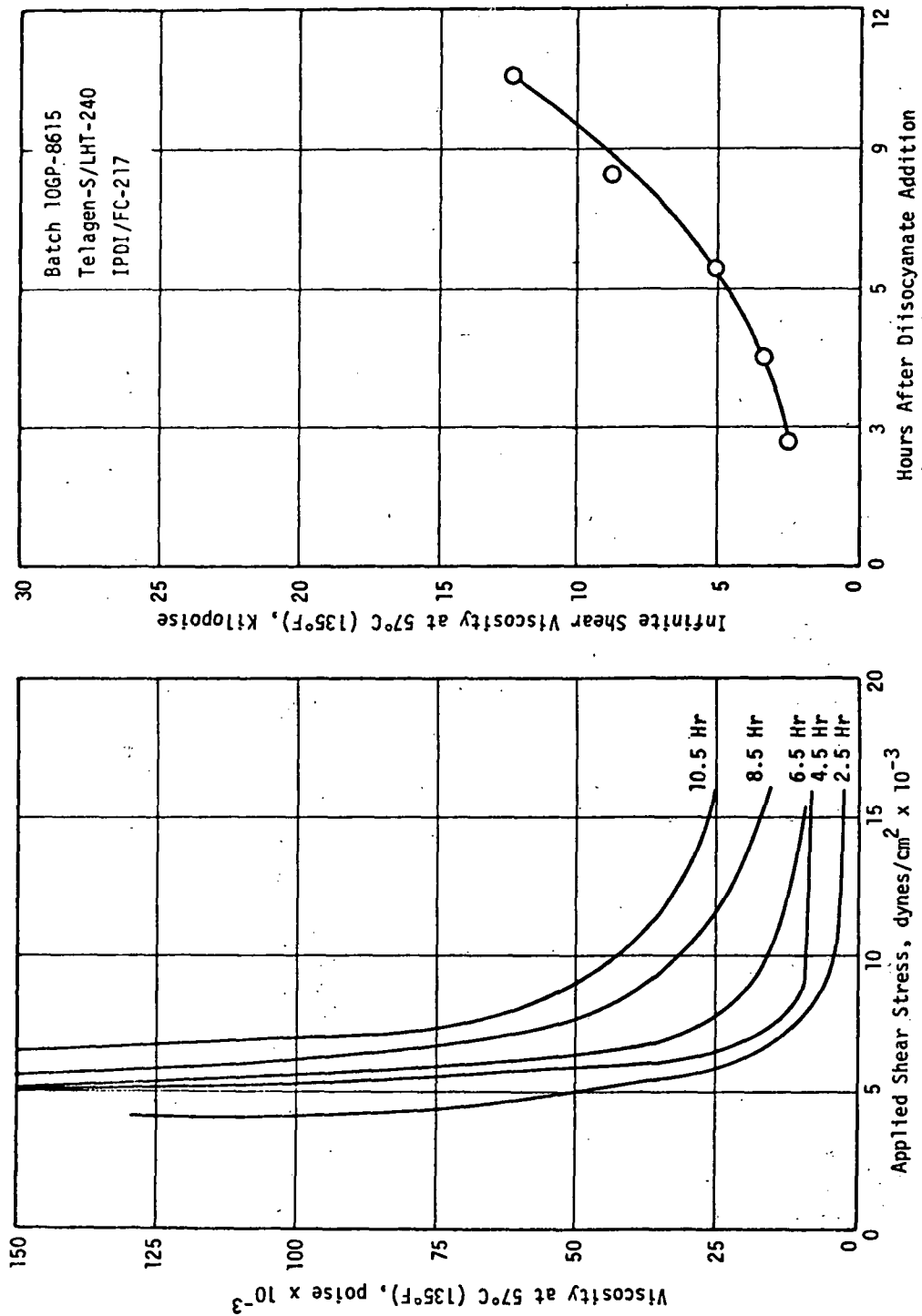
### III. EVALUATION OF PREPOLYMERS

#### A. EFFECT OF PREPOLYMER MOLECULAR WEIGHT AND DIFUNCTIONALITY CONTENT

Propellant characteristics, such as mechanical properties and processability, can be greatly influenced by the molecular weight and extent of difunctionality in the prepolymer. One of the tasks in the improved binder program was to prepare propellants with prepolymers of different molecular weights and degrees of difunctionality in order to establish guidelines for prepolymer manufacture for use in heat-sterilization applications.

An experimental prepolymer, Lot 3 HPL-219/221, which had a molecular weight of 1900 and contained 74.5% difunctional species, was obtained from the General Tire and Rubber Company. ANB-3289-3 propellant was prepared in 1-lb mixes with this material at crosslink levels of 30 to 50 equivalents of TMP. Control formulations utilizing Lot 316-AM 11/12 Telagen-S prepolymer were also prepared (M.W. of 1575 and 72% difunctionality). Visual observation showed no difference in processability between the propellants containing the two prepolymers. Mechanical properties of the propellant batches are shown in Figure 9-A.

The changes in modulus and tensile strength over the TMP concentrations used are shown graphically in Figures 10-A and 11-A. With the exception of the data points at 35 equivalents TMP, the properties show the expected trend in behavior. However, both the tensile strength and modulus



Propellant Viscosity as a Function of Shear Stress and Time from Curing Agent Addition

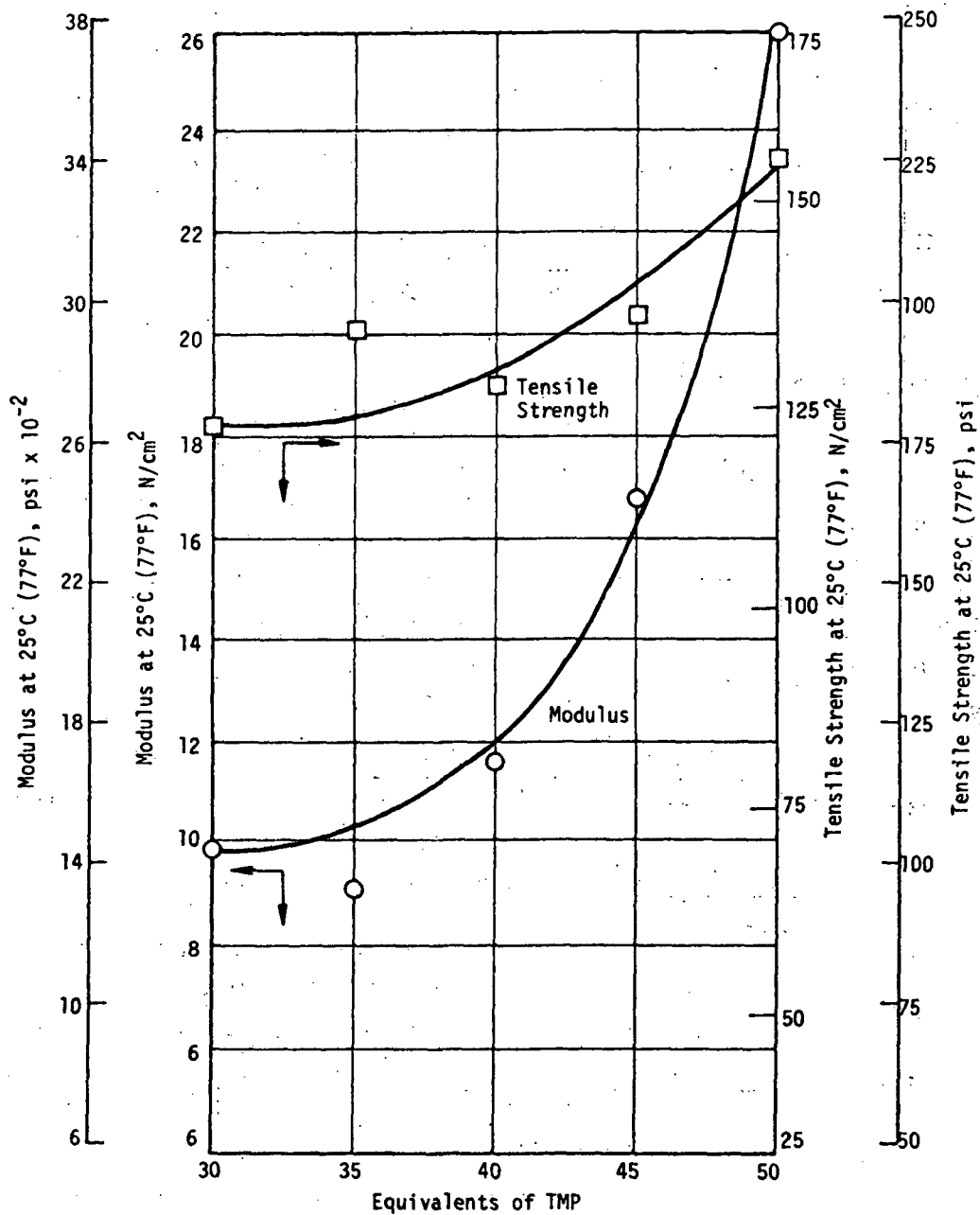
Figure 8-A

Batch No.	Equiv. of TMP	Telagen-S Lot	Mechanical Properties at 25°C (77°F)				
			$\sigma_m$ , N/cm <sup>2</sup> (psi)	$\epsilon_m$ , %	$\epsilon_b$ , %	$E_0$ , N/cm <sup>2</sup> (psi)	
GMS-54-3	30	316AM-11 & 12 (1)	107 (155)	29	49	705 (1022)	
GMS-0-18-12-1	35	316AM-11 & 12 (1)	118 (171)	30	42	531 (770)	
GMS-0-19-15-1	40	316AM-11 & 12 (1)	123 (178)	20	29	983 (1424)	
GMS-0-19-15-2	45	316AM-11 & 12 (1)	139 (201)	15	19	1460 (2116)	
7567-47-1	50	316AM-11 & 12 (1)	135 (195)	12	17	1748 (2534)	
GMS-54-1	30	3HPL-219/221 (2)	123 (178)	19	27	990 (1435)	
GMS-0-19-12-3	35	3HPL-219/221 (2)	134 (194)	22	30	910 (1319)	
7252	40	3HPL-219/221 (2)	128 (185)	17	22	1161 (1682)	
7253	45	3HPL-219/221 (2)	136 (197)	12	13	1682 (2438)	
GMS-54-2	50	3HPL-219/221 (2)	190 (275)	9	11	2602 (3771)	

- (1) 72% difunctional species, MW - 1575  
(2) 74.5% difunctional species, MW - 1900

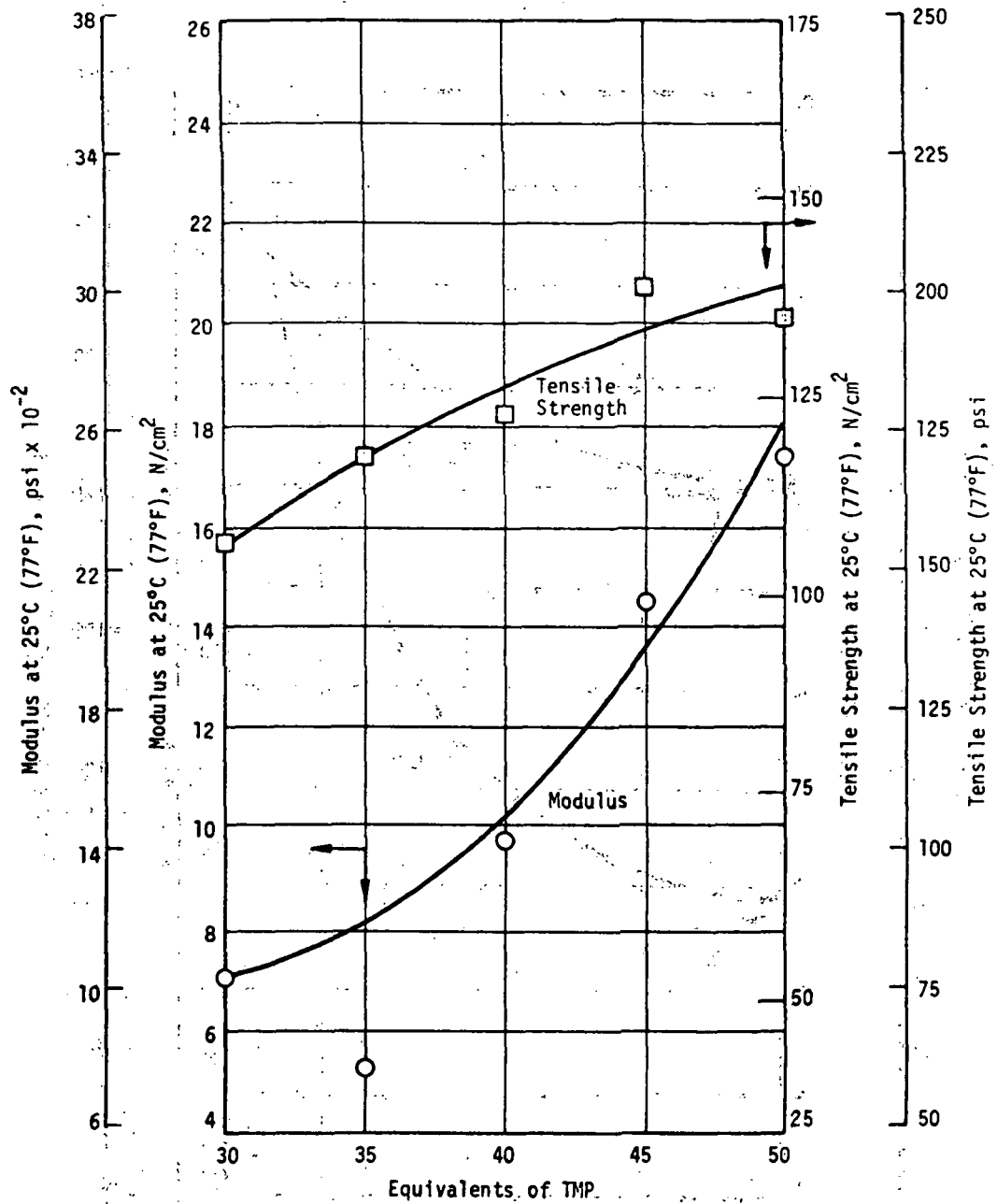
Effect of Telagen-S Functionality on Mechanical Properties  
of ANB-3289-3 Propellant Mixed in 1-lb Batches

Figure 9-A



Effect of TMP Level on Modulus and Tensile Strength of ANB-3289-3  
Propellant Prepared with Lot 3HPL-219/221 Telagen-S

Figure 10-A



Effect of TMP Level on Modulus and Tensile Strength of ANB-3289-3  
Propellant Prepared with Lot 316AM 11/12 Telagen-S

Figure 11-A



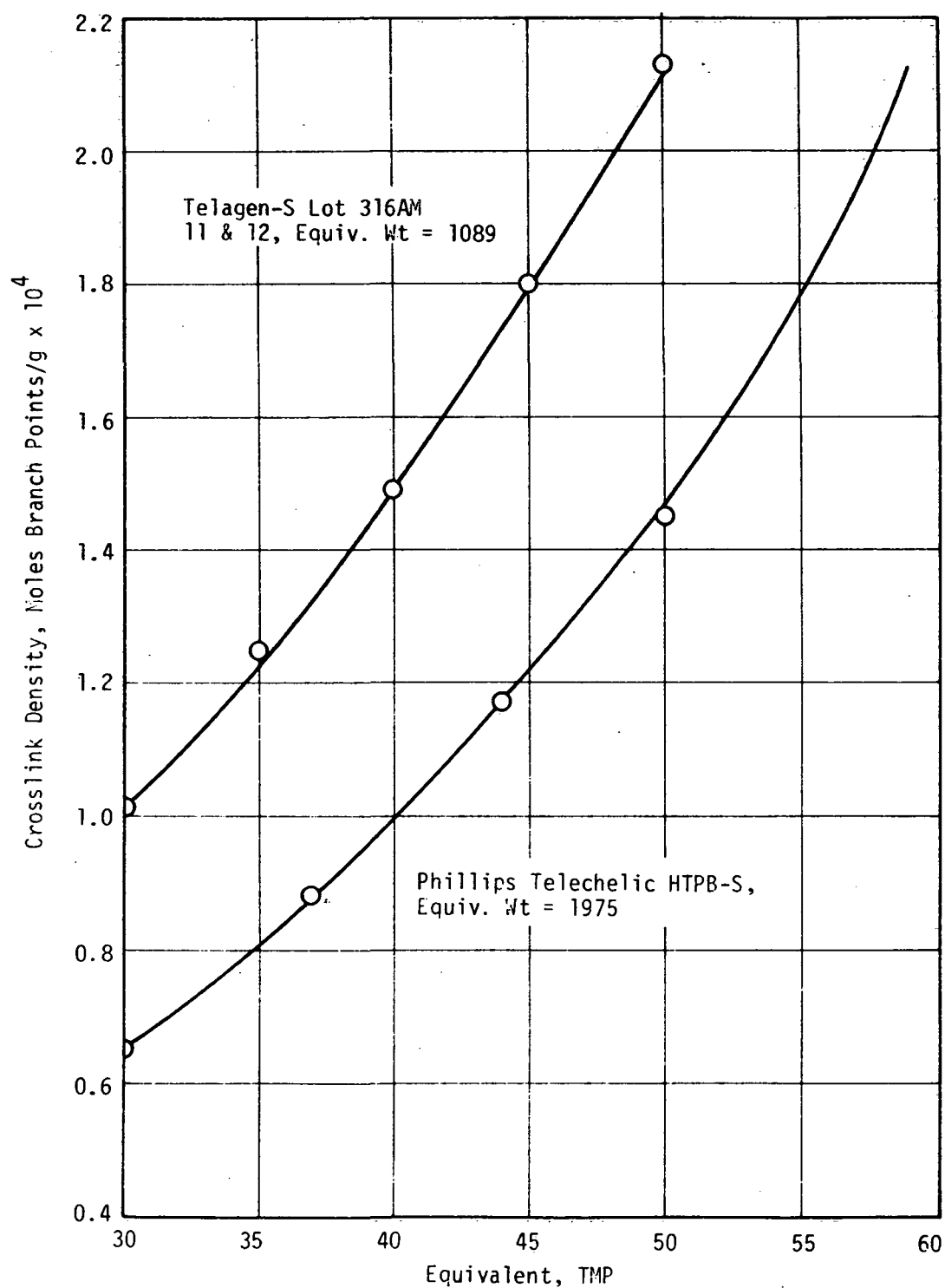
of the propellant prepared from the experimental prepolymer, Lot 3HPL-219/221 (Figure 10-A) are at a higher level than that made with Lot 316AM-11/12 Telagen-S (Figure 11-A). This is especially true of the moduli obtained at 50 equivalents TMP crosslinker.

#### B. NEW PREPOLYMER EVALUATION

Two 454g samples of saturated HTPB telechelic prepolymers were obtained from Phillips Petroleum Company. One sample had an equivalent weight of 1975, the other 1242. These values were calculated from the data supplied by the vendor. Four-hundred gram batch mixes of ANB-3289-3 propellant were made with the 1975 equivalent weight prepolymer (lot 49914) at TMP crosslinker levels of 30, 37, 44 and 50 equivalents. None of the batches reached a satisfactory cure. Increasing the TMP level to 60 equivalents resulted in a proper cure with the following mechanical properties at 25°C (77°F).

$\sigma_m$ , N/cm <sup>2</sup> (psi)	99(144)
$\epsilon_m$ , %	17
$\epsilon_b$ , %	19
$E_o$ , N/cm <sup>2</sup> (psi)	1550(2247)

This modulus compares to that obtained at a TMP level of ~47 equivalents using a Telagen-S prepolymer which has an equivalent weight of 1089. Part of the difference in properties between the two HTPB materials can be attributed to the equivalent weights which in turn affect the crosslink density of the propellant at a given TMP level. This is illustrated in Figure 12-A which shows that an increase of 10 equivalents TMP is needed to achieve the same crosslink density with the 1975 equivalent weight Phillips prepolymer as with the 1089 equivalent weight Telagen-S. The difference in equivalent weights is only part of the explanation, however, since propellants prepared with Telagen-S will cure even at low crosslink densities. Another reason for the low state of cure is that the Phillips prepolymer probably contains a lesser amount of difunctional species than does the Telagen-S. This lower difunctionality level would result in soft cure unless a high concentration of crosslinker were used.



Effect of TMP Level on Crosslink Density of Propellant Using  
Prepolymers with Different Equivalent Weights

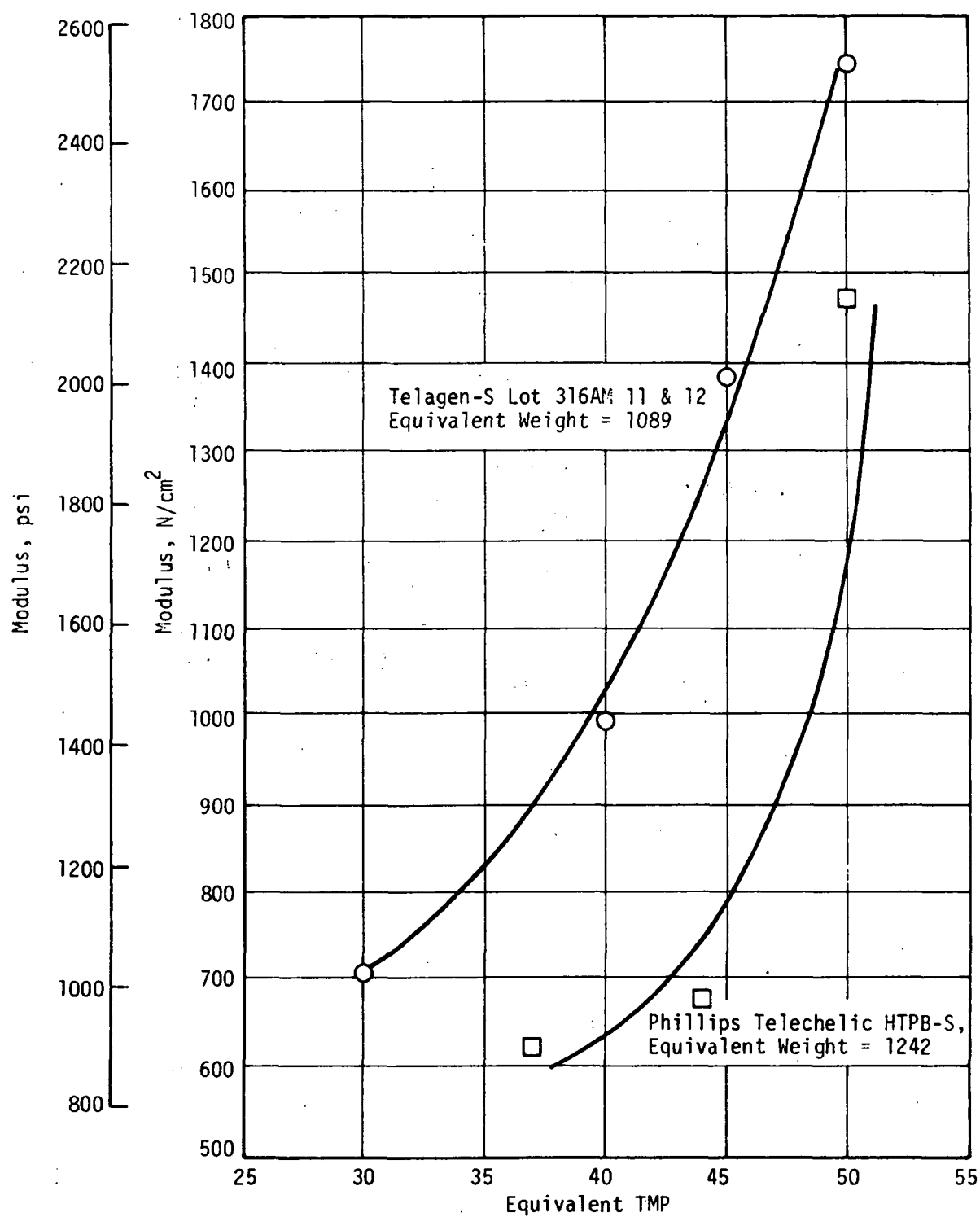
Figure 12-A

A similar series of 400g batch mixes was prepared using another Phillips experimental telechelic prepolymer (lot 49926) with an equivalent weight of 1242. These batches cured satisfactorily and exhibited the following mechanical properties.

Batch No.	Equivalents of TMP	Uniaxial Ten. Prop. at 25°C. (77°F)			
		$\sigma_m$ , N/cm <sup>2</sup> (psi)	$\epsilon_m$ , %	$\epsilon_b$ , %	$E_o$ , N/cm <sup>2</sup> (psi)
GMS-77-2	37	117(169)	30	41	626(907)
GMS-77-3	44	124(179)	26	34	686(994)
GMS-77-4	50	95(137)	12	33	1480(2145)

A comparison of the modulus versus TMP level relationship for the propellants prepared with the Phillips prepolymer (equivalent weight 1242) with that observed in the Telagen-S system is shown in Figure 13-A. An examination of the data in Figure 13-A indicates that lot 49926 Phillips prepolymer is much more similar than lot 49914 material to the Telagen-S prepolymer.

The Phillips telechelic prepolymers were also evaluated in ANB-3438 propellant which uses GTR0 as the crosslinking agent. A series of 400g batches with Phillips prepolymer (lot 49926, equiv. wt = 1242) were made over a range of crosslinker equivalents level. Mechanical property data are presented in Figure 14-A and a comparison of the modulus vs crosslinker level for propellants prepared with the Phillips and Telagen-S prepolymers is shown in Figure 15-A. With the Phillips material, the moduli showed a much greater increase as the level of crosslinker was increased (Figure 15-A). At the low level of GTR0 (35 equivalents) the elongations were quite high, 68 and 98%, respectively, for  $\epsilon_m$  and  $\epsilon_b$ . At higher crosslinker levels (higher moduli) the elongations at break ( $\epsilon_b$ ) were still high in view of the modulus levels. A comparison of the modulus vs crosslinker level relationship of propellant prepared from the two prepolymers (Figure 15-A) shows that much higher moduli are obtained with the Phillips material than with the Telagen-S prepolymer. Based on all the results obtained, it is clear that the Phillips Petroleum prepolymer can be substituted for Telagen-S in sterilizable propellants.



Effect of TMP Level on Modulus of Propellant Prepared with Different Prepolymers

Figure 13-A

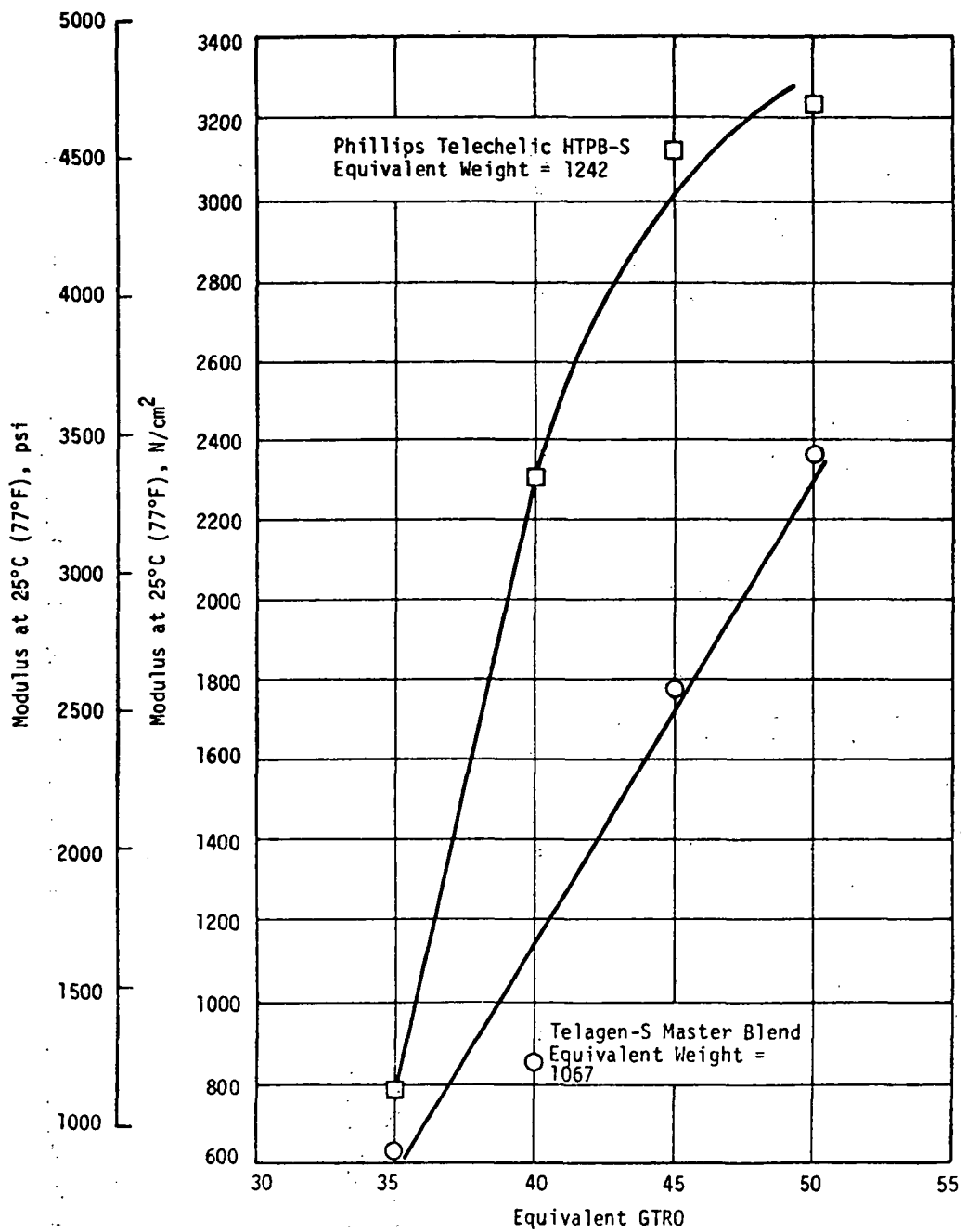
Batch No. (2)	Equiv. GTRO Crosslinker	Uniaxial Tensile Properties at 25°C (77°F)				
		$\sigma_m$ , N/cm <sup>2</sup> (psi)	$\epsilon_m$ , %	$\epsilon_b$ , %	$E_o$ , N/cm <sup>2</sup> (psi)	
1GP-9868	35	90 (130)	68	96	781	(1132)
1GP-9869	40	90 (130)	54	64	2309	(3347)
1GP-9870	45	93 (135)	4	25	3122	(4524)
1GP-9871	50	106 (154)	5	35	3235	(4689)

(1) Lot 49926, equiv. wt. - 1242

(2) 450g (1-lb) batch mixes

Mechanical Properties of ANB-3438 Propellant Prepared with Phillips Telechelic Prepolymer (1)

Figure 14-A



Effect of GTR0 Level on Modulus of ANB-3438 Propellant  
Prepared with Different Prepolymers

Figure 15-A

#### IV. EVALUATION OF AN ALTERNATIVE OXIDIZER STABILIZING AGENT

Recrystallized oxidizer containing a new stabilizing agent, FC-171, was used to prepare ANB-3289-3 propellant for comparison with that containing the currently used stabilizing agent, FC-169. A 3500g propellant batch was prepared with each stabilizing agent, and the oxidizer blend employed was a 60/40 mixture of 130 $\mu$  and 28 $\mu$  material. Blocks of the propellant (10.2 cm cubes) were subjected to heat sterilization cycles of 53 hours each at 135°C (275°F). Mechanical property data were obtained at 0, 6, and 12 sterilization cycles and are shown in Figure 16-A. The tensile strength of the propellant prepared with the FC-171 stabilized oxidizer is appreciably higher than that obtained with the FC-169 stabilized AP, 161 vs 124 N/cm<sup>2</sup> (234 vs 179 psi), respectively, for the unaged material. The propellant elongations were essentially the same. The moduli increased during the first six cycles then decreased to the approximate value of the unaged specimens during the last six cycles. The only apparent change in properties after the 12 cycles is the decrease in tensile strength.

Tests with large diameter grains of ANB-3289-3 (see Technical Discussion) propellant showed it could not survive more than two heat sterilizations under the above conditions. This problem in large grains is believed to be due to inadequate strength, as shown by the data, the FC-171 stabilizer should be useful in overcoming this problem.

#### V. REMOVAL OF BONDING AGENT

Consideration was given to the possibility that the large shift in stress-free temperature could be due partly to the secondary bonds formed between oxidizer and binder breaking and reforming at the higher temperatures. These secondary bonding forces are due mainly to bonding agent-oxidizer interactions. Therefore, the elimination of the bonding agent might cause a reduction in the stress-free temperature shifts observed in ANB-3289-3 propellant.

Batch No.	Oxidizer Stabilizing Agent (2)	Initial			After 6 Sterilization Cycles				After 12 Sterilization Cycles				
		$\sigma_m$ N/cm <sup>2</sup> (psi)	$\epsilon_m$ %	$\epsilon_b$ %	$E_o$ N/cm <sup>2</sup> (psi)	$\sigma_m$ N/cm <sup>2</sup> (psi)	$\epsilon_m$ %	$\epsilon_b$ %	$E_o$ N/cm <sup>2</sup> (psi)	$\sigma_m$ N/cm <sup>2</sup> (psi)	$\epsilon_m$ %	$\epsilon_b$ %	$E_o$ N/cm <sup>2</sup> (psi)
10GP-9414	FC-171	161 (234)	26	32	945 (1369)	145 (210)	19	23	1229 (1781)	130 (189)	24	31	983 (1424)
10GP-9435	FC-169	124 (179)	27	36	823 (1193)	126 (183)	18	22	1267 (1836)	98 (142)	24	34	903 (1308)

(1) Tested at 25°C (77°F)

(2) 0.5 wt% of oxidizer

Effect of Oxidizer Stabilizer Type on Mechanical Properties (1) of ANB-3289-3 Propellant

Figure 16-A



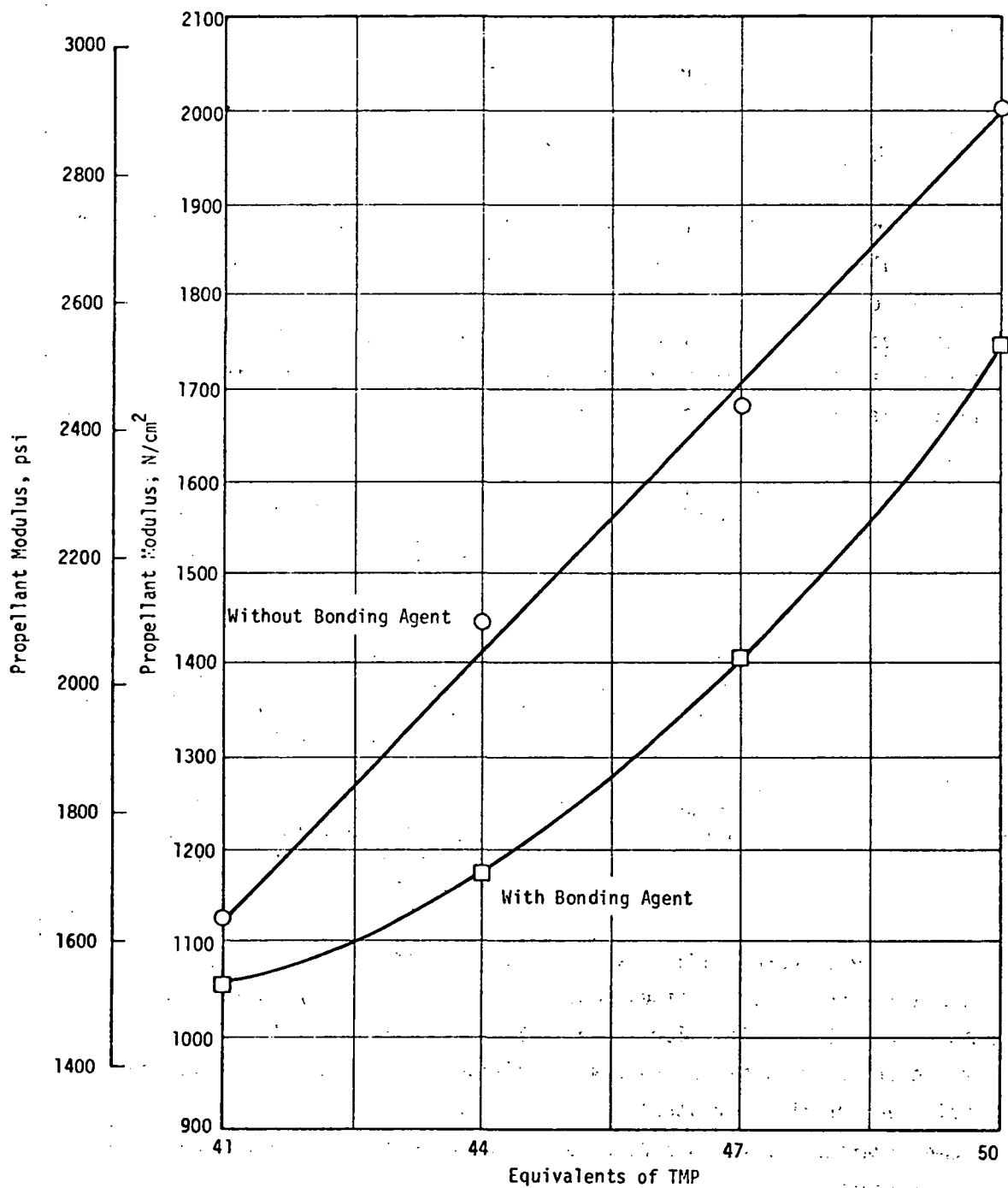
ANB-3289-3 propellant was prepared in 400g size mixes over a range of 41 to 50 equivalents TMP crosslinker, both with and without the FC-154 bonding agent. No differences could be observed visually in the as-cast propellant viscosities. Mechanical properties obtained from the two series of propellant mixes are shown in Figure 17-A. Comparative plots of modulus vs TMP level are presented in Figure 18-A. The propellants prepared with the bonding agent exhibited greater tensile strengths and lower moduli than the corresponding formulations without bonding agent. The elongations of the propellants with bonding agent were also slightly higher (perhaps not statistically significant) than those without bonding agent, at the same TMP level.

The effect of removing the bonding agent on heat sterilizability is described in the Technical Discussion.

Batch No.	TMP Equiv.	Bonding Agent	Mechanical Properties at 25°C (77°F)			
			$\sigma_m$ , N/cm <sup>2</sup> (psi)	$\epsilon_m$ , %	$\epsilon_b$ , %	$E_o$ , N/cm <sup>2</sup> (psi)
47-1	41	10 eq. FC-154	119 (172)	19	27	1054 (1528)
47-2	44	10 eq. FC-154	134 (194)	16	22	1178 (1704)
47-3	47	10 eq. FC-154	131 (190)	14	20	1411 (2045)
47-4	50	10 eq. FC-154	135 (195)	12	17	1748 (2534)
51-1	41	None	102 (148)	17	24	1130 (1638)
51-2	44	None	119 (172)	13	17	1449 (2100)
51-3	47	None	112 (163)	12	19	1684 (2440)
51-4	50	None	128 (186)	10	13	2007 (2908)

Effect of TMP Level on Mechanical Properties of ANB-3289-3 Propellant Prepared in 400 g Batches With and Without Bonding Agent

Figure 17-A



Effect of TMP Level on ANB-3289-3 Propellant Modulus  
454g (1-lb) Batches

Figure 18-A

## APPENDIX B

### INSULATION IMPROVEMENT

#### I. INTRODUCTION

In addition to the primary function of providing thermal protection, the insulation material used in heat sterilizable motor systems must also be compatible with the liner and propellant, so that the heat sterilization conditions will not cause interactions which would affect the reliability of the sterilized motor. Some of the insulation properties which could cause problems are shown below:

- |   |  |
|---|--|
| 1. Hardening during heat sterilization.                 | An undue stiffening of the insulation would cause an increase in bond stresses associated with the shift in stress-free temperature. |
| 2. Exudation of migratory species during sterilization. | Migration of liquid components would tend to weaken the insulation-to-liner and liner-to-propellant bond.                            |
| 3. Presence of metallic species.                        | Certain metal ions can catalyze the degradation of the urethane linkage at the heat sterilization temperatures.                      |

The GenGard V-4030 insulation used in the present program showed a small increase in stiffness and loss in ablative properties after the six heat sterilization cycles (53 hours each at 135°C (275°F)). While its overall performance was satisfactory for use in the design selected for the demonstration motors, a portion of the Motor Demonstration Program was devoted to the development of improved insulations.

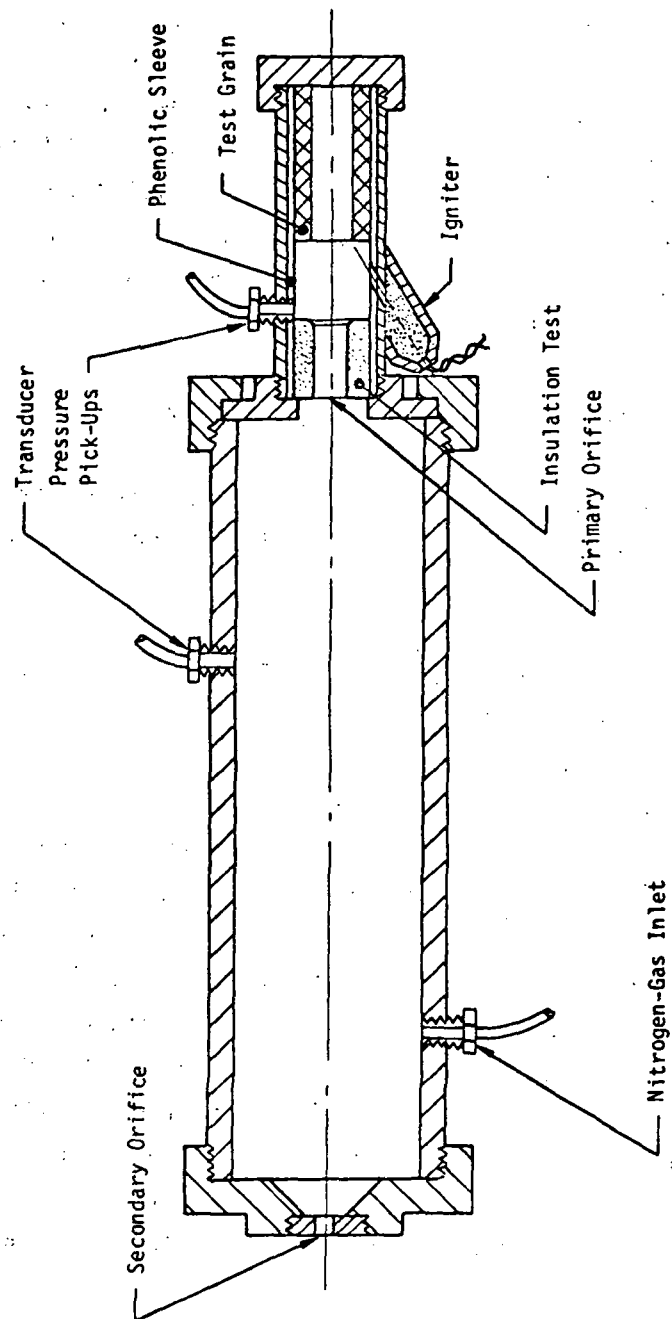
Two basic binder types were investigated, one composed of an epoxy-polyurethane system similar to that used in SD-886, the liner employed in the demonstration motors, the other based on a diisocyanate-cured saturated HTPB similar to that used in the heat sterilizable propellant binder. An additional advantage of these systems would be that the propellant bond directly without the need of additional restriction. This would result in a reduction in motor inert weight and simplify processing operations. A third material, IEM-120, a modified EPDM rubber, was also included in the evaluation as a possible improvement over the GenGard V-4030 insulation.

## II. INSULATION CONTAINING EPOXY-URETHANE BINDER

The epoxy-urethane liner system used in the demonstration motors, SD-886, was modified by adjusting the solids loading to include the following ingredients:

Ammonium sulfate	25 wt%
Kaowool fibers	25 wt%
SD-886 binder	50 wt%

The cure catalyst system was also altered to provide a longer pot life. LITE motors (Laboratory Insulation Test Evaluation motor, see Figure 1-B) were prepared with this material, half of which were test fired after being subjected to six heat sterilization cycles of 53 hours each at 135°C (275°F). The test data (Figure 2-B), reveal that the ablative properties of the unsterilized material is similar to those of GenGard V-4030. However, after the six heat sterilization properties the epoxy-urethane insulation showed a decrease in ablation rate, whereas heat sterilization caused an increase in the V-4030 ablation rate. Visual examination showed that the epoxy-urethane insulation hardened considerably after heat sterilization.



Primary Chamber Takes  
5.86 Cm (2-5/16 in.) dia  
Sleeve

Secondary Chamber  
11.4 Cm. (4-1/2 in.) I.O.

Lite Motor Schematic

Figure 1-B

Insulation	(1) Sterilized	(2)	Pressure		Burning Rate		Ablation Rate		Mass Flow	
			$\text{N/cm}^2$	(psia)	$\text{cm/sec}$	(in./sec)	$\text{cm/sec}$	(mils/sec)	$\text{g-sec/cm}^2$	(lbs-sec/in. <sup>2</sup> )
V-4030	No		348	(504)	0.424	(0.167)	0.0074	(2.9)	1.084	(0.0154)
V-4303	No		347	(503)	0.422	(0.166)	0.0076	(3.0)	1.077	(0.0153)
V-4030	Yes		349	(506)	0.424	(0.167)	0.0091	(3.6)	1.112	(0.0158)
V-4030	Yes		346	(501)	0.419	(0.165)	0.0086	(3.4)	1.112	(0.0158)
IEM-120	No		345	(500)	0.394	(0.155)	0.0086	(3.4)	1.196	(0.0170)
IEM-120	No		345	(500)	0.394	(0.155)	0.0079	(3.1)	1.189	(0.0169)
IEM-120	Yes		345	(500)	0.396	(0.156)	0.0079	(3.0)	1.309	(0.0186)
IEM-120	Yes		345	(500)	0.406	(0.160)	0.0081	(3.2)	1.365	(0.0194)
SD-886-Mod	No		345	(500)	0.386	(0.152)	0.0069	(2.7)	1.281	(0.0182)
SD-886-Mod	No		345	(500)	0.399	(0.157)	0.0071	(2.8)	1.281	(0.0182)
SD-886-Mod	Yes		345	(500)	0.399	(0.157)	0.0064	(2.5)	1.323	(0.0188)
SD-886-Mod	Yes		345	(500)	0.399	(0.157)	0.0056	(2.2)	1.288	(0.0183)

(1) V-4030 and IEM-120 are EPR rubber insulations, SD-886-Mod is SD-886 liner system modified to perform as an insulation.

(2) Sterilization treatment was six 53-hour cycles at 135°C (275°F).

Figure 2-B

Ablation Rates of Insulation Systems Lite Motor Tests with ANB-3289-3 Propellant

As mentioned previously, one of the advantages of basing the insulation on a modification of the liner system is that the propellant would bond directly to the insulation without the need of an added restriction. Bond tensile test specimens were prepared with ANB-3438 propellant cast against SD-886 liner and the SD-886 Mod insulation and tested before and after six heat sterilization cycles (53 hours each at 135°C (275°F)). The data are shown below:

	Double-Plate Tensile Strength at 25°C (77°F), N/cm <sup>2</sup> (psi)	
	<u>Initial</u>	<u>After Sterilization</u>
SD-886 Liner (control)	132 (191)	138 (200)
SD-886 Mod Insulation	112 (162)	187 (271)

The increase in bond strength is typical of previous experience with SD-886-liner and heat-sterilizable propellants utilizing saturated HTPB binder systems.

### III. INSULATIONS CONTAINING SATURATED HTPB BINDER SYSTEMS

Preliminary screening tests on binder systems based on diisocyanate-cured saturated HTPB showed that the compositions shown below were the most flexible and resistant to thermal degradation when subjected to heat sterilization tests. Formulations containing both monofunctional and difunctional epoxides (to stabilize the urethane link) were evaluated.

Formulation	Equivalentents Ratio					
	<u>1</u>	<u>2</u>	<u>3</u>	<u>4</u>	<u>5</u>	<u>6</u>
Telagen-S	55	55	55	55	55	55
GTR0	40	50	50	45	40	40
FC-154 Bonding Agent	5	5	5	5	5	5
TDI	105	105	105	105	105	105
Monofunctional Epoxide	10	20	30	-	-	-
Difunctional Epoxide	-	-	-	10	20	30



The formulations were cured at 57°C (135°F) and then subjected to a heat sterilization environment consisting of six 53-hour cycles at 135°C (275°F). No significant changes were observed after sterilization other than the heat-treated samples had darkened noticeably.

Formulations 2 and 5 containing 20 equivalents of epoxides were considered to be the best from the standpoint of flow properties and flexibility in the cured state. These binder systems were used to prepare prepare insulation materials by incorporating the following solids loading:

Carbon black	1 wt%
Kaowool fibers	15 wt%
Ammonium sulfate	35 wt%
Telagen-S binder	49 wt%

After cure and subsequent heat sterilization tests, it was noted that the insulation containing the monoepoxide remained more flexible than that which incorporated the diepoxide.

LITE motors were prepared with the insulation containing the monofunctional epoxide. However, during heat sterilization (six cycles of 53 hours each at 135°C (275°F)), the insulation sagged badly, indicating some degree of plastic flow which had been undetected previously due to the conformation of the test specimens used. As a result, LITE motor testing of the Telagen-S binder-based insulation was suspended until a tighter binder system could be developed.

#### IV. ETHYLENE-PROPYLENE-DIENE-MODIFIED (IPDM) INSULATION

An IPDM insulating material, IEM-120, developed on another program was also evaluated in LITE motor tests. This material is a calendered rubber similar to GenGard V-4030. The performance of IEM-120 was similar

to V-4030 (Figure 2-B), although there appears to be less of an affect of heat sterilization on the ablative rate of IEM-120.

## REFERENCES

1. D. O. DePree and W. L. Lambert, "Demonstration of a Sterilizable Solid Rocket Motor System", Contract NAS1-10086, NASA-CR-111889A, Addendum to The Final Report, December 1971, Aerojet Solid Propulsion Company, Sacramento, California
2. E. B. Becker and J. J. Brisbane, "Applications of the Finite Element Method to Stress Analysis of Solid Propellant Rocket Grains", Report No. S-76 Vol. 1 and 2, Rohm and Haas Co., Redstone Arsenal Research Division, Huntsville, Alabama, January 1966.
3. E. L. Wilson, L. R. Jones and T. Hsueh, "Large Displacement Analysis of Axisymmetric Shells", Report No. 69-13, Structural Engineering Lab., University of California, Berkeley, California, March 1969.
4. NASA Report SP-222, "The NASTRAN USER'S MANUAL", Caleb W. McCormick, Editor, October 1969.

\* U.S. GOVERNMENT PRINTING OFFICE: 1975-635-048 / 61



POSTMASTER: If Undeliverable (Section 158  
Postal Manual) Do Not Return

*"The aeronautical and space activities of the United States shall be conducted so as to contribute . . . to the expansion of human knowledge of phenomena in the atmosphere and space. The Administration shall provide for the widest practicable and appropriate dissemination of information concerning its activities and the results thereof."*

—NATIONAL AERONAUTICS AND SPACE ACT OF 1958

## NASA SCIENTIFIC AND TECHNICAL PUBLICATIONS

**TECHNICAL REPORTS:** Scientific and technical information considered important, complete, and a lasting contribution to existing knowledge.

**TECHNICAL NOTES:** Information less broad in scope but nevertheless of importance as a contribution to existing knowledge.

**TECHNICAL MEMORANDUMS:** Information receiving limited distribution because of preliminary data, security classification, or other reasons. Also includes conference proceedings with either limited or unlimited distribution.

**CONTRACTOR REPORTS:** Scientific and technical information generated under a NASA contract or grant and considered an important contribution to existing knowledge.

**TECHNICAL TRANSLATIONS:** Information published in a foreign language considered to merit NASA distribution in English.

**SPECIAL PUBLICATIONS:** Information derived from or of value to NASA activities. Publications include final reports of major projects, monographs, data compilations, handbooks, sourcebooks, and special bibliographies.

**TECHNOLOGY UTILIZATION PUBLICATIONS:** Information on technology used by NASA that may be of particular interest in commercial and other non-aerospace applications. Publications include Tech Briefs, Technology Utilization Reports and Technology Surveys.

*Details on the availability of these publications may be obtained from:*

**SCIENTIFIC AND TECHNICAL INFORMATION OFFICE**

**NATIONAL AERONAUTICS AND SPACE ADMINISTRATION**

**Washington, D.C. 20546**